Preface

The Standard Model (SM) is the theory that best describes the experimental results in particle physics, but some of its parameters are not very well determined by experiments because of our poor theoretical control of strong interactions. In particular the Cabibbo-Kobayashi-Maskawa (CKM) matrix elements that couple to heavy quarks are not determined with sufficient precision. These parameters are extremely important because they provide a potential signal for new physics. For example a non unitary CKM matrix would indicate a breakdown of the SM. Modern day computer facilities make it possible to adopt a brute force approach to the problem of controlling strong interactions and allow us to compute their effect systematically in a non-perturbative, model-independent way. In this thesis we present the explicit lattice evaluation of the strong interaction effects which are relevant for the processes:

- $B \to B^* + \pi$ coupling
- B^0, $\bar{B}^0$, $B^\pm$, $\Lambda_b \to X$ inclusive decays
- $B^0 \leftrightarrow \bar{B}^0$ mixing

These processes are particularly important for two reasons: first, they have just started to be explored experimentally with modern particle accelerators, therefore the corresponding CKM matrix elements are very poorly determined; second, these processes involve an heavy b quark and one expects to be able to gain, from these studies, some insight into physics at very short distances.

Organisation of the Thesis

This thesis is divided in five chapters. In the first we present a concise review of the Standard Model, its degrees of freedom and their dynamics. We also present an introduction to the phenomenology which is relevant to an understanding of the strong interactions.

In the second chapter we present a bird's eye view of the physical meaning of Regularization and Renormalization in the Kadanoff-Wilson approach, having in mind the lattice as typical regulator. We also give an introduction to the standard technique of integrating out modes, to the Operator Product Expansion and to some effective theories which are useful in the study of the Standard Model. The last section of the second chapter contains an introduction to Lattice QCD.

The third chapter contains one of the main results of this thesis: the computation of the matching factors for a complete set of 4-quark operators between continuum HQET and Lattice HQET. These factors are necessary to relate the lattice matrix elements to the experimental ones, which are usually quoted in the continuum $\overline{\text{MS}}$ renormalization scheme. The original part of this computation is published in ref. [1].

The fourth chapter is dedicated to the conputation of the $B \to B^* + \pi$ coupling and we discuss some phenomenological implications. Our results are published in ref. [2].

In the fifth chapter we compute the ratios of lifetimes $\tau(B^\pm)/\tau(B^0)$ and $\tau(\Lambda_b)/\tau(B^0)$. For the former we obtain complete agreement with the experimental results, while for the latter we find a small discrepancy with experimental data. In the evaluation of the relevant matrix elements for B mesons we find a surprising agreement between the lattice results and a naive prediction based on the vacuum saturation hypothesis. As a check we re-evaluate the B_B factor relevant for the $B^0 - \bar{B}^0$ mixing and we observe the same kind of phenomenon. In the latter analysis we adopte our values for the matching factor (including corrections to a preceding publication) finding agreement with other independent evaluations of the same quantity. These results are published in ref. [1][3] and [4].

The thesis concludes with four appendices. Their main purpose is to establish the notation and to present a set of useful formulas which may help the reader to reconstruct the crucial mathematical steps in some of the presented computations.

Acknowledgements

It has not been easy for me to come to study in England, far from the people I love, and learn to express myself in a foreign language. But here I met a lot of nice people who made my job easier. They are the staff, the postdocs and all the students of the SHEP group.

In particular I want to thank my supervisor, Chris Sachrajda, for the precious suggestions and advice he gave me during this thesis. I can truly say that I learned a lot from him.

I want to thank Jonathan Flynn for his invaluable help. He kindly let me go through his notes on the matching computation and it is there, much more than in many books, that I learned the technical details involved in this kind of computation.

I want to thank Luigi Del Debbio, Mar Bastero-Gil and Giulia De Divitiis for the many useful discussions and their comments on this thesis.

I also thank Hartmut Wittig, Chris Michael, Balint Joo, Kevin Anderson, Jacek Generowicz, Scott Griffiths and Mike Hill for their computer support, Alex Dougall, Victor Lesk and Chris Harvey-Fros for having helped me to correct this and other manuscripts of mine.

Finally I want to thank my family (Annamaria, Italo and my sister Silvia) for their economical and moral support during so many years of studies, and my girlfriend Claudia, who always understood my desire for knowledge and suffered for our distance as much as I did.

To Annamaria, Italo, Silvia and Claudia I dedicate this work.

Contents

1 The Standard Model **1**

1.1 Introduction 1

1.1.1 Lagrangian Formulation 2

1.1.2 Spontaneous symmetry breaking 7

1.1.3 Classical equations of motion 9

1.2 Phenomenology 10

1.2.1 Electroweak sector and the Higgs 12

1.2.2 Short distance physics 14

1.2.3 Long distance physics and hadronic matter 15

1.2.4 B Physics 17

1.2.5 Mixing with and without CP violation 19

1.2.6 The unitarity triangle and new physics 21

1.2.7 PCAC phase transition 21

1.2.8 Axial anomaly 22

1.2.9 Cosmological implications 22

1.2.10 Beyond the Standard Model 23

2 Effective Theories **24**

2.1 Regularization and Renormalization 24

2.1.1 Regularizing distributions 25

2.1.2 Lattice regularization and momentum cut-off 27

2.1.3 Applications to quantum mechanics 29

2.1.4 Applications to quantum field theory 30

2.1.5 Operator Product Expansion 35

2.2 Examples of interest 36

2.2.1 Heisenberg-Euler Effective Theory and quenching 36

2.2.2 Fermi Electroweak Theory 37
2.2.3 Heavy Quark Effective Theory 38
2.2.4 Goldstone Theorem and Chiral Lagrangian 40
2.3 Lattice QCD 43
2.3.1 Basic degrees of freedom and action 43
2.3.2 Simulation aspects and quenching 47
2.3.3 Correlation functions and fermions 49
2.3.4 Lattice discrete symmetries 50
2.3.5 Heavy quarks 52
2.3.6 Determining c_{SW} 52
2.3.7 Lattice errors 53

3 Perturbative Matching Coefficients 55
3.1 Continuum $\overline{\mathrm{MS}}$ vs Lattice renormalization 57
3.1.1 Renormalization of the external lines 59
3.1.2 Matching $\bar{q}\Gamma q$ type operators 60
3.1.3 Matching $\bar{b}\Gamma q$ type operators 62
3.1.4 Matching $\bar{b}\Gamma q\,\bar{q}\tilde{\Gamma} b$ type operators 62
3.1.5 Matching $\bar{b}\Gamma_i q\,\bar{b}\tilde{\Gamma}_i q$ type operators 67
3.2 Matching different scales 68
3.3 Examples of interest 70
3.3.1 Computation of Z_A^{light} 70
3.3.2 Computation of Z_A^{static} 71
3.3.3 Computation of Z_{ij} for $B-\bar{B}$ Mixing 71
3.3.4 Computation of Z_{ij} for B Decay 73
3.3.5 Computation of z_{ij} for B Decay 74

4 The $g_{B^*B\pi}$ Effective Coupling 77
4.1 Introduction 77
4.1.1 Pion reduction 79
4.2 Results 81
4.2.1 Renormalisation constants 81
4.2.2 Stochastic propagators 84
4.2.3 Lattice computation 86
4.3 Phenomenology 94

5 **Spectator Effects in Inclusive Decays of Heavy Hadrons** **97**
5.1 Introduction 97
5.1.1 Heavy Quark Expansion 99
5.2 B decays 102
5.2.1 Perturbative matching 102
5.2.2 Lattice computation and results 104
5.3 $B-\bar{B}$ mixing 110
5.3.1 Factorization 110
5.3.2 Matching 114
5.4 Λ_b decays 114
5.4.1 Perturbative matching 114
5.4.2 Lattice computation and results 117

A **Introduction to Quantum Field Theory** **122**

B **Useful Formulae and Notation** **126**
B.1 Notation in Minkowski Space-Time in $d = 4$ dimension 126
B.2 Notation in Euclidean Space-Time in $d = 4$ dimension 128
B.3 Operators and Algebra 129
B.4 Gauge groups 134
B.5 Rules for Dimensional Regularization 136

C **Units, Parameters, Particles** **139**

D **Feynman Rules** **142**
D.1 Feynman rules for QCD and HQET
(Minkowski space) 142
D.2 Feynman rules for Lattice QCD and HQET
(Euclidean space) 143
D.3 Example of computation of a Lattice Feynman diagram 144
D.4 Definition of useful parameters 146
D.5 Definition of useful integrals 147

Chapter 1

The Standard Model

1.1 Introduction

In the 1960's a plethora of particles were known to particle physicists, such as the electron, the neutrino, the proton, the neutron and a number of mesons and baryons (which are now known to be bound states of quarks in a singlet representation of the color group $SU(3)_C$). The interactions among these particles were described in terms of four distinct forces, characterised by different ranges and strengths. These were the strong force, with a range of about 10^{-15}m, the weak force, with a range of 10^{-17}m, the electromagnetic force, which has an infinite range but decreases with the inverse distance squared, and the gravitational force. The latter is very important to explain macroscopic phenomena, but it is so weak at a typical subatomic scale that it can be neglected when studying particles. It is the only force which is not taken into account by the Standard Model[1].

The observed interactions between these particles exhibit some regularities which were described in terms of conservation laws. Some of these conservation laws are known to be exact, others are only approximate, nevertheless they guided theorists toward a consistent mathematical description of those fundamental forces.

The idea of a conservation law is that it is possible to associate a quantum number to the different kinds of particles to discriminate if a particular reaction, say

$$X_a + X_b \to X_c + X_d + ... \tag{1.1}$$

is possible or not. Some of these quantum number have an additive conservation

[1]Nevertheless the gravitational force is responsible for the large scale structure of the Universe and it may be related to the other forces in some very fundamental way. For example they could all be different manifestations of just one fundamental interaction.

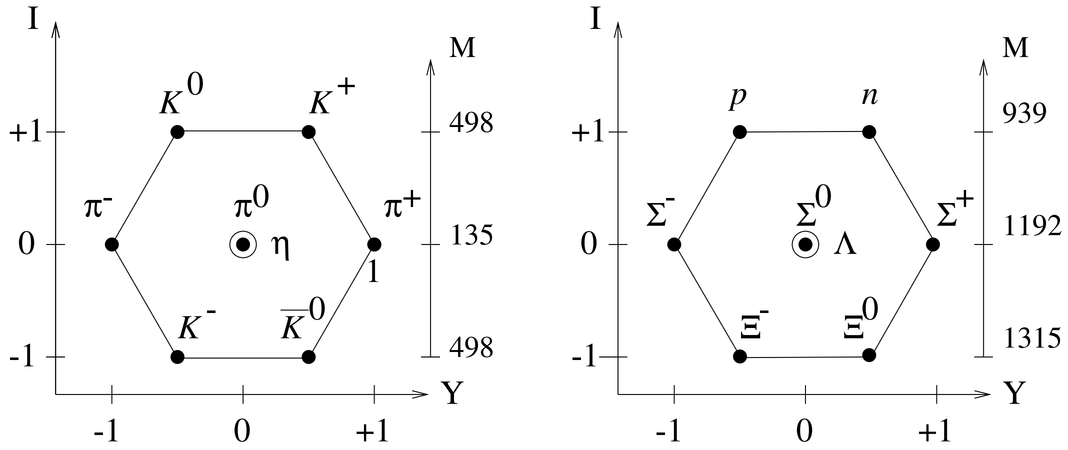

Figure 1.1: Mesonic particles with $J^P = 0^+$ (left) and Baryonic particles with $J^P = \frac{1}{2}^+$ (right). I is the isospin, Q is the electric charge and M is the mass in MeV.

law such as

$$n_a + n_b = n_c + n_d + ... \tag{1.2}$$

while others must be combined in a more complicated way (for example the spin and the isospin). Examples of additive quantum numbers are the electric charge, the hypercharge, the baryonic and leptonic number, the strangness, the charmness, the bottomness. Some of these quantum numbers are exactly conserved, some are approximatively conserved.

Each particle was identified by its mass and its quantum numbers.

At this point some patterns appeared, like those reported in figures 1.1-1.2. This suggested that some structure was hidden deep inside the known hadrons [9].

The simplest explanation was that all the mesons are bound states of quark-antiquark, while the baryons (antibaryons) are bound states of three quarks (antiquarks). The existence of some of the baryons, such as the Δ^{++}, was a puzzle in view of the Pauli exclusion principle, hence it was necessary to introduce the new quantum number called colour. The best attempt to describe experimental data from particle physics is formulated in the Standard Model[2] (SM).

1.1.1 Lagrangian Formulation

The fundamental degrees of freedom of the SM are

[2]As introductory reviews on the SM the reader can refer to [5, 6, 7, 8].

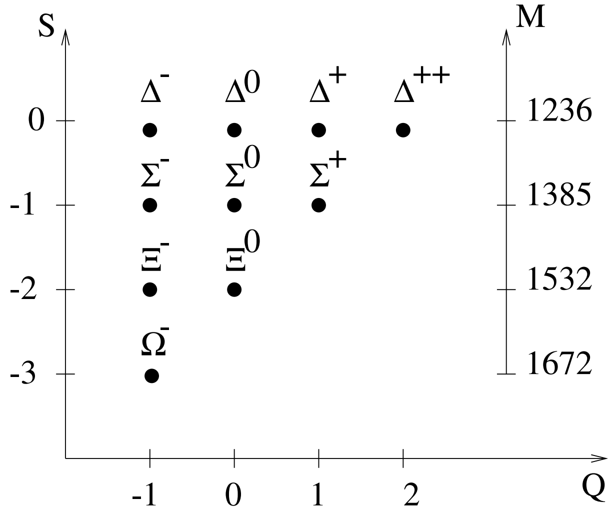

Figure 1.2: Baryonic particles with $J^P = \frac{3}{2}^+$. S is the strangeness, Q is the electric charge and M is the mass in MeV.

- Three spin $\frac{1}{2}$ particles of charge $Q = 0$, called neutrinos:

$$\nu_f \tag{1.3}$$

  where the index f is called *flavour* and runs from 1 to 3. The three neutrinos are called ν_e (*electron neutrino*), ν_μ (*muon neutrino*), ν_τ (*tau neutrino*), respectively. Their peculiar characteristic is that[3] $L\nu_f = \nu_f$.

- Three spin $\frac{1}{2}$ particles of electric charge $Q = -1$:

$$\ell_f \tag{1.4}$$

  for $f = 1, 2, 3$. They are called e^- (*electron*), μ^- (*muon*), τ^-(*tau*). They, together with neutrinos, are called *leptons*.

- Nine spin $\frac{1}{2}$ particles of electric charge $Q = \frac{2}{3}$:

$$u_f^i \tag{1.5}$$

  for $f = 1, 2, 3$. The index i is called colour and runs from 1 to 3. These nine quarks have masses which are degenerate in colour but not in flavour. The three different flavours are usually indicated with different symbols: u^i (*up quark*), c^i (*charm quark*), t^i (*top quark*).

[3] L is the projector on left-handed states, $\frac{1}{2}(1 - \gamma^5)$. $R = 1 - L$ is the complementary projector.

- Nine spin $\frac{1}{2}$ particles of electric charge $Q = -\frac{1}{3}$:

$$d^i_f \tag{1.6}$$

for $i = 1, 2, 3$ and $f = 1, 2, 3$. The three flavours are indicated as d^i (*down quark*), s^i (*strange quark*), b^i (*bottom quark*).

- One spin 0 complex field of electric charge $Q = 1$:

$$\varphi^+ \tag{1.7}$$

- One spin 0 complex field of electric charge $Q = 0$:

$$\varphi^0 \tag{1.8}$$

When it is not necessary to specify the charge or the flavour of a quark it will be referred to simply as q^i. The symbol ψ will indicate a generic spin $\frac{1}{2}$ field in the ensemble $\{\nu_f, \ell_f, u_f, d_f\}$. The greek index will be used to refer to the spin components of the fields.

It is convenient to introduce the three sets of doublets

$$\varphi \equiv \begin{pmatrix} \varphi^+ \\ \varphi^0 \end{pmatrix}, \qquad \mathcal{L}_f \equiv \begin{pmatrix} \nu_f(x) \\ \ell_f(x) \end{pmatrix}, \qquad \mathcal{Q}_f \equiv \begin{pmatrix} u_f(x) \\ d_f(x) \end{pmatrix} \tag{1.9}$$

where the first of them is called the Higgs doublet and it has never been observed.

The Lagrangian of the SM is built in accordance with the gauge principle and three fundamental symmetries:

- $U(1)_{\mathbf{Y}}$ **Group**

$$\psi(x) \to e^{iY\vartheta(x)}\psi(x) \tag{1.10}$$

where Y is an operator that has the fundamental fields as eigenstates. It is called *hypercharge*.

- $SU(2)_{\mathbf{W}}$ **Group** (for any flavour)

$$w(x) \to U(x)w(x) \tag{1.11}$$

where $U(x) \in SU(2)$ and $w(x)$ is any of the following doublets of fields:

$$L\mathcal{L}_f, \qquad L\mathcal{Q}_f, \qquad \varphi \tag{1.12}$$

	ν	$L\ell$	$R\ell$	Lu	Ru	Ld	Rd	φ^+	φ^0
S	$\frac{1}{2}$	$\frac{1}{2}$	$\frac{1}{2}$	$\frac{1}{2}$	$\frac{1}{2}$	$\frac{1}{2}$	$\frac{1}{2}$	0	0
Q	0	-1	-1	$\frac{2}{3}$	$\frac{2}{3}$	$-\frac{1}{3}$	$-\frac{1}{3}$	1	0
T_3	$\frac{1}{2}$	$-\frac{1}{2}$	0	$\frac{1}{2}$	0	$-\frac{1}{2}$	0	$\frac{1}{2}$	$-\frac{1}{2}$
Y	$-\frac{1}{4}$	$-\frac{1}{4}$	$-\frac{1}{2}$	$\frac{1}{12}$	$\frac{1}{3}$	$\frac{1}{12}$	$-\frac{1}{6}$	$\frac{1}{4}$	$\frac{1}{4}$
N_B	0	0	0	1	1	1	1	0	0
N_L	1	1	1	0	0	0	0	0	0

Table 1.1: Particle quantum numbers: spin, electric charge, isospin, hypercharge, baryon number and lepton number

The generators of this group are $T_i = \frac{\sigma_i}{2}$. Therefore the eigenvectors of T_3 are

$$T_3 \begin{pmatrix} 1 \\ 0 \end{pmatrix} = +\frac{1}{2} \begin{pmatrix} 1 \\ 0 \end{pmatrix}; \qquad T_3 \begin{pmatrix} 0 \\ 1 \end{pmatrix} = -\frac{1}{2} \begin{pmatrix} 0 \\ 1 \end{pmatrix} \tag{1.13}$$

The operator T_3 is called weak-isospin. One says that the weak-isospin of ν_f, Lu_f and φ^+ is $+\frac{1}{2}$, the weak-isospin of $L\ell_f$, Ld_f and φ^0 is $-\frac{1}{2}$, while Re, Ru, Rd have weak-isospin 0.

- $SU(3)_{\mathbf{C}}$ **Group** (colour symmetry)

$$q(x) \to U(x)q(x) \tag{1.14}$$

where $U(x) \in SU(3)$ and

$$q_f(x) = \begin{pmatrix} q_f^1(x) \\ q_f^2(x) \\ q_f^3(x) \end{pmatrix} \tag{1.15}$$

The generators of this group will be indicated with $t^a = \frac{\lambda^a}{2}$. Their explicit expression and properties are listed in Appendix B.

A summary of the values of spin, electric charge, weak-isospin and hypercharge is reported in the upper part of table (1.1).

At the moment these numbers may appear random, but they are not, in fact it is easy to check that

$$Q = 2Y + T_3 \tag{1.16}$$

The argument goes as follows: The gauge symmetries are not symmetries of the Hilbert space of the Standard Model, which is selected by imposing a gauge constraint as an operator identity on the physical states, but they are symmetries of the field theory representation of the model. Therefore one requires gauge symmetries not to be broken by the quantization procedure. In the path integral formulation of the quantum field theory this means that the regularized Jacobian of a gauge transformation must be the identity. Imposing such a condition is equivalent to eq. (1.16). This put a strong constraint on the hypercharges of the particles of the SM. There are symmetries of the action of the SM for which the corresponding Jacobian differs from the identity. This means that, at the quantum level, the symmetry is broken and the variation in the action picks up an anomalous contribution. These non-symmetries are called anomalous symmetries, or simply *anomalies*, and their corresponding charges are not conserved.

The most general Lagrangian invariant under local gauge transformations (1.14), (1.11) and (1.10) has the following structure[4]

$$\mathcal{L}_{\rm SM} \equiv \mathcal{L}_{\rm matter} + \mathcal{L}_{\rm YM} + \mathcal{L}_{\rm ssb} + \mathcal{L}_{\rm Yukawa} \tag{1.18}$$

where

$$\mathcal{L}_{\rm matter} \equiv \bar{\mathcal{L}}(i\not{D})\mathcal{L} + \bar{\mathcal{Q}}(i\not{D})\mathcal{Q} \tag{1.19}$$

$$\mathcal{L}_{\rm YM} \equiv -\frac{1}{4}G^a_{\mu\nu}G^{a,\mu\nu} - \frac{1}{4}W^i_{\mu\nu}W^{i,\mu\nu} - \frac{1}{4}B_{\mu\nu}B^{\mu\nu} \tag{1.20}$$

$$\mathcal{L}_{\rm ssb} \equiv (D_\mu\varphi)^\dagger(D^\mu\varphi) - m^2_\varphi\varphi^\dagger\varphi - \lambda\left|\varphi^\dagger\varphi\right|^2 \tag{1.21}$$

$$\mathcal{L}_{\rm Yukawa} \equiv -\bar{\mathcal{L}}_L\varphi H_{(\mathcal{L})}\mathcal{L}_R - \bar{\mathcal{Q}}_L\varphi H_{(\mathcal{Q})}\mathcal{Q}_R + h.c. \tag{1.22}$$

(the subsript L and R indicate left-handed and right-handed spinors respectively, the sum on the flavour is implicit) and we adopted the following definitions

$$D_\mu \equiv \partial_\mu + ig_1 Y B_\mu + ig_2 T^i W^i_\mu L + ig_3 t^a A^a_\mu \tag{1.23}$$

$$G^a_{\mu\nu} \equiv \partial_\mu A^a_\nu - \partial_\nu A^a_\mu - g_3 f^{abc}[A^b_\mu, A^c_\nu] \tag{1.24}$$

$$W^i_{\mu\nu} \equiv \partial_\mu W^i_\nu - \partial_\nu W^i_\mu - g_2\varepsilon^{ijk}[W^j_\mu, W^k_\nu] \tag{1.25}$$

$$B_{\mu\nu} \equiv \partial_\mu B_\nu - \partial_\nu B_\mu \tag{1.26}$$

$$H_{(\mathcal{L})} = \begin{pmatrix} 0 & 0 \\ 0 & H_{(e)} \end{pmatrix} \quad \text{and} \quad H_{(\mathcal{Q})} = \begin{pmatrix} H_{(u)} & 0 \\ 0 & H_{(d)} \end{pmatrix} \tag{1.27}$$

($H_{(e)}, H_{(u)}, H_{(d)}$, are 3×3 matrices in flavour space).

[4] In principle there is no reason why the SM Lagrangian should not contain a term of the form

$$\mathcal{L}_{\text{CP-strong}} = \theta_s \epsilon^{\mu\nu\rho\sigma} G^a_{\mu\nu} G^a_{\rho\sigma} \tag{1.17}$$

Experimental results indicates that $\theta_s < 10^{-19}$, therefore this term will be ignored. This is referred to as the strong CP problem.

1.1.2 Spontaneous symmetry breaking

The vacuum state of the SM is characterised by the minimum of the potential that appears in eq. (1.21). Assuming that $m_\varphi^2 < 0$, the φ^0 acquires a vacuum expectation value

$$v^2 \equiv \langle 0| (\varphi^0)^2 |0\rangle = \frac{\mu^2}{2\lambda} \tag{1.28}$$

Under these circumstances the Yukawa interactions of eq. (1.22) generate mass terms for the basic fermionic degrees of freedom of the SM [10]. These mass terms are conveniently expressed in terms of the unitary matrices U_e, U_u and U_d

$$vH_{(e)} = U^{-1}_{(e)L} \begin{pmatrix} m_e & & \\ & m_\mu & \\ & & m_\tau \end{pmatrix} U_{(e)R} \tag{1.29}$$

$$vH_{(u)} = U^{-1}_{(u)L} \begin{pmatrix} m_u & & \\ & m_c & \\ & & m_t \end{pmatrix} U_{(u)R} \tag{1.30}$$

$$vH_{(d)} = U^{-1}_{(d)L} \begin{pmatrix} m_d & & \\ & m_s & \\ & & m_b \end{pmatrix} U_{(d)R} \tag{1.31}$$

m_e, m_μ, m_τ are the masses of charged leptons ($Q = -1$); m_u, m_c, m_t are the masses of quarks with charge $Q = 2/3$; m_d, m_s, m_b are the masses of quarks with charge $Q = -1/3$. These are some of the fundamental parameters of the SM.

To have a diagonal mass matrix it is necessary to reabsorb the contribution of $U_{(e)}$, $U_{(u)}$ and $U_{(d)}$ with a rotation of the fields. In eq. (1.19) the term proportional to

$$\frac{g_2}{\sqrt{2}}\bar{u}\gamma_\mu L(W_1^\mu - iW_2^\mu)d + h.c. \tag{1.32}$$

picks up a contribution from this rotation of

$$\frac{g_2}{\sqrt{2}}\bar{u}\gamma_\mu L(W_1^\mu - iW_2^\mu)U_{(u)L}U^\dagger_{(d)L}d + h.c. \tag{1.33}$$

For this reason the physical states, which are mass eigenstates, couple with the charged weak currents through the 3×3 unitary matrix[5]

$$V_{CKM} \equiv U_{(u)L}U^\dagger_{(d)L} \tag{1.34}$$

[5] The leptonic sector of the SM does not get any mixing because neutrinos are supposed to be massless and there are no right-handed neutrinos. If this turn out not be the case, it may well be that this mechanism needs to be extended to leptons.

which is called the Cabibbo-Kobayashi-Maskawa matrix [11]. Its matrix elements are of central importance in particle physics. They are not predicted by the Standard Model and therefore they have to be extracted from experimental data.

After spontaneous symmetry breaking occurs it is convenient to rewrite the interacting part of the Lagrangian in terms of the four currents

$$J^{em}_\mu \equiv \bar{\psi}\gamma_\mu Q\psi \tag{1.35}$$
$$J^{nc}_\mu \equiv \bar{\psi}\gamma_\mu(T_3 - \sin^2\theta_W Q)\psi \tag{1.36}$$
$$J^{\pm}_\mu \equiv \bar{\mathcal{L}}\gamma_\mu L(T_1 \pm iT_2)\mathcal{L} + \bar{\mathcal{Q}}\gamma_\mu L(T_1 \pm iT_2)V^{\pm 1}_{CKM}\mathcal{Q} \tag{1.37}$$
$$J^a_\mu \equiv \bar{q}\gamma_\mu t^a q \tag{1.38}$$

called electromagnetic, neutral, weak charged and colour currents respectively. $\tan\theta_W \equiv g_1/g_2$ and θ_W is called the *weak mixing angle*.

It is also convenient to define the following combinations of the gauge field

$$A^{em}_\mu \equiv W^3_\mu \sin\theta_W + B_\mu \cos\theta_W \tag{1.39}$$
$$Z^0_\mu \equiv W^3_\mu \cos\theta_W - B_\mu \sin\theta_W \tag{1.40}$$
$$W^{\pm}_\mu \equiv W^1_\mu \pm iW^2_\mu \tag{1.41}$$

In this language the interaction Lagrangian describing the coupling of the matter fields with the gauge bosons can be conveniently split into three pieces:

- **Quantum Electrodynamics** [12] (electromagnetic interaction):

$$\mathcal{L}^{\rm int}_{\rm QED} = eJ^{em}_\mu A^{em\,\mu} \tag{1.42}$$

  where A^{em} is the massless gauge field associated with the photon and

$$e = g_1 \sin\theta_W \tag{1.43}$$

- **Weak Theory** [13] (weak interactions):

$$\mathcal{L}^{\rm int}_{\rm Weak} = \frac{g_2}{\cos\theta_W}J^{nc}_\mu Z^{0\mu} + \frac{g_2}{\sqrt{8}}J^+_\mu W^{-\mu} + \frac{g_2}{\sqrt{8}}J^-_\mu W^{+\mu} \tag{1.44}$$

  where Z^0 is the massive neutral vector boson and $W^{\pm}$ are the massive charged vector bosons. Their masses are given, at tree-level, by

$$m_Z = \frac{v}{2}\sqrt{g_1^2 + g_2^2} \tag{1.45}$$
$$m_W = \frac{1}{2}g_2 v \tag{1.46}$$

  (v is the expectation value of the Higgs field.)

- **Quantum Chromodynamics** [14, 15] (strong interactions) :

$$\mathcal{L}^{\rm int}_{\rm QCD} = g_3 J^a_\mu A^{a\mu} \tag{1.47}$$

where A^a is the massless non-abelian gauge field associated with the gluon. For reviews see [16, 17, 18]

- **Higgs sector**: After spontaneous symmetry breaking only one degree of freedom from the Higgs doublet survives, the Higgs boson. Its Lagrangian is quite complicated because it couples with all the fermions, $W^\pm$ and Z^0. The best present experimental value for the Higgs mass is reported in Appendix C. For reasons that will be explained in the next chapter, Higgs effects are strongly suppressed at energy scales of the order of one GeV.

Usually QED and the Weak Theory are collectively called the Electroweak Theory.

After spontaneous symmetry breaking the effective Lagrangian for the SM is function of the masses of its particles, of the three couplings and of the CKM matrix elements. The experimental values for these parameters are reported in Appendix C.

1.1.3 Classical equations of motion

The classical equation of motion for the gauge bosons of the SM are (ignoring any WWZ, WWC and Higgs intercations), in the Coulomb gauge,

- **Electromagnetic field** (the photon):

$$\Box A^{em}_\mu = e J^{em}_\mu \tag{1.48}$$

Its solution for a static electric charge gives the well known electrostatic potential $V(r) = e/r$.

- $W^\pm$ **and** Z^0 **fields** (intermediate vector bosons):

$$(\Box + m_W^2) W^\pm_\mu = \frac{g_2}{\sqrt{8}} J^\pm_\mu \tag{1.49}$$

$$(\Box + m_Z^2) Z^0_\mu = \frac{g_2}{cos\theta_W} J^{nc}_\mu \tag{1.50}$$

Their solution for a static weakly charged particle is a Yukawa-type potential $V(r) \propto r^{-1}\exp(-m_W r)$ which explains the finite range of the weak interactions.

- **Chromoelectric field** (gluons):

$$\Box A^a_\mu = g_3 f^{abc} A^b_\mu \partial^\nu A^c_\nu + g_3 J^a_\mu \tag{1.51}$$

At short distances the potential between two quarks can be modelled with $V(r) \sim 1/r$, but this is not an exact solution and it is not a good approximation for $r > 1$ fm.

The classical equation of motion for fermionic fields is the usual Dirac equation in a background field are

$$(i\not{D} - m)\psi = 0 \tag{1.52}$$

Quantum corrections spoil these naive conclusions, in particular the chromoelectric potential between two quarks at large distances turns out to be proportional to the distance: $V(r) \simeq \sigma r$ (σ is a phenomenological parameter called string tension). This result has been confirmed by many lattice simulations [19].

All the classical equations of motion and a complete Hamiltionian treatment of the SM can be found in [20].

1.2 Phenomenology

The success of the Standard Model was to combine the $SU(2)_{\rm L} \times U(1)_{\rm Y}$ Glashow - Weinberg - Salam theory of electroweak interactions [13] together with QCD [15] in one renormalizable quantum field theory. Since its formulation the Standard Model has been subject to a great deal of experimental tests, probing its predictive power well above the tree-level computations [21, 22].

At present, it seems there is no experimental evidence that is in conflict with the predictions of the Standard Model[6].

Probably one of the most striking prediction of the Standard Model, for the precision of both the perturbative calculation and the experimental result, is the anomalous magnetic moment of the electron, g_e, which can be measured form the magnetic dipole moment [6]

$$\mu = (2 + g_e)\frac{e\sigma}{2m_e} \tag{1.53}$$

The theoretical result is known up to 4 loops in QED[7]

$$g_e^{\rm th} = 0.001159652156(23) \tag{1.54}$$

[6] With the exception of the recent discovery of a neutrino mass, which is zero according to the SM. In any case this effect is so tiny that it can be verified only in huge dedicated experiments and has no measurable effect on collider physics. Many possible extensions to the SM have been proposed to take into account a neutrino mass but, at present, the experimental results do not allow discrimination between them, therefore the SM remains the best model.

[7] The possibility of carrying out this calculation with such a high degree of precision is due to the fact that the hadronic contribution and the perturbative electroweak contribution to g_e are together less than 2 10^{-12}.

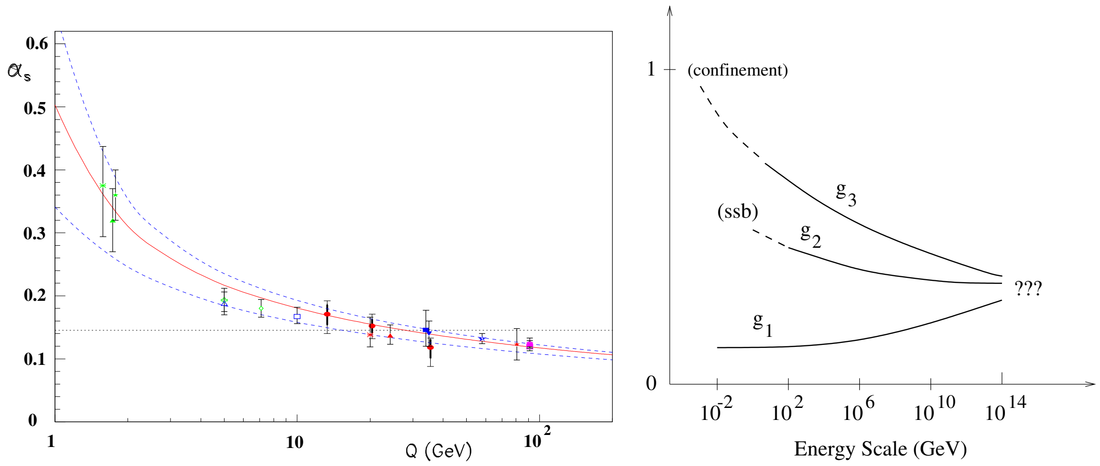

Figure 1.3: Experimental results for the running of α_s vs the momentum stransferred (left). Qualitative comparison between the running of the gauge couplings g_1, g_2 and g_3 (right).

to be compared with the experimental result

$$g_e^{\text{exp}} = 0.001159652188(3) \tag{1.55}$$

With the exception of the Higgs, all the building blocks of the SM have been directly or indirectly observed in experiments and their interactions have been observed in scattering and decay processes. The experimental cross sections and decay times agree with the perturbative theoretical predictions within less that one standard deviation.

The situation is somewhat peculiar for quarks: they have not been observed directly but there is strong indirect evidence for their existence. The renormalized strong coupling constant g_3 decreases as the energy scale increases (i.e. when probing short distances). Therefore in this domain perturbation theory is valid and this allows a number experimental tests which will be reviewed briefly. This phenomenon is called *asymptotic freedom* [23, 24]. It is a general feature of those theories with an unbroken non-abelian gauge group. At low energy scales (i.e. large distances) the perturbative expansion fails because the renormalized strong coupling g_3 (the parameter in which the perturbative expansion is done) increases and eventually becomes bigger than one. A plot of experimental values of $\alpha_s \equiv g_3^2/4\pi$ at different momentum transferred is reported in figure 1.3.

There is evidence of a net difference between the high energy perturbative regime and the low energy non-perturbative one: in the first quarks appear as the basic degrees of freedom, while in the latter only color singlet states appear, the hadrons (i.e. mesons and baryons), and quarks are confined into them [25]. At high energy (short distances) the quarks interact through the exchange of gluons, while at low energy (large distances) gluons are also confined, and their residual effect is in the short range Van der Vaals forces between hadrons[8]. The energy scale where the transition between the two regimes occurs is the fundamental parameter of QCD, and one of the most important for SM itself. It is usually indicated with the symbol Λ_{QCD}. The precise value depends on its definition and is of the order of 250 MeV. Today lattice simulations provide the only theoretical tool to explore the non-perturbative regime of QCD in a quantitative way without model dependent assumptions. In figure 1.3 the running of g_3 is compared with running of g_1 and g_2. While g_3 increases at low energies (i.e. large scale), g_1 decreases. The behaviour of g_2 is similar to that of g_3 (bacause it is associated to the non-abelian $SU(2)$ group), but it is much milder than it. In particular it never becomes bigger that one, because the low energy physics is dominated by spontaneous symmetry breaking (ssb) effects.

One consequence of the behaviour of g_3 is that, in nature, we are allowed to have "free" particles with electroweak charges different from zero, but we are not allowed to have free particles with color quantum number different from zero, for example quarks and gluons. Moreover, for electroweak interaction, perturbation theory is valid all the way down to the lowest energy scale; it is quite the opposite of what happens for strong interactions.

1.2.1 Electroweak sector and the Higgs

Electroweak interactions have been known for a long time because they are responsible for nuclear weak decays as well as many other particle decays. Originally Enrico Fermi proposed a theory to explain electroweak interactions which is based on the effective interaction Lagrangian [26]

$$\mathcal{L}_{\mathrm{Fermi}} = -\frac{G_F}{\sqrt{2}} J^+_\mu J^{-\mu} \tag{1.56}$$

The fact that this theory was not renormalizable led Glashow,Weinberg and Salam to postulate the existence of intermediate vector bosons, $W^\pm$ and Z^0 (which where later discovered) and then to formulate the SM. As will be explained in more detail in the next chapter, any perturbative result from the electroweak sector of the SM can be expanded as a series in the inverse mass of m_W. The leading contribution (order 0) in this expansion is equivalent to the corresponding

[8]An example is the force that keeps together protons and neutrons in the atomic nucleus.

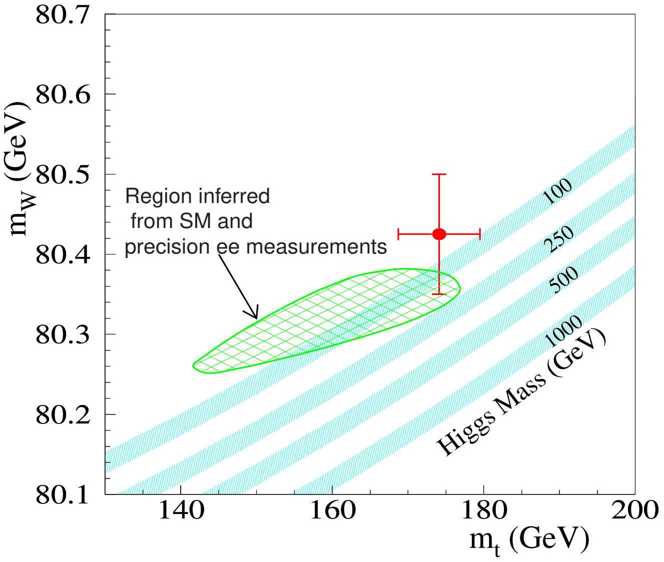

Figure 1.4: Comparison between the indirect determinations (from LEP and SLD) and the world average of direct measurements of m_W and m_t. The indirect determination (closed shaded area) is based on the measure of cross sections in $e^+e^- \rightarrow l\bar{l} + \gamma$ scattering events. The shaded bands are theoretical contraints, obatined from the SM, for different hypothetical values of the Higgs mass.

prediction of the Fermi electroweak theory with the effective coupling given by[9]

$$G_F \simeq \frac{g_2^2}{8m_W^2}\left[1 + \text{pert.corr.}\right] \tag{1.57}$$

This is one of the experimental quantities used to determine the fundamental parameters of the SM. Since the SM does not predict the values of its coupling constants, it does not predict a value for G_F.

Figure 1.4 shows a comparison between the indirect determinations and the world average of direct measurements of m_W and m_t. The shadow lines superimposed to the plot are predictions based on different possible Higgs masses. At the moment the Higgs remains the only unobserved particle of the SM, and there are two possible scenarios:

- The Higgs is too massive to be produced with present day accelerators. If this is the case, it will be discovered soon by the new Large Hadron Collider at CERN.

- The Higgs, whose existence has been postulated to explain the masses of vectorial bosons and is one of the fundamental blocks of the SM, does not

[9] Actually this relation is renormalization scheme dependent. The usual schemes consist in taking g_2, m_W and m_Z or, alternatively, g_2, G_F and m_Z as input parameters (at the m_Z pole).

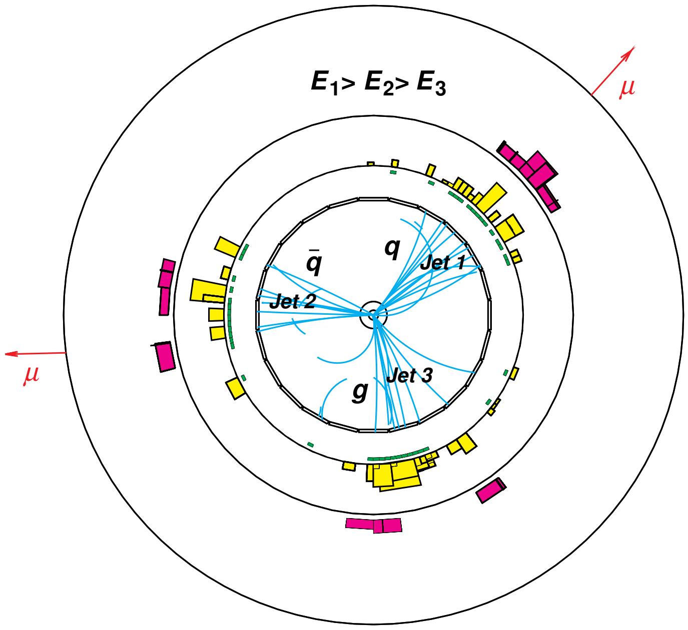

Figure 1.5: A three jet event from the OPAL experiment at LEP.

exist in real world. Hence there must be an underlying structure (above the energy scale we are able to explore today) that somehow explains the world we observe.

1.2.2 Short distance physics

The most direct evidence for existence of quarks comes from jet events in deep inelastic scattering (as well as in electron-positron annihilation, hadronic collisions and heavy quarkonia decays). The theory suggests that, if hadrons are made of quarks, the longitudinal momentum of the scattering product should be larger than its transverse part, because of the high momenum transferred in that direction. The scattering products will not be in general in a colour singlet state and will undergo the process of *hadronization*, i.e. a non singlet state will use its energy to produce pairs of quark-antiquark from the vacuum to form a colour singlet state. This process continues like in a chain reaction so that each of the original scattering products brings with itself a *jet* of particles created from the vacuum. Both a single quark or a gluon can generate a jet event.

Jet events have been observed and a snapshot is reported in figure 1.5. From the angular distribution and sphericity of jets it has been possible to measure the spin of the quarks. From 3-jet events coming from the reaction $e^+e^- \to q\bar{q}g$ (like the one in figure) it has been possible to measure directly the coupling between the gluon and quarks, g_3. From the cross section of 4-jet events, and its

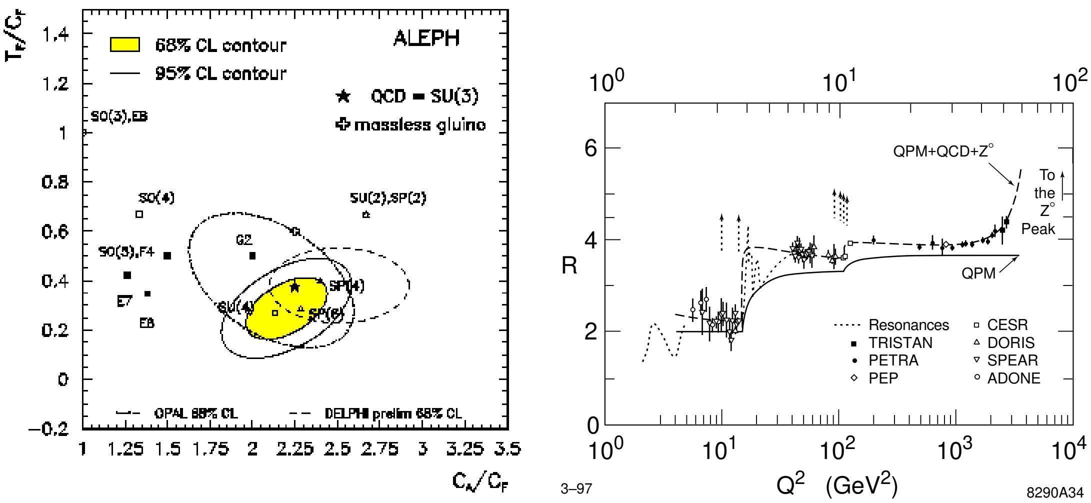

Figure 1.6: Experimental results for the Casimir invariants of QCD (left) and for the ratio R (right).

comparison with perturbative calculations, the Casimir operators[10] for the QCD gauge group have been measured. This has made it possible to check that $SU(3)$ is the appropriate gauge group to describe QCD. Combined results are reported in figure 1.6(left).

One direct measurement of the number of colors, N_C comes form the experimental ratio [27]

$$R \equiv \frac{\sigma^{\exp}(e^+e^- \to \text{hadrons})}{\sigma^{\text{th}}_{\text{QED}}(e^+e^- \to \mu^+\mu^-)} = N_{\text{c}} \sum_f Q_f^2 \left[1 + \text{pert.corr.}\right] \tag{1.58}$$

where Q_f is the electric charge of the quark of flavor f and perturbative corrections are known up to three loops. Some experimental results for R as function of the center of mass energy are reported in figure 1.6(right). The dashed line is the prediction of the SM with $N_{\text{c}} = 3$. It fits the data remarkably well.

1.2.3 Long distance physics and hadronic matter

At energies below Λ_{QCD}, i.e. at a length scale bigger than $\Lambda_{\text{QCD}}^{-1} \simeq 1\text{fm}$ the world appears to be completely different from the naive picture of quarks and gluons interacting. The predictions of the SM for low energy physics is a world made

[10]Casimir operators are the gauge invariant operators that commute with the generators of the gauge group. They are C_F, C_A and T_F. Their definitions are reported in Appendix A.

of colourless bound states of quarks, called hadrons. This phenomenon is called *confinement* [25].

At tree level there are two basic ways of constructing colourless bound states of quarks

$$\mathcal{M}_{f,f'} = q_f^i \bar{q}_{f'}^i \tag{1.59}$$

$$\mathcal{B}_{f,f',f''} = q_f^i q_{f'}^j q_{f''}^k \varepsilon_{ijk} \tag{1.60}$$

Since the quarks have spin $\frac{1}{2}$ the former must be bosons (spin 0 or 1) and the latter must be fermions (spin $\frac{1}{2}$ and $\frac{3}{2}$). Their properties depend essentially on their internal structure and mainly on the flavour of their constituent quarks (f, f', f''). In nature particles with the same quantum numbers as $\mathcal{M}$ and $\mathcal{B}$ are observed and they are called *mesons* and *baryons* respectively. Many of their properties can be deduced from this naive quark constituent model. A list of all the known mesons and baryons (excluding their higher excitations) is reported in Appendix C. In particular the proton p and the neutron n, of which we have daily experience, are spin $\frac{1}{2}$ bound states of u and d quarks with 1 and 0 electric charge respectively.

The quantum numbers (I, I_3), the isospin (not to be confused with the weak-isospin T_3), are defined to be $(\frac{1}{2}, +\frac{1}{2})$ for the u quark, $(\frac{1}{2}, -\frac{1}{2})$ for the d quark, $(0, 0)$ for all the other particles (antiparticles have the opposite I_3). Originally the isospin was introduced to discriminate between the proton and the neutron but it is useful to build the representations of all the particles made of u and d quarks.

For example, a meson with isospin (I, I_3) is[11]

$$|I, I_3\rangle = C^{I,\frac{1}{2},\frac{1}{2}}_{I_3,+\frac{1}{2},+\frac{1}{2}} \left|u\bar{d}\right\rangle + C^{I,\frac{1}{2},\frac{1}{2}}_{I_3,+\frac{1}{2},-\frac{1}{2}} \left|u\bar{u}\right\rangle + \tag{1.61}$$

$$C^{I,\frac{1}{2},\frac{1}{2}}_{I_3,-\frac{1}{2},+\frac{1}{2}} \left|d\bar{d}\right\rangle + C^{I,\frac{1}{2},\frac{1}{2}}_{I_3,-\frac{1}{2},-\frac{1}{2}} \left|d\bar{u}\right\rangle \tag{1.62}$$

Hence the lightest scalar mesons correspond to (i.e. have the same quantum numbers as)

$$\begin{array}{llll} & & |\pi^+\rangle & \sim |1,+1\rangle \\ |\eta\rangle & \sim |0,0\rangle & |\pi^0\rangle & \sim |1,0\rangle \\ & & |\pi^-\rangle & \sim |1,-1\rangle \end{array} \tag{1.63}$$

To build a representation for vector mesons it is necessary to compose the spin of the constituent quarks in a similar way to that shown for isospin.

[11] The coefficients are the well known Clebsch-Gordan coefficients.

Analogously a baryon with isospin (I, I_3) is[12]

$$
\begin{aligned}
|I, I_3\rangle \;=\; & D^I_{I_3,\frac{1}{2},\frac{1}{2},\frac{1}{2}} |uuu\rangle + D^I_{I_3,\frac{1}{2},\frac{1}{2},-\frac{1}{2}} |uud\rangle + && (1.66)\\
& D^I_{I_3,\frac{1}{2},-\frac{1}{2},\frac{1}{2}} |udu\rangle + D^I_{I_3,-\frac{1}{2},\frac{1}{2},\frac{1}{2}} |duu\rangle + && (1.67)\\
& D^I_{I_3,-\frac{1}{2},-\frac{1}{2},\frac{1}{2}} |ddu\rangle + D^I_{I_3,-\frac{1}{2},\frac{1}{2},-\frac{1}{2}} |dud\rangle + && (1.68)\\
& D^I_{I_3,\frac{1}{2},-\frac{1}{2},-\frac{1}{2}} |udd\rangle + D^I_{I_3,-\frac{1}{2},-\frac{1}{2},-\frac{1}{2}} |ddd\rangle && (1.69)
\end{aligned}
$$

Hence one can identify the following equivalences

$$
\begin{array}{lll}
|p\rangle & \sim & \left|\frac{1}{2}, +\frac{1}{2}\right\rangle \\
|n\rangle & \sim & \left|\frac{1}{2}, -\frac{1}{2}\right\rangle
\end{array}
\qquad
\begin{array}{lll}
|\Delta^{++}\rangle & \sim & \left|\frac{3}{2}, +\frac{3}{2}\right\rangle \\
|\Delta^{+}\rangle & \sim & \left|\frac{3}{2}, +\frac{1}{2}\right\rangle \\
|\Delta^{0}\rangle & \sim & \left|\frac{3}{2}, -\frac{1}{2}\right\rangle \\
|\Delta^{-}\rangle & \sim & \left|\frac{3}{2}, -\frac{3}{2}\right\rangle
\end{array}
\tag{1.70}
$$

It is trivial to observe that for these baryons $Q = I_3 + 1/2$.

Since the u and d quarks are almost degenerate in mass, so are the multiplets in the isospin that have been built (for $I = 0, 1/2, 1$ and $3/2$).

Adopting this technique, building the exact representation for any hadronic particle becomes straightforward.

1.2.4 B Physics

One pattern can be easily identified from the tables of Appendix C: there are groups of particles with almost the same mass. While for light hadrons these multiplets are explained by the fact that the mass is dominated by the binding energy of the constituents, for some of the heavy hadrons the multiplets are due to the fact that the mass is dominated by the most massive of the constituent quarks.

As an example, the quartet of heavy mesons $B^+, B^-, B^0, \bar{B}^0$ can be considered. They are almost degenerate in mass, and this mass is very big; in fact they all contain one single heavy quark b or antiquark $\bar{b}$. Using additive properties of the electric charge and the definitions of the six basic quarks (u, d, c, s, t, b) it can be

[12] The D coefficients are defined as

$$
\begin{aligned}
D^I_{I_3,m_1,m_2,m_3} \;\equiv\; & C^{I,\frac{1}{2},0}_{I_3,m_1,0} C^{0,\frac{1}{2},\frac{1}{2}}_{0,m_2,m3} + C^{I,\frac{1}{2},1}_{I_3,m_1,1} C^{1,\frac{1}{2},\frac{1}{2}}_{1,m_2,m3} + && (1.64)\\
& C^{I,\frac{1}{2},1}_{I_3,m_1,0} C^{1,\frac{1}{2},\frac{1}{2}}_{0,m_2,m3} + C^{I,\frac{1}{2},1}_{I_3,m_1,-1} C^{1,\frac{1}{2},\frac{1}{2}}_{-1,m_2,m3} && (1.65)
\end{aligned}
$$

shown that

$$\begin{array}{llll} |B^+\rangle & \sim |u\bar{b}\rangle & |B^0\rangle & \sim \left|d\bar{b}\right\rangle \\ |B^-\rangle & \sim |b\bar{u}\rangle & |\bar{B}^+\rangle & \sim \left|b\bar{d}\right\rangle \end{array} \tag{1.71}$$

The SM predicts that the decay times of each of the B's is dominated by the decay time of the b quark; therefore they must be more or less the same. The experimental results are

$$\tau(B^+) = \tau(B^-) = (1.65 \pm 0.04)10^{-12}s \tag{1.72}$$
$$\tau(B^0) = \tau(\bar{B}^0) = (1.56 \pm 0.04)10^{-12}s \tag{1.73}$$

This again is a striking prediction of the SM. But there is more: since the theoretical decay time for a free b quark can be computed from the SM, the comparison with the experimental lifetimes of the B mesons can be used to extract information from the meson decay. The theoretical decay time at tree level is given by[13]

$$\tau(B) = \mathrm{Br}_{B\to e\bar{\nu}_e X} \left(\frac{G_F^2 m_b^5}{192\pi^3} |V_{cb}|^2 \right)^{-1} \tag{1.74}$$

The comparison between (1.74) and (1.72) or (1.73) gives a rough estimation of the CKM matrix element $V_{cb} \simeq 0.04$.

In the table of baryons there is another heavy particle with almost the same mass as the B's, Λ_b, which contains the same quark, b. It is a baryon therefore it must contain two light quarks; they are a u and a d quark, in fact Λ_b is a singlet of isospin. Its decay time is

$$\tau(\Lambda_b) = (1.24 \pm 0.08)10^{-12}s \tag{1.75}$$

which is 20% less than expected from the naive picture that has been presented. One of the main goals of this thesis is to quantify this discrepancy in the framework of quantum field theory.

B mesons can be considered the hydrogen atom of QCD. In fact, as the hydrogen atom is characterised by a huge mass of the nucleus, B mesons are characterised by the mass of the b quark, which is much bigger than the mass of the so called *valence quark*. In some sense, that will be formalised in the next chapter, the b quark may be considered static thus simplifying the study of the structure of the meson. In this static approximation it has been possible to compute the wave function of the light quark in a heavy meson and the effective coupling $g_{B^*B\pi}$, which will be introduced in the next chapter.

[13] $\mathrm{Br}_{B\to e\bar{\nu}_e X}$ is the branching ratio for a B decaying into lepton and neutrino plus anything. This quantity is predicted by the SM to be 0.17 [8], while the experimental result is 0.10(2) [122].

1.2.5 Mixing with and without CP violation

The physics of K mesons and B mesons (we will concentrate on the latter as an example) is complicated by the fact that different neutral states are relevant to the analysis of different processes. For example $|B^0\rangle$ and $|\bar{B}^0\rangle$ have a definite quark content and are useful to understand scattering and decay processes, but they are not eigenstates of the Hamiltonian, hence they mix under temporal evolution. Moreover eigenstates of the Hamiltonian are not, in general, CP eigenstates.

To study a $B^0 - \bar{B}^0$ system it is convenient to introduce the mass eigenstates

$$|B_L\rangle \propto \left|B^0\right\rangle + \delta_M |\bar{B}^0\rangle \tag{1.76}$$
$$|B_H\rangle \propto \left|B^0\right\rangle - \delta_M |\bar{B}^0\rangle \tag{1.77}$$

(of mass respectively m_L and m_H) and the physical states

$$|B^0_{\text{phys}}(t)\rangle = e^{-iHt}|B^0\rangle \tag{1.78}$$
$$|\bar{B}^0_{\text{phys}}(t)\rangle = e^{-iHt}|\bar{B}^0\rangle \tag{1.79}$$

Eqs. (1.76)-(1.77) implicitly define δ_M. With some algebra one can show that CP violation in mixing can be observed through asymmetries in semileptonic decays

$$\frac{\Gamma(\bar{B}^0_{\text{phys}} \to l^+\nu X) - \Gamma(B^0_{\text{phys}} \to l^-\nu X)}{\Gamma(\bar{B}^0_{\text{phys}} \to l^+\nu X) + \Gamma(B^0_{\text{phys}} \to l^-\nu X)} = \frac{1 - |\delta_M|^4}{1 + |\delta_M|^4} \tag{1.80}$$

Therefore the parameter δ_M plays a very fundamental role. The key parameters in a theoretical study of a $B^0 - \bar{B}^0$ system are the off-diagonal elements of the Hamiltonian

$$\langle \bar{B}^0|H|B^0\rangle = M_{12} + i\Gamma_{12} \tag{1.81}$$

where M_{12} and Γ_{12} are the dispersive and absorptive parts respectively and δ_M can be expressed as function of these parameters

$$\delta_M = -\frac{M^*_{12}}{|M_{12}|}\left[1 + \text{Im}\frac{\Gamma_{12}}{M_{12}}\right] \tag{1.82}$$

The SM accounts for the quantities M_{12} and Γ_{12} by the box diagrams with intermediate top quarks

$$M_{12} = f_M\, f_B^2 m_B B_B \tag{1.83}$$
$$\Gamma_{12} = f_\Gamma\, f_B^2 m_B B_B \tag{1.84}$$

where f_M and f_Γ are kinematical factors that can be computed in perturbation

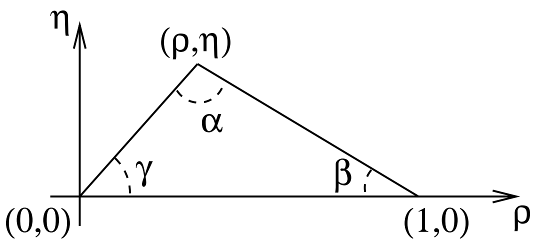

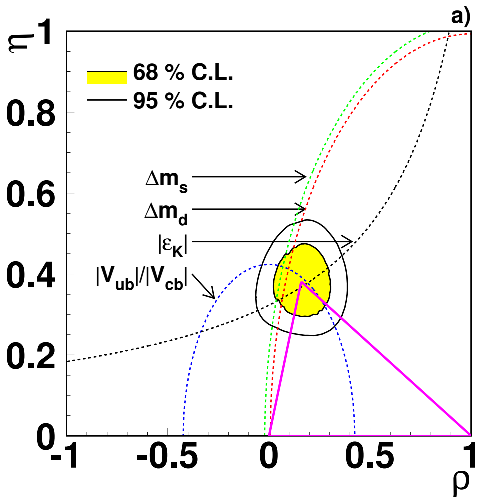

Figure 1.7: The unitarity triangle (left) and its present best constraints (right) [21].

theory and only depend on the quark masses and CKM matrix elements [28]. On the other hand

$$B_B \equiv \frac{\langle\ \bar{B}^0|\bar{b}\gamma^\mu Lq\bar{q}\gamma_\mu Lb|B^0\ \rangle}{\frac{8}{3}f_B^2 m_B^2} \tag{1.85}$$

$$f_B^2 \equiv \frac{\langle\ 0|q\gamma^5 b|B^0\ \rangle}{m_B} \tag{1.86}$$

encode nonperturbative effects due to strong interactions. f_B and B_B will be computed explicitly in chapter 5. It is important to stress that without CP violations $|\delta_M| = 1$ and the eigenstates of H would also be CP eigenstates.

The phenomenon of $K^0 - \bar{K}^0$ mixing is similar to $B^0 - \bar{B}^0$ mixing but, in the analysis of the former, the corresponding box diagrams contain s quarks in external lines (instead of a b quark). The boxes with internal u and c quarks became important and one encounters three QCD coefficients instead of one.

1.2.6 The unitarity triangle and new physics

Using unitarity the CKM matrix can be parametrized, according to Wolfenstein, in terms of four parameters [29] A, ρ, η and λ

$$V_{CKM} = \begin{pmatrix} 1-\frac{\lambda^2}{2} & \lambda & A\lambda^3(\rho - i\eta) \\ -\lambda & 1-\frac{\lambda^2}{2} & A\lambda^2 \\ A\lambda^3(1-\rho-i\eta) & -A\lambda^2 & 1 \end{pmatrix} + O(\lambda^4) \tag{1.87}$$

A, ρ and η are of order unity, and λ is the sine of the so called Cabibbo angle.

The unitarity of V_{CKM} implies that

$$V_{ub}V_{ub}^* + V_{cb}V_{cb}^* + V_{tb}V_{tb}^* = 0 \tag{1.88}$$

This can be visualized in the so called *unitarity triangle*, sketched in figure 1.7, together with the current experimental bounds.

It is extremely important to measure CKM matrix elements separately. In fact a non-unitary CKM matrix would mean a non conserved charge in the SM. Therefore the model would be non-renormalizable and one would be forced to introduce new fundamental degrees of freedom, i.e. new fundamental particles.

The presence of the complex phase η in this matrix means complex couplings in the Lagrangian, eq. (1.33), which are not invariant under time reversal. Due to the CPT theorem these interactions are not invariant under CP. This phenomenon has been observed in $K^0 - \bar{K}^0$.

Today the best determination of the CKM matrix elements, assuming three generations of quarks and imposing unitarity, are reported in Appendix C.

1.2.7 PCAC phase transition

In the same way as confinement involves the local colour symmetry, PCAC (*Partially Conserved Axial Current* [7]) involves the global chiral flavour symmetry $SU(N_f)_{L-R}$ associated to the current

$$J_\mu^{5a} \equiv \bar{q}\gamma_\mu\gamma^5 t^a q \tag{1.89}$$

This symmetry is manifestly broken by the presence of a non-vanishing quark mass matrix. On the other hand the masses of u, d and s quarks are small and one would expect this symmetry to be approximately valid at energy scales above m_s. In particular one would expect a partner of opposite chirality for the proton. But it does not seem to exist.

What happens is that the vacuum spontaneously breaks this symmetry. As a consequence of it, the Goldstone theorem states that there must be a multiplet of $N_f^2 - 1$ massless pseudoscalar bosons [30]. Actually, they will not be exactly massless, because the u, d and s quarks are not massless, but their masses will be of the order of $m_u \sim m_d$ and m_s [31].

Such a multiplet has been found in nature: it corresponds to the octet of the light pseudoscalar mesons π, K and η of figure 1.1. As consequence of the Goldstone theorem the masses of these particle verify with good approximation

$$4m_K^2 - 3m_\eta = m_\pi^2 \propto m_u + m_d \tag{1.90}$$

which is known as Gell-Mann-Okubo formula. This confirms once again the power of the SM predictions.

1.2.8 Axial anomaly

The divergence of the axial current

$$A_\mu = \bar{q}\gamma_\mu\gamma^5 q \tag{1.91}$$

should naively be proportional to the mass of the quarks. Therefore it should be almost conserved for the light u and d quarks. This does not happen because of an anomaly [7]. The anomalous Ward identity for a massless quark is

$$\partial^\mu A_\mu \propto \epsilon_{\mu\nu\rho\sigma} F^{\mu\nu} F^{\rho\sigma} \tag{1.92}$$

This equation predicts an effective coupling from the axial current to the photons. A coupling which is not in the bare Lagrangian but which is generated by the Feynman path integration. The prediction of this effective coupling is the decay of a π^0, the pseudoscalar Goldstone boson of QCD, into two photons. This phenomenon has been puzzling physicists for a long time and the SM has been able to explain it.

1.2.9 Cosmological implications

Two more quantum numbers are listed in table (1.1), they are the *baryonic number*, N_B, and the *leptonic number*, N_L. They are associated respectively to the Baryonic and Leptonic currents

$$J_\mu^B \equiv N_c^{-1} \bar{\mathcal{Q}}\gamma_\mu \mathcal{Q} \tag{1.93}$$
$$J_\mu^L \equiv \bar{\mathcal{L}}\gamma_\mu \mathcal{L} \tag{1.94}$$

It can be proved that these currents are anomalous, hence they are not separately conserved. This is an important ingredient to explain the apparent asymmetry between baryons and leptons in the Universe. On the other side $J_\mu^B - J_\mu^L$ is conserved, which means that if the global number of baryonic matter is decreased by one than the total number of antileptons is increased by one. These properties, together with the fact that SM slightly breaks CP invariance[14] gives rise to an asymmetry of particles over antiparticles if the system is out of equilibrium. This is, at the moment, the best possible explanation for the observed matter dominance in the Universe.

1.2.10 Beyond the Standard Model

There are a number of questions which are not addressed by the SM. For example it does not take into account the recent discovery of neutrino masses (and the consequent neutrino oscillations) and it becomes non-renormalizable when embedded in a curved space-time (such as the real one where the energy-momentum tensor is coupled to the gravitational tensor). But most importantly the SM does not explain why its fundamental parameters are what they are: Why is the gauge group $SU(3)_C \times SU(2)_{\mathrm{L}} \times U(1)_{\mathrm{Y}}$? Why is the strong CP phase so small that it is undetected? Why do the particles have the masses they have? Why is space-time four dimensional?

To these, many other questions could be added, originated mainly from cosmological observations. It seems reasonable to think that SM is only an effective theory (as are many other theories that have been introduced to describe particular kinematical regions) and that there is an underlying structure in our Universe. Maybe new particle accelerators will be able to explore higher energy scales and will be able to find new symmetries, such as supersymmetries; maybe they will discover that all the known particles are different excitations of the same fundamental object (a string?); perhaps they will give evidence of extra dimensions, to which we are blind today because they are compactified down to a small scale; they may even discover that we live on a four dimensional domain wall between different phases in a more-than-four dimensional manifold.

Unfortunately at the moment there is no evidence of any of the former. It is important to observe that any of the possible ways forward most likely will come from the discovery of a new particle or from the discovery of a non unitary interaction. For example a non unitary CKM matrix. This makes a good point for the quest of a better understanding of QCD in the non-perturbative regime. At the moment lattice simulations provide the only available tool to determine systematically the non-perturbative effects in particle physics, without any model-dependent assumption. The quantitative estimation of these effects is crucial to extract informations from experimental results.

[14] It means that some particle reactions have not the same rate for the corresponding antiparticle, because of the presence of imaginary terms in the CKM matrix.

Chapter 2

Effective Theories

2.1 Regularization and Renormalization

The concepts of regularization and renormalization play a fundamental role in particle physics for two reasons:

- One never measures the value of the particle fields in every point in space-time but one measures their integrals over the test function of the physical detectors, which have a finite extension. Therefore there are mathematical reasons to require that the fields are defined in the space of distributions.

- One wants to model the unknown short distance physics by introducing a Lagrangian density which contains only local (contact) interactions.

If one tries to combine the previous statements in a Quantum Field Theory, one encounters the problem of divergences and must find a way of dealing with them. The mathematical origin of these divergences is the presence of undefined formal products of distributions in the Lagrangian from which the path integral is computed. Renormalization can in fact be described in mathematical terms as the problem of defining these products of distributions[1].

In the next subsections we will analyze, as an explanatory example, the problem of defining the product of δ functions by regularizing them by a sequence of smooth functions that become more localised at zero. We will then show how an arbitrary quantum field can be expanded and regularized using delta functions and how the presence of a finite spatial cut-off in the regularized distributions is equivalent to a finite cut-off in the momentum expansion of the field itself. In the end we will relate our conclusions to ordinary Quantum Mechanics and Quantum Field Theories (in the Kadanoff-Wilson approach to renormalization). This is not intended to be an introduction to Renormalization, which the reader is supposed to be familiar with, but it is presented as an alternative view of its meaning having in mind the lattice as typical regulator.

[1] For general reviews on the subject see [32, 33]

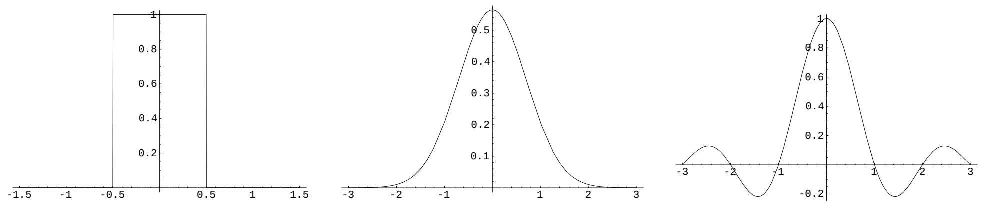

Figure 2.1: Examples of possible regularizations for a delta function. The x axis is in units of a, the y axis is in units of a^{-1}.

2.1.1 Regularizing distributions

The δ function is a distribution which is defined as

$$\int \delta(x-\overline{x})F(x)\mathrm{d}x = F(\overline{x}) \tag{2.1}$$

where $F(x)$ can be any smooth function. The same δ function can be thought of as the limit of an ordinary function $\delta(a,x)$

$$\delta(x) = \lim_{a\to 0}\delta(a,x) \tag{2.2}$$

where $\delta(a,x)$ must be smooth enough, localized in x within a precision a and its integral must be normalized to one. This procedure will be called *regularization*. Some possible regularization schemes are[2]

$$\delta(a,x) = \frac{1}{a}\left[\theta(x+a/2)-\theta(x-a/2)\right] \tag{2.3}$$

$$\delta(a,x) = \left(\pi a^2\right)^{-\frac{1}{2}}\exp(-x^2/a^2) \tag{2.4}$$

$$\delta(a,x) = \frac{\sin(\pi x/a)}{\pi x} \tag{2.5}$$

They are sketched in figure 2.1. The different schemes are equivalent in the sense that they give the same result for the following limit

$$\lim_{a\to 0}\int \delta(a,x-\overline{x})F(x)\mathrm{d}x = F(\overline{x}) \tag{2.6}$$

[2]The $\theta(x)$ function is defined to be 0 for $x<0$ and 1 for $x>0$. It is discontinuous in $x=0$.

but they do not give the same limit in expressions of the form

$$\lim_{a\to 0}\int [\delta(a, x-\overline{x})]^{n+1} F(x)\mathrm{d}x = ? \tag{2.7}$$

Moreover eq. (2.7) is likely to be divergent as a^{-n}. Suppose one wants to give a well defined meaning to the limit in eq. (2.7) by removing somehow the divergence that occurs. One way of doing it is by making $F(x)$ dependent on a, according with the prescription for $\delta(a, x)$,

$$F(x) \to F_R(a, x) = Z_R^{-n}(a)F(x) \tag{2.8}$$

where $Z_R^{-1}(a) = a + O(a^2)$. In other words the divergence of the integral is absorbed in the normalization of the function $F(x)$. This procedure is called *renormalization* and it depends on which regularization has been chosen. From now on the scheme of eq. (2.3) will be considered in particular. After renormalization

$$\int [\delta(a, x-\overline{x})]^{n+1} Z_R^{-n}(a)F(x)\mathrm{d}x = \text{const.} + O(a) \tag{2.9}$$

and its limit for $a \to 0$ becomes well defined. Therefore, up to order a terms one can redefine the integral of eq. (2.7) in the following way

$$\int [\delta(x-\overline{x})]^{n+1} F(x)\mathrm{d}x \equiv \lim_{a\to 0}\int [\delta(a, x-\overline{x})]^{n+1} Z_R^{-n}(a)F(x)\mathrm{d}x \tag{2.10}$$

The situation can be even more complicated if $F(x)$ itself is defined in terms of delta functions. For example one can consider the case when $F(x) = \exp[g\delta^2(x)]$. In this case it is not sufficient to regularize δ and renormalize F to get rid of the divergence, one is forced to renormalize g as well.

It is a general statement that, if the function $F(x, g)$ depends on some constant g, one has to renormalize the constant

$$g \to g_R(a) \tag{2.11}$$

by imposing a constraint

$$\int [\delta(a, x-\overline{x})]^{n+1} Z_R^{-n}(a)F(x, g_R(a))\mathrm{d}x = \text{const.} \tag{2.12}$$

Eq. (2.12) fixes the behaviour of $g_R(a)$ as function of a. Its solution, $g_R(a)$, can have a non-trivial behaviour in a. Eq.(2.12) is a particular case of what is generally known as the *Renormalization Group Equation* (RGE) [23]. The behaviour of $g_R(a)$ versus a is called *running*. Another common way of writing the renormalization group equation is

$$\frac{\mathrm{d}}{\mathrm{d}\log a}\int [\delta(a,x-\overline{x})]^{n+1} Z_R^{-n}(a) F(x,g_R(a))\mathrm{d}x = 0 \tag{2.13}$$

or explicitly

$$\left(a\frac{\partial}{\partial a} - \beta(g_R)\frac{\partial}{\partial g_R} + n\gamma(g_R)\right)\int [\delta(a,x-\overline{x})]^{n+1} Z_R^{-n} F(x,g_R)\mathrm{d}x = 0 \tag{2.14}$$

where

$$\beta(g_R) \equiv -\left.\frac{\partial}{\partial \log a} g_R(a)\right|_{g_R} \tag{2.15}$$

$$\gamma(g_R) \equiv \left.\frac{\partial}{\partial \log a} Z_R(a)\right|_{g_R} \tag{2.16}$$

If the original constant g is dimensionless, $g_R(a)$ must also depend on some other scale, say Λ, to cancel the dimension of a. In other words g_R must be a function of $a\Lambda$, an adimensional quantity. This simple example shows how the renormalization procedure may force one to introduce a second scale Λ of which the renormalized constant is a function. This phenomenon is called *dimensional transmutation*. In typical physical problems, a is a free parameter and it can be chosen (the physics does not depend on it providing it is small enough), while Λ characterizes the typical scale of the effect one wants to describe. One measures $g_R(a\Lambda)$ at some physical scale $a = \bar{a}$. This fixes the value of Λ and, as a consequence, the value of g_R at any other scale.

2.1.2 Lattice regularization and momentum cut-off

Any given smooth function $\phi(x)$ defined in $[-L, L]$ can be approximated with $\delta(a,x)$ functions

$$\phi(x) \simeq \phi^{\mathrm{latt}}(a,x) \equiv \sum_{k=-L/a}^{L/a} \phi_k \delta(a, x-ka) \tag{2.17}$$

with $\phi_k \equiv \phi(ka)$, or expanded in momentum

$$\phi(x) = \sum_{n=0}^{\infty} b_n e^{ip_n x} \tag{2.18}$$

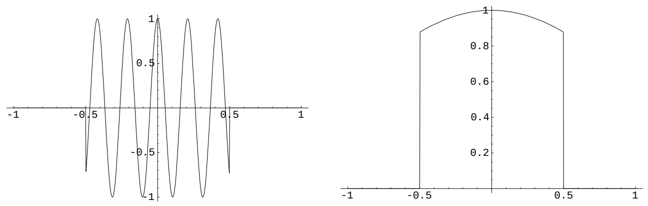

Figure 2.2: Different behaviour of the integrand of b'_n for high frequency modes (left) and low frequency modes (right) respectively.

where

$$p_n \equiv \frac{\pi n}{L}; \qquad b_n \equiv \frac{1}{2\pi}\int_{-L}^{L} \phi(x) e^{-ip_n x} dx \tag{2.19}$$

The expansion in momentum of the right hand side of eq.(2.17) can be written as

$$\phi^{\mathrm{latt}}(a,x) = \sum_{n=0}^{\infty} b'_n e^{ip_n x} \tag{2.20}$$

where

$$b'_n = \frac{1}{2\pi}\sum_{k=-L/a}^{L/a}\left[\phi_k \int_{-L}^{L} \delta(a, ka - x) e^{-ip_n x} dx\right] \tag{2.21}$$

It becomes evident that for $p_n > 1/a$ the integrand oscillates fast and the corresponding integral, b'_n, has to be small; while for $p_n < 1/a$ the integral is almost constant and approximately equal to $e^{-ip_n ka}$, therefore $b'_n \simeq b_n$. The different behaviour of the integrand is shown in figure 2.2. This proves that eq.(2.17) can be written as

$$\phi(x) \simeq \phi^{\mathrm{latt}}(a,x) \simeq \phi^{\mathrm{co}}(a,x) \equiv \sum_{n=0}^{\infty} \theta\left(\frac{1}{a} - p_n\right) b_n e^{ip_n x} \tag{2.22}$$

If $\phi(x)$ describes some physical quantity and one has a finite resolution in space, a, then $\phi(x)$ can be replaced by its Fourier expansion with a cut-off in momentum space $p_n < a^{-1}$. Therefore this technique can be regarded as a different, but in some sense equivalent, regularization scheme.

Note that b_0 is the mean value of $\phi(x)$. Moreover $p_1 = \pi/L$ represents the minimum energy/momentum mode that can propagate on a finite unidimensional volume of length $2L$.

The superscripts "latt" and "co", used to identify the two different regularizations, are abbreviations of *lattice* and *cut-off* respectively. For multi-dimensional integrals, the common regularization schemes are *Pauli-Villars* and *dimensional regularization*. The latter consists in changing the number of dimensions from 4 to $4-2\varepsilon$ and taking the limit of $\varepsilon \to 0$. Despite the fact that this is a less intuitive regularization scheme, it is the most practical for actual calculations [34, 35].

Divergences associated with limit $a \to 0$ are called ultraviolet, while those associated with limit $L \to \infty$ are called infrared divergences.

2.1.3 Applications to quantum mechanics

Suppose one studies the quantum mechanical problem of modelling a system for which the energy eigenvalues, E_n, are known and derived by an interaction potential of the form

$$V(r) = -\frac{\alpha}{r} + V^I(r) \tag{2.23}$$

but the interaction potential is not known. Therefore one wants to find a $V^I(r)$ that better predicts the data, E_n.

The standard procedure is to perform a multipole-like expansion of the potential that appear in the Schrödinger equation [36]

$$V^I(r) = c_0\delta(r) + c_1\nabla_r\delta(r) + c_2\nabla_r^2\delta(r) + ... \tag{2.24}$$

(this expansion is well defined for regularized deltas) and obtain the coefficients of the expansion by comparison between data and predictions for the energy levels, E_n. Naively one would expect to be able to reconstruct the unknown potential in this way.

This technique does not work. In fact, even at the second order in standard perturbation theory one finds a product of delta functions

$$E_n \to E_n + c_0^2 \sum_{m\neq n} \frac{\langle n|\, \delta(r)\, |m\rangle \, \langle m|\, \delta(r)\, |n\rangle}{E_n - E_m} \tag{2.25}$$

which, as it has been shown, it not uniquely defined. It is necessary to regularize the theory and renormalize the coupling constants c_0, c_1, c_2, etc.

From the physical point of view the problem arises when, in eq. (2.25), the sum runs over a complete set of states $|m\rangle$. However, since one does not have infinite resolution in experiments, one should exclude from the sum those states with energy (momentum) bigger than the inverse cut-off, a.

The fact that it is necessary to renormalize c_0 means that the parameters of the Schrödinger equation become functions of a. Nevertheless, even if the parameters of the theory depend on a, the physical quantities computed from the theory must be independent of a.

The right and well defined procedure to solve the original problem is

- Regularize the δ function
- Expand the unknown potential as

$$V_R^I(a,r) = c_{R0}(a)\delta(r) + c_{R1}(a)\nabla_r\delta(r) + c_{R2}(a)\nabla_r^2\delta(r) + ... \tag{2.26}$$

- Determine the $c_{Ri}(a)$ coefficients, up to a fixed order in perturbation theory, by comparing the predicted values for the energy level with the experimental ones.

Since the physics must be independent of a one implicitly defines a running for the $c_{Ri}(a)$. In this simple case the RGEs read

$$\frac{\mathrm{d}}{\mathrm{d}\log a}E_n(c_{R1}(a), c_{R2}(a), c_{R3}(a), ...) = 0 \tag{2.27}$$

where $E_n(c_{R1}(a), c_{R2}(a), c_{R3}(a), ...)$ are the theoretical values for the energy levels as function of the constants $c_{Ri}(a)$.

The lesson one learns is that, as in the multipole expansion, one can mimic the complex high momentum, short distance structure of the "real theory" (whatever it is) by a generic set of simple point-like interactions. The couplings are the analogues of the multipole moments, while the delta functions are analogues to the multipoles that generate the field. It is not true that, as higher order corrections are added, the potential of eq. (2.26) will eventually become identical to the true one (assuming it exists). There are infinitely many theories which share the same low energy behaviour. Generally speaking our low energy experimental data do not contain enough information to probe, and completely specify, the high energy structure of the underlying theory.

2.1.4 Applications to quantum field theory

While in quantum mechanics one computes energy levels, in quantum field theory (QFT) one computes n-point Green functions, which are integrals of the form

$$\langle 0|\, T\{\phi(x_1)...\phi(x_n)\}\,|0\rangle = \int [\mathrm{d}\phi]\phi(x_1)...\phi(x_n)e^{i\int \mathcal{L}[\phi(x),g]\mathrm{d}^4x} \tag{2.28}$$

(T stands for the time ordered product) which we rewrite in the compact notation

$$\langle 0|\, T\{\phi(x_1)...\phi(x_n)\}\, |0\rangle = \int [\mathrm{d}\phi] F^n[\phi(x), g] \tag{2.29}$$

where $\int [d\phi]$ is a sum over all the possible field configurations, and

$$F^n[\phi(x), g] = \phi(x_1)...\phi(x_n) e^{i \int \mathcal{L}[\phi(x), g] \mathrm{d}^4 x} \tag{2.30}$$

is a non-linear functional in $\phi(x)$ depending on some coupling constant(s) g. An important point here is that $F^n[\phi(x), g]$ contains terms like ϕ^2, ϕ^3, ... coming from the expansion of the action. For simplicity it will be assumed that the field has a one dimensional domain $[-L, L]$. There are two natural ways of formally defining the integral (2.29).

- Introduce a cut-off a, approximate the field as in eq.(2.17), and integrate over all the ϕ_i

$$\langle 0|\, T\{\phi(x_1)...\phi(x_n)\}\, |0\rangle^{\mathrm{latt},a} = \left(\prod_{i=-L/a}^{L/a} \int \mathrm{d}\phi_i \right) F^n[\phi^{\mathrm{latt}}(a, x), g] \tag{2.31}$$

- Introduce a momentum cut-off $p_N \simeq a^{-1}$, expand ϕ in Fourier components as in eq. (2.18) and integrate over the coefficients of the expansion

$$\langle 0|\, T\{\phi(x_1)...\phi(x_n)\}\, |0\rangle^{\mathrm{co},a} = \left(\prod_{n=0}^{N} \int \mathrm{d}b_n \right) F^n[\phi^{\mathrm{co}}(a, x), g] \tag{2.32}$$

In both cases the integral may diverge, therefore it becomes necessary to renormalize the functional $F^n[...]$ (i.e. the field ϕ itself) or the coupling constant(s) g. Usually both of them[3].

Analogously to the quantum mechanical example, the problem of ultraviolet divergences (associated to the limit $a \to 0$) arises because one would like the fields to be defined in the space of distributions and, at the same time, one is modelling unknown physics with a local Lagrangian density. Therefore any non-trivial functional of these fields would be divergent [32]. It become necessary to introduce a finite cut-off a and regularize the theory. Again one must impose the condition that physical predictions are independent of the regularization scheme and from the cut-off, a. Therefore one needs one RGE for each parameter of the

[3] In case of a multidimensional domain for the fields, one generally prefers to use dimensional regularization because it preserves Poincaré invariace and gauge invariance of the theory.

theory[4].

For example in a theory where

$$\mathcal{L}[\phi] = \frac{1}{2}(\partial_\mu\phi)^2 - \frac{1}{2}m^2\phi^2(x) - g\phi^3(x) \tag{2.33}$$

one uses the 2-point Green function to renormalize the coupling m, i.e. the mass, and the 3-point Green function to renormalize the coupling g. In other words one imposes a constraint on the values of mass and coupling constant which are predicted by the theory, by equating them to the experimental results. From these RGEs one obtains the running for the mass m and the coupling constant(s) g.

Usually one distinguishes between the "bare" parameters that appear in the regularized Lagrangian (for a finite value of the cut-off, a) and the "dressed", "physical" or "renormalized" parameters that are defined and measured by actual experiments. If one takes the limit $a \to 0$, the bare parameters lose any physical meaning and one must carefully define the renormalized ones (one says to choose a prescription). If one is happy of keeping the cut-off small but finite one is allowed to identify the renormalized and the bare parameters, because these can now be measured. This is the approach one uses on the lattice and it corresponds to the Kadanoff-Wilson approach to renormalization.

One can write a RGE both for the bare parameters (as function of the cut-off) or, equivalently, for the renormalized ones (as function of the renormalization scale, i.e. the scale at which one performs the measurements). The two equations are formally identical at first order in pertubation theory[5]. This is not surprising because one can always define the renormalized coupling at a scale $\bar{a}$ to be equivalent to the bare coupling with a cut-off $a = \bar{a}$.

The general form for the RGEs of the n-point Green functions, eq. (2.31) is

$$\left(a\frac{\partial}{\partial a} - \beta(g_R)\frac{\partial}{\partial g_R} + n\gamma(g_R)\right)\langle 0|\,\phi(x_1)...\phi(x_n)\,|0\rangle^{\text{latt},a} \equiv 0 \tag{2.34}$$

where

$$\beta(g_R) \equiv -\left.\frac{\partial}{\partial \log a} g_R(a)\right|_{g_R} \tag{2.35}$$

$$\gamma(g_R) \equiv \left.\frac{1}{2}\frac{\partial}{\partial \log a} Z_R(a)\right|_{g_R} \tag{2.36}$$

[4]In analogy with the RGE eq. (2.14).

[5]Only at second order in perturbation theory the RGE for the renormalized parameters shows a dependence from their exact definition, the renormalization prescription.

and $Z_R(a)$ is defined as the wave function renormalization factor

$$\phi_R(x) = Z_R^{-1/2}\phi_{\text{bare}}(x) \tag{2.37}$$

For non-abelian gauge theories in four dimensions without symmetry breaking (such as QCD), at one loop, $g_R(a)$ turns out to satisfy the equation[6]

$$\beta(g_R) \equiv -a\frac{\partial g_R(a)}{\partial a} = -\beta_0^{\text{QCD}}\frac{g_R^3(a)}{(4\pi)^2} + O(g_R^5) \tag{2.38}$$

where

$$\beta_0^{\text{QCD}} = \frac{11 - 2N_f}{3} \tag{2.39}$$

Its solution can be written in the form

$$\alpha_s(a) \equiv \frac{g_R^2}{4\pi} = \frac{2\pi}{\beta_0^{\text{QCD}}\log(a\Lambda_{\text{QCD}})} \tag{2.40}$$

and therefore g_R decreases (increases) when a decreases (increases). This phenomenon was already presented in the last chapter and is called *asymptotic freedom* [24]. The scale Λ_{QCD} is due to dimensional transmutation and can be thought of as the typical energy scale of QCD. The presence of this physical scale breaks the scale invariance of the theory. For QCD this is related to the presence of the so called *trace anomaly*.

For an abelian gauge theory (such as QED) $g_R(a)$ obeys the equation

$$\beta(g_R) \equiv -a\frac{\partial g_R(a)}{\partial a} = \beta_0^{\text{QED}}\frac{g_R^3(a)}{(4\pi)^2} + O(g_R^5) \tag{2.41}$$

where $\beta_0^{\text{QED}} = 4N_f/3$. Note that the right hand side of eq.(2.41) has an opposite sign than the right hand side of eq.(2.38). In fact the renormalized coupling constant of QED decreases (increases) when a increases (decreases), quite the opposite of QCD.

It has been seen how, in QFT, one is forced to introduce two different energy scales:

- Λ: the typical scale of the effect being studied. This scale is in nature and there is no freedom to fix it. For QCD it is $\Lambda_{\text{QCD}} \simeq 250\text{MeV}$.
- $\mu = a^{-1}$: the scale that corresponds to the precision of the mathematical description, the cut-off in the Kadanoff-Wilson approach to Renormalization Group. The theory is said to be renormalizable if this scale can be

[6] RGE are commonly written in terms of $\mu = a^{-1}$ and not of a.

arbitrarily large. This does not mean that one can trust the predictions of the theory with arbitrary precision.

It is usually possible to model the same phenomenon using different QFTs, which differ in the regularization-renormalization prescription and/or the renormalization scale. The predictions of these different theories must be compatible with each other apart from order $O(a)$ corrections.

Some QFTs have a finite number of coupling constants and it is possible to give a well defined meaning to the limit $a \to 0$ because all the possible divergencies can be absorbed in the renormalized constants. These QFTs are said to be renormalizable. Other QFTs are not renormalizable because it is not possible to absorb all the divergencies in a finite set of constants. The possible Green functions, at different orders in perturbation theory, exhibit an infinite variety of divergent behaviour. Originally it was believed that only renormalizable QFT made sense[7]. The modern picture is different: if the world is described by a continuous QFT, it must be a renormalizable one. But the world could have a minimum length scale and the renormalization requirement is no longer a fundamental one. Perhaps the most important modern interpretation of these results is that, if one wants to formulate a QFT to describe physics down to a finite resolution, say a, and one does not pretend it to be the theory of everything, it does not have to be renormalizable (because one does not pretend to send the scale a to zero) [37]. These particular kind of theories are called *effective theories*[8].

In the real world, there might be new supersymmetric interactions or superstring, or electrons and muons may have internal stucture, none of which is incorporated in the SM. Nevertheless the SM has been formulated and still explains the results of our experiments with a typical accuracy of 10%. Renormalization saved us by saying that one does not need to know what happens at very high momenta in order to understand low momentum experiments.

Wilson showed that any information about physics above the renormalization scale is contained in the coefficients of the effective theory.

The procedure to relate the renormalized parameters/operators between two different theories, or different regularization schemes, is called matching[9].

For renormalizable effective theories this procedure is stated in the Appelquist-Carazzone theorem [38]. It states that, under some given conditions, the effects of high energy modes ($p_n > a^{-1}$) only appear in the low energy mode physics ($p_n < a^{-1}$) through corrections which are proportional to a, or through renormalization.

It has been shown by Symanzik [39] that it is possible to improve the convergence of an effective theory to its continuum limit ($a \to 0$) from $O(a)$ to $O(a^{n+1})$.

[7] This requirement led Weinberg, Glashow and Salam to formulate the Standard Model.

[8] E.g. the Fermi theory of electroweak interactions is not renormalizable but it is able to describe with good accuracy weak interactions at energy scales below m_W

[9] An explicit example will be give in the next chapter.

In order to achieve this, it is necessary to add to the effective Lagrangian terms which are proportional to $a, a^2, ..., a^n$ and adjust the corresponding coefficients. This *improvement* technique is heavily used in lattice simulations where the minimum length scale, the lattice spacing a, cannot be reduced arbitrarily, therefore one desires the dependence on a of the Green functions to be as small as possible. In the next sections some effective theories will be introduced, which will be used in the later study of heavy mesons and baryons.

2.1.5 Operator Product Expansion

Another way to view the conclusions of the previous section is to say that one can study an interaction that is fundamentally a product of currents by replacing this product of operators by a sum of local operators. As an example of interest we consider here the following expansion of a product of two operators

$$\mathcal{O}_A(x)\mathcal{O}_B(0) \simeq \sum_n C_n(x)\mathcal{O}_n(0) \tag{2.42}$$

where the coefficients $C_n(x)$ are unknown c-number functions and the operators $\mathcal{O}_n$, organized by their dimension, are constructed from the basic field considering they must have the same transformation properties as the left-hand side.

The expansion (2.42) implies a relation between Green functions

$$\langle 0| T\{\mathcal{O}_A(x)\mathcal{O}_B(0)...\} |0\rangle^{\mathrm{latt},a} \simeq \sum_n C_n(x,a) \langle 0| T\{\mathcal{O}_n(0)...\} |0\rangle^{\mathrm{latt},a} \tag{2.43}$$

where the dots represent any arbitrary product of fields. One can write the RGE for the Green functions that appear on the left-hand side and those that appear on the right-hand side of eq. (2.43). Their difference uniquely determine a RGE for the $C_n(x,a)$ coefficients

$$\left(a\frac{\partial}{\partial a} - \beta\frac{\partial}{\partial g} - (\gamma_A + \gamma_B - \gamma_n) \right) C_n(x,a) = 0 \tag{2.44}$$

where γ_A, γ_B and γ_n are the anomalous dimensions of $\mathcal{O}_A$,$\mathcal{O}_B$ and $\mathcal{O}_n$ respectively. The one loop solution of eq. (2.44) is

$$C_n(x,a) = \frac{\mathrm{const.}}{|x|^{d_A+d_B-d_n}} \left(\frac{\alpha_s(x)}{\alpha_s(a)}\right)^{(\hat\gamma_A+\hat\gamma_B-\hat\gamma_n)/2\beta_0} \tag{2.45}$$

where $\hat\gamma_A$, $\hat\gamma_B$ and $\hat\gamma_n$ are the numerical coefficients of the 1-loop anomalous dimensions of $\mathcal{O}_A$,$\mathcal{O}_B$ and $\mathcal{O}_n$ respectively, and d_A, d_B and d_n are the dimensions of the corresponding operators.

The expansion (2.42) is called Operator Product Expansion and it is a particularly useful tool in QCD to disentangle the perturbative physics, encoded in the coefficients $C_n(x)$, from the non perturbative physics, encoded in the expectation values of the local operators O_n. The former are computed in perturbation theory, while the latter can be measured or evaluated using lattice, Sum Rules or model dependent assumptions.

2.2 Examples of interest

2.2.1 Heisenberg-Euler Effective Theory and quenching

As a first example one can try to formulate an effective theory for QED. In particular one may be interested in modelling QED at energy scales below the electron mass, m_e. In this kinematic region the electron (and other fermions) cannot be produced directly but, instead, influences the physics of photons only through virtual processes. In other words one may be interested in formulating an effective Lagrangian $\mathcal{L}_{eff}$ which generates the same Green functions for photons as

$$\mathcal{L}_{QED} = -\frac{1}{4}F_{\mu\nu}F^{\mu\nu} + \bar{\psi}(i\not{D} - m_e)\psi \tag{2.46}$$

does. More formally one can write

$$\int [\mathrm{d}A_\mu] e^{i\int \mathrm{d}^4x \mathcal{L}_{eff}} \propto \int [\mathrm{d}A_\mu][\mathrm{d}\psi][\mathrm{d}\bar{\psi}] e^{i\int \mathrm{d}^4x \mathcal{L}_{QED}} \tag{2.47}$$

The path integral in the fermionic modes can be done, as was shown in eq.(2.32), thus obtaining an implict form for the, so called, Heisenberg-Euler effective Lagrangian [40]

$$\int \mathrm{d}^4x \mathcal{L}_{E-H} = -\frac{1}{4}\int \mathrm{d}^4x F_{\mu\nu}F^{\mu\nu} - i\mathrm{tr}\ln\left[\frac{i\not{D} - m_e}{i\not{\partial} - m_e}\right] \tag{2.48}$$

This procedure is called *integrating out modes.* The right hand side can be expanded in powers of $1/m_e$

$$\mathcal{L}_{E-H} = -\frac{1}{4}F_{\mu\nu}F^{\mu\nu} + \frac{e^2}{240\pi^2 m_e^2}F_{\mu\nu}\Box F^{\mu\nu} + O(\frac{1}{m_e^4}) + O(e^4) \tag{2.49}$$

Note how the first term gives a contribution to the photon propagator which is equivalent to the one-loop correction of QED. Corrections to this effective Lagrangian can be of two forms:

- At any finite order in α, one has to add terms of any order in $1/m_e^2$

- The coefficients of terms of any order in $1/m_e^2$ receive corrections of arbitrarily high order in α, because of multi-loop diagrams.

The theory described by the effective Lagrangian (2.49) is not renormalizable because it would be necessary to include terms of arbitrary order in $1/m_e^2$ to cancel its perturbative divergences.

This is an example of what has been discussed in the section 2.1.2. The fact that loop effects are proportional to the inverse mass square of the particle in the loop tells us that loops of massive particles can be neglected. This is why, for example, one can neglect effects of particles more massive than the electron, when computing quantum corrections to atomic spectra.

The approximation of neglecting corrections of the order $1/m_e^2$ is called *quenching* and is a peculiar characteristic of many lattice simulations of QCD.

2.2.2 Fermi Electroweak Theory

Exactly as was done for QED, one can integrate out modes of heavy particles in the theory of weak interactions. In this case the most massive modes are associated with $W^{\pm}$ and Z^0 bosons. Ignoring the latter one can write

$$\int [\mathrm{d}\psi][\mathrm{d}\bar{\psi}]e^{i\int \mathrm{d}^4x\mathcal{L}_{eff}} \propto \int [\mathrm{d}W_\mu][\mathrm{d}\psi][\mathrm{d}\bar{\psi}]e^{i\int \mathrm{d}^4x\mathcal{L}_{\mathrm{Weak}}} \tag{2.50}$$

thus obtaining for the interactive part of the Lagrangian

$$\mathcal{L}_{eff}^{\mathrm{int}} = \mathcal{L}_{\mathrm{Fermi}} + O(\frac{1}{m_W^4}) \tag{2.51}$$

where $\mathcal{L}_{Fermi}$ is the Fermi interaction Lagrangian [26] of eq. (1.56). m_W is much bigger than the typical hadronic scale, Λ_{QCD}, therefore one can consider $\mathcal{L}_{\mathrm{Fermi}}$ a good approximation of $\mathcal{L}_{\mathrm{weak}}$ when studying non-perturbative QCD corrections to hadronic matrix elements.

In practice, if one wants to compute perturbative corrections to Green functions and keep the renormalization scale μ below m_W, one is allowed to perform the following approximation when computing Feynman diagrams involving W propagators

$$\frac{g_2^2}{8}\int J^{+\mu}(p)\frac{1}{p^2-m_W^2}J_\mu^-(p)\mathrm{d}^4p \simeq -\frac{g_2^2}{8m_W^2}\int J^{+\mu}(p)J_\mu^-(p)\mathrm{d}^4p \tag{2.52}$$

where J^μ are charged weak currents. This is because of the cut-off in momentum space induced by the renormalization procedure.

2.2.3 Heavy Quark Effective Theory

In the preceding example only modes that did not appear in the external asymptotic states were integrated out. In practice loops of heavy particles in Feynman diagrams have been absorbed in corrections to the Lagrangian. One may be interested in a different problem, that is integrating out modes of a particle that does appear in the external states, for example a heavy quark (which will be indicated with the symbol h). In the external states the heavy quark cannot be a free particle (because of confinement) but it must be in an hadronic bound state. Therefore it is not an on-shell particle and the off-shell component of its momentum is due to the exchange of gluons within the hadron. One can describe the behaviour of this heavy quark with an effective theory in which modes with energy above $\Lambda \ll m_b$ have been integrated out and only appear in the parameters of the theory. Moreover one requires $\Lambda_{\rm QCD} \ll \Lambda$. In such a theory the off-shell component of a heavy quark, bounded in an hadronic state, is only due to the exchange of soft gluons and it is of the order of Λ.

In this framework, the momentum of the heavy quark can be written as

$$p_\mu = p_\mu^{\text{on-shell}} + k_\mu \tag{2.53}$$

where k_μ is the off-shell part of it and $k^2 \sim \Lambda^2$. On the other hand the hadron, of which the heavy quark is a constituent, must be on-shell and one can measure its momentum and hence its velocity, v_μ. The on-shell components of the heavy quark momentum can be expressed in terms of the velocity of the hadron,

$$p_\mu^{\text{on-shell}} \equiv m_h v_\mu \Rightarrow \left|p_\mu^{\text{on-shell}}\right|^2 = m_h^2 \tag{2.54}$$

This statement is not rigorous because there are ambiguities in the definition of the mass of the quarks, since they cannot be observed as free particles. However it can be proven that the following reasoning can be made consistent whichever definition is taken.

Since in the effective theory that is considered a natural momentum cut-off, Λ is present the free propagator of the heavy quark can be expanded in $1/m_h$

$$\frac{1}{\not{p} - m_h} = \left(\frac{1+\not{v}}{2}\right)\frac{1}{k_\mu v^\mu} + O(\frac{\Lambda}{m_h}) \tag{2.55}$$

The same propagrator can be obtained by the effective Lagrangian

$$\mathcal{L}_{\rm HQET} = \bar{h}\left(\frac{1+\not{v}}{2}\right)(D_\mu v^\mu)h + O(\frac{\Lambda}{m_h}) \tag{2.56}$$

The expansion (2.55) can be carried out to obtain those terms of higher order both in $1/m_h$ and in α_s, in the same fashion as what was done to construct the

Heisenberg-Euler Lagrangian. The effective Lagrangian (2.56) is called *Heavy Quark Effective Theory*[10] (HQET).

Note the presence of the projector $(1+\not{v})/2$ in the tree level HQET. In this low energy description loops of heavy quarks have been integrated out, therefore a second quantization description of these particles becomes redundant. The projector in the effective Lagrangian means that anti-particles, at tree level, do not couple to the effective degrees of freedom. An analogous description for anti-particles would have been possible, and the effective Lagrangian would have had a projector on anti-particles instead, $(1-\not{v})/2$.

One prediction of the theory is that, at tree-level and for a static hadron (i.e. $v_\mu = (1, \mathbf{0})$), the heavy quark only couples to the temporal component of the gauge field. In other words the interaction between spin and colour magnetic field is of higher order in $1/m_h$. Correspondingly, a symmetry emerges between those states which differ only by the spin orientation of the heavy quark[11]. The pseudo-scalar and vector mesons, B and B^* (both are ground states of zero orbital angular momentum), present an example of such a spin degeneracy. In fact, up to corrections of the order $1/m_h = 1/m_b$, they are degenerate in mass (as was observed in the preceeding chapter) and the wave functions of their light constituent quarks coincide. This statement is crucial in determining their wave function. This will be done in chapter 4.

Another important conclusion comes from the fact that, at tree-level, the HQET Lagrangian (2.56) does not depend on m_h. Therefore if there is more than one heavy quark, the theory must be symmetric with respect to the interchange between them. This phenomenon is called *heavy quark symmetry.* It predicts that the wave function of a heavy meson is independent of the flavour and spin of the heavy quark, leading to a covariant representation of heavy mesonic states [41]. The angular momentum J and the parity P of the light degrees of freedom determine a degenerate doublet of states with spin-parity J^P.

An example of this are the families of B and D mesons. The former is characterised by a heavy b quark and the latter by a c quark with $\Lambda_{\mathrm{QCD}} < m_c < m_b$. The heavy quark symmetry is manifest in the spectrum, in fact it predicts

$$m_{B^*}^2 - m_B^2 \simeq m_{D^*}^2 - m_D^2 \tag{2.57}$$

Experimentally $m_{B^*}^2 - m_B^2 = 0.49\mathrm{GeV}^2$, $m_{D^*}^2 - m_D^2 = 0.55\mathrm{GeV}^2$ while the correction to the prediction of the heavy quark symmetry are of order $0.1\mathrm{GeV}^2$. Therefore it works as well as one should expect. Moreover the heavy quark sym-

[10] For reference see [41, 42]

[11] If, instead of a heavy quark, one considers a heavy nucleus in an atom, this is saying that all the spin of the atom is carried by the nucleus and it is not affected by electro-magnetic interaction at the typical energy scale of chemical reactions. This statement is crucial in techniques of magnetic resonance, where one uses huge magnetic fields to interact with the magnetic moment of the nucleus (which is proportional to the spin) without any screening effect by the electrons.

metry is mainly a symmetry between the dynamical parameters that characterise hadrons containing heavy quarks of different flavour, in fact they have the same wave function and the same QCD corrections to their spectrum[12]. A practical effect of heavy quark symmetry is that

$$\langle D|\,\bar{c}\gamma^0 b\,|B\rangle = \sqrt{2m_B}\sqrt{2m_D}\;\xi(\omega = v_D\cdot v_B) \tag{2.58}$$

where $\xi(\omega)$ is called *Isgur-Wise function.* $\xi(0) = 1$, because of the heavy quark symmetry combined with the conservation of the vectorial current $V^\mu = \bar{b}\gamma^\mu b$

2.2.4 Goldstone Theorem and Chiral Lagrangian

The Goldstone theorem, when applied to the axial current, states that, if one computes the Green function

$$G^a_\mu(q^2) = \int \mathrm{d}^3x\,\langle 0|\,J^{5a}_\mu(x)\Phi(0)\,|0\rangle\, e^{-iqx} \tag{2.59}$$

where Φ is any operator that creates any field configuration which has a non-vanishing expectation value that breaks the symmetry associated with the charged axial current J^{5a}_μ, one finds that

$$\lim_{q\to 0} q^\mu G^a_\mu(q^2) \neq 0 \tag{2.60}$$

and the Green function $G^a_\mu(q^2)$ must have a pole at $q^2 = 0$. In other words there must be massless particles associated to this pole, the Goldstone bosons.

It has been seen in chapter 1 that J^{5a}_μ is spontaneously broken; this is because the chiral condensate $\bar{q}q$ acquires a vacuum expectation value. The corresponding Goldstone bosons are the pseudo-scalar mesons that can be built with the lightest of the quarks: u, d and s. They are the eight particles

$$\pi^\pm \quad \pi^0 \quad K^\pm \quad K^0 \quad \bar{K}^0 \quad \eta$$

Since m_u, m_d and m_s are not exactly zero, these particles are called pseudo-Goldstone bosons and their masses squared are expected to be of the order of the masses of the constituent quarks.

It is convenient to arrange these particle in a 3×3 multiplet according with their transformation properties under $SU(N_f)_L \times SU(N_f)_R$

$$\mathcal{M} = \begin{pmatrix} \pi^0/\sqrt{2}+\eta/\sqrt{6} & \pi^+ & K^+ \\ \pi^- & -\pi^0/\sqrt{2}+\eta/\sqrt{6} & K^0 \\ K^- & \bar{K}^0 & -\sqrt{2/3}\eta \end{pmatrix} \tag{2.61}$$

[12] In the same way as different isotopes of the same atom have different masses but have the same electronic wave functions, the same energy levels and, therefore, the same chemical properties.

In this language a $SU(N_f)_R$ transformation corresponds to $\mathcal{M} \to U\mathcal{M}$ while a $SU(N_f)_L$ transformation corresponds to $\mathcal{M} \to \mathcal{M}U^\dagger$ (in both cases $U \in SU(N_f)$). The most general effective Lagrangian for this multiplet (2.61) has the form

$$\mathcal{L}_\chi = \frac{1}{4} F_\pi^2 \mathrm{tr}\left\{\partial_\mu \xi \partial^\mu \xi^\dagger + 2M(\xi + \xi^\dagger)\right\} + O(p^2) \tag{2.62}$$

where $\xi = \exp(i\mathcal{M}/F_\pi)$, while F_π and Λ_0 are phenomenological parameters. Eq.(2.62) constitutes one more example of an effective Lagrangian. It is called *Chiral Lagrangian* [43]. It has a phenomenological origin and its range of validity is below the energy scale given by the lightest resonance in the particle spectrum, $m_\rho \simeq 770\mathrm{MeV}$. Higher order correction to this Lagrangian can appear in off-diagonal matrix elements in M, in terms involving more than two derivatives and in the renormalization of the constants. Assuming degenerate light quark masses, i.e. $m_u = m_d = \hat{m}$, a comparison with tree-level predictions of the SM suggests that

$$F_\pi \simeq f_\pi \equiv \frac{1}{m_\pi^2} \langle 0| \partial^\mu A_\mu \left|\pi^0(p)\right\rangle \tag{2.63}$$

$$M \simeq \Lambda_0 \begin{pmatrix} \hat{m} & 0 & 0 \\ 0 & \hat{m} & 0 \\ 0 & 0 & m_s \end{pmatrix} \tag{2.64}$$

$$\Lambda_0 \simeq -\frac{1}{f_\pi} \langle 0| \bar{q}q |0\rangle \tag{2.65}$$

(the masses of the u and d quarks are assumed to be same). Using eq. (2.64) in eq. (2.62) one obtains

$$m_\pi^2 = 2\hat{m}\Lambda_0 \tag{2.66}$$

$$m_K^2 = (\hat{m} + m_s)\Lambda_0 \tag{2.67}$$

$$m_\eta^2 = \frac{2}{3}(\hat{m} + 2m_s)\Lambda_0 \tag{2.68}$$

which prove the Gell-Mann-Okubo formula of eq. (1.90).

All the parameters of the Chiral Lagrangian can be calculated from first principles (i.e. from QCD) by performing lattice simulations. In particular f_π will be computed explicitly in chapter 4.

A combination of heavy quark symmetry and chiral symmetry has been used in recent years to develop the *Heavy Meson Chiral Lagrangian* (HMχ), describing the interactions of low-momentum pions with mesons containing a single heavy quark[13] [44].

[13] for reviews see [45, 46].

The pseudoscalar and vector mesons, B and B^*, are described by a 4×4 Dirac matrix H with two spinor indices, one for the heavy quark and one for the light degrees of freedom. In terms of the effective meson fields

$$H = \frac{1+\not{v}}{2}\left[B^*_\mu \gamma^\mu - B\gamma_5\right]; \qquad \bar{H} = \gamma^0 H^\dagger \gamma^0 \tag{2.69}$$

where v is the velocity of the meson and B and B^* are the annihilation operators for particles containing a b quark in the initial state. These meson fields are used in the effective Lagrangian to describe the heavy mesons. The light mesons are treated as an octet of pseudo-Goldstone bosons according to the usual Chiral Lagrangian formalism. At low-momentum the strong interactions of B and B^* mesons with light pseudoscalars are described by the couplings in the effective Lagrangian; the lowest order interaction is given by [44, 46]:

$$\mathcal{L}^{\rm int}_{\rm HM\chi} = g\,{\rm tr}(\bar{H}_a H_b \mathcal{A}^{ba}_\mu \gamma^\mu \gamma^5) \tag{2.70}$$

where

$$\mathcal{A}_\mu = \frac{i}{2}(\xi^\dagger \partial^\mu \xi - \xi \partial^\mu \xi^\dagger) \tag{2.71}$$

The Roman indices a and b denote light quark flavour and, as usual, repeated indices are summed over $1, 2, 3$. The expansion of $\mathcal{A}$ in terms of pion fields begins with a linear term,

$$\mathcal{A}_\mu = -\frac{1}{F_\pi}\partial_\mu \mathcal{M} + ... \tag{2.72}$$

The coupling g in eq. (2.70) can easily be related to the $B^*B\pi$ coupling defined as [105, 75]

$$\langle B^0(p)\pi^+(q)|B^{*+}(p')\rangle = -g_{B^*B\pi}(q^2) q_\mu \eta^\mu(p')\,(2\pi)^4\,\delta(p'-p-q) \tag{2.73}$$

where η^μ is the polarization vector of the B^* and the physical states are relativistically normalised

$$\langle B(p)|B(p')\rangle = 2p^0(2\pi)^3\delta^{(3)}(\mathbf{p}-\mathbf{p}') \tag{2.74}$$

The physical coupling $g_{B^*B\pi}$ is given by the value of the above form factor for an on-shell pion

$$g_{B^*B\pi} = \lim_{q^2 \to m_\pi^2} g_{B^*B\pi}(q^2) \tag{2.75}$$

At tree level in the heavy meson chiral lagrangian, the above matrix element is

$$\langle B^0(p)\pi^+(q)|B^{*+}(p')\rangle = -\frac{2m_B}{f_\pi}\, g\, q_\mu \eta^\mu(p')(2\pi)^4\delta^{(4)}(p'-p-q) \tag{2.76}$$

which therefore yields:

$$g_{B^*B\pi} = \frac{2m_B}{f_\pi} g \tag{2.77}$$

As a result, g and $g_{B^*B\pi}$ can be considered as equivalent. The above relation can be extended to take into account higher-order terms in the HMχ lagrangian [47, 48, 50]. The effective coupling g will be computed explicitly in chapter 4.

2.3 Lattice QCD

At the typical hadronic scale, while electroweak effects can computed in the standard perturbative way, QCD effects are non-perturbative. Therefore it becomes necessary to formulate QCD in such a way to make it possible to perform a numerical computation of the Green functions.

This is done by choosing the lattice regularization scheme and re-writing the action of QCD in terms of some effective degrees of freedom, as will be briefly explained[14].

2.3.1 Basic degrees of freedom and action

The Aharonov-Bohm experiment revealed that the gauge field $A_\mu = t^a A^a_\mu$ is not observable, because it is gauge dependent, but the phase of a particle in a gauge field background, moving from x to y, is an observable

$$\mathcal{P}e^{ig\int_x^y A_\mu \mathrm{d}x^\mu} \tag{2.78}$$

($\mathcal{P}$ indicates a path-ordered exponential). For a finite lattice spacing a, it becomes convenient to write the action of QCD in terms of the quark fields (which are associated to the lattice sites) and of the phases associated to the shortest paths on the lattice

$$U_\mu(x) \equiv e^{ig\int_x^{x+a\mu} A_\mu \mathrm{d}x^\mu} \simeq 1 + igaA_\mu(x + a\widehat{\mu}/2) \tag{2.79}$$

$$U_{-\mu}(x) \equiv e^{ig\int_x^{x-a\mu} A_\mu \mathrm{d}x^\mu} = U^\dagger_\mu(x - a\widehat{\mu}) \simeq 1 - igaA_\mu(x - a\widehat{\mu}/2) \tag{2.80}$$

[14] For reviews see [51, 19, 53, 54]. This introduction will not cover the technical aspects of implementing lattice simulation on a computer. For a basic review on the subject and some C++ code one can refer to the free package **mdpqcd** described in ref. [98].

(which are associated to the links between two consecutive lattice sites). In QCD U are 3×3 complex matrices, called links.

The basic discretized operators which appear in the Lagrangian, are:

- Ordinary derivative[15]:

$$\partial_\mu \psi(x) \equiv \frac{1}{2a}\left[\psi(x + a\widehat{\mu}) - \psi(x - a\widehat{\mu})\right] \tag{2.81}$$

- Covariant derivative:

$$D_\mu \psi(x) \equiv \frac{1}{2a}\left[U_\mu(x)\psi(x + a\widehat{\mu}) - U_{-\mu}(x)\psi(x - a\widehat{\mu})\right] \tag{2.82}$$

  It is trivial to check that in the continuum limit it is equivalent to the usual covariant derivative of QCD. In fact, up to order a corrections,

$$\begin{aligned} D_\mu \psi(x) =& \frac{1}{2a}\big[(1 + igaA_\mu(x) + ...)(1 + a\partial_\mu + ...)\psi(x) - \\ & \quad (1 - igaA_\mu(x) + ...)(1 - a\partial_\mu + ...)\psi(x)\big] \\ =& (\partial_\mu + igA_\mu(x) + ...)\psi(x) \end{aligned} \tag{2.83}$$

- Field-strengh tensor:

$$\begin{aligned} G_{\mu\nu}(x) = \frac{1}{8a^2}\big[& P_{\mu\nu}(x) + P_{\mu\nu}(x - a\widehat{\mu}) + P_{\mu\nu}(x - a\widehat{\nu}) + \\ & P_{\mu\nu}(x - a\widehat{\mu} - a\widehat{\nu})\big] - (\mu \leftrightarrow \nu) \end{aligned} \tag{2.84}$$

  where $P_{\mu\nu}$ is called plaquette and is defined as

$$P_{\mu\nu}(x) \equiv U_\mu(x)U_\nu(x + a\widehat{\mu})U_{-\mu}(x + a\widehat{\mu} + a\widehat{\nu})U_{-\nu}(x + a\widehat{\nu}) \tag{2.85}$$

  It can be proved that, expanding in a, one obtains

$$P_{\mu\nu}(x) = 1 + ia^2 g t^a G^a_{\mu\nu}(x) - \frac{a^4 g^2}{4} G^a_{\mu\nu}(x) G^{a\mu\nu}(x) + ... \tag{2.86}$$

  which substitued into eq. (2.84) justifies the definition.

For practical purposes, that will be examined below, one is usually interested in the Euclidean formulation of Lattice QCD. This is achieved by performing the

[15]We remark that a different choice could be made as long as in the limit $a \to 0$ one recovers the ordinary derivative.

Wick rotation[16]

$$x_0 \to ix_0; \qquad x_i \to x_i \tag{2.87}$$

Under this rotation the exponential term in the action becomes real

$$e^{i\mathcal{S}} = e^{ia^4 \sum_x \mathcal{L}} \to e^{-\mathcal{S}_E} = e^{-a^4 \sum_x \mathcal{L}_E} \tag{2.88}$$

From now on all the quoted quantities (including γ matrices) will be Euclidean. In terms of the links, any Green function of QCD can be written as

$$\langle 0| \mathcal{O}(...) |0\rangle^{\text{latt}} = \int [\mathrm{d}U][\mathrm{d}\psi][\mathrm{d}\bar{\psi}]\mathcal{O}(...)e^{-\mathcal{S}_E[U,\psi,\bar{\psi}]} \tag{2.89}$$

where [55]

$$\mathcal{S}_E^{\text{gauge}} = \beta \sum_{x,\mu,\nu} \left[1 - \frac{1}{3}\text{Re tr}P_{\mu\nu}(x)\right] = a^4 \sum_x \frac{1}{4}\text{tr}G^a_{\mu\nu}(x)G^{a\mu\nu}(x) + O(a^2) \tag{2.90}$$

$$\mathcal{S}_E^{\text{quark}} = a^4 \sum_x \bar{\psi}(x)(\gamma^\mu D_\mu + m)\psi(x) + O(a) \tag{2.91}$$

The variable $\beta = 6/g^2(a)$ has been introduced to conform to the standard notation of Lattice QCD. In the gauge part of the action there are no order a corrections and the first corrections arise at the order a^2. On the other side, in the quark part of the Lagrangian, order a corrections play, in general, a very important role for the following two reasons:

- If one neglects order a corrections and naively uses the lattice covariant derivative to implement $\mathcal{S}_E^{\text{quark}}$, one obtains a free quark propagator of the form

  $$S(p) = \frac{a}{i\gamma^\mu \sin(p_\mu a) + am} \tag{2.92}$$

  which has 16 zeros in the Brillouin zone in the limit $m \to 0$, to be confronted with the single zero of the continuum propagator

  $$S(p) = \frac{1}{i\gamma^\mu p_\mu + m} \tag{2.93}$$

  This problem is known as doubling. To get rid of this proliferation of zero

[16] The way how different quantities transform under the Wick rotation is reported in table (B.14)

modes Wilson proposed to add to the action a term of order a of the form

$$-a^5 \frac{r}{2} \sum_{x,\mu} \bar{\psi}(x) \frac{1}{a^2} \left[U_\mu(x)\psi(x+a\widehat{\mu}) - 2\psi(x) + U_{-\mu}(x)\psi(x-a\widehat{\mu})\right] \tag{2.94}$$

(this is not the only possible solution to the problem but it is the one of interest in this thesis). In practical simulations r is fixed to be 1, nevertheless it is convenient to show its dependence. Note that eq. (2.94) is a mass term therefore it explicitly breaks chiral symmery.

- When computing Green functions one is always interested in the limit $a \to 0$ and one would like to improve the convergence of Green functions from order a to order a^2. This can be done by adding to the Action terms of order a that compensate for the discretization errors up to the same order [57]. In particular one can choose a term of the form

$$-a^5 \frac{c_{SW}}{4} \sum_{x,\mu>\nu} \bar{\psi}(x)\gamma^\mu\gamma^\nu G_{\mu\nu}(x)\psi(x) \tag{2.95}$$

where the constant c_{SW} must be fixed somehow. This term is usually referred to as *clover term*.

Including these $O(a)$ corrections the quark part of the action can be re-written as

$$\mathcal{S}_E^{\text{quark}}[U,\psi,\bar{\psi}] = \frac{a^3}{2\kappa} \sum_y \bar{\psi}(x) Q_{xy}[U]\psi(y) \tag{2.96}$$

where

$$\begin{aligned} Q_{xy}[U] = \delta_{xy} - \kappa \sum_\mu &\left[(r-\gamma^\mu)U_\mu(x)\delta_{x,y-\mu} + (r+\gamma^\mu)U_{-\mu}(x)\delta_{x,y+\mu}\right] \\ &- \frac{\kappa c_{SW}}{2} \sum_{\mu>\nu} \gamma^\mu\gamma^\nu G_{\mu\nu}(x)\delta_{xy} \end{aligned} \tag{2.97}$$

and, at tree-level[17]

$$\beta = \frac{6}{g^2(a)}; \qquad \kappa = \frac{1}{2ma+8r}; \qquad c_{SW} = 1 \tag{2.99}$$

The action (2.96-2.97) is referred to as *Shiikoleslami-Wolhert action* (SW) [56].

The coefficient $a^3/2\kappa$ can be absorbed in the definition of the fermionic fields, ψ and $\bar{\psi}$.

Note that the lattice spacing a is not an input parameter but, because of dimensional transmutation, its value uniquely depends on the value of β. From the lattice one measures the spectrum as function of β and κ in units of $1/a$ and, by comparison with the physical spectrum one extracts the value of a and the mass of the quark that corresponds to each given value of κ. c_{SW} on the other side is uniquely dependent on the scale (i.e. on β or, equivalently, on g) and it must be determined by fine tuning.

2.3.2 Simulation aspects and quenching

First of all, one can consider Green functions that do not depend on quark fields and integrate out the quarks

$$\begin{aligned}\langle 0|\,\mathcal{O}(...)\,|0\rangle^{\mathrm{latt}} &= \int [\mathrm{d}U][\mathrm{d}\psi][\mathrm{d}\bar{\psi}]\mathcal{O}(...[U])e^{-\mathcal{S}_E[U,\psi,\bar{\psi}]} \\ &= \int [\mathrm{d}U]\mathcal{O}(...[U])\det Q[U]e^{-\mathcal{S}_E^{\mathrm{gauge}}[U]} \\ &= \int [\mathrm{d}U]\mathcal{O}(...[U])P[U]\end{aligned} \tag{2.100}$$

where

$$P[U] = e^{-\mathcal{S}_E^{\mathrm{gauge}}[U]+\ln\det Q[U]} \tag{2.101}$$

In practice one neglects the contribution of $\ln\det Q[U]$ in the probability $P[U]$, eq. (2.101). This is called the *quenched approximation*. Its only motivation is the limitation in present computer power. It introduces a systematic error in the computations that has to be quantified.

[17] The fact that Lattice QCD with the action of eq. (2.97) is $O(a)$ improved for on-shell quantities does not simply appear form a Taylor expansion. To show the improvement it is necessary to list all dimension 5 operators, use the equations of motion to reduce some of them and absorb the contribution of the remaining two operators in the coupling constant and mass renormalization

$$g^2 \to g^2(1+b_g ma); \qquad m \to m(1+b_m ma) \tag{2.98}$$

State	I^G	J^{PC}	Operator J
scalar	1^-	0^{++}	$\bar{q}q'$
	1^-	0^{++}	$\bar{q}\gamma^0 q'$
pseudoscalar	1^-	0^{-+}	$\bar{q}\gamma^5 q'$
	1^-	0^{-+}	$\bar{q}\gamma^0\gamma^5 q'$
vector	1^+	1^{--}	$\bar{q}\gamma^\mu q'$
	1^+	1^{--}	$\bar{q}\gamma^\mu\gamma^0 q'$
axial	1^-	1^{++}	$\bar{q}\gamma^\mu\gamma^5 q'$
tensor	1^+	1^{+-}	$\bar{q}\gamma^\mu\gamma^j q'$
octet	$\frac{1}{2}$	$\frac{1}{2}^-$	$(q^{Ti}\gamma^2\gamma^0 q'^j)(\gamma^5 q''^k)\varepsilon_{ijk}$
	$\frac{1}{2}$	$\frac{1}{2}^-$	$(q^{Ti}\gamma^2\gamma^0\gamma^5 q'^j)(q''^k)\varepsilon_{ijk}$
decuplet	$\frac{3}{2}$	$\frac{3}{2}^+$	$(q^{Ti}\gamma^2\gamma^0\gamma^i q'^j)(q''^k)\varepsilon_{ijk}$

Table 2.1: Example of currents used on lattice and their relative quantum numbers. q, q' and q'' are different flavours. The superscripts i, j and k are color labels.

The probability $P[U]$ is real (this is why Lattice computations are performed in Euclidean space) and resembles a Boltzman weight factor. Therefore standard statistical mechanics techniques can be applied.

Any standard lattice simulation begins with the creation of an ensemble of gauge configurations $\{U^i\}$. It is created through a Markov process [53], i.e. each configuration U^i is generated from the preceding one, U^{i-1}, using a stochastic algorithm satisfying the condition

$$P(U^{i-1} \to U^i)P[U^{i-1}] = P(U^i \to U^{i-1})P[U^i] \tag{2.102}$$

where $P(U \to U')$ is the probability of generating the configurations U' from the configuration U. Such an algorithm is called a *Monte Carlo Algorithm*. Note that $P[U]$ depends on $\beta = 6/g^2(a)$ which is the parameter that fixes the lattice scale. The initial configuration U^0 can be chosen to be "cold", i.e. when all its links are the identity, or "hot", when each link is a random $SU(N)$ matrix [58, 59].

The computation of any Green function, defined in eq. (2.100), can be approximated as an average over the ensemble of gauge configurations

$$\langle 0| \mathcal{O}(...) |0\rangle^{\text{latt}} \simeq \frac{1}{N}\sum_{\{U_i\}} \mathcal{O}(...[U^i]) \tag{2.103}$$

where N is the number of generated configurations.

2.3.3 Correlation functions and fermions

The typical quantities that are measured on the lattice are the two and three-point correlation functions between currents and their Fourier transforms at zero momentum [60]

$$C_2(t_x) = \int \mathrm{d}^3\mathbf{x}\langle 0|J(0)J^\dagger(x)|0\rangle \tag{2.104}$$

$$C_{3\mathcal{O}}(t_x, t_y) = \int \mathrm{d}^3\mathbf{x}\mathrm{d}^3\mathbf{y}\langle 0|J(-y)\mathcal{O}(0)J^\dagger(x)|0\rangle \tag{2.105}$$

Since the lattice metric is Euclidean, the asymptotic behaviour of the spatial Fourier transform of the two point correlation function, in the limit $t_x \to \infty$, is given by

$$C_2(t_x) \sim Z_J^2 e^{-m_J t_x} \tag{2.106}$$

where m_J is the mass of the lightest state $|1_J\rangle$ created by the current $J^\dagger$ and

$$Z_J = |\langle 1_J|\, J^\dagger(0)\, |0\rangle| \tag{2.107}$$

From the measurement of $C_2(t_x)$ and its fit to (2.106), it is possible to extract masses of particles, m_J. In the same fashion from the asymptotic behaviour of the ratio between the three and two-point correlation functions it is possible to extract matrix elements [60]

$$\frac{C_{3\mathcal{O}}(t_x, t_y)}{C_2(t_x)C_2(t_y)} \sim \frac{1}{Z_J^2}\frac{\langle 1_J|\mathcal{O}|1_J\rangle}{2m_J} \tag{2.108}$$

The most general current $J(x)$ is expressed in terms of fundamental fermionic fields $q_\alpha^i(x)$ (the quark fields). A list of some interesting currents J is reported in table 2.1. In expressions like eq.(2.104) and (2.105) these fields are Wick contracted

$$\langle 0|\{q_\alpha^i(x), \bar{q}_\beta^j(y)\}|0\rangle = S_{\alpha\beta}^{ij}(x, y) \tag{2.109}$$

Despite the fact that fermions are neglected when gauge configurations are created, they are re-introduced at a later stage as particles propagating in the gluonic background field. Therefore the two and three point correlation functions can be written as appropriate traces of propagators, $S_{\alpha\beta}^{ij}(x, y, [U])$, in the backgroud gluonic field U. For example the propagator of a pseudoscalar meson (associated to the current $J = \bar{u}^i \gamma^5 d^i$), from x to y can be computed as

$$\begin{aligned} \langle 0| J(y) J^\dagger(x) |0\rangle &= \langle 0| \bar{u}^i(y)\gamma^5 d^i(y) \bar{d}^j(x)\gamma^5 u^j(x) |0\rangle \\ &= \langle 0| \operatorname{tr}\left\{ S_d^{ij}(y,x)\gamma^5 S_u^{ji}(x,y)\gamma^5 \right\} |0\rangle \\ &= \frac{1}{N}\sum_{\{U\}} \operatorname{tr}\left\{ S_d^{ij}(y,x,[U])\gamma^5 S_u^{ji}(x,y,[U])\gamma^5 \right\} \end{aligned} \tag{2.110}$$

On each gauge configuration U, the fermion propagator S is computed by inverting the fermionic matrix

$$S(x,y,[U]) = (Q[U])^{-1}_{xy} \tag{2.111}$$

This is the most expensive part of any lattice calculations. In the computation of the propagator κ and c_{SW} are input parameters. The former is in one to one correspondence with the fermion mass

$$m = \frac{1}{2a}\left(\frac{1}{\kappa} - \frac{1}{\kappa_{crit}}\right) \tag{2.112}$$

and κ_{crit} is a parameter depending on β. The chiral limit corresponds to the limit $\kappa \to \kappa_{crit}$, when the quark becames massless. In practice any inversion algorithm for eq.(2.111) converges slower and slower as the chiral limit is approached and this can never be reached.

There are two standard ways of computing the fermion propagator: exact and stochastic. The former is very time expensive therefore it is usual normal practice to compute propagators ending in one single point of the lattice. The latter is less precise but allows one to compute propagators from each point to each point of the lattice in a feasible time.

2.3.4 Lattice discrete symmetries

The lattice formulation of QCD is invariant under the following discrete symmetries of the quark propagator [61]

- **Parity,** P:

$$S^{ij}_{\alpha\beta}(x,y,[U]) = \gamma^0_{\alpha\alpha'} S^{ij}_{\alpha'\beta'}(x^P, y^P, [U^P])\gamma^0_{\beta'\beta} \tag{2.113}$$

- **Charge conjugation,** C:

$$S^{ij}_{\alpha\beta}(x,y,[U]) = (\gamma^0\gamma^2)_{\alpha\alpha'} S^{ji}_{\alpha'\beta'}(y,x,[U^C])(\gamma^2\gamma^0)_{\beta'\beta} \tag{2.114}$$

- **Time reversal,** T:

$$S^{ij}_{\alpha\beta}(x,y,[U]) = (\gamma^0\gamma^5)_{\alpha\alpha'} S^{ij}_{\alpha'\beta'}(x^T,y^T,[U^T])(\gamma^5\gamma^0)_{\beta'\beta} \tag{2.115}$$

- H **symmetry**:

$$S^{ij}_{\alpha\beta}(x,y,[U]) = \gamma^5_{\beta\alpha'} S^{ji}_{\alpha'\beta'}(y,x,[U])\gamma^5_{\beta'\alpha} \tag{2.116}$$

U^P, U^C, U^T are the parity reversed, charge conjugate, time reversed gauge configuration respectively.

These discrete symmetries play a very important role because they put some contraint on the Euclidean Green functions. In particular one can consider Green function of the form

$$G^{(n,m)}(\vec{p}_1,...,\vec{p}_n) = \int \mathrm{d}^4x_1 e^{ip_1x_1}...\mathrm{d}^4x_n e^{ip_nx_n} \langle 0|\, \mathrm{tr}\{S\gamma^{\mu_1}S\gamma^{\mu_2}...S\gamma^{\mu_m}\}\, |0\rangle \tag{2.117}$$

where the trace is in spin and colour, and S are quark propagators connecting an arbitrary couple of points in the ensemble $\{x_1,...,x_n\}$. Imposing invariance under P (parity), one obtains that

$$G^{(n,m)}(\vec{p}_1,...,\vec{p}_n) = (-1)^N G^{(n,m)}(-\vec{p}_1,...,-\vec{p}_n) \tag{2.118}$$

where N is the number of indices μ_1,...,μ_m that differ from 0. Eq. (2.118) is true also in the Minkowski space.

Imposing invariance under PCH one obtains that

$$G^{(n,m)}(\vec{p}_1,...,\vec{p}_n) = (-1)^N \left[G^{(n,m)}(\vec{p}_1,...,\vec{p}_n)\right]^* \tag{2.119}$$

This tells whether any Green function is real or imaginary.

Eq. (2.119) is not true in Minkowski space. In fact it is replaced by an equivalent expression where N counts the total number of indices μ_1,...,μ_m that are equal to 5.

As an example one can consider

$$G^{(3,2)}(\vec{p}) = \int \mathrm{d}^4x e^{ipx} \langle 0|\, S(x,0)\gamma^i\gamma^5 S(0,x)\gamma^j\, |0\rangle \tag{2.120}$$

Since $N = 3$, eq. (2.118) tells that it is odd under parity and eq. (2.119) tells that it is imaginary. Moreover for $p = 0$ it must be zero (because it is odd under parity).

2.3.5 Heavy quarks

Lattice simulations can be combined with HQET to simulate the behaviour of a heavy quark. In the limit where its mass is bigger than $1/a$ the heavy quark (anti-quark) can be considered static and its propagator (derived for the discretized version of the HQET Lagrangian) is

$$\begin{aligned} S^{ij}_{\alpha\beta}(x,y,[U]) = & \left(\frac{1+\gamma^0}{2}\right)_{\alpha\beta} \left[U_0^\dagger(x-a\widehat{0})...U_0^\dagger(y)\right]^{ij} \theta(t_x-t_y)\delta_{\mathbf{x},\mathbf{y}} + \\ & \left(\frac{1-\gamma^0}{2}\right)_{\alpha\beta} \left[U(x)_0...U_0(y-a\widehat{0})\right]^{ij} \theta(t_y-t_x)\delta_{\mathbf{x},\mathbf{y}} \end{aligned} \qquad (2.121)$$

It includes the contribution of both a quark (propagating forward in time) and of an anti-quark (propagating backward in time).

2.3.6 Determining c_{SW}

There are three standard techniques to fix the parameter c_{SW}

- 1-loop improvement [112]

$$c_{SW} = 1 + 1.5954/\beta \qquad (2.122)$$

- Tadpole improvement [111] (i.e. resumming the contribution of all tadpole graphs to the renormalization of the tree-level c_{SW}).

$$c_{SW} = \frac{1}{u_0^3} \qquad (2.123)$$

  where u_0 is the gauge average of $\frac{1}{3}\mathrm{Re}\,\mathrm{tr}P_{\mu\nu}$. It can be extracted from numerical simulations.

- Non-perturbative improvement [112]. This is the most sophisticated technique. The idea behind it is that of determining the improvement coefficients for the different operators (including c_{SW}) by measuring independently on lattice the left and right-hand side of Ward identities and imposing the constraint that they coincide. The table of results for c_{SW} can be summarized by the following fitting function (valid only for $\beta > 5.7$)

$$c_{SW} = \frac{\beta^3 - 3.648\beta^2 - 7.254\beta + 6.642}{\beta^3 - 5.2458\beta^2} \qquad (2.124)$$

Even if different techniques may give different results for c_{SW} they are consistent with each other providing the operators are improved adopting the corresponding procedure. Whichever improvement technique is used, the SW action generates Green functions that converge to the continuum limit up to correction of the second order in a and order 1 in α (for 1-loop) or exactly (for non-perturbative improvement).

2.3.7 Lattice errors

Numerical simulations of Lattice QCD are characterized by a number of statistical and systematical errors which will have to be taken into account when quoting lattice results. What follows is a list of the most common errors one has to consider, possibly reduce and, hopefully, quantify:

- **Statistical errors**. All Monte Carlo simulations are based on statistical sampling therefore they introduce a statistical error that is expected to decrease with $1/\sqrt{N}$ where N is the number of independent measurements (in case of one measurement for gauge configuration, N is the number of gauge configurations). Since the gauge configurations are created using a Markov chain based on small changes to link variables, one may be worried about correlations among the different configurations. Because of modern day computational power it is possible to generate reasonable statistical samples and this is no more a major problem.

- **Finite volume**. Because of the finite volume, periodic or anti-periodic boundary conditions are imposed for the field. Therefore every observable which is computed on the lattice suffers from an unphysical contribution of mirror states. In any case, these finite-volume contributions to the Green functions falls off exponentially with the lattice length and they are usually negligible for a lattice size L bigger than $5/m_\pi$. On the other side the effects of mirror states are crucial in preventing a direct determination of scattering phases from lattice [62].

- **Quenched approximation**. This approximation is the hardest to justify. Its only reason is the present limitation in computational power. As a consolation one can argue that present exploratory unquenched simulations suggest that the effects of the quark loops in the mass spectrum are small, but the error introduced by quenching in the determination of a^{-1} can be as big as 10%-20%.

- **Finite lattice spacing,** a. Physical results are extracted from lattice in the limit of $a \to 0$. This limit cannot be reached in real lattice simulation and in practice one performs simulations with a finite (as small as possible) lattice spacing. The discrepancy between the computed Green functions and their continuum limit is usually of the order of a (or a^2 for improved lattice actions). In typical simulations $1/a = 1 \div 3\text{GeV}$.

- **Chiral extrapolation**. It has been shown that because of the finite volume effects, an infrared cut-off is naturally associated with the lattice and u and d quarks are too light to be simulated, even by modern day computers. Therefore one usually performs lattice simulations for values of $m_u = m_d$ much bigger of the physical values (typically of the order of 100 MeV), then performs an extrapolation of the results to the limit $m_u = m_d = 0$. This extrapolation is called the *chiral extrapolation*. It corresponds to the limit $\kappa \to \kappa_{crit}$ For the masses of light particles (the pseudo-Goldstone boson) this extrapolation is guided by predictions of the chiral Lagrangian such as the Gell-Mann-Okubo formula, eq. (1.90)

- **Heavy quarks**. The c and b quarks are too heavy to propagate on a typical lattice, therefore there are two possible approaches. One possibility is to simulate these quarks with a mass smaller than the physical one and then to perform an extrapolation to the physical mass. This approach is similar to the chiral extrapolation for the heavy quark. The second possibility is to implement the HQET on lattice. This implies that one considers the heavy quark as static and, in principle, systematically computes corrections to this approximation in the $1/m_h$ expansion. This is the approach that will be used in the rest of the thesis when simulating heavy hadrons.

- **Matching between lattice and continuum scheme**. Experimental data are analyzed using some continuum renormalization scheme, usually dimensional regularization with the $\overline{\text{MS}}$ prescription. To confront Lattice QCD results with phenomenology it is therefore necessary to match the matrix elements between the two different schemes. In general

$$\langle 0| \mathcal{O}_i(...) |0\rangle^{\overline{\text{MS}}} = Z_{ij} \langle 0| \mathcal{O}_j(...) |0\rangle^{\text{latt}} \tag{2.125}$$
$$= (\delta_{ij} + O(\alpha_s)) \langle 0| \mathcal{O}_j(...) |0\rangle^{\text{latt}} \tag{2.126}$$

  where Z_{ij} are called matching coefficients and have a perturbative origin. The matching coefficients are computed in perturbation theory and usually they are known only at 1-loop. One explicit example of a matching computation will be given in the next chapter. Since α_s is big at the typical lattice energy scale, corrections of higher order in α_s can contribute to an error in the matching of as much as 10%. Moreover in the matching procedure it is common that matrix elements of some continuum operator mix with the corresponding matrix elements of new operators that appear on lattice, because Z_{ij} is, in general, non diagonal. The contribution of these operators can be big and must be taken into account.

Chapter 3

Perturbative Matching Coefficients

This is the most technical chapter of the thesis and it can be skipped in a first reading. In section 3.1 the matching coefficients for a general set of 2- and 4-quark operators (namely $\bar{q}\Gamma q$, $\bar{b}\Gamma q$, $\bar{b}\Gamma q\bar{q}\tilde{\Gamma}b$ and $\bar{b}\Gamma q\bar{b}\tilde{\Gamma}q$) renormalized in the continuum and in the lattice theory will be computed explicitly

$$(\bar{q}\Gamma_i q)^{\overline{\mathrm{MS}},\mu} = Z_{ij}^{\mathrm{light}}(\mu,a)(\bar{q}\Gamma_j q)^{\mathrm{latt},a} \tag{3.1}$$

$$(\bar{b}\Gamma_i q)^{\overline{\mathrm{MS}},\mu} = Z_{ij}^{\mathrm{static}}(\mu,a)(\bar{b}\Gamma_j q)^{\mathrm{latt},a} \tag{3.2}$$

$$(\bar{b}\Gamma_i^A q\bar{q}\tilde{\Gamma}_i^A b)^{\overline{\mathrm{MS}},\mu} = Z_{ij}^{\Delta B=0}(\mu,a)(\bar{b}\Gamma_j^A q\bar{q}\tilde{\Gamma}_j^A b)^{\mathrm{latt},a} \tag{3.3}$$

$$(\bar{b}\Gamma_i^A q\bar{b}\tilde{\Gamma}_i^A q)^{\overline{\mathrm{MS}},\mu} = Z_{ij}^{\Delta B=2}(\mu,a)(\bar{b}\Gamma_j^A q\bar{b}\tilde{\Gamma}_j^A q)^{\mathrm{latt},a} \tag{3.4}$$

In the continuum, dimensional regularization with modified minimal subtraction, $\overline{\mathrm{MS}}$ is used. The superscripts "$\overline{\mathrm{MS}}$" and "latt" refer to the renormalization scheme and μ, a^{-1}, μ' to the renormalization energy scales. The index A represents both color and spin indices that are contracted between the two matrices Γ and $\tilde{\Gamma}$. b will be considered a static quark, as prescribed by the HQET, while q will be considered massless. Infrared divergences will be cured by giving an infinitesimal mass to the gluon, λ. (Any dependence on λ cancels in the final results.)

At 1-loop the matching coefficients Z_{ij} will be written as

$$Z_{ij}(\mu,a) = \delta_{ij} + \frac{\alpha_s}{4\pi}\left(-\gamma_{ij}\log\mu^2a^2 + d_{ij}^{\overline{\mathrm{MS}}} - d_{ij}^{\mathrm{latt}}\right) \tag{3.5}$$

where the coefficients γ_{ij}, $d_{ij}^{\overline{\mathrm{MS}}}$ and d_{ij}^{lett} will be computed for each of the different operators in the corresponding subsection, see eqs. (3.39)-(3.41), eqs. (3.51)-(3.53) and tables 3.2, 3.4.

In section 3.2 the matching coefficients for the same set of operators renor-

Γ_i	$\omega_{1,i}$	$\omega_{2,i}$	$\omega_{3,i}$
I	4	-2	1
γ^5	-4	2	-1
γ^0	-2	2	1
γ^i	-2	2	-1
$\gamma^0\gamma^5$	2	-2	-1
$\gamma^i\gamma^5$	2	-2	1
$\sigma^{\mu\nu}$	1	2	-1

$\Gamma_i^A \otimes \tilde{\Gamma}_i^A$	$\Omega_{1,i}$	$\Omega_{2,i}$	$\Omega_{3,i}$	$\Omega_{4,i}$
$L \otimes L$	4	$3/2$	-4	$-3/2$
$L \otimes R$	4	$3/2$	-4	$-3/2$
$R \otimes L$	4	$3/2$	-4	$-3/2$
$R \otimes R$	4	$3/2$	-4	$-3/2$
$\gamma^\mu L \otimes \gamma_\mu L$	$-1/2$	0	-5	0
$\gamma^\mu L \otimes \gamma_\mu R$	5	0	$1/2$	0
$\gamma^\mu R \otimes \gamma_\mu L$	5	0	$1/2$	0
$\gamma^\mu R \otimes \gamma_\mu R$	$-1/2$	0	-5	0

Table 3.1: Choice of basis of spin matrices, Γ_i (left) and $\Gamma_i \otimes \tilde{\Gamma}_i$ (right).

malized at different scales, but in the same scheme, will be computed

$$(\bar{q}\Gamma_i q)^{\overline{\text{MS}},\mu} = z_{ij}^{\text{light}}(\mu,\mu')(\bar{q}\Gamma_j q)^{\overline{\text{MS}},\mu'} \tag{3.6}$$

$$(\bar{b}\Gamma_i q)^{\overline{\text{MS}},\mu} = z_{ij}^{\text{static}}(\mu,\mu')(\bar{b}\Gamma_j q)^{\overline{\text{MS}},\mu'} \tag{3.7}$$

$$(\bar{b}\Gamma_i^A q\bar{q}\tilde{\Gamma}_i^A b)^{\overline{\text{MS}},\mu} = z_{ij}^{\Delta B=0}(\mu,\mu')(\bar{b}\Gamma_j^A q\bar{q}\tilde{\Gamma}_j^A b)^{\overline{\text{MS}},\mu'} \tag{3.8}$$

$$(\bar{b}\Gamma_i^A q\bar{b}\tilde{\Gamma}_i^A q)^{\overline{\text{MS}},\mu} = z_{ij}^{\Delta B=2}(\mu,\mu')(\bar{b}\Gamma_j^A q\bar{b}\tilde{\Gamma}_j^A q)^{\overline{\text{MS}},\mu'} \tag{3.9}$$

The coefficients z_{ij}, in the leading log approximation, will be expressed as

$$z_{ij}(\mu,\mu') = \delta_{ij} + \frac{\gamma_{ij}}{N_c^2}\left[\left(\frac{\alpha(\mu')}{\alpha(\mu)}\right)^{\frac{N_c^2}{2\beta_0}} - 1\right] \tag{3.10}$$

i.e. as function of the perturbative coefficient γ_{ij} that were computed before. β_0 is β_0^{QCD} defined in eq. (2.39) and N_c is the number of colours, i.e. 3 for QCD.

In section 3.3 some examples will be given in detail to clarify the usage of our results for some parameters of practical interest in this thesis.

For $\bar{q}\Gamma_i q$ and $\bar{b}\Gamma_i q$ type operators the basis of table 3.1(left) has been chosen, while for $\bar{b}\Gamma_i^A q\bar{q}\tilde{\Gamma}_i^A b$ and $\bar{b}\Gamma_i^A q\bar{b}\tilde{\Gamma}_i^A q$ the basis of table 3.1(right) is used. The constants $\omega_{1,i}$, $\omega_{2,i}$ and $\omega_{3,i}$ that appear in table 3.1 are defined in the dimensional regularization scheme in $D = 4 - 2\varepsilon$ dimensions from the implicit relations

$$\gamma^\mu\Gamma_i\gamma_\mu = (\omega_{1,i} + \omega_{2,i}\varepsilon)\Gamma_i \tag{3.11}$$

$$\gamma^0\Gamma_i\gamma_0 = \omega_{3,i}\Gamma_i \tag{3.12}$$

The origin of the constants $\Omega_{1,i}$, $\Omega_{2,i}$, $\Omega_{3,i}$ and $\Omega_{4,i}$ will be explained later, together with the problem of evanescent operators. To keep the results as general as possible all the results will be expressed as function of the ω's and the Ω's.

3.1 Continuum $\overline{\mathrm{MS}}$ vs Lattice renormalization

The idea behind the matching is that physical results must be independent of the renormalization scheme that is used in the computation. At a perturbative level one writes this statement in mathematical language as

$$\mathcal{O}_i^{\overline{\mathrm{MS}}} = \left[\delta_{ij} + \frac{\alpha_s^{\overline{\mathrm{MS}}}(\mu)}{4\pi}(\gamma_{ij}\log\lambda^2\mu^{-2} + d_{ij}^{\overline{\mathrm{MS}}}) + O(\alpha^2)\right]\mathcal{O}_j^{\mathrm{tree}} \tag{3.13}$$

$$\mathcal{O}_i^{\mathrm{latt}} = \left[\delta_{ij} + \frac{\alpha_s^{\mathrm{latt}}(\mu)}{4\pi}(\gamma_{ij}\log\lambda^2 a^2 + d_{ij}^{\mathrm{latt}}) + O(\alpha^2)\right]\mathcal{O}_j^{\mathrm{tree}} \tag{3.14}$$

Where the terms in square brackets are the 1- 2- ... n-loops perturbative correction in the appropriate renormalization scheme. γ_{ij} is called the *anomalous dimension matrix*. In the simplest cases γ_{ij} is diagonal. From now on we will be interested in the 1-loop relation between the two renormalization schemes. At this order

$$\frac{\alpha_s^{\overline{\mathrm{MS}}}}{4\pi} = \left[1 + \frac{\alpha_s}{4\pi} + O(\alpha^2)\right]\frac{\alpha_s^{\mathrm{latt}}}{4\pi} \tag{3.15}$$

and one, up to order α^2 terms, can easily invert the perturbative coefficients and can identify

$$\left[\delta_{ij} - \frac{\alpha_s}{4\pi}(\gamma_{ij}\log\lambda^2\mu^{-2} + d_{ij}^{\overline{\mathrm{MS}}}) + O(\alpha^2)\right]\mathcal{O}_j^{\overline{\mathrm{MS}}} \tag{3.16}$$

with

$$\left[\delta_{ij} - \frac{\alpha_s}{4\pi}(\gamma_{ij}\log\lambda^2 a^2 + d_{ij}^{\mathrm{latt}}) + O(\alpha^2)\right]\mathcal{O}_j^{\mathrm{latt}} \tag{3.17}$$

(it does not matter in which scheme $\frac{\alpha_s}{4\pi}$ is renormalized). Therefore one deduces the 1-loop relation

$$\mathcal{O}_i^{\overline{\mathrm{MS}}} = Z_{ij}(\mu,a)\mathcal{O}_j^{\mathrm{latt}} = \left[\delta_{ij} + \frac{\alpha_s}{4\pi}\left(-\gamma_{ij}\log\mu^2 a^2 + d_{ij}^{\overline{\mathrm{MS}}} - d_{ij}^{\mathrm{latt}}\right)\right]\mathcal{O}_j^{\mathrm{latt}} \tag{3.18}$$

What is left to do is to list all of the 1-loop relevant diagrams contributing to the renormalization of the set of operators in which we are interested, $\mathcal{O}_i$, and compute them in each of the two renormalization schemes. The sum of the terms proportional to $\frac{\alpha_s}{4\pi}\log\lambda^2$ will give a contribution to the anomalous dimension matrix γ_{ij} and it will turn out to be the same in the two renormalization schemes. If one identifies the two renormalization scales $\mu = a^{-1}$ any logarithmic dependence on the renormalization scale disappears in the matching.

The computation of Feynman diagrams is performed using the Feynman rules which are given in Appendix D, both for the continuum QCD (the rules for modified minimal substraction, $\overline{\mathrm{MS}}$ are given in Appendix B) and for lattice QCD.

In the lattice case many more diagrams appear, at the same order, than in the continuum case and we will distinguish between those diagrams that originate from the standard Wilsonian action and those diagrams originated from the SW improvement, eq. (2.96): the new quark-gluon interaction derived from the clover term, eq. (2.95) will be represented by a grey blob. This vertex is denoted in Appendix D by the symbol $V^I_\mu(p,q)$. The improvement technique prescribes that the addition of the clover term to the Wilsonian Lagrangian must be accompanied by a transformation of the quark fields in fermionic operators

$$q \;\rightarrow\; \left[1-\frac{1}{4}ar(\overrightarrow{\not{D}}-m_q)\right]q \tag{3.19}$$

$$\bar{q} \;\rightarrow\; \bar{q}\left[1+\frac{1}{4}ar(\overleftarrow{\not{D}}-m_q)\right] \tag{3.20}$$

where D are the usual covariant derivatives. This is necessary to cancel order a corrections in the numerical evaluation of the expectation values of operators involving light quarks. Under this rotation the operator $\bar{q}\Gamma q$ transforms as follows

$$\bar{q}\Gamma q \rightarrow \bar{q}\Gamma q + \frac{1}{4}ar\bar{q}\left[\overleftarrow{\not{D}}\,\Gamma - \Gamma\,\overrightarrow{\not{D}}\right]q \tag{3.21}$$

This new order a contribution can be read in the Feynman language as two additional Feynman rules for the rotated operator, coming from $\frac{1}{2}ar\not{\partial}$ and from $\frac{1}{2}ar\not{A}$ respectively. These two new Feynman vertices are represented by a grey star (note that the static quarks are not rotated). The complete set of lattice diagrams that will be relevant to the present calculations are reported in

- fig. (3.1): Corrections to massless quark and static quark propagators.
- fig. (3.2): Corrections to $\bar{q}\Gamma q$ vertex.
- fig. (3.3): Corrections to $\bar{b}\Gamma q$ vertex.
- fig. (3.4): Corrections to 4-quark operators.

All these figures are at the end of the chapter. The diagrams have been labelled with a progressive number going from 01) to 61) and they will be referred to by the corresponding number.

The explicit evaluation of diagram 27) is reported step by step, as an example, in Appendix D.

It has not been possible to solve symbolically the integrals originated in the lattice diagrams, therefore they have been expressed in terms of some parameters

c, e, f, v, h, m, l, q etc. which are also defined in Appendix D. These parameters have been integrated numerically using the CERN libraries. Divergences have been removed from the numerical integration by subtracting a small ball (of radius 1) from the integration domain. The intergration on the ball is performed exactly.

Some of these parameters were already introduced by Eichten and Hill [63], Flynn *et al.* [64], Borrelli *et al.* [65]. In a few cases we found some disagreement with the results of the latter, but our results are in agreement with the recent paper [121].

3.1.1 Renormalization of the external lines

The quark self energy contributes to the constants Z through the renormalization of the external lines. In fact each external quark line is renormalized according with

$$u(\mathbf{p}) \to Z_2^{1/2} u(\mathbf{p}) \tag{3.22}$$

where the renrmalization constant Z_2 for QCD, at one loop, is defined as

$$Z_2 = 1 + \frac{\partial}{\partial \not{p}} \Sigma(p) \Big|_{\not{p}=0} \tag{3.23}$$

and, for a massless quark, $\Sigma(p)$ corresponds to the Feynman diagram

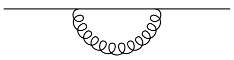

$$\begin{aligned} &= \Sigma(p) \\ &= \int d_4k (-ie\gamma^\mu t^a) \frac{i}{\not{p} - \not{k}} \frac{g_{\mu\nu}}{k^2 - \lambda^2} (-ie\gamma^\nu t^a) \\ &= \frac{\alpha_s}{4\pi} C_F (\text{divergence} + \log \lambda^2 \mu^{-2} + \text{finite part}) \not{p} \end{aligned} \tag{3.24}$$

For what follows we are interested in the "log + finite part" of the 1-loop Z_2 renormalization constant in the following four cases.

- Massless quark in the continuum scheme:

$$\frac{\partial}{\partial \not{p}} \left[\quad \right] = \frac{\alpha_s}{4\pi} C_F (\log \lambda^2 \mu^{-2} + \frac{1}{2}) \tag{3.25}$$

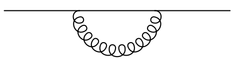

- Static quark in the continuum scheme [63]:

$$\frac{\partial}{\partial p_0} \left[\quad \right] = \frac{\alpha_s}{4\pi} C_F (-2 \log \lambda^2 \mu^{-2}) \tag{3.26}$$

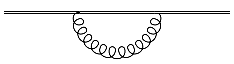

Note that the static-quark propagtor, eq. (D.4), depends only on p_0 therefore $\Sigma(p) \propto p_0$.

- Massless quark in the lattice scheme [64, 65]:

$$\frac{\partial}{\partial \not{p}}\Big[01)\Big] = \frac{\alpha_s}{4\pi} C_F(\log \lambda^2 a^2 + f) \tag{3.27}$$

$$\frac{\partial}{\partial \not{p}}\Big[02) + 03) + 04)\Big] = \frac{\alpha_s}{4\pi} C_F(f^I) \tag{3.28}$$

- Static quark in the lattice scheme [64]:

$$\frac{\partial}{\partial p_0}\Big[06)\Big] = \frac{\alpha_s}{4\pi} C_F(-2\log \lambda^2 a^2 + e) \tag{3.29}$$

3.1.2 Matching $\bar{q}\Gamma q$ type operators

To perform this matching we now proceed in evaluating all the 1-loop perturbative corrections to $\bar{q}\Gamma q$ in the continuum and in the lattice scheme to obtain the coefficients γ_{ij} and d_{ij} of eq. (3.18).

- Vertex correction in the continuum scheme

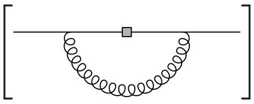

$$= \frac{\alpha_s}{4\pi}\Big[(-\omega_{1,i}^2/4)\log \lambda^2 \mu^{-2} + (\omega_{1,i}\omega_{2,i}/2 + 3\omega_{1,i}^2/8)\Big]\bar{q}(t^a \Gamma_i t^a) q \tag{3.30}$$

where $\omega_{1,i}$ and $\omega_{2,1}$ depend on the Γ_i spin matrix are are tabulated in table 3.1 for our choice of a basis.

- Vertex corrections in the lattice scheme (all the relevant diagrams, excluding the contribution of the external lines, are reported in fig. (3.2)):

$$
\begin{aligned}
07) &= \frac{\alpha_s}{4\pi}\left[(-\omega_{1,i}^2/4)\log\lambda^2 a^2 + \right.\\
&\qquad \left. -v_1 - (\omega_{1,i}^2-4)v_2/12 + \omega_{1,i}w\right]\bar{q}(t^a\Gamma_i t^a)q && (3.31)\\
08) &= 10) = \frac{\alpha_s}{4\pi}\left[-(\omega_{1,i}^2-4)v_1^I/12 + \omega_{1,i}w_1^I\right]\bar{q}(t^a\Gamma_i t^a)q && (3.32)\\
10) &= \frac{\alpha_s}{4\pi}\left[-(\omega_{1,i}^2-4)v_2^I/12 + \omega_{1,i}w_2^I\right]\bar{q}(t^a\Gamma_i t^a)q && (3.33)\\
11) &= \frac{\alpha_s}{4\pi}2\left[s_1 + (\omega_{1,i}^2-4)s_2/12 + \omega_{1,i}s_3/4\right]\bar{q}(t^a\Gamma_i t^a)q && (3.34)\\
12) &= 13) = \frac{\alpha_s}{4\pi}2\left[(\omega_{1,i}^2-4)s_4/12 + \omega_{1,i}s_5/4\right]\bar{q}(t^a\Gamma_i t^a)q && (3.35)\\
14) &= \frac{\alpha_s}{4\pi}2\left[(\omega_{1,i}^2-4)s_6/12 + \omega_{1,i}s_7/4\right]\bar{q}(t^a\Gamma_i t^a)q && (3.36)\\
15) &= 17) = \frac{\alpha_s}{4\pi}(-m)\bar{q}(\Gamma_i t^a t^a)q && (3.37)\\
16) &= 18) = \frac{\alpha_s}{4\pi}(-l)\bar{q}(\Gamma_i t^a t^a)q && (3.38)
\end{aligned}
$$

Summing all the contributions (and including the renormalization factors $Z_2^{1/2}$ for each of the two external light quarks) one gets

$$
\begin{aligned}
\gamma_{ij} &= \delta_{ij}C_F(1-\omega_{1,i}^2/4) && (3.39)\\
d_{ij}^{\overline{\text{MS}}} &= \delta_{ij}C_F(1/4 + \omega_{1,i}\omega_{2,i}/2 + 3\omega_{1,i}^2/8) && (3.40)\\
d_{ij}^{\text{latt}} &= \delta_{ij}C_F\left[\frac{1}{2}(f+f^I) - v_1 + 2s_1 - m - l + \right.\\
&\qquad +(\omega_{1,i}^2-4)(2s_2+2s_4+2s_6-v_2-v_1^I-v_2^I)/12\\
&\qquad \left. +\omega_{1,i}(w+w_1^I+w_2^I+s_3/2+s_5/2+s_7/2)\right]\\
&= \delta_{ij}C_F\left[1.0\omega_{1,i}^2 - 2.4\omega_{1,i} + 3.1\right] && (3.41)
\end{aligned}
$$

We observe that for the vector and axial currents, $\Gamma_i = \gamma^\mu, \gamma^\mu\gamma^5$ the anomalous dimension is exactly zero (because in these cases $\omega_{1,i}^2 = 4$, see table 3.1). In fact these two currents are conserved. Moreover we observe that the matching factors are diagonal, i.e. different operators do not mix. This is not true in general for a different basis of Γ_i matrices. Consider for example

$$
\bar{q}Lq = \frac{1}{2}\left[\bar{q}Iq - \bar{q}\gamma^5 q\right] \tag{3.42}
$$

the two operators on the right have multiplicative matching factors, but they are different, therefore $\bar{q}Lq$ mixes with $\bar{q}Rq$.

3.1.3 Matching $\bar{b}\Gamma q$ type operators

Following the same procedure as in the last subsection we will proceed evaluating all the 1-loop perturbative corrections to the operator $\bar{b}\Gamma_i q$ in the continuum and in the lattice scheme.

- Vertex correction in the continuum scheme

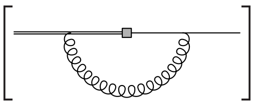

$$= \frac{\alpha_s}{4\pi}(-\log\lambda^2\mu^{-2}+1)\bar{b}(t^a\Gamma_i t^a)q \tag{3.43}$$

- Vertex corrections in the lattice scheme

$$
\begin{aligned}
19) &= \frac{\alpha_s}{4\pi}(-\log\lambda^2 a^2+d_1)\bar{b}(t^a\Gamma_i t^a)q+\frac{\alpha_s}{4\pi}(d_2)\bar{b}(t^a\gamma^0\Gamma_i\gamma^0 t^a)q && (3.44)\\
20) &= \frac{\alpha_s}{4\pi}(-d^I)\bar{b}(t^a\gamma^0\Gamma_i\gamma^0 t^a)q && (3.45)\\
21) &= \frac{\alpha_s}{4\pi}(n)\bar{b}(t^a\Gamma_i t^a)q+\frac{\alpha_s}{4\pi}(-d^I)\bar{b}(t^a\gamma^0\Gamma_i\gamma^0 t^a)q && (3.46)\\
22) &= \frac{\alpha_s}{4\pi}(-q)\bar{b}(t^a\gamma^0\Gamma_i\gamma^0 t^a)q && (3.47)\\
23) &= \frac{\alpha_s}{4\pi}(-m)\bar{b}(\Gamma_i t^a t^a)q && (3.48)\\
24) &= \frac{\alpha_s}{4\pi}(-l)\bar{b}(\Gamma_i t^a t^a)q && (3.49)\\
25) &= \frac{\alpha_s}{4\pi}(h)\bar{b}(t^a\gamma^0\Gamma_i\gamma^0 t^a)q && (3.50)
\end{aligned}
$$

Our results can be summarized in the three parameters which appear in eq. (3.18):

$$
\begin{aligned}
\gamma_{ij} &= \delta_{ij}C_F(-3/2) && (3.51)\\
d_{ij}^{\overline{\mathrm{MS}}} &= \delta_{ij}C_F(5/4) && (3.52)\\
d_{ij}^{\overline{\mathrm{MS}}} &= \delta_{ij}C_F\Big[\frac{1}{2}(e+f+f^I)+d_1+n-m-l+\\
&\qquad \omega_{3,i}(d_2-2d^I-q-h)\Big]\\
&= \delta_{ij}C_F\Big[-6.89\omega_{3,i}+9.37\Big] && (3.53)
\end{aligned}
$$

where $\omega_{3,i}$ is defined in eq. (3.12) and tabulated in table 3.1 for our basis.

3.1.4 Matching $\bar{b}\Gamma q\,\bar{q}\tilde{\Gamma}b$ type operators

The matching of 4-quark type operators is more difficult because there are two different fermion lines in each Feynman diagram.

We distinguish five categories of loop corrections to the general operator

$$\mathcal{O}_i = \bar{b}\Gamma_i^A q\bar{q}\tilde{\Gamma}_i^A b \tag{3.54}$$

They are:

I. Corrections to the external lines, 01)-06), which have been computed in subsection 3.1.1.

II. Vertex corrections to each of the quark bilinears, 19)-25), which have been computed in subsection 3.1.3.

III. Correction in which the gluon couples to both static-quark propagators, 26).

IV. Corrections in which the gluon couples to one static-quark propagator, 27),28),30),31),47)-50),55),56).

V. Corrections in which the gluon does not couple to static-quarks, 29),32)-46),51)-54),57)-61).

First of all we proceed by computing the missing diagrams in the continuum scheme.

III. Corrections in which the gluon couples to both static quarks

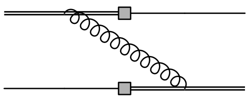

$$= \frac{\alpha_s}{4\pi}(2\log\lambda^2\mu^{-2})\bar{b}(t^a\Gamma_i)q\bar{q}(\tilde{\Gamma}_i t^a)b \tag{3.55}$$

IV. Corrections in which the gluon couples to one static-quark propagator

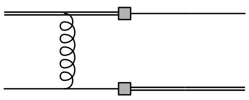

$$= \frac{\alpha_s}{4\pi}(\log\lambda^2/\mu^{-2} - 1)\bar{b}(t^a\Gamma_i)q\bar{q}(t^a\tilde{\Gamma}_i)b \tag{3.56}$$

and

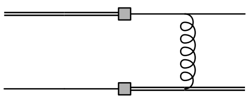

$$= \frac{\alpha_s}{4\pi}(\log\lambda^2\mu^{-2} - 1)\bar{b}(\Gamma_i t^a)q\bar{q}(\tilde{\Gamma}_i t^a)b \tag{3.57}$$

V. Corrections in which the gluon does not couple to static quarks

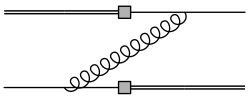

$$\begin{aligned} = \;& \frac{\alpha_s}{4\pi}(-\log\lambda^2\mu^{-2} + \Omega_{1,i})\bar{b}(\Gamma_i t^a)q\bar{q}(t^a\tilde{\Gamma}_i)b + \\ & \frac{\alpha_s}{4\pi}\left[(-1/4)\log\lambda^2\mu^{-2} + \Omega_{2,i}\right] \times \\ & \quad \bar{q}(\Gamma_i\sigma^{\mu\nu}t^a)q\bar{q}(t^a\sigma^{\nu\mu}\tilde{\Gamma}_i)b \end{aligned} \tag{3.58}$$

Apparently the choice of a regularization scheme, such as NDR (Naive Dimensional Regularization), HV ('t Hooft-Veltman) or DRed (Dimensional Reduction), together with a subtraction prescription (in our case $\overline{\text{MS}}$) makes the continuum operators completely defined. A more careful analysis demonstrates, however, that this is not the case if more than one fermion line is present in the Feynman diagrams. In this case one has to specify how to deal with *evanescent operators* (i.e. operators that do not exist in four dimensions) that appear in $D = 4 - 2\varepsilon$ dimensions. The problem arises because the two rules

$$\gamma^\mu \gamma^\nu \gamma^\rho \gamma^\sigma = i\varepsilon^{\mu\nu\rho\sigma}\gamma^5 \tag{3.59}$$

and

$$\{\gamma^\mu, \gamma^5\} = 0 \tag{3.60}$$

are not compatible in arbitrary dimensions. Therefore there is not a unique definition of γ^5. Each regularization scheme provides a different definition for γ^5, but none of them provides a unique definition of tensor products of gamma matrices containing γ^5. This ambiguity becomes manifest if one tries to compute the following evanescent operator in $D = 4 - 2\varepsilon$ dimensions

$$\mathcal{O}_\varepsilon = \gamma^\mu \gamma^\nu \gamma^\rho L \otimes \gamma_\mu \gamma_\nu \gamma_\rho L - 16\gamma^\mu L \otimes \gamma_\mu L \tag{3.61}$$

which vanishes linearly in ε. When an operator of this kind is produced in a divergent diagram (proportional to $1/\varepsilon$), it gives rise to a finite contribution to the diagram, even when the limit $D \to 4$ is taken.

One way of removing any ambiguity is choosing a basis of $\Gamma_i \otimes \tilde{\Gamma}_i$ in D dimensions on which to project every possible gamma structure. Another possible choice is fixing the order ε contribution of each evanescent operator.

Our renormalization prescription for evanescent operators in D dimension is completely specified by order ε terms in

$$\gamma^\mu \gamma^\nu \gamma^\rho \otimes \gamma_\mu \gamma_\nu \gamma_\rho = (10 - 6\varepsilon)\gamma^\mu \otimes \gamma_\mu + (6 + 2\varepsilon)\gamma^\mu \gamma^5 \otimes \gamma_\mu \gamma^5 \tag{3.62}$$

together with the usual prescriptions of the HV scheme[1]. Our choice coincides with that of Flynn *et al.* for $\Delta B = 2$ operators. The coefficients $\Omega_{1,i}$, $\Omega_{2,i}$, $\Omega_{3,i}$ and $\Omega_{4,i}$ of table 3.1 (on which the matching coefficients depend) depend on this choice.

The lattice counterpart of the matching does not suffer from this ambiguity and it is uniquely defined at each stage.

We will proceed by listing the contribution of all of the lattice corrections.

[1] γ^5 anticommutes with γ^μ for $\mu = 0, 1, 2, 3$ and commutes with the other γ^μ matrices; the gamma structure that comes form original operator, not from the perturbative correction, is not extended to D dimensions.

III. Correction in which the gluon couples to both static quarks

$$26) = \frac{\alpha_s}{4\pi}(2\log\lambda^2a^2)\bar{b}(t^a\Gamma_i)q\bar{q}(\tilde{\Gamma}_it^a)b \tag{3.63}$$

IV. Corrections in which the gluon couples to one static-quark propagator

$$\begin{aligned}
27) \quad &= \quad \frac{\alpha_s}{4\pi}(\log\lambda^2a^2 - d_1)\bar{b}(t^a\Gamma_i)q\bar{q}(t^a\tilde{\Gamma}_i)b + \\
&\quad\ \frac{\alpha_s}{4\pi}(d_2)\bar{b}(t^a\gamma^0\Gamma_i)q\bar{q}(t^a\gamma^0\tilde{\Gamma}_i)b & (3.64)\\
28) \quad &= \quad \frac{\alpha_s}{4\pi}(\log\lambda^2a^2 - d_1)\bar{b}(\Gamma_it^a)q\bar{q}(\tilde{\Gamma}_it^a)b + \\
&\quad\ \frac{\alpha_s}{4\pi}(d_2)\bar{b}(\Gamma_i\gamma^0t^a)q\bar{q}(\tilde{\Gamma}_i\gamma^0t^a)b & (3.65)\\
30) \quad &= \quad \frac{\alpha_s}{4\pi}(-d^I)\bar{b}(t^a\gamma^0\Gamma_i)q\bar{q}(t^a\gamma^0\tilde{\Gamma}_i)b & (3.66)\\
31) \quad &= \quad \frac{\alpha_s}{4\pi}(-d^I)\bar{b}(\Gamma_i\gamma^0t^a)q\bar{q}(\tilde{\Gamma}_i\gamma^0t^a)b & (3.67)\\
47) \quad &= \quad \frac{\alpha_s}{4\pi}(-n)\bar{b}(\Gamma_it^a)q\bar{q}(\tilde{\Gamma}_it^a)b + \\
&\quad\ \frac{\alpha_s}{4\pi}(-d^I)\bar{b}(\Gamma_i\gamma^0t^a)q\bar{q}(\tilde{\Gamma}_i\gamma^0t^a)b & (3.68)\\
48) \quad &= \quad \frac{\alpha_s}{4\pi}(-q)\bar{b}(\Gamma_i\gamma^0t^a)q\bar{q}(\tilde{\Gamma}_i\gamma^0t^a)b & (3.69)\\
49) \quad &= \quad \frac{\alpha_s}{4\pi}(-n)\bar{b}(t^a\Gamma_i)q\bar{q}(t^a\tilde{\Gamma}_i)b + \\
&\quad\ \frac{\alpha_s}{4\pi}(-d^I)\bar{b}(t^a\gamma^0\Gamma_i)q\bar{q}(t^a\gamma^0\tilde{\Gamma}_i)b & (3.70)\\
50) \quad &= \quad \frac{\alpha_s}{4\pi}(-q)\bar{b}(t^a\gamma^0\Gamma_i)q\bar{q}(t^a\gamma^0\tilde{\Gamma}_i)b & (3.71)
\end{aligned}$$

V. Corrections in which the gluon does not couple to static quarks

$$\begin{aligned}
29) \quad &= \quad \frac{\alpha_s}{4\pi}(-\log\lambda^2a^2 - v_1)\bar{b}(\Gamma_it^a)q\bar{q}(t^a\tilde{\Gamma}_i)b + \\
&\quad\ \frac{\alpha_s}{4\pi}((-1/4)\log\lambda^2a^2 - v_2/12)\bar{b}(\Gamma_i\sigma^{\mu\nu}t^a)q\bar{q}(t^a\sigma^{\nu\mu}\tilde{\Gamma}_i)b + \\
&\quad\ \frac{\alpha_s}{4\pi}(w)\bar{b}(\Gamma_i\gamma^\mu t^a)q\bar{q}(t^a\gamma^\mu\tilde{\Gamma}_i)b & (3.72)\\
32) \quad &= \quad 33) = \frac{\alpha_s}{4\pi}(-v_1^I/12)\bar{b}(\Gamma_i\sigma^{\mu\nu}t^a)q\bar{q}(t^a\sigma^{\nu\mu}\tilde{\Gamma}_i)b + \\
&\quad\ \frac{\alpha_s}{4\pi}(w_1^I)\bar{b}(\Gamma_i\gamma^\mu t^a)q\bar{q}(t^a\gamma^\mu\tilde{\Gamma}_i)b & (3.73)\\
34) \quad &= \quad \frac{\alpha_s}{4\pi}(-v_2^I/12)\bar{b}(\Gamma_i\sigma^{\mu\nu}t^a)q\bar{q}(t^a\sigma^{\nu\mu}\tilde{\Gamma}_i)b + \\
&\quad\ \frac{\alpha_s}{4\pi}(w_2^I)\bar{b}(\Gamma_i\gamma^\mu t^a)q\bar{q}(t^a\gamma^\mu\tilde{\Gamma}_i)b & (3.74)
\end{aligned}$$

$$\begin{aligned}
35) &= 39) = \frac{\alpha_s}{4\pi}(s_1)\bar{b}(\Gamma_i t^a)q\bar{q}(t^a\tilde{\Gamma}_i)b + \\
&\frac{\alpha_s}{4\pi}(s_2/12)\bar{b}(\Gamma_i\sigma^{\mu\nu}t^a)q\bar{q}(t^a\sigma^{\nu\mu}\tilde{\Gamma}_i)b + \\
&\frac{\alpha_s}{4\pi}(s_3/4)\bar{b}(\Gamma_i\gamma^{\mu}t^a)q\bar{q}(t^a\gamma^{\mu}\tilde{\Gamma}_i)b && (3.75) \\
36) &= 37) = 40) = 41) = && (3.76) \\
&\frac{\alpha_s}{4\pi}(s_4/12)\bar{b}(\Gamma_i\sigma^{\mu\nu}t^a)q\bar{q}(t^a\sigma^{\nu\mu}\tilde{\Gamma}_i)b + \\
&\frac{\alpha_s}{4\pi}(s_5/4)\bar{b}(\Gamma_i\gamma^{\mu}t^a)q\bar{q}(t^a\gamma^{\mu}\tilde{\Gamma}_i)b && (3.77) \\
38) &= 42) = \frac{\alpha_s}{4\pi}(s_6/12)\bar{b}(\Gamma_i\sigma^{\mu\nu}t^a)q\bar{q}(t^a\sigma^{\nu\mu}\tilde{\Gamma}_i)b + \\
&\frac{\alpha_s}{4\pi}(s_7/4)\bar{b}(\Gamma_i\gamma^{\mu}t^a)q\bar{q}(t^a\gamma^{\mu}\tilde{\Gamma}_i)b && (3.78) \\
43) &= \frac{\alpha_s}{4\pi}(t_4)\bar{b}(\Gamma_i t^a)q\bar{q}(t^a\tilde{\Gamma}_i)b + \\
&\frac{\alpha_s}{4\pi}(t_5/12)\bar{q}(\Gamma_i\sigma^{\mu\nu}t^a)b\bar{q}(t^a\sigma^{\nu\mu}\tilde{\Gamma}_i)b + \\
&\frac{\alpha_s}{4\pi}(t_6/4)\bar{b}(\Gamma_i\gamma^{\mu}t^a)q\bar{q}(t^a\gamma^{\mu}\tilde{\Gamma}_i)b && (3.79) \\
44) &= 45) = \frac{\alpha_s}{4\pi}(t_7/12)\bar{b}(\Gamma_i\sigma^{\mu\nu}t^a)q\bar{q}(t^a\sigma^{\nu\mu}\tilde{\Gamma}_i)b + \\
&\frac{\alpha_s}{4\pi}(t_8/4)\bar{b}(\Gamma_i\gamma^{\mu}t^a)q\bar{q}(t^a\gamma^{\mu}\tilde{\Gamma}_i)b && (3.80) \\
46) &= \frac{\alpha_s}{4\pi}(t_9/12)\bar{b}(\Gamma_i\sigma^{\mu\nu}t^a)q\bar{q}(t^a\sigma^{\nu\mu}\tilde{\Gamma}_i)b + \\
&\frac{\alpha_s}{4\pi}(t_{10}/4)\bar{b}(\Gamma_i\gamma^{\mu}t^a)q\bar{q}(t^a\gamma^{\mu}\tilde{\Gamma}_i)b && (3.81) \\
51) &= 53) = \frac{\alpha_s}{4\pi}(-m/4)\bar{b}(\Gamma_i\gamma^{\mu}t^a)q\bar{q}(t^a\gamma^{\mu}\tilde{\Gamma}_i)b && (3.82) \\
52) &= 54) = \frac{\alpha_s}{4\pi}(-l/4)\bar{b}(\Gamma_i\gamma^{\mu}t^a)q\bar{q}(t^a\gamma^{\mu}\tilde{\Gamma}_i)b && (3.83) \\
55) &= \frac{\alpha_s}{4\pi}(h)\bar{b}(t^a\gamma^0\Gamma_i)q\bar{q}(t^a\gamma^0\tilde{\Gamma}_i)b && (3.84) \\
56) &= \frac{\alpha_s}{4\pi}(h)\bar{b}(\Gamma_i\gamma^0 t^a)q\bar{q}(\tilde{\Gamma}_i\gamma^0 t^a)b && (3.85) \\
57) &= 59) = \frac{\alpha_s}{4\pi}(t_2/4)\bar{b}(\Gamma_i\gamma^{\mu}t^a)q\bar{q}(t^a\gamma^{\mu}\tilde{\Gamma}_i)b && (3.86) \\
58) &= 60) = \frac{\alpha_s}{4\pi}(t_3/4)\bar{b}(\Gamma_i\gamma^{\mu}t^a)q\bar{q}(t^a\gamma^{\mu}\tilde{\Gamma}_i)b && (3.87) \\
61) &= \frac{\alpha_s}{4\pi}(t_1/4)\bar{b}(\Gamma_i\gamma^{\mu}t^a)q\bar{q}(t^a\gamma^{\mu}\tilde{\Gamma}_i)b && (3.88)
\end{aligned}$$

Our results for the coefficients γ_{ij} and d_{ij} are presented in table 3.2. Note that the index j does not span the basis of table 3.1 but it spans the set of operators $\mathcal{O}_j$ of table 3.2, which depend on $\mathcal{O}_i$. This notation is particularly convenient because it applies to any operator, whatever the spin and color structure are.

j (categ.)	γ_{ij}	$d_{ij}^{\overline{\rm MS}}$	$d_{ij}^{\rm latt}$	$\mathcal{O}_j^{\rm latt}(\Delta B=0)$
1 (I,II)	-1	$\frac{1}{2}$	6.36	$C_F\,\bar{b}\Gamma_i^A q\,\bar{q}\tilde{\Gamma}_i^A b$
2 (II)	$-\frac{3}{2}$	1	6.19	$\bar{b}(t^a\Gamma_i^A t^a)q\,\bar{q}\tilde{\Gamma}_i^A b+\bar{b}\Gamma_i^A q\,\bar{q}(t^a\tilde{\Gamma}_i^A t^a)b$
3 (II)	0	0	-6.89	$\bar{b}(t^a\gamma^0\Gamma_i^A\gamma^0 t^a)q\,\bar{q}\tilde{\Gamma}_i^A b+\bar{b}\Gamma_i^A q\,\bar{q}(t^a\gamma^0\tilde{\Gamma}_i^A\gamma^0 t^a)b$
4 (III)	2	0	-4.53	$\bar{b}(t^a\Gamma_i^A)q\,\bar{q}(\tilde{\Gamma}_i^A t^a)b$
5 (IV)	1	-1	-6.19	$\bar{b}(\Gamma_i^A t^a)q\,\bar{q}(\tilde{\Gamma}_i^A t^a)b+\bar{b}(t^a\Gamma_i^A)q\,\bar{q}(t^a\tilde{\Gamma}_i^A)b$
6 (IV)	0	0	-6.89	$\bar{b}(\Gamma_i^A\gamma^0 t^a)q\,\bar{q}(\tilde{\Gamma}_i^A\gamma^0 t^a)b+\bar{b}(t^a\gamma^0\Gamma_i^A)q\,\bar{q}(t^a\gamma^0\tilde{\Gamma}_i^A)b$
7 (V)	-1	$\Omega_{1,i}$	5.12	$\bar{b}(\Gamma_i^A t^a)q\,\bar{q}(t^a\tilde{\Gamma}_i^A)b$
8 (V)	$-\frac{1}{4}$	$\Omega_{2,i}$	1.05	$\bar{b}(\Gamma_i^A\sigma^{\mu\nu}t^a)q\,\bar{q}(t^a\sigma^{\nu\mu}\tilde{\Gamma}_i^A)b$
9 (V)	0	0	-2.43	$\bar{b}(\Gamma_i^A\gamma^\mu t^a)q\,\bar{q}(t^a\gamma^\mu\tilde{\Gamma}_i^A)b$

Table 3.2: Values of the contributions to γ_{ij} and d_{ij} for $\Delta B=0$ 4-quark operators.

The symbolic expression for the coefficients $d_{ij}^{\rm latt} = d_j^W + d_j^{SW}$ is given in table 3.3, where the components proportional to the d_i^W would be the results if the Wilson formulation of the quark action had been used, and those proportional to d_i^{SW} are the additional contributions which result from the use of the SW improved action.

3.1.5 Matching $\bar{b}\Gamma_i q\,\bar{b}\tilde{\Gamma}_i q$ type operators

There are many parallels between the calculations of matrix elements of spectator effects in inclusive decays and that of the matrix elements of the $\Delta B=2$ operators which contribute, for example, to the important process of B^0-$\bar{B}^0$ mixing. Indeed, we have recomputed the matrix elements of the $\Delta B=2$ operators and compared the results to those in ref. [67] as a check on our procedures and programs. The calculation of the matching factors are also similar in the two cases, and we have exploited this fact as a check on our perturbative calculation.

The difference between the matching of $\Delta B=0$ operators ($\bar{b}\Gamma_i q\bar{q}\tilde{\Gamma}_i b$) and $\Delta B=2$ operators ($\bar{b}\Gamma_i q\bar{b}\tilde{\Gamma}_i q$) is in the direction of one of the two fermionic lines

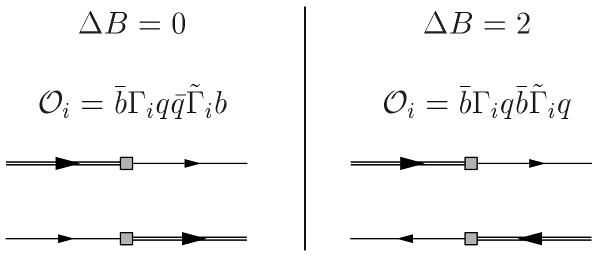

Wilson contribution	SW contribution
$d_1^W = f + e = 17.89$	$d_1^{SW} = f^I - 2(l+m) = -11.53$
$d_2^W = d_1 = 5.46$	$d_2^{SW} = n = 0.73$
$d_3^W = d_2 = -7.22$	$d_3^{SW} = h - 2d^I - q = 0.33$
$d_4^W = -c = -4.53$	$d_4^{SW} = 0$
$d_5^W = -d_1 = -5.46$	$d_5^{SW} = -n = -0.73$
$d_6^W = d_2 = -7.22$	$d_6^{SW} = c_3^{SW} = 0.33$
$d_7^W = -v_1 = 4.85$	$d_7^{SW} = 2s_1 + t_4 = 0.27$
$d_8^W = -v_2/12 = 0.17$	$d_8^{SW} = (-v^I + s - 2s_1 - t_4 + t_B)/12 = 0.87$
$d_9^W = w = -1.21$	$d_9^{SW} = w^I + (-2l - 2m + s + t_A)/4 = -1.22$

Table 3.3: Values of the coefficients d_i^W and d_i^{SW}. Their symbolic expressions are given in terms of the variables defined in Appendix D.

Therefore the evaluation of the various contributions to the d_{ij}'s for $\Delta B = 2$ operators parallels that of the operator $\mathcal{O}_i$ for spectator effects in inclusive decays. In particular each of the lattice Feynman diagrams that has been computed in the last subsection can easily be mapped in the corresponding diagram for $\Delta B = 2$ operator. The numerical part of these diagram can be even or odd under this map, depending on the structure of the Feynman integrand. The explicit computation shows that only corrections that fall in the categories $j = 4, 5, 7, 8$ are odd, while the others are even.

In the case of continuum diagrams it was not possible to find an exact transformation, therefore they have been recomputed and expressed in terms of the parameters $\Omega_{3,i}$ and $\Omega_{4,i}$ of table 3.1(right).

The results of our analysis are reported in table 3.4.

In considering the crossing relations between inclusive decays and mixing, we note that in the latter process, one of the $\bar{b}$ fields destroys a quark (so that $\bar{b}\gamma^0 = \bar{b}$) and the other creates an antiquark (so that $\bar{b}\gamma^0 = -\bar{b}$).

3.2 Matching different scales

We will here consider a different problem: the computation of the matching coefficients between operators regularized in the same theory but renormalized at different scales. This can be done by imposing a Renormalization Group Equation (RGE) for the amplitudes of each of the operators $\mathcal{O}_i$ between an initial state $|i\rangle$ and a final state $|f\rangle$. Introducing the definition

$$G_i(\mu, g) = \langle f|\, \mathcal{O}_i^{\overline{\mathrm{MS}},\mu}\, |i\rangle \tag{3.89}$$

j (categ.)	γ_{ij}	$d_{ij}^{\overline{\mathrm{MS}}}$	d_{ij}^{latt}	$\mathcal{O}_j^{\mathrm{latt}}(\Delta B = 2)$
1 (I,II)	-1	$\frac{1}{2}$	6.36	$C_F\,\bar{b}\Gamma_i^A q\,\bar{b}\tilde{\Gamma}_i^A q$
2 (II)	$-\frac{3}{2}$	1	6.19	$\bar{b}(t^a\Gamma_i^A t^a)q\,\bar{b}\tilde{\Gamma}_i^A q + \bar{b}\Gamma_i^A q\,\bar{b}(t^a\tilde{\Gamma}_i^A t^a)q$
3 (II)	0	0	-6.89	$\bar{b}(t^a\gamma^0\Gamma_i^A\gamma^0 t^a)q\,\bar{b}\tilde{\Gamma}_i^A q + \bar{b}\Gamma_i^A q\,\bar{b}(t^a\gamma^0\tilde{\Gamma}_i^A\gamma^0 t^a)q$
4 (III)	-2	-0	4.53	$\bar{b}(t^a\Gamma_i^A)q\,\bar{b}(t^a\tilde{\Gamma}_i^A)q$
5 (IV)	-1	1	6.19	$\bar{b}(\Gamma_i^A t^a)q\,\bar{b}(t^a\tilde{\Gamma}_i^A)q + \bar{b}(t^a\Gamma_i^A)q\,\bar{b}(\tilde{\Gamma}_i^A t^a)q$
6 (IV)	0	0	-6.89	$\bar{b}(\Gamma_i^A\gamma^0 t^a)q\,\bar{b}(t^a\gamma^0\tilde{\Gamma}_i^A)q + \bar{b}(t^a\gamma^0\Gamma_i^A)q\,\bar{b}(\gamma^0\tilde{\Gamma}_i^A t^a)q$
7 (V)	1	$\Omega_{3,i}$	-5.12	$\bar{b}(\Gamma_i^A t^a)q\,\bar{b}(\tilde{\Gamma}_i^A t^a)q$
8 (V)	$\frac{1}{4}$	$\Omega_{4,i}$	-1.05	$\bar{b}(\Gamma_i^A\sigma^{\mu\nu}t^a)q\,\bar{b}(\tilde{\Gamma}_i^A\sigma^{\mu\nu}t^a)q$
9 (V)	0	0	-2.43	$\bar{b}(\Gamma_i^A\gamma^\mu t^a)q\,\bar{b}(\tilde{\Gamma}_i^A\gamma^\mu t^a)q$

Table 3.4: Values of the contributions to γ_{ij} and d_{ij} for $\Delta B = 2$ 4-quark operators.

the form of the RGE at one loop is

$$\left[\mu\frac{\partial}{\partial\mu} - \beta_0\frac{g^3}{16\pi^2}\frac{\partial}{\partial g} + \hat{\gamma}\frac{g^2}{16\pi^2} + O(g^4)\right]_{ij} G_j(\mu, g) = 0 \tag{3.90}$$

where $\hat{\gamma}$ is the one loop anomalous dimension matrix (of which γ_{ij} are elements) for the operators $\mathcal{O}_i$ renormalized in the continuum at the scale μ. β_0 is β_0^{QCD} of eq. (2.39). For an asymptotically free theory one can neglect the contributions of higher order terms and the solution of eq. (3.90) is

$$G_i(\mu, g) = \left[\exp\left(-\frac{\hat{\gamma}}{\beta_0}\int_{\bar{g}}^{g}\frac{dg}{g}\right)\right]_{ij} G_j(\bar{\mu}, \bar{g}) \tag{3.91}$$

where $\bar{\mu}$ and $\bar{g} \equiv g(\bar{\mu})$ are constant values. Integrating it explicitly one obtains

$$G_i(\mu, g) = \left[g(\mu)^{-\hat{\gamma}/\beta_0}\right]_{ij} G_j(\bar{\mu}, \bar{g}) = \left[\alpha(\mu)^{-\gamma/2\beta_0}\right]_{ij} \bar{G}_j \tag{3.92}$$

where $\bar{G}_j$ are constant values.

Going back to the definition, eq. (3.89), one can rewrite eq. (3.92) for the renormalized operators

$$\mathcal{O}_i^{\overline{\mathrm{MS}},\mu} = z_{ij}(\mu, \mu')\mathcal{O}_j^{\overline{\mathrm{MS}},\mu'} = \left[\left(\frac{\alpha(\mu')}{\alpha(\mu)}\right)^{\hat{\gamma}/2\beta_0}\right]_{ij} \mathcal{O}_j^{\overline{\mathrm{MS}},\mu'} \tag{3.93}$$

In the simplest cases, since the anomalous dimension matrix is diagonal, one obtains

$$z_{ij}^{\text{light}}(\mu,\mu') = \delta_{ij}\left(\frac{\alpha(\mu')}{\alpha(\mu)}\right)^{\frac{4-\omega_{1,i}^2}{6\beta_0}} \tag{3.94}$$

$$z_{ij}^{\text{static}}(\mu,\mu') = \delta_{ij}\left(\frac{\alpha(\mu')}{\alpha(\mu)}\right)^{\frac{1}{\beta_0}} \tag{3.95}$$

For $\bar{b}\Gamma_i q\bar{q}\tilde{\Gamma}_i b$ and $\bar{b}\Gamma_i q\bar{b}\tilde{\Gamma}_i q$ type operators it is necessary to reduce the operators $\mathcal{O}_j$ of tables (3.2-3.4) to the same basis of the original operators before computing the exponential. This computation is straightforward but tedious and depends on the particular basis in which one is interested in. Therefore we will later present the result only for those operators which are needed in the rest of the thesis.

Alternatively one can make use of the relation

$$a^{bc} = e^{b\log a^c} \simeq 1 + b\log a^c = 1 + b(a^c - 1) \tag{3.96}$$

which is true for small values of $a^c - 1$ and can simplify eq. (3.93). One obtains

$$z_{ij}(\mu,\mu') = \left[\left(\frac{\alpha(\mu')}{\alpha(\mu)}\right)^{\hat{\gamma}/2\beta_0}\right]_{ij} \simeq \delta_{ij} + \frac{\gamma_{ij}}{N_c^2}\left[\left(\frac{\alpha(\mu')}{\alpha(\mu)}\right)^{\frac{N_c^2}{2\beta_0}} - 1\right] \tag{3.97}$$

This expression is known as the leading log approximation and it is appropriate even when the two indices i and j span different bases. Therefore eq. (3.97) is immediately applicable to the results of tab. 3.2 and 3.4.

3.3 Examples of interest

3.3.1 Computation of Z_A^{light}

By the symbol Z_A^{light} we refer (as in standard literature) to the matching coefficient for the axial current $A^\mu = \bar{q}\gamma^\mu\gamma^5 q$ between continuum and lattice schemes

$$(\bar{q}\gamma^\mu\gamma^5 q)^{\overline{\text{MS}},\mu} = Z_A^{\text{light}}(\mu,a)(\bar{q}\gamma^\mu\gamma^5 q)^{\text{latt},a} \tag{3.98}$$

Therefore we look in subsection 3.1.2 for the coefficients γ_{ij}, $d_{ij}^{\overline{\text{MS}}}$ and d^{latt} ,i.e. eqs.(3.39-3.41), and evaluate them for the values of the parameters ω corresponding to Γ_i=$\gamma^\mu\gamma^5$. From table 3.1(left) we read $\omega_{1,i} = 2$ and $\omega_{2,i} = -2$. Hence

$$\gamma_{ij} = 0 \tag{3.99}$$
$$d_{ij}^{\overline{\text{MS}}} = \delta_{ij} C_F \frac{1}{4} \tag{3.100}$$
$$d_{ij}^{\text{latt}} = \delta_{ij} C_F (2.3) \tag{3.101}$$

Therefore using eq. (3.18) we get

$$Z_A^{\text{light}} = 1 + \frac{\alpha_s}{4\pi} C_F(-2.1) \tag{3.102}$$

We observed that $\gamma^\mu\gamma^5$ is a conserved current (apart from the anomaly) therefore the associated Ward identity implies $\gamma_{ij} = 0$, in agreement with our finding.

3.3.2 Computation of Z_A^{static}

By the symbol Z_A^{static} we refer to the matching coefficient for zero component of the axial current $A^0 = \bar{b}\gamma^0\gamma^5 q$ (which corresponds to an interpolating operator that creates a static B meson) between continuum and lattice schemes

$$(\bar{b}\gamma^0\gamma^5 q)^{\overline{\text{MS}},\mu} = Z_A^{\text{static}}(\mu, a)(\bar{b}\gamma^0\gamma^5 q)^{\text{latt},a} \tag{3.103}$$

Therefore we look in subsection 3.1.3 for the coefficients γ_{ij}, $d_{ij}^{\overline{\text{MS}}}$ and d^{latt} ,i.e. eqs.(3.51-3.53), and evaluate them for the values of the parameters ω corresponding to Γ_i=$\gamma^0\gamma^5$. From table 3.1(left) we read $\omega_{3,i} = -1$. Hence

$$\gamma_{ij} = \delta_{ij} C_F(-3/2) \tag{3.104}$$
$$d_{ij}^{\overline{\text{MS}}} = \delta_{ij} C_F (5/4) \tag{3.105}$$
$$d_{ij}^{\text{latt}} = \delta_{ij} C_F (19.44) \tag{3.106}$$

Therefore using eq. (3.18) we get

$$Z_A(\mu, a)^{\text{static}} = 1 + \frac{\alpha_s}{4\pi} C_F (3/2 \log \lambda^2 a^2 + 5/4 - 21.6) \tag{3.107}$$

3.3.3 Computation of Z_{ij} for $B - \bar{B}$ Mixing

We are particularly interested in the operator whose matrix elements contains the non-perturbative QCD effects for B^0-$\bar{B}^0$ mixing:

$$\mathcal{O}_L^{\overline{\text{MS}}} = \frac{1}{2}\left[\bar{b}_1\gamma^\rho L q_2\, \bar{b}_3\gamma_\rho L q_4 - \bar{b}_1\gamma^\rho L q_4\, \bar{b}_3\gamma_\rho L q_2\right] \tag{3.108}$$

The indices $1, 2, 3$ and 4 are fictitious quantum numbers used to track the two possible inequivalent Wick contractions of the fields when computing matrix elements. In this case the different operators $\mathcal{O}_j$ of table 3.4 reduce to 3 independent ones:

$$\mathcal{O}_R^{\mathrm{latt}} = \frac{1}{2}\left[\bar{b}_1\gamma^\rho Rq_2\,\bar{b}_3\gamma_\rho Rq_4 - \bar{b}_1\gamma^\rho Rq_4\,\bar{b}_3\gamma_\rho Rq_2\right] \tag{3.109}$$

$$\begin{aligned}\mathcal{O}_N^{\mathrm{latt}} &= \bar{b}_1 Lq_2\,\bar{b}_3 Rq_4 + \bar{b}_1 Rq_2\,\bar{b}_3 Lq_4 + \frac{1}{2}\bar{b}_1\gamma^\rho Lq_2\,\bar{b}_3\gamma_\rho Rq_4 + \frac{1}{2}\bar{b}_1\gamma^\rho Rq_2\,\bar{b}_3\gamma_\rho Lq_4 \\ &- \bar{b}_1 Lq_4\,\bar{b}_3 Rq_2 - \bar{b}_1 Rq_4\,\bar{b}_3 Lq_2 - \frac{1}{2}\bar{b}_1\gamma^\rho Lq_4\,\bar{b}_3\gamma_\rho Rq_2 - \frac{1}{2}\bar{b}_1\gamma^\rho Rq_4\,\bar{b}_3\gamma_\rho Lq_2\end{aligned} \tag{3.110}$$

as well as $\mathcal{O}_L^{\mathrm{latt}}$ itself. In fact when one computes perturbative corrections to $\mathcal{O}_L$ the operators $\mathcal{O}_j$ of table 3.4 can be simplified using Fierz identities:

$$\mathcal{O}_1 = \mathcal{O}_2 = 2\left(\frac{1}{N}+1\right)\mathcal{O}_L \tag{3.111}$$

$$\mathcal{O}_2 = 2\left(\frac{1}{N}+1\right)\mathcal{O}_L \tag{3.112}$$

$$\mathcal{O}_3 = -\left(\frac{1}{N}+1\right)\mathcal{O}_N \tag{3.113}$$

$$\mathcal{O}_4 = -2\left(\frac{N-1}{2N}\right)\mathcal{O}_L \tag{3.114}$$

$$\mathcal{O}_5 = \left(\frac{1}{N}-1\right)\mathcal{O}_N \tag{3.115}$$

$$\mathcal{O}_6 = \mathcal{O}_7 = \mathcal{O}_8 = -\left(\frac{N-1}{2N}\right)\mathcal{O}_L \tag{3.116}$$

$$\mathcal{O}_9 = -\left(\frac{N-1}{2N}\right)\mathcal{O}_R \tag{3.117}$$

Adding the different contributions with the appropriate coefficients d_{ij} we get

$$\mathcal{O}_L^{\overline{\mathrm{MS}}} = (1+\frac{\alpha_s}{4\pi}D_L)\mathcal{O}_L^{\mathrm{latt}} + \frac{\alpha_s}{4\pi}D_N\mathcal{O}_N^{\mathrm{latt}} + \frac{\alpha_s}{4\pi}D_R\mathcal{O}_R^{\mathrm{latt}} \tag{3.118}$$

where

$$D_L = -22.4\ ,\quad D_N = -13.8 \quad \text{and } D_R = -3.2\ \ . \tag{3.119}$$

The results for D_L and D_N in eq. (3.119) agree with those in the literature [66], whereas that for D_R does not (a similar conclusion was reached independently

D_{ij}	$i=1$	$i=2$	$i=3$	$i=4$	$\mathcal{O}_j^{\mathrm{latt}}$
$j=1$	-21.64	-	2.06	0.54	$\bar{b}\gamma^\mu Lq\,\bar{q}\gamma^\mu Lb$
$j=2$	-	-21.64	2.16	2.40	$\bar{b}Lq\,\bar{q}Rb$
$j=3$	9.29	2.43	-10.80	2.83	$\bar{b}\gamma^\mu Lt^a q\,\bar{q}\gamma^\mu Lt^a b$
$j=4$	9.72	10.79	11.34	-9.05	$\bar{b}Lt^a q\,\bar{q}Rt^a b$
$j=5$	-18.37	-	-3.06	-	$\bar{b}\gamma^\mu Rq\,\bar{q}\gamma^\mu Lb$
$j=6$	36.75	18.37	6.12	3.06	$\bar{b}Lq\,\bar{q}Lb$
$j=7$	-13.78	-	6.89	-	$\bar{b}\gamma^\mu Rt^a q\,\bar{q}\gamma^\mu Lt^a b$
$j=8$	27.56	13.78	-13.78	-6.89	$\bar{b}Lt^a q\,\bar{q}Lt^a b$

Table 3.5: Coefficients D_{ij} for the four operators of eqs. (3.123)-(3.126).

by Giménez [121]). In ref. [66] the quoted result is $D_R = -5.4$ [2].

3.3.4 Computation of Z_{ij} for B Decay

In the computation of inclusive decay times, in chapter 5, we will need the matching coefficients for the four operators

$$\mathcal{O}_1^{\overline{\mathrm{MS}}} = \bar{b}\gamma^\mu Lq\,\bar{q}\gamma^\mu Lb \tag{3.123}$$

$$\mathcal{O}_2^{\overline{\mathrm{MS}}} = \bar{b}Lq\,\bar{q}LRb \tag{3.124}$$

$$\mathcal{O}_3^{\overline{\mathrm{MS}}} = \bar{b}\gamma^\mu Lt^a q\,\bar{q}\gamma^\mu Lt^a b \tag{3.125}$$

$$\mathcal{O}_4^{\overline{\mathrm{MS}}} = \bar{b}Lt^a q\,\bar{q}\gamma^\mu Rt^a b \tag{3.126}$$

[2] We believe that the reason is that in eq. (B.16) of ref. [65] there should be a correction:

$$(\ldots) + \frac{g^2}{16\pi^2}\frac{4}{3}(\omega+\omega^I) \to (\ldots) - \frac{g^2}{16\pi^2}\frac{4}{3}(\omega+\omega^I)\,O_R^{\mathrm{latt}}\ , \tag{3.120}$$

eq. (B.26) should be replaced by

$$D_R^I = \frac{1}{3}[s + 4\omega^I - 2(l+m)] \tag{3.121}$$

and that in table 3

$$D_R^I = -0.38 \ \text{ for } r = 1\ . \tag{3.122}$$

There errors are carried forward into successive papers [66], [67] and [68]. Moreover in the same paper, in the definition of v^I (eq. (B.17)), the term Δ_2 at the denominator should be replaced by Δ_2^2 (the correct expression is reported in Appendix D).

For each of them we pick up the d^{ij} coefficients from table 3.2 and we project the operators $\mathcal{O}_j$ on a convenient basis. In the basis of table 3.5 we can reexpress our results in the formula

$$\mathcal{O}_i^{\overline{\rm MS}} = Z_{ij}\mathcal{O}_j^{\rm latt} = \mathcal{O}_i^{\rm latt} + \frac{\alpha_s}{4\pi}D_{ij}\mathcal{O}_j^{\rm latt} \tag{3.127}$$

where the D_{ij} coefficients are also reported in table 3.5.

3.3.5 Computation of z_{ij} for B Decay

In the computation of inclusive decay times, in chapter 5, we will also need the matching coefficients for the two 4-quark operators

$$\mathcal{O}_1^{\overline{\rm MS}} = \bar{b}\gamma^\mu Lq\bar{q}\gamma_\mu Lb \tag{3.128}$$
$$\mathcal{O}_2^{\overline{\rm MS}} = \bar{b}\gamma^\mu Lt^a q\bar{q}\gamma_\mu Lt^a b \tag{3.129}$$

In this basis one can rearrange the coefficients γ_{ij} of table (3.2) and, for three colours, one finds

$$\hat{\gamma} = \begin{pmatrix} 8 & 6 \\ -4/3 & 1 \end{pmatrix} \tag{3.130}$$

Therefore using the leading log approximation, eq. (3.97), one gets

$$\left(\frac{\alpha(\mu')}{\alpha(\mu)}\right)^{\hat{\gamma}/2\beta_0} = 1 + \begin{pmatrix} 8/9 & -2/3 \\ -4/27 & 1/9 \end{pmatrix}\left[\left(\frac{\alpha(\mu')}{\alpha(\mu)}\right)^{18/\beta_0} - 1\right] \tag{3.131}$$

which is the same result quoted by Neubert and Sachrajda in ref. [91].

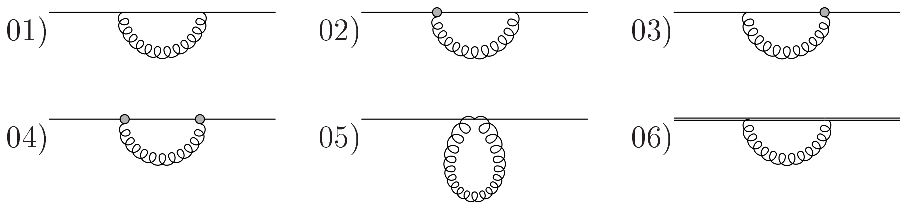

Figure 3.1: Lattice Feynman graphs contributing to 1-loop corrections to light and heavy quark propagators.

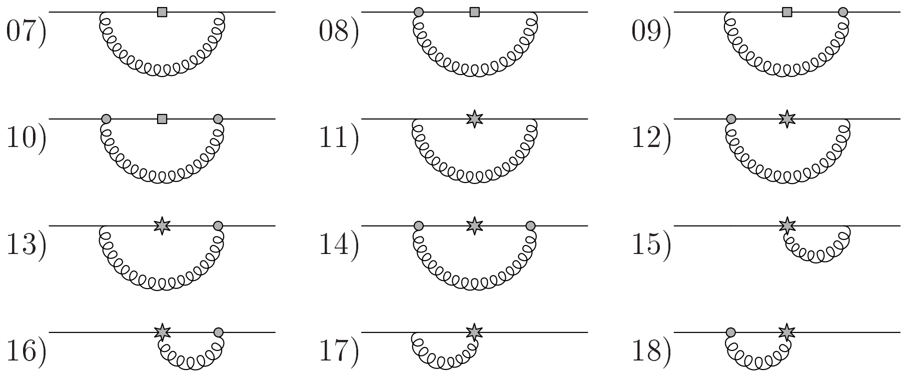

Figure 3.2: Lattice Feynman graphs contributing to 1-loop corrections to $\bar{q}\Gamma_i q$ type operators.

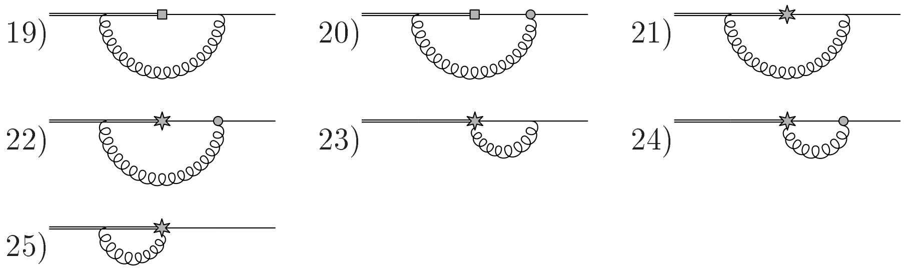

Figure 3.3: Lattice Feynman graphs contributing to 1-loop corrections to $\bar{b}\Gamma_i q$ type operators.

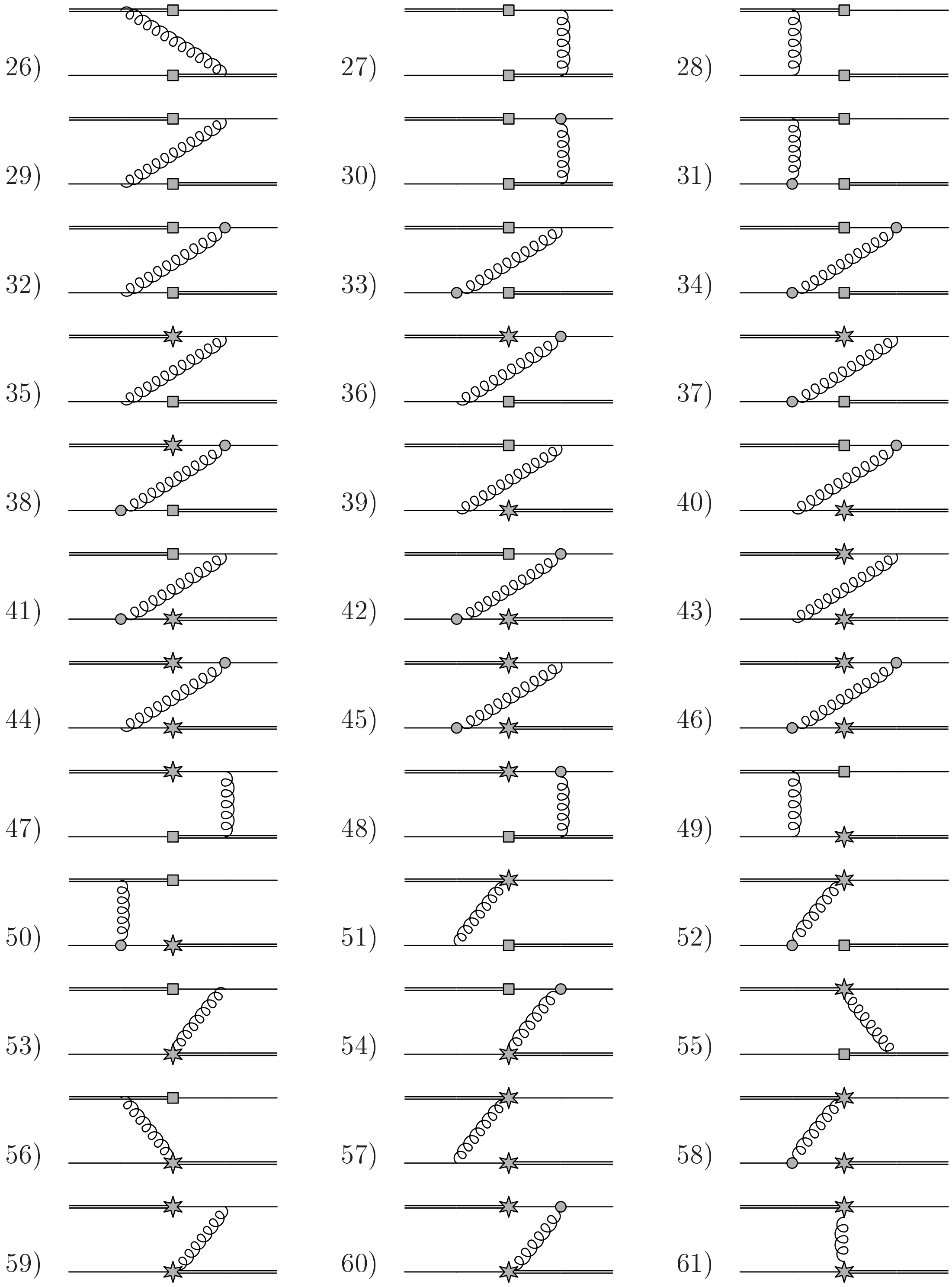

Figure 3.4: Lattice Feynman graphs contributing to 1-loop corrections to $\bar{b}\Gamma_i q\bar{q}\tilde{\Gamma}_i b$ and $\bar{b}\Gamma_i q\bar{b}\tilde{\Gamma}_i q$ type operators.

Chapter 4

The $g_{B^*B\pi}$ Effective Coupling

This chapter is based on the published paper:
G. De Divitiis, L. Del Debbio, M. Di Pierro, J. Flynn, C. Michael and J. Peisa [UKQCD Collaboration], "Towards a lattice determination of the $g_{B^*B\pi}$ coupling", JHEP **9810** (1998) 010; hep-lat/9807032

4.1 Introduction

We showed in chapter 2 that the form factor $g_{B^*B\pi}(q^2)$ that appears in eq. (2.73)

$$\langle B^0(p)\pi^+(q)|B^{*+}(p')\rangle = -g_{B^*B\pi}(q^2)q_\mu\eta^\mu(p')\,(2\pi)^4\,\delta(p'-p-q) \tag{4.1}$$

is related, for an on-shell pion, to the coupling constant g that appears in the Heavy Meson Chiral Lagrangian, eq. (2.70),

$$g \equiv \frac{f_\pi}{2m_B} g_{B^*B\pi} \tag{4.2}$$

where $g_{B^*B\pi}$ is defined as

$$g_{B^*B\pi} = \lim_{q^2\to m_\pi^2} g_{B^*B\pi}(q^2) \tag{4.3}$$

Moreover starting from eq. (4.1) and performing an LSZ reduction of the pion field, we find that the coupling $g_{B^*B\pi}$ is related to the form factor at zero momentum-transfer of the axial current between hadronic states. Such a relation is the analog, in the $B\pi$ system, of the Goldberger-Treiman relation, relating the nucleon electromagnetic form factor to the nucleon-nucleon-pion coupling. An important consequence of the Goldberger-Treiman relation, for our purposes, is that it allows a numerical evaluation of the $g_{B^*B\pi}$ coupling, as the form factors of the axial current can be evaluated by a lattice simulation. The details of the pion reduction are presented in Section 4.1.1.

The interest of such a computation is two-fold. From a theoretical point-of-view, it is interesting *per se* to be able to fix, from lattice QCD, the coupling appearing in the heavy meson chiral lagrangian. In addition, it is important to stress that this determination also has phenomenological motivations. Assuming vector meson dominance (VMD) in the $B \to \pi l \nu$ decay, the coupling $g_{B^*B\pi}$ fixes the normalisation of the form factors used to parametrise the matrix element of the weak vector current, $V^\mu = \bar{u}\gamma^\mu b$, between hadronic states. Defining the form factors by

$$\begin{aligned} \langle \pi^+(p')|V^\mu|\bar{B}(p)\rangle &= f_1(q^2)(p+p'-\frac{m_B^2-m_\pi^2}{q^2}q)^\mu + f_0(q^2)\frac{m_B^2-m_\pi^2}{q^2}q^\mu \\ &= f_+(q^2)(p+p')^\mu + f_-(q^2)q^\mu \end{aligned} \tag{4.4}$$

where $q = p - p'$ is the transferred momentum, the contribution from the B^* channel is easily evaluated

$$f_1(q^2) = \frac{g_{B^*B\pi}}{2f_{B^*}} \frac{1}{1-q^2/m_{B^*}^2} \tag{4.5}$$

The normalisation of the form factor therefore depends on the $B^*B\pi$ coupling and the decay constant of the vector meson, defined as

$$\langle 0|V^\mu|\bar{B}^*(p)\rangle = i\frac{m_{B^*}^2}{f_{B^*}}\eta^\mu(p) \tag{4.6}$$

Heavy quark symmetry and chiral symmetry justify this pole form for f_1 when q^2 is close to $q^2_{\mathrm{max}} = (m_B - m_\pi)^2$ [44, 47, 48, 50, 69, 70]. For q^2 far from q^2_{max}, the pole form may be taken as a phenomenological ansatz. However, we note that the functional dependence of the form factor in eq. (4.5) cannot be simultaneously consistent with heavy quark symmetry at large q^2, which demands that $f_1(q^2_{\mathrm{max}}) \sim m_B^{1/2}$ and the light-cone sum rule scaling relation at $q^2 = 0$, which states $f_1(q^2{=}0) \sim m_B^{-3/2}$ [71][1]. Nonetheless, by fitting lattice results, which are available in the high q^2 region where the pole form is justified, we can determine the parameters in eq. (4.5).

It is interesting to remark that the interplay of the effective Lagrangian approach and lattice simulations provides another determination of the form factors for the heavy-to-light B decays and therefore sheds further light on the theoretical determination of the non-perturbative effects mentioned at the beginning. This result can be compared with direct computations of the same quantities obtained by fitting lattice data [73], using unitarity bounds [74] and sum rules [75, 76].

In the work described here, the matrix element of the light quark axial current between the heavy mesons is computed in a quenched lattice simulation of QCD

[1] Light-cone sum rules have also been applied at large q^2 and reproduce the $m_B^{1/2}$ scaling behaviour of f_1 as demanded by heavy quark symmetry [72]

in the static heavy quark limit, using stochastic methods to compute the desired light quark propagators, as described in Section 4.2. The discussion of systematic errors is an important issue in any lattice calculation and plays a crucial part in estimating the error on the final result. In this respect, it is important to stress here that we are presenting an exploratory study. Our main concern is therefore to test the possibility of extracting the coupling defined above, rather than presenting its best lattice determination. Such a task would require a more extensive simulation and is left for further studies.

Renormalisation constants are needed in order to connect lattice results with continuum physical observables. Those relevant for the action and the quantities considered in this paper are summarised in section 4.2.1.

The best estimate we obtain for g is

$$g \equiv \frac{f_\pi}{2m_B} g_{B^*B\pi} = 0.42(4)(8) \tag{4.7}$$

The phenomenological implications of this result are discussed in section 4.3.

The value of g enters many phenomenological quantities of interest calculated in heavy meson chiral perturbation theory, including the form factors for semileptonic $B \to \pi$ decays mentioned here, as well as $B^* \to \pi$ decays and other quantities such as ratios of heavy meson leptonic decay constants, heavy meson mass splittings and radiative decays. Even the relatively crude estimate obtained here should be interesting for heavy meson phenomenology, but we believe future more precise lattice computations would be valuable.

4.1.1 Pion reduction

An LSZ reduction of the pion in the definition of $g_{B^*B\pi}$, eq. (4.1), yields

$$\langle B^0(p)\pi^+(q)|B^{*+}(p+q)\rangle = i(m_\pi^2 - q^2)\int_x e^{iq\cdot x}\langle \bar{B}(p)|\pi(x)|B^*(p+q)\rangle \tag{4.8}$$

Using the PCAC relation

$$\pi(x) = \frac{1}{m_\pi^2 f_\pi}\partial^\mu A_\mu(x) \tag{4.9}$$

where A_μ is, as usual, the QCD axial current, eq. (4.8) becomes

$$\langle B^0(p)\pi^+(q)|B^{*+}(p+q)\rangle = q^\mu \frac{1}{f_\pi}\frac{m_\pi^2 - q^2}{m_\pi^2}\int_x e^{iq\cdot x}\langle \bar{B}(p)|A_\mu(x)|B^*(p+q)\rangle \tag{4.10}$$

The matrix element of the axial current is parametrised in terms of three form factors

$$\begin{aligned}\langle B^0(p)|A_\mu(0)|B^{*+}(p+q)\rangle &= \eta_\mu F_1(q^2) + (\eta\cdot q)\,(2p+q)_\mu F_2(q^2) \\ &\quad + (\eta\cdot q)\,q_\mu F_3(q^2)\end{aligned} \tag{4.11}$$

yielding for the $B^*B\pi$ coupling

$$g_{B^*B\pi}(q^2) = -\frac{1}{f_\pi}\frac{m_\pi^2-q^2}{m_\pi^2}\left[F_1(q^2) + \left(m_{B^*}^2 - m_B^2\right)F_2(q^2) + q^2F_3(q^2)\right] \tag{4.12}$$

In the static limit in which our simulation is performed, the B and B^* mesons are degenerate, so that the form factor F_2 can be discarded.

Analytical continuation of eq. (4.12) towards the soft–pion limit ($q^2 \to 0$), leads to

$$g_{B^*B\pi}(0) = -\frac{1}{f_\pi}F_1(0) \tag{4.13}$$

It is commonly assumed, when deriving the Goldberger-Treiman relation, that $g_{B^*B\pi}$ is a smooth function of q^2, and, therefore, that the physical coupling can be approximated by

$$g_{B^*B\pi} = g_{B^*B\pi}(m_\pi^2) \approx g_{B^*B\pi}(0) \tag{4.14}$$

The above equation explicitly shows that, in the soft–pion limit, the $B^*B\pi$ coupling is related to the form factor of the axial current between B and B^* states. If one were working in the chiral limit from the very beginning, the same Goldberger-Treiman relation, eq. (4.13), would be obtained from the conservation of the axial current.

The relation between $g_{B^*B\pi}$ and g mentioned earlier can be rederived by comparing the matrix element of the Noether current associated to chiral symmetry both in HMχ and QCD. In the chiral limit, the Noether currents associated with chiral symmetry, in QCD and in HMχ, are respectively

$$A^{ab}_{\mathrm{QCD},\mu} = \bar{q}^a\gamma_\mu\gamma_5 q^b \tag{4.15}$$

and

$$A^{ab}_{\mathrm{HM}\chi,\mu} = f_\pi\partial_\mu\mathcal{M}^{ab} - 2g\left(B_\mu^{*\,a\,\dagger}B^b + B^{a\,\dagger}B_\mu^{*\,b}\right) + \cdots \tag{4.16}$$

where the ellipsis denotes terms with more than one pion or terms containing both heavy-mesons and pions.

The form factors of the axial current in QCD are related to the coupling of the

Figure 4.1: Tree-level diagrams needed to compute the matrix element of the axial current in HMχ. The dot ($\bullet$) represents the g-vertex in the HMχ lagrangian; the squares are insertions of the axial current in eq. (4.16).

heavy meson chiral lagrangian by matching the two theories at tree level. The diagrams needed at tree level to evaluate the matrix element in eq. (4.11) for the HMχ current are depicted in fig. 4.1. A straightforward computation leads to

$$\begin{aligned} F_1(q^2) &= -2g\, m_B \\ F_3(q^2) &= \frac{2g}{q^2} m_B \end{aligned}$$

which, together with the Golberger-Treiman relation, reproduces eq. (2.77). One may also work away from the chiral and heavy quark limits and include corrections for finite mass pions and heavy quarks in this result.

The determination of g is therefore reduced to the computation of the matrix element of the light-light axial vector current between hadronic states. Such an evaluation can be performed using three-point correlation functions on the lattice. The details of the calculation are reported in the next section.

4.2 Results

4.2.1 Renormalisation constants

Quantities that will be evaluated on the lattice are connected to their continuum counterparts by a finite renormalisation. In order to extract physical information, the matrix element of a bilinear quark operator defined on the lattice, $\mathcal{O}^{\mathrm{latt},a}$, has to be multiplied by the corresponding renormalisation constant

$$\mathcal{O}^{\overline{\mathrm{MS}},\mu} = Z(a\mu, g)\, \mathcal{O}^{\mathrm{latt},a} \tag{4.17}$$

which in general depends on the renormalisation scale μ and the details of the lattice discretization (a single continuum operator may also match onto a set of lattice operators). For partially conserved currents, the μ dependence disappears in the above definition, the associated anomalous dimension being equal to zero. This is the case for the QCD light-light axial current considered here. It is also the case for the heavy-light current in full QCD, but not for the static-light current onto which it matches in the effective theory: hence the renormalisation constant $Z_A^{\rm static}$ in eq. (4.25) below, which converts the lattice matrix element to the physical $f_B^{\rm static}$, includes the effect of running between different scales in the effective theory.

In our simulation, we use the standard gluon action and the tadpole-improved Sheikholeslami-Wohlert [111, 56] fermion action for the light quarks. Our value of $\beta = 5.7$ implies $a^{-1} = 1.10$GeV and $c_{SW} = 1.57$.

The matrix element of the light-light axial current between an initial state i and a final state f in the continuum can be written as[2]

$$\langle f|\, A_\mu \,|i\rangle^{\overline{\rm MS}} = Z_A^{\rm tadpole} \langle f|\, A_\mu \,|i\rangle^{\rm latt} = Z_A^{1-{\rm loop}} \frac{u_0}{u_0^{1-{\rm loop}}} \langle f|\, A_\mu \,|i\rangle \tag{4.18}$$

The factor u_0, a measure of the average link variable, can be interpreted as a non-perturbative rescaling of the quark fields in the tadpole improvement prescription. For our lattice $u_0 = 0.86081$.

The perturbative part reads

$$\frac{Z_A^{1-{\rm loop}}}{u_0^{1-{\rm loop}}} = \frac{1+\frac{\alpha C_F}{4\pi}\zeta_A}{1+\frac{\alpha C_F}{4\pi}\lambda} \simeq 1 + \frac{\alpha C_F}{4\pi}(\zeta_A - \lambda) \tag{4.19}$$

where $\lambda = -\pi^2$ for the plaquette definition used for u_0 and $\zeta_A = -13.8$ [112, 113].

We note here that the removal of tree-level $O(a)$ discretisation errors is achieved by combining the Sheikholeslami-Wohlert action for $c_{SW} = 1$ with improved operators, found by redefining or "rotating" the quark fields [114]. In our simulation, the rotation has not been applied to the quarks, so the perturbative coefficient ζ above is calculated using the improved action only. Moreover, in perturbation theory, $c_{SW} = 1 + O(\alpha)$, so we quote ζ above calculated for $c_{SW} = 1$, without rotated light quark fields. In [115] the light fermion bilinear operator renormalisations are given as functions of c_{SW} and an arbitrary amount of field rotation: using our actual value of $c_{SW} = 1.57$, with no field rotation, in those results would increase Z_A by 5%.

The mean-field improved perturbative expansion is performed in terms of a boosted coupling constant, $\tilde{\alpha}$, which in our case is chosen as $\tilde{\alpha} = \alpha_0/u_0^4$, where α_0 is the bare lattice coupling constant. We use $\tilde{\alpha}$ for α in eq. (4.19). For our lattice, with $\beta = 5.7$ and $u_0 = 0.86081$ from the average plaquette, this leads to

$$Z_A^{\rm tadpole} = Z_A^{1-{\rm loop}} \frac{u_0}{u_0^{1-{\rm loop}}} = 0.806. \tag{4.20}$$

[2]Note that $Z_A^{\text{1-loop}}$ is computed similarly to $Z_A^{\rm light}$ of eq. (3.102) but the former does not include contributions from the rotation of the operator, while the latter does. In this case the former is used for consistency with the tadpole improved action.

In the same way it is necessary to match the renormalized current that we use to create a B (or equivalently a B^*) meson

$$\langle 0|\, J_0^B \,|B\rangle^{\overline{\rm MS}} = Z_A^{\rm static} \,\langle 0|\, J_0^B \,|B\rangle^{\rm latt} \tag{4.21}$$

Using the results of chapter 3, we obtain

$$Z_A^{\rm static} = 1 - 20\frac{\alpha_s^{\rm latt}(a^{-1})}{4\pi} = 0.75 \tag{4.22}$$

As an alternative method, we also computed $Z_A^{\rm static}$ using a more sophisticated technique proposed by Lepage and Mackenzie [111]. We performed the matching at a different scale, q^*, which is determined from the expectation value of $\ln(qa)^2$ in the one-loop lattice perturbation theory integrals for the corrections to the renormalisation constant, including the perturbative tadpole improvement corrections for the chosen definition of u_0. For the improved, $c_{SW} = 1$, action and plaquette definition of u_0, Giménez and Reyes [121] quote $q^*a = 2.29$. We used this value. We will also adopt a plaquette definition of the lattice coupling constant according to (for zero flavours)

$$\frac{1}{3}\ln\, {\rm tr}P_{\mu\nu} = -\frac{4\pi}{3}\alpha_s(3.41/a)(1-1.19\alpha_s) \tag{4.23}$$

Once α_s is determined, we can use the equation for the running of α_s, at two loops,

$$\alpha_s(q) = \frac{2\pi}{\beta_0\ln(q/\Lambda) + \frac{\beta_1}{2\beta_0}\ln\left(2\ln(q/\Lambda)\right)} \tag{4.24}$$

to determine $\alpha_s(q^*)$. In the quenched theory, $\beta_0 = 11$ and $\beta_1 = 102$. We find $a\Lambda = 0.294$ and $\alpha_s(q^*) = 0.216$.

Since $q^* = 2.52$GeV (extracted from ref. [121] using our value for a^{-1}) is between the charm and b quark thresholds we perform the continuum running with four active flavours. From the Particle Data Group (PDG) [122], we take $\Lambda_{QCD}^{\overline{\rm MS}\,(5)} = 237^{+26}_{-24}$MeV using two-loop running, and find $\Lambda_{QCD}^{\overline{\rm MS}\,(4)}$ using continuity of the strong coupling at the b quark threshold. This threshold value is given by m_b satisfying $m_b^{\overline{\rm MS}}(m_b) = m_b = 4.25$GeV, using the average of the range, 4.1–4.4GeV, quoted by the PDG [122].

The overall renormalisation constant is thus given by:

$$\begin{aligned} Z_A^{\rm static} &= \left(\frac{\alpha_s(m_b)}{\alpha_s(q^*)}\right)^{-\frac{6}{25}}\left\{1-\frac{8}{3}\frac{\alpha(m_b)}{4\pi}+0.91\frac{\alpha(q^*)-\alpha(m_b)}{4\pi}\right\} \\ &\quad\times\sqrt{u_0}\left\{1+\frac{\alpha_V(q^*)}{4\pi}\left[4\ln(q^*a)-19.36+\frac{2}{3}\pi^2\right]\right\} \end{aligned} \tag{4.25}$$

Using the inputs given above, we find

$$Z_A^{\text{static}} = 0.78 \tag{4.26}$$

in agreement with our naive estimate of eq. (4.22). Independent variations of $\Lambda^{(5)}$ and m_b to the ends of the ranges quoted above and $\pm 10\%$ variation in a^{-1} change this value by 1.3% or less. Changing q^* to $1/a$ or π/a reduces Z_A^{static} by 13% or raises it by 1.3% respectively.

We close this section by noting that both Z_A^{tadpole} and Z_A^{static} are evaluated in the chiral limit and so do not depend on the light quark mass used in the simulation.

4.2.2 Stochastic propagators

The numerical analysis is carried out on 20 quenched gauge configurations, generated on a $12^3 \times 24$ lattice at $\beta = 5.7$, corresponding to $a^{-1} = 1.10$ GeV. The heavy quark propagators are evaluated in the static limit [63]. Stochastic propagators [107, 108] are used to invert the fermionic matrix for the light quarks. They can be used in place of light quark propagators calculated with the usual deterministic algorithm. The stochastic inversion is based on the relation

$$S_{ij} = (Q^{-1})_{ij} = \frac{1}{Z} \int [\mathrm{d}\phi] \; (Q_{jk}\phi_k)^* \phi_i \; \exp\left(-\phi_i^* (Q^\dagger Q)_{ij} \phi_j\right) \tag{4.27}$$

where, in our case, Q is the tadpole improved SW fermionic operator of eq. (2.97) and the indices i, j, k represent simultaneously the space-time coordinates, the spinor and colour indices. Two values of κ are considered, $\kappa_1 = 0.13843$ and $\kappa_2 = 0.14077$, with $c_{SW} = 1.57$. The heavier value, κ_1, corresponds to a bare mass of the light quark around $m = 140$ MeV and κ_2 corresponds to a lighter mass $m = 75$ MeV. The chiral limit corresponds to $\kappa_{crit} = 0.14351$ [109]. For every gauge configuration, an ensemble of 24 independent fields ϕ_i is generated with gaussian probability

$$P[\phi] = \frac{1}{Z} \exp\left(-\phi_i^* (Q^\dagger Q)_{ij} \phi_j\right) \tag{4.28}$$

All light propagators are computed as averages over the pseudo-fermionic samples:

$$S_{ij} = \begin{cases} \langle (Q\phi)_j^* \phi_i \rangle \\ \text{or} \\ \langle (\gamma_5 \phi^*)_j \, (Q\phi\gamma_5)_i \rangle \end{cases} \tag{4.29}$$

where the two expressions are related by the H symmetry: $S = \gamma_5 S^\dagger \gamma_5$. Moreover, the maximal variance reduction method is applied in order to minimise the statistical noise [107]. Maximal variance reduction involves dividing the lattice into two boxes ($0 < t < T/2$ and $T/2 < t < T$) and solving the equation of motion numerically within each box, keeping the spinor field ϕ on the boundary fixed. According to the maximal reduction method, the fields which enter the correlation functions must be either the original fields ϕ or solutions of the equation of motion in disconnected regions. The stochastic propagator is therefore defined from each point in one box to every point in the other box or on the boundary. For this reason, when computing a three-point correlation function

$$\langle 0|J(t_1,x)\mathcal{O}(t_0,y)J^\dagger(t_2,z)|0\rangle \tag{4.30}$$

one operator — $\mathcal{O}$ in the present work — is forced to be on the boundary ($t_0 = 0$ or $T/2$) and the other two must be in different boxes, while the spatial coordinates are not constrained. If j is a point of the boundary, not all the terms in $(Q\phi)_j$ lie on the boundary because the operator Q involves first neighbours in all directions. Hence, whenever a propagator S_{ij} is needed with one of the points on the boundary, we use whichever of the two expressions in eq. (4.29) has the spinor $Q\phi$ computed away from the boundary.

It is generally advantageous to "smear" the interpolating operators J and $J^\dagger$ over the spatial coordinates, in order to enhance the overlap with the ground state. In our simulations spatial fuzzed links are used for smearing the hadronic interpolating operators [110, 107]. This technique consists in replacing light quark field $q(x)$, by a "fuzzed" field

$$q^F(x) = \sum_{i=1,2,3} U_i^F(x)q(x+\hat{\imath}) + U_{-i}^F(x)q(x-\hat{\imath}) \tag{4.31}$$

where $U_{\pm i}^F(x)$ are defined by the recursive relations

$$U_i^F(x) = \mathcal{P}_{SU(2)}\Big[\zeta\, U_i^F(x) + \sum_{j\neq i} U_j^F(x)U_i^F(x+\hat{\jmath})U_{-j}^F(x+\hat{\imath}+\hat{\jmath}) + \tag{4.32}$$

$$U_{-j}^F(x)U_i^F(x-\hat{\jmath})U_j^F(x+\hat{\imath}-\hat{\jmath})\Big] \tag{4.33}$$

$$U_{-i}^F(x) = \mathcal{P}_{SU(2)}\Big[\zeta\, U_{-i}^F(x) + \sum_{j\neq i} U_j^F(x)U_{-i}^F(x+\hat{\jmath})U_{-j}^F(x-\hat{\imath}+\hat{\jmath}) + \tag{4.34}$$

$$U_{-j}^F(x)U_{-i}^F(x-\hat{\jmath})U_j^F(x-\hat{\imath}-\hat{\jmath})\Big] \tag{4.35}$$

starting with initial values $U_i^F(x) = U_i(x)$ and $U_{-i}^F(x) = U_i^\dagger(x-\hat{\imath})$. $\mathcal{P}_{SU(2)}$ is a projector on $SU(2)$, implemented as in the Cabibbo-Marinari cooling algorithm, and $\zeta = 2.5$ is a constant value. The recursive procedure to compute $U_{\pm i}^F(x)$ has been applied twice.

4.2.3 Lattice computation

In order to extract g, the three-point correlation function C_3 and the two-point correlation function C_2 for local (L) and fuzzed (F) sources are computed. The FF three-point function is defined as

$$C_{3\ \mu\nu}^{FF}(\mathbf{x};t_1,t_2) = \frac{1}{V}\int d^3y\ \langle 0|J_\nu^{B^*}(\mathbf{y},-t_1)A_\mu(\mathbf{x}+\mathbf{y},0)J^{B\ \dagger}(\mathbf{y},t_2)|0\rangle \quad (4.36)$$

where $J_\nu^{B^*}$ and J^B are fuzzed operators with the quantum numbers corresponding respectively to the B^* and B states. Analogous definitions hold for the FL and LL cases. For time separations that are large enough to isolate the lowest energy states, the three-point function is related to the axial current matrix element

$$\begin{aligned} C_{3\ \mu\nu}^{FF}(\mathbf{x};t_1,t_2) &\to \langle 0|J_\nu^{B^*}|B^*,\xi\rangle\frac{\langle B^*,\xi|A_\mu(\mathbf{x})|B\rangle}{2m_B\,2m_B}\langle B|J^{B\ \dagger}|0\rangle e^{-M_B(t_1+t_2)} \\ &= Z^F\eta_\nu^\xi(0)\frac{\langle B^*,\xi|A_\mu(\mathbf{x})|B\rangle}{2m_B}Z^F e^{-M_B(t_1+t_2)} \quad (4.37)\end{aligned}$$

where ξ is the polarisation label of the vector particle, and the sum over polarisations is omitted. In the static limit considered in this paper, the slope of the exponential time-decay is not the physical mass of the mesons; it can be interpreted as a binding energy. Moreover, the two-point functions for the vector and pseudoscalar particles are degenerate, leading to the same binding energies and Z factors for both the B and B^*. In order to avoid confusion, the physical mass is denoted by m_B and the binding energy by M_B. Z^F is the overlap of the interpolating operator with the physical state, defined from the two-point functions

$$\begin{aligned} C_2^{FF}(t) &= \frac{1}{V}\int_V d^3y\ \langle 0|J^B(\mathbf{y},0)J^{B\ \dagger}(\mathbf{y},t)|0\rangle \\ &\to (Z^F)^2 e^{-M_B t} \quad (4.38)\end{aligned}$$

Integrating the three-point function over $\mathbf{x}$ gives the matrix element for zero momentum transfer. In this limit, the latter can be expressed in terms of the form factor $F_1(q^2)$ in eq. (4.11).

The sum over polarisations in eq. (4.37) yields

$$\int d^3x\ C_{3\ \mu\nu}^{FF}(\mathbf{x};t_1,t_2) \to (Z^F)^2(g_{\mu\nu} - \frac{p_\mu p_\nu}{m_B^2})F_1(0)e^{-M_B(t_1+t_2)} \quad (4.39)$$

The last equation shows that the three-point functions with $\mu \neq \nu$ and $\mu = \nu = 0$ should vanish. Therefore, only the correlators with $\mu = \nu = 1,2,3$ are henceforth considered.

Moreover, taking rotational symmetry into account, $C_3^{FF}(\mathbf{x};t_1,t_2)$ is expected to be a function of the distance r only, up to cut-off effects. The three-point functions measured on the lattice are averaged over equivalent $\mathbf{x}$ positions[3]. The desired matrix element is obtained from the ratio

$$E_\mu(r,t) \stackrel{\text{def}}{=} (Z^F)^2 \overline{\sum_r}^x \frac{C_{3\ \mu\mu}^{FF}(\mathbf{x},t,t)}{C_2^{FF}(t)C_2^{FF}(t)} \to \frac{\langle B^*|A_\mu(r)|B\rangle}{2m_B}\eta_\mu \tag{4.40}$$

where the time-dependence cancels when the three-point function is divided by the product of two-point functions.

The coefficients Z^F and Z^L are extracted from the exponential fit of the two point correlation functions C_2. The data are reported in fig. 4.2. As one can see from the plots, the two-point functions already exhibit a single-exponential behaviour at moderate time separations. The main sources of error in this computation are expected to stem from the determination of the three-point function and from the value of the light quark masses, which are far from the chiral limit. Thus, a single exponential fit of the two-point functions turns out to be accurate enough for the scope of this study. The value of Z^F is extracted from a direct fit of C_2^{FF}, while Z^L is obtained from C_2^{FF} and C_2^{FL}. The results of the fit are shown directly on the plot. It is worth remarking that, in all the channels considered, single-exponential fits yield reasonable values for the reduced χ^2.

The B meson decay constant, in the static approximation, can be extracted from

$$f_B^{\text{static}} = Z_A^{\text{static}} \sqrt{\frac{2}{m_B}} Z^L a^{-3/2} \tag{4.41}$$

where Z_A^{static} is the renormalisation constant for the axial current in the static theory, which was defined in eq. (4.25). The aim here is not a precise determination of the pseudoscalar decay constant, f_B^{static}. Rather, the result is presented to allow an estimate of the systematic errors in our computation of the HMχ

[3]The symbol

$$\overline{\sum_r}^x$$

indicates the average on all the spatial positions on the lattice compatible with the constraint $|x| = r$. On a finite lattice $V = L^3$, only some distances are allowed

$$r = \sqrt{x_1^2 + x_2^2 + x_3^2}$$

because each x_i must be an integer between 0 and L/2. For each allowed distance r, a given number of terms N_r appears in the above sum, yielding a relative error on each point $\delta E_\mu(r,t) \sim N_r^{-1/2}$, e.g.

$$N_0 = 1;\ N_1 = 6;\ N_{\sqrt{2}} = 12;\ N_{\sqrt{3}} = 6;\ \ldots;\ N_{\sqrt{108}} = 1$$

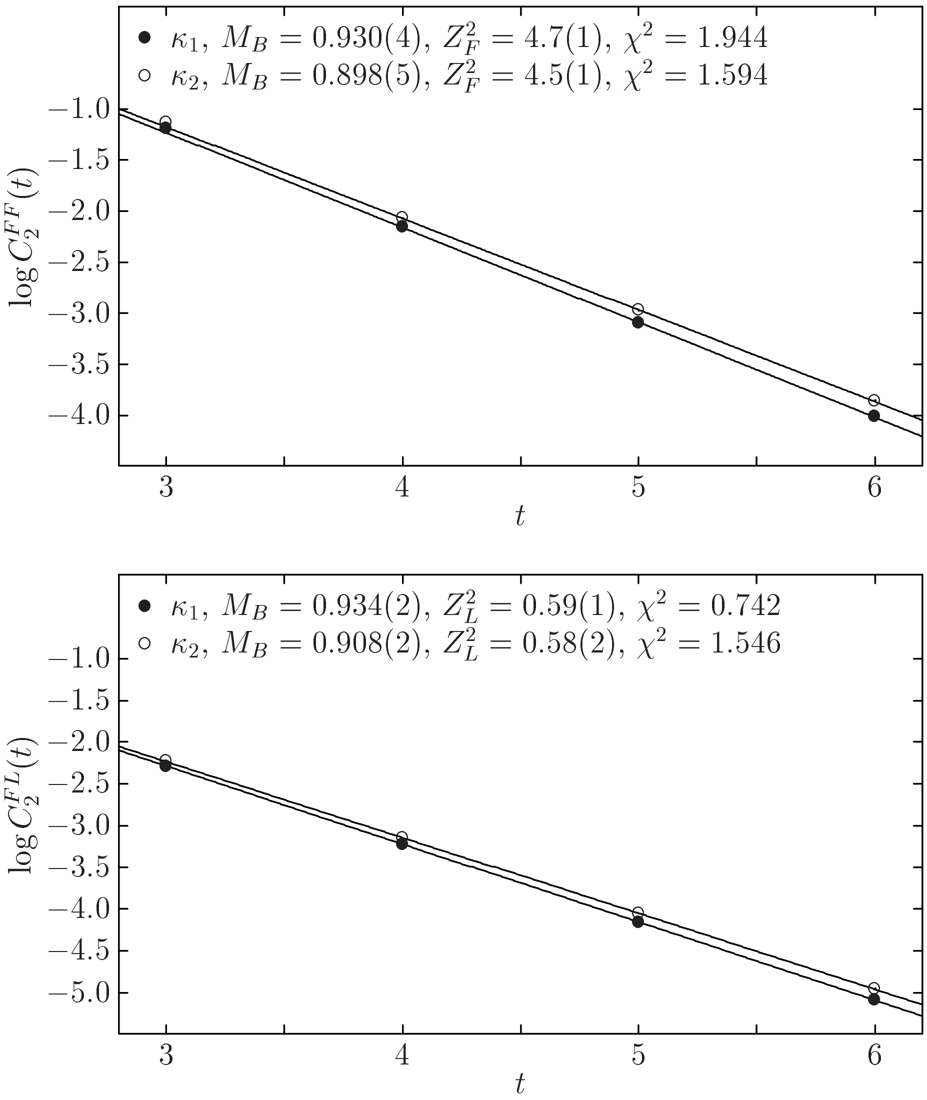

Figure 4.2: Logarithmic plots of $C_2^{FF}(t)$ and $C_2^{FL}(t)$ for both values of κ. The quoted values refer to the reduced χ^2.

	κ_1	κ_2	κ_{crit}
$M_B a$	0.930(4)	0.898(5)	0.862(7)
$(Z^F)^2$	4.75(10)	4.57(10)	4.37(15)
$(Z^L)^2$	0.59(1)	0.58(2)	0.57(3)
$f_B^{\rm static}$(GeV)	0.43(1)	0.43(1)	0.42(2)

Table 4.1: Values for Z^F, Z^L, M_B and $f_B^{\rm static}$ obtained from fitting the two-point functions.

coupling, g.

The results of the fits, together with the values for $f_B^{\rm static}$ are summarised in table 4.1. The B meson binding energies obtained from the fits of C_2^{FF} and C_2^{FL} are consistent with each other. However, our determination appears to be slightly different from the one published in [107]. The discrepancy can be explained as a contribution from excited states, which is subtracted in [107] where a multi-exponential fit is performed. The 1-state fit yields a value of Z^L approximately 20% higher than the one obtained from the 3-state fit. Hence the value obtained for the static B decay constant lies above other lattice calculations of this quantity [106]. We take into account this effect by adding a systematic error to our results of the order 20%.

This is a first, exploratory, direct lattice determination of the coupling g, so the discrepancies noted above are perhaps expected and could easily arise from various lattice artefacts. Our value of β is far from the continuum limit, while our action and operators are not fully $O(a)$ improved. We have not tried to optimise the smearing or fitting procedures. Our ensemble of gauge configurations and the collection of spinor configurations on each gauge sample are quite small. The calculation is also performed in the quenched approximation. All of these issues could be addressed in a further simulation, but here we will keep in mind that the uncertainties will propagate as systematic errors to our final result for the $B^*B\pi$ coupling.

The generation of stochastic propagators for the light quark and the static approximation for the heavy quark have proved to be useful tools in this investigation. However, neither is strictly necessary to calculate the axial current matrix element of interest. One could combine static heavy quarks with light quark propagators determined by standard deterministic methods. A full $O(a)$-improved simulation with heavy quark masses around the charm mass would allow one to go beyond the static approximation and study the dependence of g on the heavy mass. The freedom allowed in lattice calculations to tune quark masses would also allow the light quark mass dependence, noted above as strikingly absent, to be investigated in more detail.

Returning to the results of the present simulation, the quantity $E_0(x,t)$, which

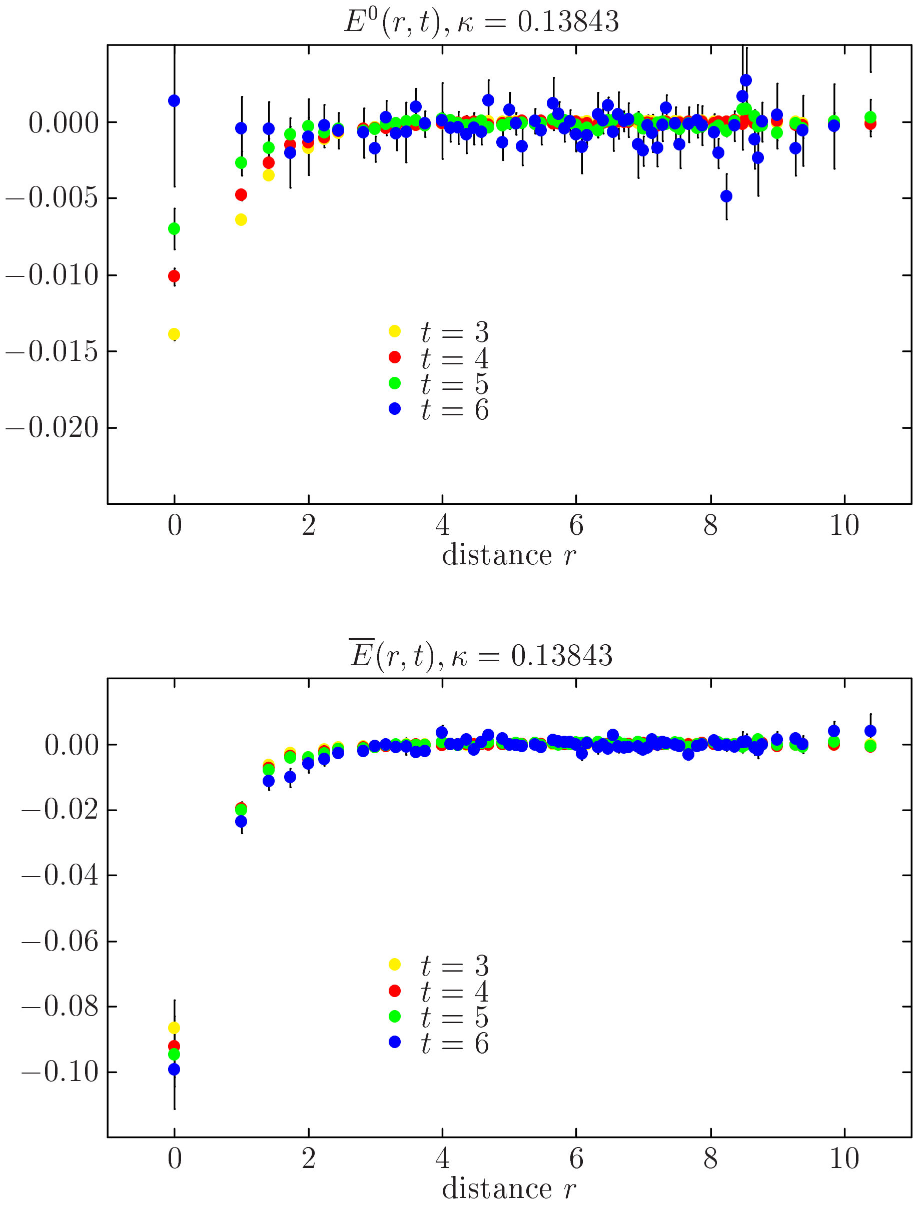

Figure 4.3: Plots of $E^0(r,t)$ and $\overline{E}(r,t)$ as functions of r for different values of t $(= 3, 4, 5, 6)$ for $\kappa = 0.13843$.

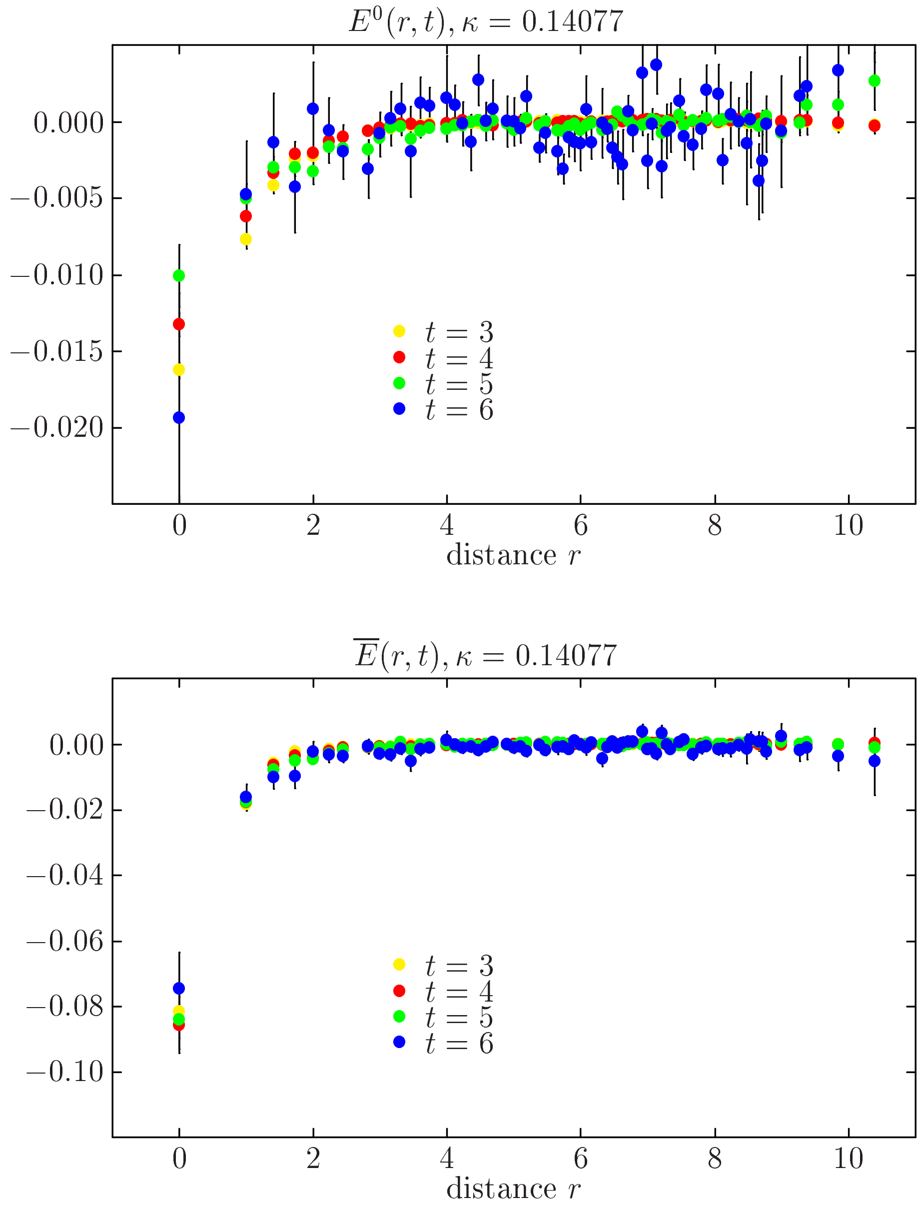

Figure 4.4: Plots of $E^0(r,t)$ and $\overline{E}(r,t)$ as functions of r for different values of t $(= 3, 4, 5, 6)$ for $\kappa = 0.14077$.

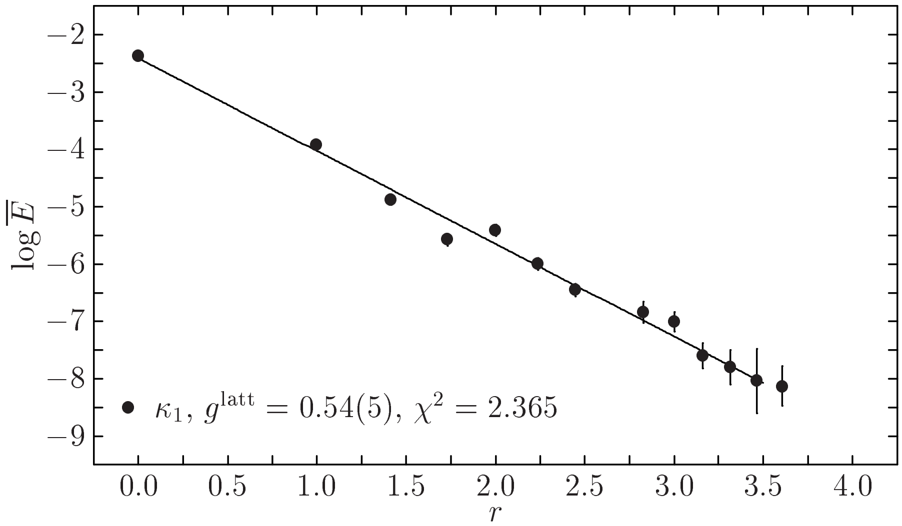

Figure 4.5: Plot of $\overline{E}(r)$ as a function of r for $\kappa = 0.13843$.

is expected to vanish, is measured as a further consistency check. The data reported in figs. 4.3 and 4.4 show a much smaller signal than the one obtained for $E_i(x,t)$. As t is increased, the fictitious peak at zero distance decreases, while the noise increases.

Using rotational invariance, the average of the three spatial components of $E_i(r,t)$

$$\overline{E}(r,t) = \frac{1}{3}(E_1(r,t) + E_2(r,t) + E_3(r,t)) \tag{4.42}$$

is measured. The results are reported in figs. 4.3 and 4.4, for the two values of κ used in this simulation. At fixed r, $\overline{E}(r,t)$ is expected to be independent of t. As this behaviour is confirmed by the data, the signal can be improved by averaging the values at different times, each weighted with its error, yielding a function of the spatial distance $\overline{E}(r)$, which needs to be integrated over the three-dimensional volume. Since this is an exploratory calculation we have neglected the effects of correlations between neighbouring time slices on the error in the average. Our choice increases the statistical error in our result. However, we note that the systematic errors considered below in any case dominate the uncertainty in the values at each time. The time-slices considered in the average are $t = 4, 5, 6$. Logarithmic plots of $\overline{E}(r)$ is displayed in figs. 4.5 and 4.6 for both values of κ, suggesting that the data are consistent with an exponential decay.

To evaluate the volume integral, $\overline{E}(r)$ is fitted with a two-parameter expo-

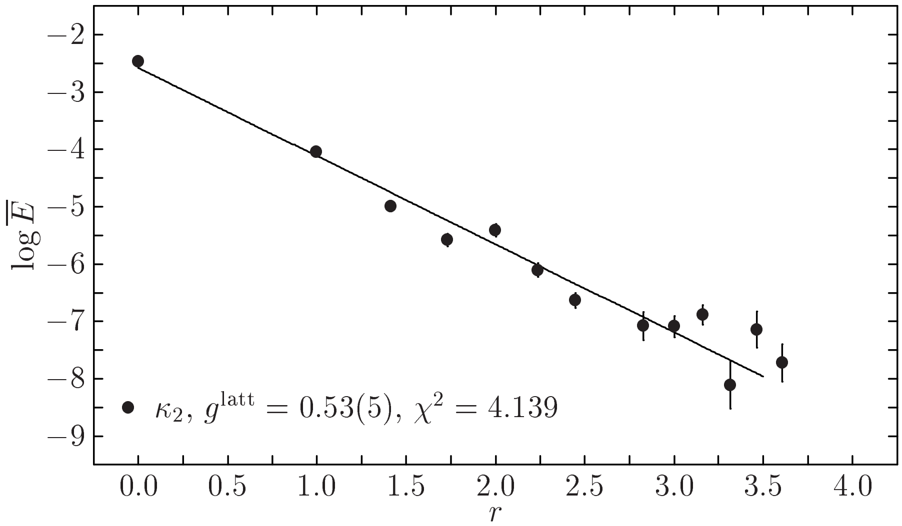

Figure 4.6: Plot of $\overline{E}(r)$ as a function of r for $\kappa = 0.14077$.

nential for each value of κ,

$$f(r) = Se^{-r/r_0} \tag{4.43}$$

The results of the fit and the values of the reduced χ^2 are recorded on the figures. The coupling g is finally obtained by integrating analytically the fitted function:

$$g^{\rm latt} = -\int_0^\infty 4\pi r^2 \overline{E}(r)dr = -\int_0^\infty 4\pi r^2 f(r)dr \tag{4.44}$$

The superscript "latt" indicates, as usual, that these numbers are defined on the lattice using operators renormalised at the lattice energy scale $a^{-1} = 1.10$ GeV. As for the two-point functions, the value of $g^{\rm L}$ does not appear to depend on the mass of quarks. It is not clear from this simulation, whether this is a genuine physical feature or, as explained earlier, an artefact of the lattice used here. Further studies should aim to clarify this point.

The best estimate for $g^{\rm latt}$ at $\kappa = \kappa_{crit}$ is thus obtained from a weighted average of the results at the two kappas used in our simulations

$$g^{\rm latt} = 0.52(5)(10) \tag{4.45}$$

The first error is statistical; the second is an estimate of the systematic error of 20%, based on the systematic error observed in the estimate of f_B.

Reference	g	Reference	g
[75]	0.32(2)	[125]	0.7
[126]	0.39	[105]	0.75-1.0
[46][a]	0.44 (16)	[127, 128]	0.4-0.7
		[129]	0.38

[a] Combined sum rule + lattice results

Table 4.2: Recent determinations of the coupling constant g

4.3 Phenomenology

We now combine the lattice matrix element with its renormalisation factor to find the continuum value for g. Since we observe no light quark mass dependence in g^{latt} and evaluated the renormalisation constant in the chiral limit, we multiply the lattice matrix element in eq. (4.45) by the renormalisation constant in eq. (4.20), to obtain the value

$$g^{\overline{\text{MS}}} = Z_A^{\text{tadpole}} g^{\text{latt}} = 0.42(4)(8) \tag{4.46}$$

for the coupling of the heavy mesons with the Goldstone bosons.

The direct decay $B^* \to B\pi$ is kinematically forbidden. However, the corresponding reaction occurs in the D system, where the coupling $g_{D^*D\pi}$ is also related to g by an expression analogous to eq. (2.77), although the $1/m_Q$ corrections are expected to be larger in the charm case. A recent analysis [123], incorporating chiral symmetry breaking corrections plus $1/m_c$ corrections in the HMχ lagrangian and fitting to the branching ratios for $D^{*0} \to D^0\pi^0$, $D^{*+} \to D^+\pi^0$ and $D_s^* \to D_s\pi^0$ (together with radiative decay rates for the same D^* mesons), gives respectively

$$g = 0.27^{+4+5}_{-2-2} \qquad (D^{*0} \to D^0\pi^0) \tag{4.47}$$

$$g = 0.76^{+3+2}_{-3-1} \qquad (D_s^* \to D_s\pi^0) \tag{4.48}$$

The two fold ambiguity can be resolved by imposing the experimental limit $\Gamma(D^{*+}) < 0.13\text{MeV}$ [124], which gives $g < 0.52$ to a good approximation [123].

Other estimates of g are derived using constituent quark models and sum rules. Starting from the non-relativistic result $g = 1$, quark models can be improved using more sophisticated assumptions to describe the quark dynamics inside the meson. Independent estimates are obtained from computing QCD correlation functions in the framework of sum rules. To give an idea of the range spanned by different determinations, some recent results are listed in table 4.2, while our value together with the average of other determinations is displayed in fig. 4.7.

The best estimate from a global analysis of available results, quoted in the

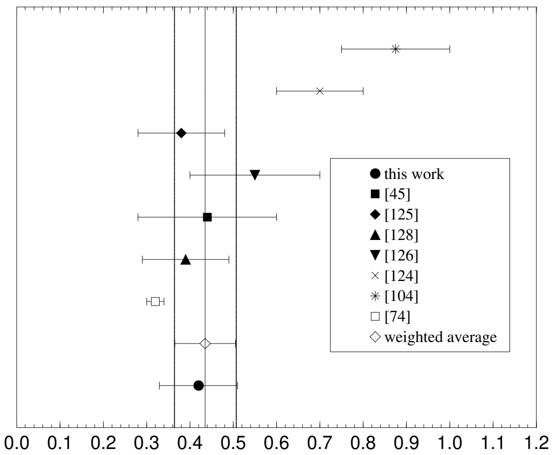

Figure 4.7: Comparison of various estimates of the coupling g.

review [46], is

$$g \simeq 0.38 \tag{4.49}$$

with a total uncertainty of 20%; the latter being comparable with the estimated systematic error from our lattice computation. Not only is the result presented in this paper compatible with the previous estimates; the systematic error is also competitive when compared to the above results.

The agreement with other previous estimates is pleasing, but the value of the coupling g can also be used to check the consistency of the heavy quark symmetry predictions in the soft pion limit for the lattice results.

The form factor f_1 of the semileptonic decay $B \to \pi l \nu$ is predicted to have the expression given earlier in eq. (4.5). This behaviour for $f_1(q^2)$ is expected to be valid near zero recoil ($q^2 \to q^2_{\text{max}}$), where the closest vector resonance dominates, even beyond the leading approximation in $1/m_b$ in HQET [70]. One also obtains this behaviour from the heavy meson chiral lagrangian [44, 47, 48, 50], valid for a low momentum pion. It is perhaps surprising that such a behaviour is found by sum rules to hold reasonably, at least for the D meson, also at $q^2 \to 0$ [75]. In this case the coupling g would fix the normalisation of the form factor f_1 . The extension of the validity of the vector pole dominance for general values of q^2 has no simple theoretical justification. It can be argued that the contributions from different resonances can lead to a single pole behaviour; however, in this case, the relation between g and $f_1(0)$ would be spoilt.

Lattice data for the semi-leptonic B decay form factors have been fitted assuming a pole behaviour for f_1 [73], yielding $f_1(0) = 0.44(3)$, to be compared with eq. (4.5) in the VMD hypothesis

$$f_1(0)|_{\mathrm{VMD}} = \frac{g_{B^*B\pi}}{f_{B^*}} = \frac{m_B}{f_\pi f_{B^*}} g = 0.50(5)(10) \tag{4.50}$$

which is in good agreement with the direct fit. Such an agreement should not come as a surprise: the lattice data, after chiral extrapolation, turn out to be close to the end-point of the phase space kinematically allowed for $B \to \pi$ decays ($q^2 \simeq q^2_{max}$). The lattice normalisation of the form factor comes therefore from a fit in a region where vector dominance does hold. Hence, the above agreement should be seen as a consistency check of the two lattice computations. It is nevertheless important to see that the two results are not contradictory.

Assuming a pole form for f_1, an independent bound on the value of the residue is obtained by enforcing the theory to satisfy unitarity [130]. The bound quoted in [130] is

$$m^2_{B^*} f_1(0) \leq 10\mathrm{GeV}^2 \tag{4.51}$$

which translates into

$$f_1(0) \leq 0.4 \tag{4.52}$$

This, again, agrees reasonably with the determination obtained from VMD, using our value for g, and the one coming from the direct fit of the lattice form factors.

As the lattice determinations will improve in the future, the comparison of the three results summarised here could become an effective way to constrain the residue at the B^* pole.

Chapter 5

Spectator Effects in Inclusive Decays of Heavy Hadrons

This chapter is based on the published papers:
M. Di Pierro and C.T. Sachrajda [UKQCD Collaboration], "A Lattice study of spectator effects in inclusive decays of B mesons", Nucl. Phys. **B534** (1998) 373 hep-lat/9805028.
M. Di Pierro and C.T. Sachrajda [UKQCD Collaboration], "Spectator effects in inclusive decays of beauty hadrons", hep-lat/9809083.
M. Di Pierro and C.T. Sachrajda [UKQCD Collaboration], "A Lattice study of spectator effects in inclusive decays of Λ_b baryons", (in preparation)

5.1 Introduction

Inclusive decays of heavy hadrons can be studied in the framework of the heavy quark expansion, in which widths and lifetimes are computed as series in inverse powers of the mass of the b-quark [83, 84, 85][1]. The leading term of this expansion corresponds to the decay of a free-quark and is universal, contributing equally to the lifetimes of all beauty hadrons (see eq. (1.74). Remarkably there are no corrections of $O(1/m_b)$, and the first corrections are of $O(1/m_b^2)$ [88, 85]. "Spectator effects", i.e. contributions from decays in which a light constituent quark also participates in the weak process, enter at third order in the heavy-quark expansion, i.e. at $O(1/m_b^3)$. However, as a result of the enhancement of the phase space for 2→2 body reactions, relative to 1→3 body decays, the spectator effects are likely to be larger than estimates based purely on power counting, and may well be significant. The need to evaluate the spectator effects is reinforced by the striking discrepancy between the experimental result for the

[1] For recent reviews and additional references see refs. [86, 87].

ratio of lifetimes [89]:

$$\frac{\tau(\Lambda_b)}{\tau(B_d)} = 0.78 \pm 0.04 \ , \tag{5.1}$$

and the theoretical prediction

$$\frac{\tau(\Lambda_b)}{\tau(B_d)} = 0.98 + O(1/m_b^3) \ . \tag{5.2}$$

In order to explain this discrepancy in the conventional approach, the higher order terms in the heavy quark expansion, and the spectator effects in particular, would have to be surprisingly large. We evaluate these spectator effects for B mesons and the Λ_b baryon.

The experimental value of the ratio of lifetimes of the charged and neutral B-mesons is [89]

$$\frac{\tau(B^-)}{\tau(B_d^0)} = 1.06 \pm 0.04 \ , \tag{5.3}$$

to be compared to the theoretical prediction

$$\frac{\tau(B^-)}{\tau(B_d^0)} = 1 + O(1/m_b^3) \ . \tag{5.4}$$

Below we determine the contribution to the $O(1/m_b^3)$ term on the right-hand side of eq. (5.2) and (5.4) coming from spectator effects, which we believe to be the largest component.

Our results for the ratios of lifetimes are

$$\frac{\tau(B^-)}{\tau(B^0)} = 1.03(2)(3) \tag{5.5}$$

$$\frac{\tau(\Lambda_b)}{\tau(B^0)} = \begin{cases} 0.91(1) & \text{for } m_u = m_d = 140 \text{ MeV} \\ 0.93(1) & \text{for } m_u = m_d = 75 \text{ MeV} \end{cases} \tag{5.6}$$

For the second ratio it was not possible to perform a chiral extrapolation, therefore we quoted the results for two different values of the light quark mass.

Our results indicate that spectator effects are not negligible, and indeed they are bigger than naive estimations based purely on power counting. Although they do not appear to be sufficiently large to account fully for the discrepency.

We remark that the matrix elements between B mesons are evaluated on a $24^3 \times 48$ lattice at $\beta = 6.2$, while the matrix elements between Λ_b states are evaluated on a $16^3 \times 24$ lattice at $\beta = 5.7$ (the same used in the simulation which is discussed in chapter 4) therefore, having established that spectator effects are significant, a future study on a bigger lattice (with larger β) is required in order to improve the precision of our results.

The results of our calculations indicate that the vacuum saturation hypothesis is (surprisingly?) well satisfied. In other words we find that the lattice matrix elements that are relevant to spectator effects for B decays factorize within the statistical errors

$$\langle B|\,\bar{b}\Gamma q\,\bar{q}\tilde{\Gamma}b\,|B\rangle \simeq \langle B|\,\bar{b}\Gamma q\,|0\rangle\,\langle 0|\,\bar{q}\tilde{\Gamma}b\,|B\rangle \tag{5.7}$$

The present calculation is very similar to that of the B_B-parameter of B-$\bar{B}$ mixing (see section 1.2.5), for which several recent simulations have been performed [67, 68, 94], including one using the same configurations used in this study [67]. We use the calculations of the B_B parameter as a comparison and check on our results, both for the perturbative matching coefficients and for the evaluation of the matrix elements. We also stress that the feature that the values of the matrix elements of the operators (5.13)-(5.16) are close to those expected from the vacuum saturation hypothesis is also present in the evaluation of the B_B-parameter.

The plan of the remainder of this chapter is as follows. In the next subsection we show the relation, at tree-level in perturbation theory, between the inclusive decay times of heavy hadrons and the matrix elements of the operators defined in eqs. (5.13)-(5.16). In the successive three sections we will present our results for $\tau(B^-)/\tau(B^0)$, B_B-parameter and $\tau(\Lambda_b)/\tau(B^0)$ respectively. We remind the reader that all the matching factors which are required in this chapter are computed in chapter 3.

5.1.1 Heavy Quark Expansion

Using the optical theorem, the inclusive decay time of a hadron H_b, containing a b quark, can be written as the following matrix element

$$\tau(H_b)^{-1} = \frac{1}{m_{H_b}}\int \mathrm{d}^4x\,\langle H_b|\,T\left\{\mathcal{L}_{eff}(x),\mathcal{L}_{eff}(0)\right\}|H_b\rangle \tag{5.8}$$

where $\mathcal{L}_{eff}$ is that part of the effective weak Lagrangian involving an heavy b quark. At the renormalization scale $\mu = m_b$ electroweak corrections are negligible and can be ignored, while strong perturbative corrections must be taken into account. The explicit form of $\mathcal{L}_{eff}$, including strong perturbative corrections to

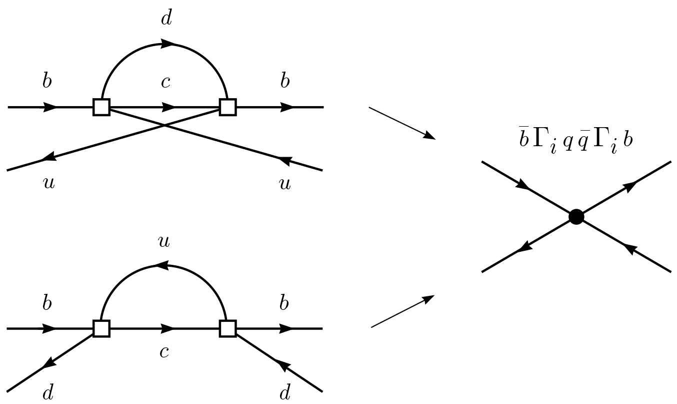

Figure 5.1: Spectator contributions to the transition operator $T\{\mathcal{L}_{eff}(x), \mathcal{L}_{eff}(0)\}$ (left), and the corresponding operator in the OPE (right). Here Γ_i denotes some combination of Dirac and colour matrices.

the coefficients, is

$$\begin{aligned}\mathcal{L}_{eff} = -\frac{G_F}{\sqrt{2}}V_{cb}\Big\{ & c_1(m_b)\left[V_{ud}\bar{d}\gamma_\mu Lu\,\bar{c}\gamma^\mu Lb + V_{sc}\bar{s}\gamma_\mu Lc\,\bar{c}\gamma^\mu Lb\right] + \\ & c_2(m_b)\left[V_{ud}\bar{c}\gamma_\mu Lu\,\bar{d}\gamma^\mu Lb + V_{sc}\bar{c}\gamma_\mu Lc\,\bar{s}\gamma^\mu Lb\right] + \\ & \sum_{\ell=e,\mu,\tau}\left[\bar{\ell}\gamma_\mu L\nu_\ell\,\bar{c}\gamma^\mu Lb\right] + \text{h.c.}\Big\}\end{aligned} \tag{5.9}$$

where

$$c_1(m_b) = \frac{1}{2}\left(\frac{\alpha_s(m_W)}{\alpha_s(m_b)}\right)^{a_+} + \frac{1}{2}\left(\frac{\alpha_s(m_W)}{\alpha_s(m_b)}\right)^{a_-} \simeq 1.10 \tag{5.10}$$

$$c_1(m_b) = \frac{1}{2}\left(\frac{\alpha_s(m_W)}{\alpha_s(m_b)}\right)^{a_+} - \frac{1}{2}\left(\frac{\alpha_s(m_W)}{\alpha_s(m_b)}\right)^{a_-} \simeq -0.25 \tag{5.11}$$

and $a_- = -2a_+ = -4/\beta_0^{QCD}$. In the numerical analysis $\alpha_s(m_W) = 0.117$ is used, following ref. [91].

The inverse decay time of eq. (5.8) is written in terms a non local product of operators but it can be expanded in terms of local operators using the Operator Product Expansion. We perform the OPE in a series of local operators with increasing dimension, whose coefficients contain inverse powers of the b quark mass:

$$\tau(H_b)^{-1} = \frac{G_F^2 m_b^5 |V_{cb}|^2}{192\pi^3} \frac{1}{2m_{H_b}} \Big\{ c_3 \langle H_b | \bar{b}b | H_b \rangle + \frac{c_5}{m_b^2} \langle H_b | \bar{b}\sigma^{\mu\nu} t^a G^a_{\mu\nu} b | H_b \rangle + \sum_i \frac{c_{6,i}}{m_b^3} \langle H_b | \mathcal{O}_i | H_b \rangle + \ldots \Big\} \tag{5.12}$$

where four dimension 6 operators contribute to the spectator effect of $O(m_b^{-3})$

$$\mathcal{O}_1 = \bar{b}\gamma^\mu L q \; \bar{q}\gamma_\mu L b \tag{5.13}$$
$$\mathcal{O}_2 = \bar{b}L q \; \bar{q} R b \tag{5.14}$$
$$\mathcal{O}_3 = \bar{b}\gamma^\mu L t^a q \; \bar{q}\gamma_\mu L t^a b \tag{5.15}$$
$$\mathcal{O}_4 = \bar{b}L t^a q \; \bar{q} R t^a b \tag{5.16}$$

The operators $\mathcal{O}_i$ arise from the tree-level contractions (reported in fig. 5.1) in the transition operator of eq. (5.8). The matching coefficients, c_3, c_5 and $c_{6,i}$, contain information about short disctance physics and are determined at tree-level in [91]. It is remarkable that there is no contribution of terms of order $1/m_b$ because there is no way of building a non trivial operator of dimension four.

Since we are performing an expansion in the heavy quark mass and this quantity cannot be measured directly, there is an ambiguity in defining the kinetic-energy of the b quark. This has the practical effect that some of the matrix elements that appear in the expansion (5.12) are divergent and their divergence is cancelled by an opposite divergence in the matching coefficients of the corresponding operators. This cancellation occurs only at an infinite order in perturbation theory and one, in practice, cannot reach such a theoretical precision. This problem is known as renormalon ambiguity. One way to go around the problem is that of taking a ratio of lifetimes and expanding it in $1/m_b$ so that only differences of matrix elements of the same operators appear. This cancels the divergences. In particular we are interested in B and Λ_b decays and, up to order $O(1/m_b^3)$, from eq. (5.12) one obtains

$$\frac{\tau(B^-)}{\tau(B^0)} = 1 + \sum_i \frac{c_{6i}}{m_b^3} \left[\frac{\langle B^0 | \mathcal{O}_i | B^0 \rangle}{2m_B} - \frac{\langle B^- | \mathcal{O}_i | B^- \rangle}{2m_B} \right] \tag{5.17}$$

$$\frac{\tau(\Lambda_b)}{\tau(B^0)} = 1 + \Delta + \sum_i \frac{c_{6,i}}{m_b^3} \left[\frac{\langle B | \mathcal{O}_i | B \rangle}{2m_B} - \frac{\langle \Lambda_b | \mathcal{O}_i | \Lambda_b \rangle}{2m_{\Lambda_b}} \right] \tag{5.18}$$

where Δ is the contribution of order 0 and $1/m_b^2$. It only depends on m_b and the two phenomenological quantities

$$\frac{\langle B|\,\bar{b}b\,|B\rangle}{2m_B} - \frac{\langle \Lambda_b|\,\bar{b}b\,|\Lambda_b\rangle}{2m_{\Lambda_b}} = 0.04(1) \tag{5.19}$$

$$\frac{\langle B|\,\bar{b}\sigma Gb\,|B\rangle}{2m_B} - \frac{\langle \Lambda_b|\,\bar{b}\sigma Gb\,|\Lambda_b\rangle}{2m_{\Lambda_b}} = 0.72 \text{ GeV}^2 \tag{5.20}$$

These numerical values are extracted from experiments: the mass spectrum and the B-B^* mass splitting, respectively.

After the substitutions of eqs.(5.19), (5.20) and the numerical values for the coefficients, the ratios in eqs. (5.17) and (5.18) can be written as linear combination of six matrix elements of the four 4-quark operators (5.13)-(5.16)

$$\frac{\tau(B^-)}{\tau(B^0)} = a_0 + a_1\varepsilon_1 + a_2\varepsilon_2 + a_3 B_1 + a_3 B_2 \tag{5.21}$$

$$\frac{\tau(\Lambda_b)}{\tau(B^0)} = b_0 + b_1\varepsilon_1 + b_2\varepsilon_2 + b_3 L_1 + b_4 L_2 \tag{5.22}$$

where [2]

$$B_1 \equiv \frac{8}{f_B^2 m_B}\frac{\langle B|\,\mathcal{O}_1\,|B\rangle}{2m_B}; \qquad B_2 \equiv \frac{8}{f_B^2 m_B}\frac{\langle B|\,\mathcal{O}_2\,|B\rangle}{2m_B} \tag{5.23}$$

$$\varepsilon_1 \equiv \frac{8}{f_B^2 m_B}\frac{\langle B|\,\mathcal{O}_3\,|B\rangle}{2m_B}; \qquad \varepsilon_2 \equiv \frac{8}{f_B^2 m_B}\frac{\langle B|\,\mathcal{O}_4\,|B\rangle}{2m_B} \tag{5.24}$$

$$L_1 \equiv \frac{8}{f_B^2 m_B}\frac{\langle \Lambda|\,\mathcal{O}_1\,|\Lambda\rangle}{2m_\Lambda}; \qquad L_2 \equiv \frac{8}{f_B^2 m_B}\frac{\langle \Lambda|\,\mathcal{O}_3\,|\Lambda\rangle}{2m_\Lambda} \tag{5.25}$$

The numerical values for the coefficients a_i and b_i have been computed in [91] and are reported in table 5.1 for operators renormalized in the continuum $\overline{\text{MS}}$ renormalization scheme at the scale $\mu = m_B$.

5.2 B decays

5.2.1 Perturbative matching

Since the Wilson coefficient functions of the operators (5.13)–(5.16) in the OPE for inclusive decay rates have been evaluated only at tree-level [91], at the same

[2] In terms of the parameters $\widetilde{B}$ and r introduced in ref. [91]

$$\begin{aligned} r &= -6L_1 \\ \widetilde{B} &= -2L_2/L_1 - 1/3 \end{aligned}$$

	value		value
a_0	$+1.00$	b_0	$+0.98$
a_1	-0.697	b_1	-0.173
a_2	$+0.195$	b_2	$+0.195$
a_3	$+0.020$	b_3	$+0.030$
a_4	$+0.004$	b_4	-0.252

Table 5.1: a_i and b_i coefficients corresponding to operators renormalized in the continuum $\overline{\rm MS}$ at the scale $\mu = m_B$.

level of precision it is sufficient to compute the matrix elements in any "reasonable" renormalization scheme. We present our results for the matrix elements of the HQET operators in the $\overline{\rm MS}$ scheme at a renormalization scale m_b [3]. In order to obtain these from the matrix elements of bare operators in the lattice theory, with cut-off a^{-1} (where a is the lattice spacing), which we compute directly in our simulations, we require the corresponding matching coefficients.

It is convenient to perform the matching in two steps:

i) The first step is the evaluation of the coefficients which relate the HQET operators in the continuum ($\overline{\rm MS}$) and lattice schemes, both defined at the scale a^{-1},

$$\mathcal{O}_i^{\overline{\rm MS},a^{-1}} = Z_{ij}\mathcal{O}_j^{\rm latt,a} = \mathcal{O}_i^{\rm latt,a} + \frac{\alpha_s}{4\pi} D_{ij}\mathcal{O}_j^{\rm latt,a} \tag{5.26}$$

where the lattice (continuum) operators are labelled by the superscript "latt" ($\overline{\rm MS}$). The coefficients D_{ij} for the operators of interest have been computed in chapter 3 and are reported in table 3.5. The mixing of operators is such that it is necessary to compute the matrix elements of eight lattice operators $\mathcal{O}_j^{\rm latt,a}$ (see table 3.5). They are the original four (5.13)-(5.16) and the four new ones

$$\mathcal{O}_5 = \bar b\gamma^\mu R q\ \bar q\gamma_\mu L b \tag{5.27}$$
$$\mathcal{O}_6 = \bar b L q\ \bar q L b \tag{5.28}$$
$$\mathcal{O}_7 = \bar b\gamma^\mu R t^a q\ \bar q\gamma_\mu L t^a b \tag{5.29}$$
$$\mathcal{O}_8 = \bar b L t^a q\ \bar q L t^a b \tag{5.30}$$

ii) We then evolve the HQET operators in the continuum scheme from renor-

[3] From these it is possible to obtain the matrix elements in any other renormalization scheme using perturbation theory.

malization scale $\mu = a^{-1}$ to scale $\mu = m_b$,

$$\mathcal{O}_i^{\overline{\mathrm{MS}},m_b} = z_{ij}(m_b, a^{-1})\mathcal{O}_j^{\overline{\mathrm{MS}},a^{-1}} \ . \tag{5.31}$$

This evolution, sometimes known as "hybrid renormalization", requires knowledge of the anomalous dimension matrix [95, 96, 97] (see also section 3.3.5).

The matching procedure involves short-distance physics only, and so can be carried out in perturbation theory. Lattice perturbation theory generally converges very slowly, and therefore, where possible, the matching should be performed non-perturbatively so as to minimise these systematic errors. We, however, do not use a non-perturbative renormalization, but, when evaluating the matching coefficients, we do use a "boosted" lattice coupling constant in order to partially resum the large higher order contributions (e.g. those coming from tadpole graphs).

In order to obtain the parameters B_i and ε_i it is also necessary to determine the normalization of the axial current [65]. In this case there is a single coefficient Z_A^{static} defined by

$$\langle 0|\, J_0^B \,|B\rangle^{\overline{\mathrm{MS}}} = Z_A^{\mathrm{static}} \langle 0|\, J_0^B \,|B\rangle^{\mathrm{latt}} \tag{5.32}$$

both renormalized at the scale $\mu = a^{-1}$ (see section 3.3.2). J_0^B is the temporal component of the current associated to a B meson. From now on the subscript 0 and superscript B will be omitted. At one loop order in perturbation theory the expression for this coefficient was computed in section 3.3.2. For our value of α_s

$$Z_A^{\mathrm{static}} = 1 - 20\,\frac{\alpha_s(a^{-1})}{4\pi} = 0.79 \tag{5.33}$$

Using hybrid renormalization one can obtain the axial current in the $\overline{\mathrm{MS}}$ scheme at scale m_b. We stress again that the results presented for the B_i's and ε_i's below were obtained with both the four quark operators and the axial current defined in the HQET in the $\overline{\mathrm{MS}}$ scheme at the scale m_b [4].

In the following subsection we combine the results of the matrix elements computed on the lattice with the perturbative coefficients presented in this section to obtain the B_i's and ε_i's.

5.2.2 Lattice computation and results

The non-perturbative strong interaction effects in spectator contributions to inclusive decays are contained in the matrix elements of the eight four-quark operators, $\mathcal{O}_j$, given in table 3.5. We evaluate these matrix elements in a quenched

[4] These differ at one-loop level from the corresponding operators in QCD.

simulation on a $24^3 \times 48$ lattice at $\beta = 6.2$ using the SW tree-level improved action [56]: The use of this action reduces the errors due to the granularity of the lattice to ones of $O(\alpha_s a)$, where a is the lattice spacing. We use the 60 SU(3) gauge-field configurations, and the light quark propagators corresponding to hopping parameters $\kappa =$ 0.14144, 0.14226 and 0.14262 which have been used previously to obtain the B-parameter of B^0-$\bar{B}^0$ mixing [67] and other quantities required for studies of B-physics. The value of the hopping parameter in the chiral limit is given by $\kappa_{crit} = 0.14315$. The calculation of the matrix elements of the operators in table 3.5 is very similar to that of the $\Delta B = 2$ operators from which the B-parameter is extracted, and we exploit the similarities to perform checks on our calculations (see section 5.3 and Appendix B).

The evaluation of the matrix elements requires the computation of two- and three-point correlation functions

$$C_2(t_x) \equiv \sum_{\vec{x}} \langle 0|\, J(x) J^\dagger(0)\, |0\rangle \tag{5.34}$$

where we have assumed that $t_x > 0$, and

$$C_{3j}(t_x, t_y) \equiv \sum_{\vec{x},\vec{y}} \langle 0|\, J(y) \mathcal{O}_j(0) J^\dagger(x)\, |0\rangle^{\text{latt}} \tag{5.35}$$

where $t_y > 0 > t_x$. In eqs. (5.34) and (5.35) $J^\dagger$ and J are interpolating operators which can create or destroy a heavy pseudoscalar meson (containing a static heavy quark) and $\mathcal{O}_j$ is one of the operators whose matrix element we wish to evaluate. In practice we choose J to be the fourth component of an axial current. It is generally advantageous to "smear" the interpolating operators J and $J^\dagger$ over the spatial coordinates, in order to enhance the overlap with the ground state. Following ref. [67] we have used several methods of smearing and checked that the results for the matrix elements of $\mathcal{O}_j$ are independent of the choice of smearing. In this paper we present as our "best" results those obtained using a gauge-invariant smearing based on the Jacobi algorithm described in ref. [99]. The smeared heavy-quark field at time t, $b^S(\vec{x}, t)$, is defined by

$$b^S(x) = \sum_{\vec{x}'} M(\vec{x}, \vec{x}') b(\vec{x}', t) \ , \tag{5.36}$$

where

$$M(\vec{x}, \vec{x}') = \sum_{n=0}^{N} \kappa_S \Delta^n(\vec{x}, \vec{x}') \tag{5.37}$$

and Δ is the three-dimensional version of the Laplace operator. The parameter κ_S and the number of iterations can be used to control the smearing radius, and here we present our results for $\kappa_S = 0.25$ and $N = 140$ which corresponds to an rms smearing radius $r_0 = 6.4a$ [100]. The smeared interpolating operator is then chosen to be $J^S(x) = \bar{b}^S(x)\gamma_5 q(x)$, where q is the field of the light quark. The local interpolating operator is simply defined to be $J^L(x) = \bar{b}(x)\gamma_5 q(x)$.

The eight matrix elements $\langle B| \mathcal{O}_j(0) |B\rangle^{\text{latt}}$ are determined by computing the ratios:

$$R_j(t_1, t_2) \equiv \frac{4C_{3j}^{SS}(-t_1, t_2)}{C_2^{LS}(-t_1)C_2^{LS}(t_2)} \ , \tag{5.38}$$

where t_1 and t_2 are positive and sufficiently large to ensure that only the ground state contributes to the correlation functions. The indices S and L denote whether the interpolating operators are smeared or local. It is convenient to choose both J and $J^\dagger$ to be smeared in the three-point function K_j and to evaluate the two-point functions with a local operator at the source and a smeared one at the sink. At large time separations t_1 and t_2,

$$R_j(t_1, t_2) \to \frac{2}{m_B (Z^L)^2} \langle B| \mathcal{O}_j(0) |B\rangle^{\text{latt}} \tag{5.39}$$

where Z^L is given by

$$\langle 0| J^L(0) |B\rangle^{\text{latt}} \equiv \sqrt{2m_B} Z^L \ . \tag{5.40}$$

The R_j defined in eq.(5.38) contribute directly to the B_i's and the ε_i's, apart from perturbative matching factors. To see this, note that the leptonic decay constant of the B-meson in the static limit (i.e. infinite mass limit for the b-quark) is given by

$$f_B^2 = \frac{2(Z_A^{\text{static}} Z^L)^2}{m_B} \ , \tag{5.41}$$

so that

$$R_j(t_1, t_2) \to \frac{2}{m_B (Z^L)^2} \langle B| \mathcal{O}_j(0) |B\rangle^{\text{latt}} = \frac{4(Z_A^{\text{static}})^2}{f_B^2 m_B^2} \langle B| \mathcal{O}_j(0) |B\rangle^{\text{latt}} \tag{5.42}$$

which corresponds precisely to the normalization of the B_i's and ε_i's in eqs.(5.23)–(5.24) (apart from the matching factors Z_A^{static} and that of the four-quark operator $\mathcal{O}_j$ described in section 5.2.1).

In these computations it is particularly important to establish that the contribution from the ground-state has been isolated. The natural way to do this is to look for plateaus, i.e. for regions in t_1 and t_2 for which $R_j(t_1, t_2)$ is independent of t_1 and t_2. Since the statistical errors grow fairly quickly with $t_{1,2}$ our

	Gauge Inv.	Exponential	Gaussian	Cube	Double Cube
$R_1(3,3)$	1.02(3)	1.03(2)	1.04(3)	1.03(2)	1.07(8)
$R_2(3,3)$	1.00(2)	1.01(2)	1.01(3)	1.01(2)	1.00(5)
$R_3(3,3)$	0.00(1)	−0.00(1)	−0.00(2)	−0.00(1)	−0.03(3)
$R_4(3,3)$	0.00(1)	0.00(1)	0.01(1)	0.00(1)	0.01(2)
$R_5(3,3)$	−0.99(4)	−1.01(3)	−1.01(4)	−1.00(3)	−1.01(7)
$R_6(3,3)$	−0.99(3)	−1.00(2)	−1.01(3)	−1.00(3)	−1.01(6)
$R_7(3,3)$	−0.04(2)	−0.03(2)	−0.04(2)	−0.03(2)	−0.09(5)
$R_8(3,3)$	−0.00(1)	−0.00(1)	−0.01(1)	−0.01(1)	−0.02(2)

Table 5.2: Values of the $R_j(3,3)$ obtained with different smearing methods for a light quark with $\kappa = 0.14226$.

ability to verify the existence of plateaus is limited. For example in fig. 5.2 we present our results for $R_j(t_1,t_2)$, obtained with the light quark mass corresponding to $\kappa = 0.14226$ as a function of t_2 for $t_1 = 3$. The results are consistent with being constant, but the errors are uncomfortably large for $t_2 > 5$ or so. An alternative, and perhaps more convincing, way to confirm that the contribution from the ground-state has been isolated is to check that the values of the R_j are independent of the method of smearing used to define the smeared interpolating operators. Following ref. [67], in addition to the gauge invariant prescription for smearing described above, we have defined the smeared field in four other ways (having transformed the fields to the Coulomb gauge). For these additional four cases, $M(\vec{x},\vec{x}')$ of eq. (5.37) is replaced by the following

$$\text{Exponential}: \quad M(\vec{x},\vec{x}') = \exp(-|\vec{x}-\vec{x}'|/r_0), \tag{5.43}$$

$$\text{Gaussian}: \quad M(\vec{x},\vec{x}') = \exp(-|\vec{x}-\vec{x}'|^2/r_0^2), \tag{5.44}$$

$$\text{Cube}: \quad M(\vec{x},\vec{x}') = \prod_{i=1}^{3} \Theta(r_0 - |\vec{x}_i - x_i'|), \tag{5.45}$$

$$\text{Double Cube}: \quad M(\vec{x},\vec{x}') = \prod_{i=1}^{3} \left(1 - \frac{|x_i - x_i'|}{2r_0}\right) \Theta(2r_0 - |x_i - x_i'|), \tag{5.46}$$

and we have chosen $r_0 = 5$. As an example, we present in table 5.2 the results for the $R_j(t_1,t_2)$ for $t_1 = 3$ and $t_2 = 3$, again for the middle value of the three κ's, $\kappa = 0.14226$.

We take as our best results those obtained with the gauge invariant smearing, and with $t_1 = t_2 = 3$. After extrapolating to the chiral limit we find the following

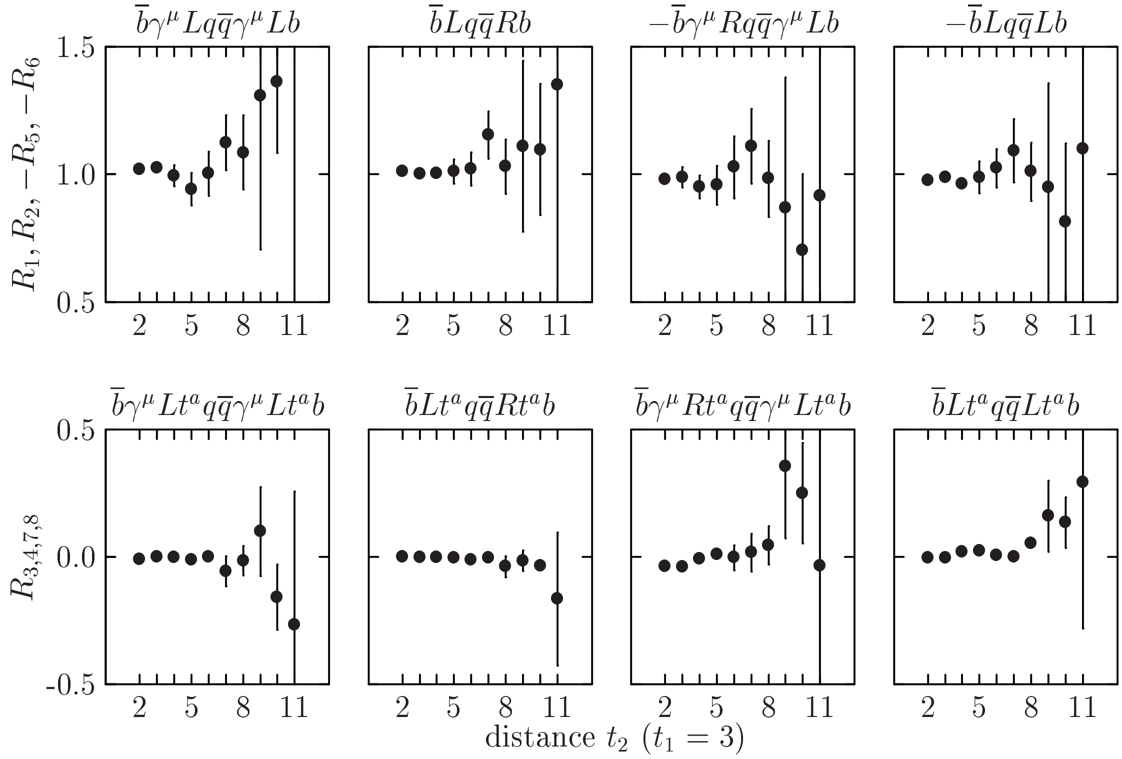

Figure 5.2: Results for the R_j, $j = 1 \cdots 8$ as a function of t_2 for $t_1 = 3$. The value of the quark mass corresponds to $\kappa = 0.14226$.

results for the R_j

$$R_1(3,3) = 1.04 \pm 0.04 \qquad R_2(3,3) = 1.00 \pm 0.03 \tag{5.47}$$

$$R_3(3,3) = -0.01 \pm 0.02 \qquad R_4(3,3) = -0.00 \pm 0.01 \tag{5.48}$$

$$R_5(3,3) = -0.97 \pm 0.06 \qquad R_6(3,3) = -0.98 \pm 0.05 \tag{5.49}$$

$$R_7(3,3) = -0.03 \pm 0.03 \qquad R_8(3,3) = -0.01 \pm 0.01 \tag{5.50}$$

We now combine these results with the matching coefficients presented in section 5.2.1 to determine the B_i's and the ε_i's. For the value of the lattice coupling constant we take one of the standard definitions of the boosted coupling

$$\frac{\alpha_s(a^{-1})}{4\pi} = \frac{6(8\kappa_c)^4}{(4\pi)^2\beta_0} = 0.0105 \ . \tag{5.51}$$

Here β_0 is β_0^{QCD} of eq. (2.39) for $N_f = 0$, because we performed a quenched simulation, i.e. zero quark flavours. Using the coefficients from table 3.5 we then obtain

$$\begin{aligned}
B_1^{\overline{\mathrm{MS}},a^{-1}} &= \left(Z_A^{\mathrm{static}}\right)^{-2}\left(\delta_{1j}+\frac{\alpha_s(a^{-1})}{4\pi}D_{1j}\right)R_j = 0.98(8)\\
B_2^{\overline{\mathrm{MS}},a^{-1}} &= \left(Z_A^{\mathrm{static}}\right)^{-2}\left(\delta_{2j}+\frac{\alpha_s(a^{-1})}{4\pi}D_{2j}\right)R_j = 0.93(5)\\
\varepsilon_1^{\overline{\mathrm{MS}},a^{-1}} &= \left(Z_A^{\mathrm{static}}\right)^{-2}\left(\delta_{3j}+\frac{\alpha_s(a^{-1})}{4\pi}D_{3j}\right)R_j = 0.01(3)\\
\varepsilon_2^{\overline{\mathrm{MS}},a^{-1}} &= \left(Z_A^{\mathrm{static}}\right)^{-2}\left(\delta_{4j}+\frac{\alpha_s(a^{-1})}{4\pi}D_{4j}\right)R_j = 0.00(2)
\end{aligned}$$

We now evolve these coefficients to the scale m_b, using the relation 3.131, which we rewrite in the form

$$B_i^{\overline{\mathrm{MS}},m_b} = \left(1+\frac{8}{9}\delta\right)_i B^{\overline{\mathrm{MS}},a^{-1}} + \left(-\frac{2}{3}\delta\right)\varepsilon_i^{\overline{\mathrm{MS}},a^{-1}} \tag{5.52}$$

$$\varepsilon_i^{\overline{\mathrm{MS}},m_b} = \left(1+\frac{1}{9}\delta\right)\varepsilon_i^{\overline{\mathrm{MS}},a^{-1}} + \left(-\frac{4}{27}\delta\right)B_i^{\overline{\mathrm{MS}},a^{-1}} \tag{5.53}$$

where

$$\delta \equiv \left(\frac{\alpha_s(a^{-1})}{\alpha_s(m_b)}\right)^{9/2\beta_0} - 1 = 0.09(3) \tag{5.54}$$

In estimating δ and its uncertainty we have allowed for a conservative variation of the parameters around the "central" values ($\Lambda_{QCD} = 250\,\mathrm{MeV}$, $a^{-1} = 2.9\,\mathrm{GeV}$, $m_b = 4.5\,\mathrm{GeV}$ and $\beta_0 = 9$). We finally obtain[5]:

$$B_1^{\overline{\mathrm{MS}},m_b} = 1.06(8) \qquad B_2^{\overline{\mathrm{MS}},m_b} = 1.01(6) \tag{5.55}$$

$$\varepsilon_1^{\overline{\mathrm{MS}},m_b} = -0.01(3) \qquad \varepsilon_2^{\overline{\mathrm{MS}},m_b} = -0.01(2)\ . \tag{5.56}$$

Using the results in eqs. (5.55) and (5.56) we obtain the following value for the ratio of lifetimes for the neutral and charged B-mesons:

$$\frac{\tau(B^-)}{\tau(B_d)} = a_0 + a_1B_1 + a_2B_2 + a_3\varepsilon_1 + a_4\varepsilon_2 = 1.03(2)(3) \tag{5.57}$$

where the coefficients a_i are taken from ref. [91] and reported in table 5.1. The first error in eq. (5.57) is from the uncertainty in the values of the matrix elements in eqs. (5.55) and (5.56), whereas the second is an estimate of the uncertainty due to our ignorance of the one-loop contribution to the Wilson coefficient function

[5] These matrix elements have also been evaluated using QCD sum-rules [101]. These authors find $B_1^{\overline{\mathrm{MS}},m_b} = 0.96(4)$, $B_2^{\overline{\mathrm{MS}},m_b} = 0.95(2)$, $\varepsilon_1^{\overline{\mathrm{MS}},m_b} = -0.14(1)$ and $\varepsilon_2^{\overline{\mathrm{MS}},m_b} = -0.08(1)$, differing somewhat (particularly for the ε_i's) from our values.

in the OPE (this was estimated by varying the matching scale from $m_b/2$ to $2m_b$ using the procedure described in ref. [91]). The value in eq. (5.57) is in good agreement with the experimental results in eq. (5.3).

5.3 $B - \bar{B}$ mixing

In this section we revisit the phenomenologically important process of B-$\bar{B}$ mixing. The computation of the matrix elements of the relevant lattice operators on the same gauge configurations has already been presented in [67], and we do not add to these lattice computations. We do, however, wish to make two observations

i) The matrix elements of the lattice $\Delta B = 2$ operators relevant for B-$\bar{B}$ mixing factorize with a similar precision to that found for the four-quark operators considered in section 5.2.2. Because of the way in which lattice computations are usually organised, this property is not as readily manifest for the ΔB=2 operators as it is for the spectator effects. However, by using colour and spin Fierz identities, we demonstrate that the values of the matrix elements of the lattice $\Delta B = 2$ operators are very close to those expected using factorization. Some of our observations have already been noted in ref. [94], where the Wilson formulation for the light quarks was used. We extend this investigation of factorization, and show that each contribution to the matrix elements (i.e. each Wick contraction) is close to the estimated value obtained using the factorization and vacuum saturation hypothesis.

ii) We believe that there is an error in the published value of the matching factors for the $\Delta B = 2$ operators using the SW action for the light quarks. We discussed this in some detail in chapter 3. In this section we briefly comment on the consequences of this error.

We now consider these two observations in turn.

5.3.1 Factorization

In order to determine the B-parameter of B-$\bar{B}$ mixing, eq. (1.85), we need to compute the matrix element of the operator $\mathcal{O}_L$, defined in eq. (3.108), in the $\overline{\text{MS}}$ scheme at the scale m_b. In the matching between the continuum scheme and the lattice scheme this operator mixes with the three lattice operators $\mathcal{O}_L$, $\mathcal{O}_R$ and $\mathcal{O}_N$ defined in eqs.(3.108)-(3.110) of chapter 3, as well as with

$$\mathcal{O}_S = \frac{1}{2}\left[\bar{b}_1 L q_2\, \bar{b}_3 L q_4 - \bar{b}_1 L q_4\, \bar{b}_3 L q_2\right] \tag{5.58}$$

which arises from the matching between the continuum full theory and the continuum effective theory [64]. At order α_s we rewrite the definition 1.85, in terms of the matching factors and the lattice parameters, as

$$B_B^{\overline{\mathrm{MS}},m_b} = (Z_A^{\mathrm{static}})^{-2}\left\{\left[1+\frac{\alpha_s}{4\pi}(4\log m_b^2a^2+C_L+D_L)\right]R_L + \frac{\alpha_s}{4\pi}D_RR_R+\frac{\alpha_s}{4\pi}D_NR_N+\frac{\alpha_s}{4\pi}C_SR_S\right\} \tag{5.59}$$

where the coefficients D_L, D_R and D_N have been computed in section 3.3.3, the coefficients $C_L=-14$ and $C_S=-8$ are computed in ref. [64] and R_j are defined as

$$R_j = \frac{3}{8}\frac{2}{m_B(Z_L)^2}\langle\, B^0|\mathcal{O}_j|\bar{B}^0\,\rangle^{\mathrm{latt},a} = \frac{3(Z_A^{\mathrm{static}})^2}{8f_B^2m_B^2}\langle\, B^0|\mathcal{O}_j|\bar{B}^0\,\rangle^{\mathrm{latt},a} \tag{5.60}$$

for each of the operators $\mathcal{O}_L^{\mathrm{latt},a}$, $\mathcal{O}_R^{\mathrm{latt},a}$, $\mathcal{O}_N^{\mathrm{latt},a}$ and $\mathcal{O}_S^{\mathrm{latt},a}$.

We now show that these matrix elements (and related ones) are reproduced remarkably accurately by assuming the factorisation hypothesis and vacuum saturation. For each of these operators ($\mathcal{O}_j$) we define the ratio $R_j(t_1,t_2)$ analogously to eq.(5.38) as follows

$$R_j(t_1,t_2) \equiv \frac{3}{8}\frac{C_{3j}^{SS}(t_1,t_2)}{C^{LS}(-t_1)C^{LS}(t_2)}\ , \tag{5.61}$$

where the correlation functions C and C_{3j} are defined in eqs.(5.34) and (5.35), except that in the C_{3j} the operators $\mathcal{O}_j$ are now $\Delta B=2$ operators, and the interpolating operators destroy a B-meson and create a $\bar{B}$-meson.

We start by explaining explicitly what we mean by factorization (combined with vacuum saturation). The evaluation of the B-parameter requires the computation of three-point functions $C_{3j}(t_1,t_2)$, which are of the form[6]

$$\langle 0|\,\bar{q}(y)\gamma^5 b(y)\ \bar{b}(0)\Gamma q(0)\,\bar{b}(0)\tilde{\Gamma}q(0)\ \bar{q}(x)\gamma^5 b(x)\,|0\rangle \tag{5.62}$$

There are four Wick contractions which contribute to the correlation function, and it is convenient to track these by introducing a fictitious quantum number, labelled by an integer suffix on each field, so that the correlation function is written in the form

$$\langle 0|\,\bar{q}_2(y)\gamma^5 b_1(y)\ \mathcal{O}_{\Gamma\otimes\tilde{\Gamma}}(0)\ \bar{q}_4(x)\gamma^5 b_3(x)\,|0\rangle \tag{5.63}$$

[6]The extension of this discussion to include smeared interpolating operators is completely straightforward.

where

$$\mathcal{O}_{\Gamma\otimes\tilde{\Gamma}} \equiv \bar{b}_1\Gamma q_2\ \bar{b}_3\tilde{\Gamma}q_4\ + \bar{b}_3\Gamma q_4\ \bar{b}_1\tilde{\Gamma}q_2\ - \bar{b}_1\Gamma q_4\ \bar{b}_3\tilde{\Gamma}q_2\ - \bar{b}_3\Gamma q_2\ \bar{b}_1\tilde{\Gamma}q_4 \tag{5.64}$$

and $\Gamma, \tilde{\Gamma}$ are Dirac matrices. The contraction of spinor (α, β) and colour (a) indices in each bilinear in eq. (5.64) is implicit (e.g. $\bar{b}_1\Gamma q_2 = \bar{b}^a_{1,\alpha}\Gamma_{\alpha,\beta}q^a_{2,\beta}$). Only contractions between fields with the same suffix are allowed, and the four terms in eq. (5.64) correspond to the four original Wick contractions. For all the operators of interest, by using colour and spin Fierz identities, it is possible to rewrite each of the four terms into sums of operators of the form $(\bar{b}_1\Gamma' q_2)\,(\bar{b}_3\tilde{\Gamma}' q_4)$ and $(\bar{b}_1\Gamma' t^a q_2)\,(\bar{b}_3\tilde{\Gamma}' t^a q_4)$, for some γ-matrices Γ' and $\tilde{\Gamma}'$. In the factorization and vacuum saturation hypothesis

$$\langle\, \bar{B}\,|(\bar{b}_1\Gamma' t^a q_2)\,(\bar{b}_3\tilde{\Gamma}' t^a q_4)\,|\,B\,\rangle \simeq 0\ , \tag{5.65}$$

and

$$\left\langle \bar{B}\right|(\bar{b}_1\Gamma' q_2)\,(\bar{b}_3\tilde{\Gamma}' q_4)\,|B\rangle \simeq \left\langle \bar{B}\right|(\bar{b}_1\Gamma' q_2)\,|0\rangle\,\langle 0|\,(\bar{b}_3\tilde{\Gamma}' q_4)\,|B\rangle \tag{5.66}$$

Lorentz invariance implies that each of the matrix elements on the right-hand side of eq. (5.66) vanishes or is proportional to the leptonic decay constant f_B.

We now consider each of the operators in turn:

- $\mathcal{O}_L$ and $\mathcal{O}_R$: The factor of 3/8 in eq. (5.61) was chosen so that the factorization hypothesis gives $R_L = R_R = 1$. Numerically we find:

$$\frac{R_L(3,3) + R_R(3,3)}{2} = 0.95(3) \tag{5.67}$$

- $\mathcal{O}_S$: Lorentz invariance implies that the matrix element $\langle\, B\,|\bar{b}\sigma^{\mu\nu}(1-\gamma^5)q\,|\,0\,\rangle$ vanishes. Using this fact we deduce that factorization implies that $R_S \simeq 5/8$. The numerical result for R_S is 0.60(3), in very good agreement with the estimate based on factorization.

- $\mathcal{O}_N$: Finally factorization implies that $R_N \simeq 1$, in good agreement with the numerical value 0.97(4).

In order to illustrate further that the numerical results quoted above are in agreement with expectations based on factorization and vacuum saturation we present separately in fig. 5.3 the contributions to each of the ratios from the two independent contractions:

$$R^a = \langle\, \bar{B}\,|(\bar{b}_1\Gamma' q_2)\,(\bar{b}_3\tilde{\Gamma}' q_4)\,|\,B\,\rangle \tag{5.68}$$

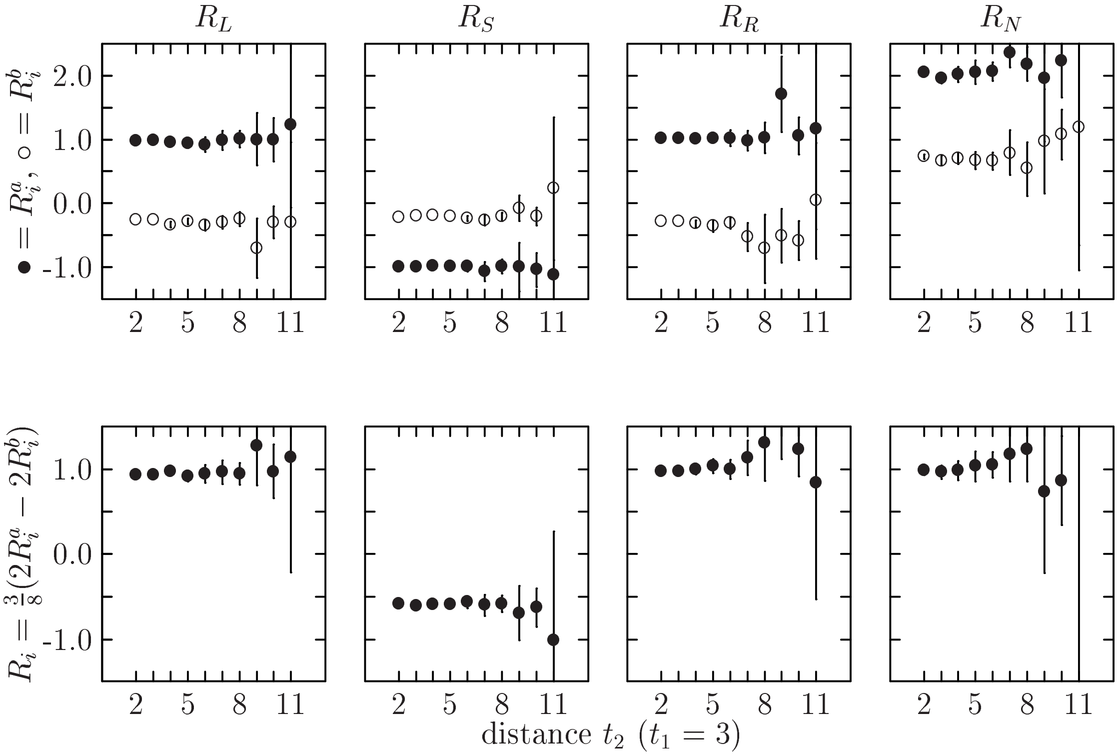

Figure 5.3: Results for the R_j^a, R_j^b and R_j $(j = L, S, R, N)$ as a function of t_2 for $t_1 = 3$. The value of the quark mass corresponds to $\kappa = 0.14226$.

and

$$R^b = \langle \bar{B} | \, (\bar{b}_1 \Gamma' q_4) \, (\bar{b}_3 \tilde{\Gamma}' q_2) \, | B \rangle \tag{5.69}$$

as well as the total combination

$$R = \frac{3}{8}(2R^a - 2R^b) \tag{5.70}$$

We see that not only are the values of the R's quoted above in agreement with expectations from factorization, but the values of each of the R^a and R^b are also those we would expect on this assumption:

$$R_L^a \simeq 1 \qquad R_L^b \simeq -\frac{1}{3} R_L^a \qquad ; \qquad R_S^a \simeq -1 \qquad R_S^b \simeq \frac{1}{6} R_S^a \tag{5.71}$$

$$R_R^a \simeq 1 \qquad R_R^b \simeq -\frac{1}{3} R_L^a \qquad ; \qquad R_N^a \simeq 2 \qquad R_N^b \simeq \frac{1}{3} R_N^a \tag{5.72}$$

In this subsection we have demonstrated that the surprising precision of predictions for matrix elements obtained using the factorization hypothesis in inclusive decays, which was discussed in section 5.2.2, also applies to existing results for B-$\bar{B}$ mixing.

5.3.2 Matching

In this subsection we discuss very briefly the implications of the error in the published value of the perturbative matching factors in B-$\bar{B}$ mixing (see appendix B). For example, we take method (a) of ref. [67] (in which each of the ratios R_i is fitted separately) and, substituting our values in eq. (5.59), we find

$$B_B^{\overline{\rm MS},m_b} = 0.66(2)\ , \qquad B_B = \alpha_s^{-6/23} B_B^{\overline{\rm MS},m_b} = 0.96(3) \tag{5.73}$$

where $B_B^{\overline{\rm MS},m_b}$ and B_B are the B-parameter in the $\overline{\rm MS}$ scheme at scale m_b and the renormalization group invariant B-parameter respectively. For the comparison we only quote the statistical error. In order to see the effect of the error in the matching coefficient, the result in eq. (5.73) should be compared with that obtained in ref. [67] using an identical procedure (except for the values of the matching coefficients):

$$B_B^{\overline{\rm MS},m_b} = 0.69(2)\ , \qquad B_B = \alpha_s^{-6/23} B_B^{\overline{\rm MS},m_b} = 1.02(3) \tag{5.74}$$

Giménez and Martinelli had pointed out that the authors of ref. [67] had used matching coefficient which did not include the contributions to the $O(a^2)$ terms in the lattice operators which they had used [68]. As explained in ref. [68], this leads to a negligible correction to the B-parameter. The differences in the values in eqs. (5.73) and (5.74) are therefore largely due to the error discussed in appendix B.

5.4 Λ_b decays

The main motivation for this study is that, as a result of the enhancement of the phase space for $2 \to 2$ body reaction, relative to $1 \to 3$ body decays, we expect the spectator effects in Λ_b decays to be larger than estimates based purely on power counting. This preliminary study seems to indicate that this is not the case, but further investigation will be required. We will proceed by evaluating the two missing matrix elements L_1 and L_2 of eq. (5.22), since ε_1 and ε_2 have already been computed in section 5.2. Our results will be summarized in eq. (5.97).

5.4.1 Perturbative matching

In lattice simulations we compute matrix elements of bare operators with ultraviolet cut-off a^{-1} (where a is the lattice spacing). We wish to determine matrix elements of renormalised operators in some standard renormalisation scheme (the $\overline{\rm MS}$ scheme for example), and this can be done in perturbation theory. We have discussed this in some detail earlier in this chapter, and here we briefly repeat the main points relevant for the evaluation of the matrix elements L_1 and L_2.

We start by relating the matrix elements L_1 and L_2 (defined in the $\overline{\rm MS}$ scheme say) renormalised at m_b to those renormalised at a^{-1}. The Wilson coefficient functions in the OPE expansion have been evaluated at tree level[91] only and at the same level of precision the relevant matching coefficients are [95, 96]

$$L_1^{\overline{\rm MS},m_b} = \left(1+\frac{8}{9}\delta\right) L_1^{\overline{\rm MS},a^{-1}} + \left(-\frac{2}{3}\delta\right) L_2^{\overline{\rm MS},a^{-1}} \qquad (5.75)$$

$$L_2^{\overline{\rm MS},m_b} = \left(1+\frac{1}{9}\delta\right) L_2^{\overline{\rm MS},a^{-1}} + \left(-\frac{4}{27}\delta\right) L_1^{\overline{\rm MS},a^{-1}} \qquad (5.76)$$

where

$$\delta \equiv \left(\frac{\alpha_s(a^{-1})}{\alpha_s(m_b)}\right)^{9/2\beta_0} - 1 = 0.40(5) \qquad (5.77)$$

In estimating δ we have used $\Lambda_{\rm QCD} = 250$ MeV, $a^{-1} = 1.10$ GeV, $m_b = 4.5$ GeV and $\beta_0 = 9$. The error in δ is evaluated allowing a conservative 20% uncertainty for $\Lambda_{\rm QCD}$.

The second step of the matching relates the matrix elements renormalised in the continuum to those regularized on lattice (both at the same energy scale, the inverse lattice spacing). Although this involves corrections of $O(\alpha_s)$, which are in principle beyond the precision which we require, we do include them because the perturbative coefficients in lattice perturbation are generally large. This computation, for the most general four quark operator involving one heavy quark, appears in the appendix of ref. [1]. In the present case this matching can be written in the form

$$L_1^{\overline{\rm MS},a^{-1}} = \frac{8}{f_B^2 m_B}\left[h_{11}M_1 + h_{12}M_2 + h_{13}M_3 + h_{14}M_4\right] \qquad (5.78)$$

$$L_2^{\overline{\rm MS},a^{-1}} = \frac{8}{f_B^2 m_B}\left[h_{21}M_1 + h_{22}M_2 + h_{23}M_3 + h_{24}M_4\right] \qquad (5.79)$$

coefficient	expression	value
h_{11}	$1+\frac{\alpha}{4\pi}\left[\frac{10}{3}-\frac{4}{3}d_{11}-\frac{8}{3}d_{12}\right]$	0.737
h_{12}	$\frac{\alpha}{4\pi}\left[-\frac{4}{3}d_{13}\right]$	0.112
h_{13}	$\frac{\alpha}{4\pi}\left[-\frac{5}{2}-d_{14}-2d_{15}-d_{17}\right]$	0.113
h_{14}	$\frac{\alpha}{4\pi}\left[-d_{16}\right]$	0.084
h_{21}	$\frac{\alpha}{4\pi}\frac{2}{9}\left[-\frac{5}{2}-d_{14}-2d_{15}-d_{17}\right]$	0.025
h_{22}	$\frac{\alpha}{4\pi}\left[-\frac{2}{9}d_{16}\right]$	0.019
h_{23}	$1+\frac{\alpha}{4\pi}\left[\frac{5}{12}-\frac{4}{3}d_{11}+\frac{1}{3}d_{12}-\frac{7}{6}d_{14}+\frac{2}{3}d_{15}-\frac{7}{6}d_{17}\right]$	0.869
h_{24}	$\frac{\alpha}{4\pi}\left[\frac{1}{2}d_{16}\right]$	−0.042

Table 5.3: Matching coefficients for the matrix elements M_1 and M_2, renormalised on lattice at an energy scale $a^{-1} = 1.10$ GeV. The constants d_{ij} correspond to the lattice matching factors $d_{ij}^{\rm latt}$ of table 3.2

where

$$M_1 = \frac{\langle\Lambda_b|\,\bar{b}\gamma^\mu Lq\bar{q}\gamma^\mu Lb\,|\Lambda_b\rangle}{2m_{\Lambda_b}} \tag{5.80}$$

$$M_2 = \frac{\langle\Lambda_b|\,\bar{b}\gamma^\mu L\gamma^0 q\bar{q}\gamma^\mu Lb\,|\Lambda_b\rangle}{2m_{\Lambda_b}} + \frac{\langle\Lambda_b|\,\bar{b}\gamma^\mu Lq\bar{q}\gamma^0\gamma^\mu Lb\,|\Lambda_b\rangle}{2m_{\Lambda_b}} \tag{5.81}$$

$$M_3 = \frac{\langle\Lambda_b|\,\bar{b}\gamma^\mu Lt^a q\bar{q}\gamma^\mu Lt^a b\,|\Lambda_b\rangle}{2m_{\Lambda_b}} \tag{5.82}$$

$$M_4 = \frac{\langle\Lambda_b|\,\bar{b}\gamma^\mu L\gamma^0 t^a q\bar{q}\gamma^\mu Lt^a b\,|\Lambda_b\rangle}{2m_{\Lambda_b}} + \frac{\langle\Lambda_b|\,\bar{b}\gamma^\mu Lt^a q\bar{q}\gamma^0\gamma^\mu Lt^a b\,|\Lambda_b\rangle}{2m_{\Lambda_b}} \tag{5.83}$$

are the bare lattice matrix elements regularised at the appropriate lattice scale. The coefficients h_{ij} are listed in table (1.1) where, for the lattice coupling constant we have used a boosted coupling equal to

$$\frac{\alpha_s^{\rm latt}(a^{-1})}{4\pi} = \frac{6(8\kappa_{crit})^4}{(4\pi)^2\beta_0} \simeq 0.01216\ . \tag{5.84}$$

The matching coefficients corresponding to the lattice action which we are using are reported in table (5.3).

A consequence of the Heavy Quark Effective Theory, and the fact that the light quarks in the Λ_b are in a spin zero combination, is that the number of lattice operators whose matrix elements have to be evaluated is four rather than eight, which is the case for heavy mesons.

In order to obtain the factor $f_B^2 m_B$ it is also necessary to determine the

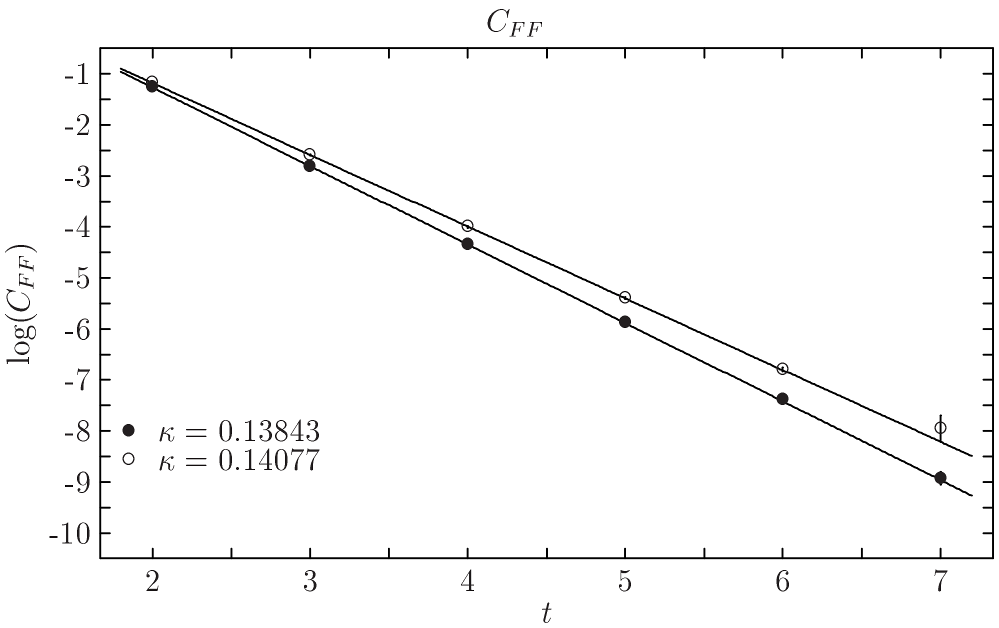

Figure 5.4: Plot of C_2^{FF} after the substraction for the contribution of excited states.

normalization of the axial current, Z_A,

$$f_B m_B = \langle 0|\, J_0^B \,|B\rangle^{\overline{\mathrm{MS}},a^{-1}} = Z_A^{\mathrm{static}} \langle 0|\, J_0^B \,|B\rangle^{\mathrm{latt},a} = \sqrt{2m_B} Z_A^{\mathrm{static}} Z_L \ , \tag{5.85}$$

where J_0^B is the time component of the axial current defined on the lattice and Z_L is obtained from the numerical value of its matrix element determined from numerical simulations At our value of the lattice spacing

$$Z_A^{\mathrm{static}} = 1 - 20.0 \frac{\alpha_s^{\mathrm{latt}}(a^{-1})}{4\pi} = 0.75 \tag{5.86}$$

In the following section we combine the results for the matrix elements computed on the lattice, M_i and Z_L, with the perturbative coefficients presented in this section, h_{ij} and Z_A^{static}, to obtain the required values for $L_1(m_b)$ and $L_2(m_b)$.

5.4.2 Lattice computation and results

The non-perturbative strong interaction effects in spectator contributions to inclusive decays are contained in the matrix elements M_i (5.83). They have been evaluated in a quenched simulation on a $12^3 \times 24$ lattice at $\beta = 5.7$ using the SW tree-level improved action [56]. We use 20 gauge-field configurations and the light quark propagators are computed using a stochastic inversion for the light propagators.

The use of this stochastic inversion technique makes it possible to compute a light-quark propagator from each point on the lattice with $0 < t \leq 12$ (we call this region box I) to each point with $12 < t \leq 24 = 0$ (box II). As already explained in chapter 4, this doubles the effective statistics in the computation of the matrix elements.

In this exploratory study we have performed the calculations at $c_{\rm SW} = 1.57$, and with two values of the light-quark mass, $m = 140$MeV and $m = 75$MeV, corresponding to $\kappa_1 = 0.13847$ and $\kappa_2 = 0.14077$ respectively. For this value of $c_{\rm SW}$ $\kappa_{crit} \simeq 0.14351$. The origin of our value for $c_{\rm SW}$ is discussed in chapter 4.

The same lattice has been used to compute, with satisfactory results, the wave function of a B-meson and the effective $B^* \to B + \pi$ coupling constant (in the Heavy Meson Chiral Lagrangian). This computation was described in chapter 4.

The evaluation of the matrix elements requires the computation of 2- and 3-point correlation functions of the form,

$$C_2(t_x) = \sum_{x} \langle 0|\, J(x) J^\dagger(0)\, |0\rangle \tag{5.87}$$

where we have assumed $t_x > 0$, and

$$C_{3j}(t_x, t_y) = \sum_{x,y} \langle 0|\, J(y) \mathcal{O}_j(0) J^\dagger(x)\, |0\rangle \tag{5.88}$$

where $t_y > 0 > t_x$. In eqs. (5.87) and (5.88) J and $J^\dagger$ are interpolating operators which can destroy/create the Λ_b baryon. Our choice is

$$J^\dagger_\gamma = \sum_{a,b,c,\alpha,\beta} \varepsilon_{abc} \left[\overline{u}^a_\alpha \left(\gamma^5 C\right)_{\alpha\beta} \overline{d}^b_\beta \overline{b}^c_\gamma \right] \tag{5.89}$$

where $\overline{u}$, $\overline{d}$ and $\overline{b}$ are creation operators for the quarks.

Moreover we define a quantity Z_Λ that encodes the superposition between this current and the desired ground state

$$Z_\Lambda u^{(s)}_\gamma(\mathbf{0}) = \frac{\langle \Lambda_b, s|\, J^\dagger_\gamma(0)\, |0\rangle}{\sqrt{2m_\Lambda}} \tag{5.90}$$

where s is the spin (up or down) of the baryon.

In order to enhance the contribution of the ground state to the correlation functions, it is useful to "smear" the interpolating operators J and $J^\dagger$ (see e.g. ref. [100] and references therein). In this section we will follow ref. [81] and adopt the type of smearing known as "fuzzing", already described in some detail in section 4.2.2. We introduce two superscipts on each correlation function, each of which can be either "F" or "L" depending whether the interpolating operators J and $J^\dagger$ are fuzzed or local.

The standard technique to extract hadronic matrix elements of the type $\langle\Lambda_b|\,\mathcal{O}_j\,|\Lambda_b\rangle$ is to look for plateaus in the ratios

$$R_j(t_1,t_2) = Z_\Lambda^2 \frac{C_{3j}^{FF}(t_1,t_2)}{C_2^{LF}(t_1)C_2^{LF}(t_2)}\ . \tag{5.91}$$

In our analysis, however, even with the use of fuzzed interpolating operators J and $J^\dagger$, it is not possible to eliminate entirely the effects of excited states from the three-point correlation functions $C_{3j}^{FF}(t_1,t_2)$. On the other hand we do find that the ground state does dominate the two-point correlation function $C_2^{FF}(t)$ for $t>3$, and the masses we obtain in this way agree, within errors, with those found by Chris Michael on the same lattice using a 3-mass correlated fit for different smeared correlators.

We have followed the following procedure to extract the matrix elements $\langle\Lambda_b|\,\mathcal{O}_j\,|\Lambda_b\rangle$:

- For each value of the light-quark mass we start by fitting the two-point correlation function for $t>3$ with a single exponential

$$C_2^{FF}(t) = (Z_{\Lambda_1}^F)^2 \exp(-m_\Lambda t) \tag{5.92}$$

  thus obtaining the mass of the ground state, m_Λ.

- In order to be able to subtract the effects of the excited state from the three point correlation functions, we now fit $C_2^{FF}(t)$ for $t>1$ with a double exponential

$$C_2^{FF}(t) = (Z_\Lambda^F)^2 e^{-m_\Lambda t} + (Z_{\Lambda_1}^F)^2 e^{-m_{\Lambda_1} t} \tag{5.93}$$

  keeping m_Λ and Z_Λ^F fixed at the values obtained from the single exponential fit above.

- For each of the operators of interest, $\mathcal{O}_j$, we then fit the three-point correlation function $C_{3j}^{FF}(t_1,t_2)$ to

$$\begin{aligned} C_{3j}^{FF}(t_1,t_2) &= \frac{\langle\Lambda_b|\mathcal{O}_j|\Lambda_b\rangle}{2m_\Lambda}(Z_\Lambda^F)^2 e^{-m_\Lambda(t_1+t_2)} && (5.94)\\ &+ C\left[e^{-m_\Lambda t_1 - m_{\Lambda_1} t_2} + e^{-m_\Lambda t_1 - m_{\Lambda_1} t_2}\right] && (5.95)\end{aligned}$$

  thus obtaining values for the two unknown parameters $\langle\Lambda_b|\,\mathcal{O}_j\,|\Lambda_b\rangle$ and the constant C, which encodes the contribution from excited states.

This procedure has been repeated for each of the 4 relevant operators, on 40 jackknife samples to extract the statistical errors (twice the number of gauge

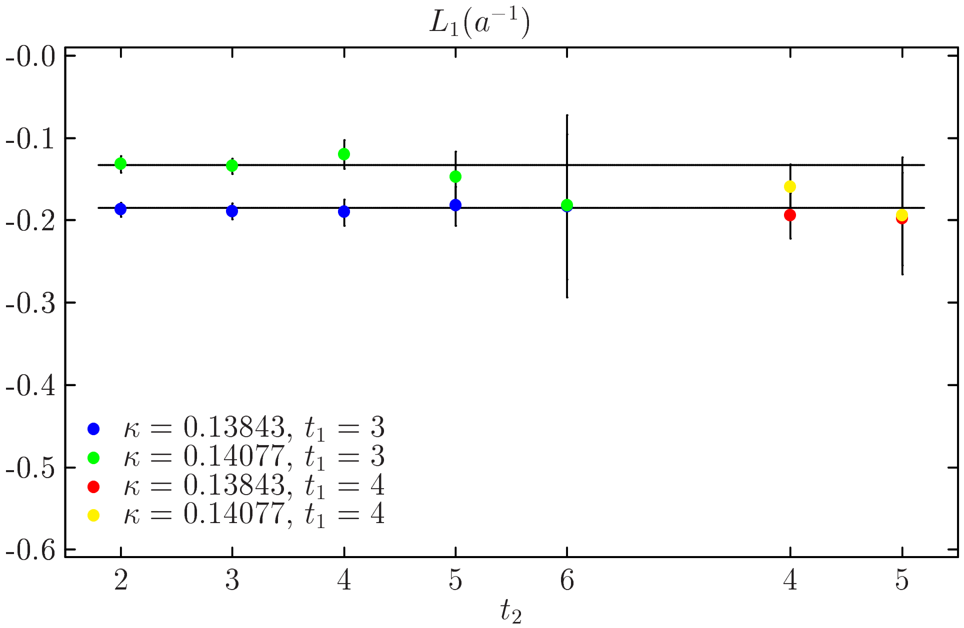

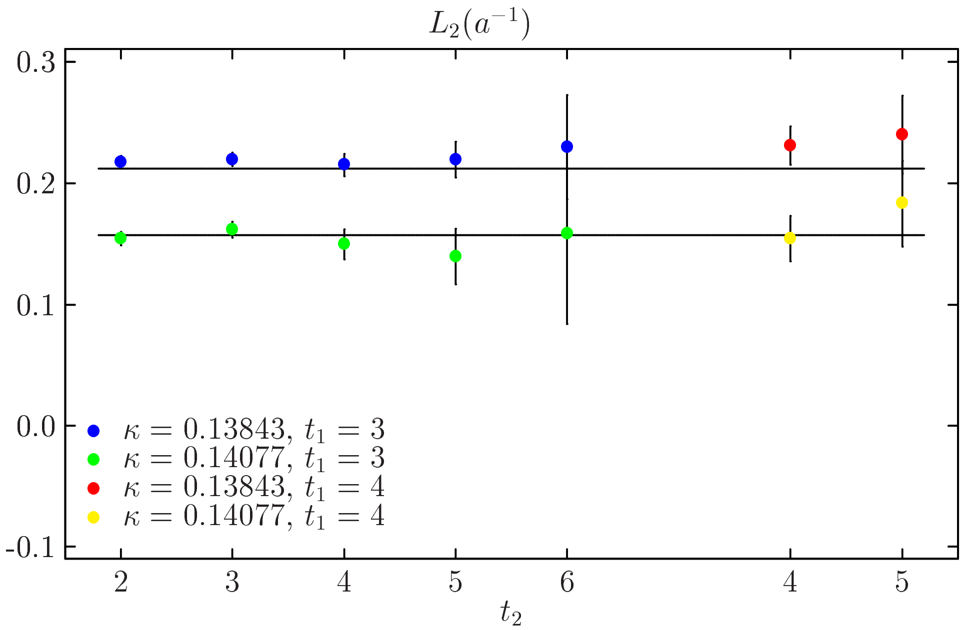

Figure 5.5: Plot of the matrix elements $L_1^{\overline{\rm MS},a^{-1}}$ and $L_2^{\overline{\rm MS},a^{-1}}$ computed after the substraction of excited states.

expression	κ_1	κ_2
$Z_A^2 Z_L^2 = f_B^2 m_B/2$	$0.33(1)$	$0.33(1)$
M_1	$-0.026(3)$	$-0.019(3)$
M_2	$0.045(4)$	$0.038(5)$
M_3	$0.018(2)$	$0.013(2)$
M_4	$-0.040(4)$	$-0.031(4)$
$L_1^{\overline{\mathrm{MS}},a^{-1}}$	$-0.18(2)$	$-0.13(3)$
$L_2^{\overline{\mathrm{MS}},a^{-1}}$	$0.21(2)$	$0.16(2)$
$L_1^{\overline{\mathrm{MS}},m_b}$	$-0.31(3)$	$-0.22(4)$
$L_2^{\overline{\mathrm{MS}},m_b}$	$0.23(2)$	$0.17(2)$

Table 5.4: Lattice results for the matrix elements computed on lattice, M_i, the combined matrix elements at two different scales, L_i, and the physical ratio of lifetimes.

configurations because of the two boxes into which the maximal variance reduction divides the lattice).

In order to justify the above procedure a posteriori, we subtract the contributions from the excited state obtained above from the two- and three-point correlation functions, and look for plateaus in the ratios:

$$R_j(t_1, t_2) = Z_\Lambda^2 \frac{\tilde{C}_{3j}^{FF}(t_1, t_2)}{\tilde{C}_2^{LF}(t_1)\tilde{C}_2^{LF}(t_2)} \tag{5.96}$$

where $\tilde{C}$ indicates that contribution from excited states has been substracted from the correlation function C. The subtracted two-point correlation function is reported in fig. 5.4. Fig. 5.5 shows the plateaus of R for those operators that correspond to L_1 and L_2 (with the appropriate normalization factor $\frac{8}{f_B^2 m_B}$). The plateaus in fig. 5.5 give us confidence in our treatment of the subtraction of the contribution of the excited state. The results for the operators obtained from eq. (5.96) agree to within 1% with those obtained from eq. (5.95).

Our results for the two values of κ are reported in table (5.4). Combining them with eq. (5.22) we obtain

$$\frac{\tau(\Lambda_b)}{\tau(B^0)} = \begin{cases} 0.91(1) & \text{for } m_u = m_d = 140 \text{ MeV} \\ 0.93(1) & \text{for } m_u = m_d = 75 \text{ MeV} \end{cases} \tag{5.97}$$

Appendix A

Introduction to Quantum Field Theory

Consider a system described by a set of fields $\{\phi_i(x)\}$ and a Lagrangian which is function of $\phi_i(x)$, $\partial_\mu \phi_i(x)$ and eventually some external fields

$$\mathcal{L} = \mathcal{L}_0 + \mathcal{L}_I \tag{A.1}$$

$\mathcal{L}_I$ is the interactive part of the Lagrangian. The equations of motion are given by

$$\partial_\mu \frac{\partial \mathcal{L}}{\partial(\partial_\mu \phi_i)} - \frac{\partial \mathcal{L}}{\partial \phi_i} = 0 \tag{A.2}$$

Noether's theorem: If, under the general infinitesimal transformation of space-time coordinates and fields (functions of the infinitesimal parameters $\delta\alpha_a$)

$$x_\mu \to x'_\mu = x_\mu + X^a_\mu \delta\alpha_a \tag{A.3}$$

$$\phi_i(x) \to \phi'_i(x') = \phi_i(x) + \Phi^a_i(x)\delta\alpha_a \tag{A.4}$$

the Lagrangian transforms in the following way

$$\mathcal{L}(x)\mathrm{d}^4x \to \mathcal{L}'(x')\mathrm{d}^4x' = [\mathcal{L}(x) + \partial^\mu Z^a_\mu(x)\delta\alpha_a]\mathrm{d}^4x \tag{A.5}$$

then the transformation is a symmetry of the equation of motion and there is a conserved current associated to it

$$J^{\mu a} = \frac{\partial \mathcal{L}}{\partial(\partial_\mu \phi_i)}(\partial^\nu \phi_i X^a_\nu - \Phi^a_i) - \mathcal{L} X^a_\mu \tag{A.6}$$

with $\partial_\mu J^{\mu a} = 0$. The generators of the transformation are the conserved charges given by

$$Q^a(t_x) = \int \mathrm{d}^3\mathbf{x} J^{0a}(\mathbf{x}, t_x) \tag{A.7}$$

If in the transformation (A.4) the parameter $\delta\alpha_a$ is function of x, the transformation is called a gauge transformation.

The generator of temporal translations is called the Hamiltonian and it is defined as

$$H(t) = H_0(t) + H_I(t) = \int \mathrm{d}^3x \frac{\partial \mathcal{L}}{\partial(\partial_0 \phi_i)}(\partial_0 \phi_i) - \mathcal{L} \tag{A.8}$$

where $H_I(t) = -\int \mathrm{d}^3x \mathcal{L}_I(\mathbf{x}, t_x)$.

Green functions: The vacuum expectation value of a set of fields is defined as

$$\begin{aligned} G_{i_1,\ldots,i_n}(x_1,\ldots,x_n) &\equiv \langle 0| T\{\phi_{i_1}(x_1),\ldots,\phi_{i_n}(x_n)\} |0\rangle \\ &\equiv \lim_{T\to\infty} \langle \mathbf{0}| T\{\phi_{i_1}(x_1),\ldots,\phi_{i_n}(x_n), e^{-i\int_{-T}^{+T} H_I(t)\mathrm{d}t}\} |\mathbf{0}\rangle \\ &= \int [\mathrm{d}\phi]\, \phi_{i_1}(x_1)\ldots\phi_{i_n}(x_n) e^{i\int \mathrm{d}^4x\mathcal{L}} \\ &= \frac{1}{Z[0]} \frac{-i\delta}{\delta J_{i_1}(x_1)} \cdots \frac{-i\delta}{\delta J_{i_n}(x_n)} Z[J_1,\ldots,J_n] \end{aligned} \tag{A.9}$$

where

$$Z[J_1,\ldots,J_n] \equiv \int [\mathrm{d}\phi]\, e^{i\int \mathrm{d}^4x\mathcal{L} + \sum_i J_i\phi_i} \tag{A.10}$$

The latter expression is called the generating functional (or partition function after the Wick rotation).

Note the distinction between $|\mathbf{0}\rangle$, a state containing 0 particles, and $|0\rangle$, interpreted as the physical vacuum state. Eq. (A.9) may be interpreted together as a definition of $G(...)$ and $|0\rangle$. The symbol $\phi_i(x)$ in eq. (A.9)) has to be interpreted as an operator in the Fock space, while in eq. (A.10) it has to be interpreted as a quantum field defined in some appropriate physical Hilbert space. Since there is a $1-1$ correspondence between them, the same symbol can be used without generating ambiguities.

LSZ reduction formula: In the context of the scattering processes and decay processes it is often convenient to define in and out states as

$$|\phi_1(x_1)\phi_2(x_2)...\rangle_{in} = \lim_{T\to-\infty} e^{+iH_0T}e^{-iHT}\overline{\phi}_1(x_1)\overline{\phi}_2(x_2)...\,|0\rangle \tag{A.11}$$

$$|\phi_3(x_3)\phi_4(x_4)...\rangle_{out} = \lim_{T\to+\infty} e^{+iH_0T}e^{-iHT}\overline{\phi}_3(x_4)\overline{\phi}_3(x_4)...\,|0\rangle \tag{A.12}$$

The state *in* (*out*) has to be interpreted as the state which asymptotic behaviour for large negative (positive) time is that given by $\overline{\phi}_1(x_1)\overline{\phi}_2(x_2)...\,|0\rangle$ ($\overline{\phi}_3(x_4)\overline{\phi}_3(x_4)...\,|0\rangle$).

It is possible to construct a Hilbert space for the *in* states and associate a Fock representation to it. It is important to stress that this representation is isomorphic but not coincident with the analogous representation for *out* states. The two are related by the so called $\mathcal{S}$ matrix

$$|\phi_1(x_1)\phi_2(x_2)...\rangle_{out} \equiv \mathcal{S}^\dagger\,|\phi_1(x_1)\phi_2(x_2)...\rangle_{in} \tag{A.13}$$

and the $\mathcal{S}$ matrix is formally defined as

$$\mathcal{S} \equiv : \exp\left[\int \mathrm{d}^4x \sum_i \phi_{i,in}(x)K_{i,x}\frac{\delta}{\delta J_i(x)}\right] : Z[J_1,...,J_n] \tag{A.14}$$

where $K_{i,x}\phi_i(x)$ is the free classical equation of motion for the field $\phi_i(x)$ derived by the Lagrangian $\mathcal{L}$. In the case of a scalar theory $K_{i,x} = (\Box_x + m_i)$ is the Klein-Gordon functional and m_i is the mass associated to the field ϕ_i. Eq. A.14 is called LSZ reduction formula.

Optical Theorem: Because of restrictions imposed by causality the $\mathcal{S}$ matrix has to be hemitian. In terms of the transition matrix $\mathcal{T}$, implicitly defined by

$\mathcal{S} = 1 + i\mathcal{T}$, the theorem states that

$$\mathcal{T}^\dagger \mathcal{T} = 2\text{Im}(\mathcal{T}) \tag{A.15}$$

Decay and Scattering: One is usually interested in the transition matrix elements between some asymptotic *in* and *out* states

$$\begin{aligned} {}_{out}\langle f|i\rangle_{in} &= {}_{in}\langle f|\,\mathcal{S}\,|i\rangle_{in} \\ &= \delta_{fi} - i(2\pi)^4\delta^4(p_1 + p_2 + ... - p_3 - p_4 - ..)\mathcal{M}_{fi} \end{aligned} \tag{A.16}$$

$\mathcal{M}_{fi}$ is the transition amplitude that appears in the formulas for the decay rate (A.17) and for the cross section (A.18). In practice $\mathcal{M}_{fi}$ can be computed directly from the Green function (A.9), isolating the connected contribution and omitting the propagators for external particles.

The formula for the inverse decay time of a particle of 4-momentum $p = (E_{\mathbf{p}}, \mathbf{p})$ is

$$\tau^{-1} = \frac{1}{2E_{\mathbf{p}}} \int \left(\prod_{i>1} \frac{\mathrm{d}_3\mathbf{p}_i}{2E_{\mathbf{p}_i}} \right) (2\pi)^4\delta^4(p - \sum_{i>1} p_i)\, |\mathcal{M}_{fi}|^2 \tag{A.17}$$

The formula for the cross section of two scattering particles of momenta p_1 and p_2 respectively is

$$\sigma = \frac{1}{4\sqrt{(p_1 \cdot p_2)^2 - p_1^2 p_2^2}} \int \left(\prod_{i>2} \frac{\mathrm{d}_3\mathbf{p}_i}{2E_{\mathbf{p}_i}} \right) (2\pi)^4\delta^4(p_1 + p_2 - \sum_{i>2} p_i)\, |\mathcal{M}_{fi}|^2 \tag{A.18}$$

where $E_{\mathbf{p}} = \sqrt{m^2 + \mathbf{p}^2}$ and $\mathrm{d}_n = (2\pi)^{-n}\mathrm{d}^n$.

Appendix B

Useful Formulae and Notation

B.1 Notation in Minkowski Space-Time in $d = 4$ dimension

- Metric

$$g^{\mu\nu} = \mathrm{diag}(1, -1, -1, -1) \tag{B.1}$$

- Pauli matrices

$$\sigma_1 = \begin{pmatrix} 0 & 1 \\ 1 & 0 \end{pmatrix} \qquad \sigma_2 = \begin{pmatrix} 0 & -i \\ i & 0 \end{pmatrix} \qquad \sigma_3 = \begin{pmatrix} 1 & 0 \\ 0 & -1 \end{pmatrix} \tag{B.2}$$

they undergo the commutation relation

$$[\sigma_i, \sigma_j] = 2i\varepsilon^{ijk}\sigma_k \tag{B.3}$$

- Dirac matrices (Dirac representation)

$$\gamma^0 = \begin{pmatrix} \mathbf{1} & 0 \\ 0 & -\mathbf{1} \end{pmatrix} \qquad \gamma^i = \begin{pmatrix} 0 & \sigma_i \\ -\sigma_i & 0 \end{pmatrix} \qquad \gamma^5 = \begin{pmatrix} 0 & 1 \\ 1 & 0 \end{pmatrix} \tag{B.4}$$

- Dirac matrices (Chiral representation)

$$\gamma^0 = \begin{pmatrix} 0 & \mathbf{1} \\ \mathbf{1} & 0 \end{pmatrix} \qquad \gamma^i = \begin{pmatrix} 0 & \sigma_i \\ -\sigma_i & 0 \end{pmatrix} \qquad \gamma^5 = \begin{pmatrix} -\mathbf{1} & 0 \\ 0 & \mathbf{1} \end{pmatrix} \tag{B.5}$$

In both the representations γ^0 and γ^5 are hermitian and γ^i are anti-hermitian. The following relations hold

$$g^{\mu\nu} = \frac{1}{2}\{\gamma^\mu, \gamma^\nu\} \tag{B.6}$$

$$\sigma^{\mu\nu} = \frac{i}{2}[\gamma^\mu, \gamma^\nu] \tag{B.7}$$

$$\gamma_5 = \gamma^5 = i\gamma^0\gamma^1\gamma^2\gamma^3 \tag{B.8}$$

- Projectors

$$L = \frac{1-\gamma^5}{2} \qquad R = \frac{1+\gamma^5}{2} \tag{B.9}$$

- Traces

$$\mathrm{tr}(\gamma^\mu\gamma^\nu) = 4g^{\mu\nu} \tag{B.10}$$

$$\mathrm{tr}(\gamma^\mu\gamma^\nu\gamma^\rho) = 0 \tag{B.11}$$

$$\mathrm{tr}(\gamma^\mu\gamma^\nu\gamma^\rho\gamma^\sigma) = 4(g^{\mu\nu}g^{\rho\sigma} - g^{\mu\rho}g^{\nu\sigma} + g^{\mu\sigma}g^{\rho\nu}) \tag{B.12}$$

$$\mathrm{tr}(\gamma^5\gamma^\mu\gamma^\nu\gamma^\rho\gamma^\sigma) = 4i\epsilon^{\mu\nu\rho\sigma} \tag{B.13}$$

where $\epsilon^{0123} = -\epsilon_{0123} = 1$.

B.2 Notation in Euclidean Space-Time in $d = 4$ dimension

- Wick rotation prescription (E for Euclidean, M for Minkowski)

$$\begin{array}{|cc|cc|} \hline \mathrm{E} & \mathrm{M} & \mathrm{E} & \mathrm{M} \\ \hline x^0 & ix^0 & x^i & x^i \\ \partial^0 & -i\partial_0 & \partial^i & \partial_i \\ A^4 & -iA_0 & A^i & A_i \\ F^0 i & -iF_{0i} & F^{ij} & F_{ij} \\ \gamma^0 & \gamma^0 & \gamma^i & -i\gamma^i \\ \gamma^5 & \gamma^5 & & \\ \hline \end{array} \tag{B.14}$$

The integration measure transform as follow

$$\exp(-\mathcal{S}_E) = \exp(i\mathcal{S}_M) \tag{B.15}$$

where

$$\mathcal{S}_E = \int \mathrm{d}^4 x_E \mathcal{L}_E[...] = -i \int \mathrm{d}^4 x_M \mathcal{L}_M[...] \tag{B.16}$$

The choice $\mathrm{d}^4 x_E = i\mathrm{d}^4 x_M$ can be made, hence $\mathcal{L}_E[...] = -\mathcal{L}_M[...]$

- Metric

$$g_E^{\mu\nu} = -\delta^{\mu\nu} = \mathrm{diag}(-1,-1,-1,-1) \tag{B.17}$$

- Dirac matrices (Dirac representation)

$$\gamma^0 = \begin{pmatrix} \mathbf{1} & 0 \\ 0 & -\mathbf{1} \end{pmatrix} \qquad \gamma^i = \begin{pmatrix} 0 & -i\sigma_i \\ i\sigma_i & 0 \end{pmatrix} \qquad \gamma^5 = \begin{pmatrix} 0 & 1 \\ 1 & 0 \end{pmatrix} \tag{B.18}$$

Dirac matrices (Chiral representation)

$$\gamma^0 = \begin{pmatrix} 0 & \mathbf{1} \\ \mathbf{1} & 0 \end{pmatrix} \qquad \gamma^i = \begin{pmatrix} 0 & -i\sigma_i \\ i\sigma_i & 0 \end{pmatrix} \qquad \gamma^5 = \begin{pmatrix} -\mathbf{1} & 0 \\ 0 & \mathbf{1} \end{pmatrix} \tag{B.19}$$

All the Euclidean Dirac matrices are hermitian. The following relations hold

$$g^{\mu\nu} = \frac{1}{2}\{\gamma^\mu, \gamma^\nu\} = \delta^{\mu\nu} \tag{B.20}$$

$$\sigma^{\mu\nu} = \frac{i}{2}[\gamma^\mu, \gamma^\nu] \tag{B.21}$$

$$\gamma^5 = \gamma^0\gamma^1\gamma^2\gamma^3 \tag{B.22}$$

and all the $\sigma^{\mu\nu}$ are hermitian.

- Projectors

$$L = \frac{1-\gamma^5}{2} \qquad R = \frac{1+\gamma^5}{2} \tag{B.23}$$

- Traces

$$\mathrm{tr}(\gamma^\mu\gamma^\nu) = 4\delta^{\mu\nu} \tag{B.24}$$

$$\mathrm{tr}(\gamma^\mu\gamma^\nu\gamma^\rho) = 0 \tag{B.25}$$

$$\mathrm{tr}(\gamma^\mu\gamma^\nu\gamma^\rho\gamma^\sigma) = 4(\delta^{\mu\nu}\delta^{\rho\sigma} - \delta^{\mu\rho}\delta^{\nu\sigma} + \delta^{\mu\sigma}\delta^{\rho\nu}) \tag{B.26}$$

$$\mathrm{tr}(\gamma^5\gamma^\mu\gamma^\nu\gamma^\rho\gamma^\sigma) = 4\epsilon_E^{\mu\nu\rho\sigma} \tag{B.27}$$

where $\epsilon_E^{0123} = -1$.

B.3 Operators and Algebra

- Fourier decomposition of the basic fields (of spin 0, 1/2 and 1 respectively) in a basis of creation-annihilation operators (using the relativistic normalization)

$$\varphi(x) = \int \frac{\mathrm{d}_3\mathbf{p}}{2E_{\mathbf{p}}} \left[a(\mathbf{p})e^{-ipx} + a^\dagger(\mathbf{p})e^{ipx}\right] \tag{B.28}$$

$$\psi_\alpha(x) = \int \frac{\mathrm{d}_3\mathbf{p}}{2E_{\mathbf{p}}} \sum_{s=-\frac{1}{2},\frac{1}{2}} \left[b(\mathbf{p},s)u_\alpha(\mathbf{p},s)e^{-ipx} + d^\dagger(\mathbf{p},s)v_\alpha(\mathbf{p},s)e^{ipx}\right] \tag{B.29}$$

$$A_\mu(x) = \int \frac{\mathrm{d}_3\mathbf{p}}{2E_{\mathbf{p}}} \sum_{s=1,2,3} \left[\epsilon_\mu(\mathbf{p},s)c(\mathbf{p},s)e^{-ipx} + \epsilon^*_\mu(\mathbf{p},s)c^\dagger(\mathbf{p},s)e^{ipx}\right] \tag{B.30}$$

where $E_{\mathbf{p}} = \sqrt{m^2 + \mathbf{p}^2}$ and $\mathrm{d}_n = (2\pi)^{-n}\mathrm{d}^n$.

The creation-annihilation operators satisfy commutation relations deduced by the theorem of "spin and statistics" and causality.

- Commutation relations for bosons

$$[a(\mathbf{p}), a(\mathbf{p}')] = [a^\dagger(\mathbf{p}), a^\dagger(\mathbf{p}')] = 0 \tag{B.31}$$

$$[a(\mathbf{p}), a^\dagger(\mathbf{p}')] = 2E_{\mathbf{p}}(2\pi)^3\delta^3(\mathbf{p} - \mathbf{p}') \tag{B.32}$$

$$\left[c(\mathbf{p},s), c^\dagger(\mathbf{p}',s')\right] = 2E_{\mathbf{p}}\delta_{s,s'}(2\pi)^3\delta^3(\mathbf{p} - \mathbf{p}') \tag{B.33}$$

- Commutation relations for fermions

$$\{b(\mathbf{p},s), b(\mathbf{p}',s')\} = \left\{b^\dagger(\mathbf{p},s), b^\dagger(\mathbf{p}',s')\right\} = 0 \tag{B.34}$$

$$\{d(\mathbf{p},s), d(\mathbf{p}',s')\} = \left\{d^\dagger(\mathbf{p},s), d^\dagger(\mathbf{p}',s')\right\} = 0 \tag{B.35}$$

$$\left\{b(\mathbf{p},s), b^\dagger(\mathbf{p}',s')\right\} = 2E_{\mathbf{p}}\delta_{s,s'}(2\pi)^3\delta^3(\mathbf{p} - \mathbf{p}') \tag{B.36}$$

$$\left\{d(\mathbf{p},s), d^\dagger(\mathbf{p}',s')\right\} = 2E_{\mathbf{p}}\delta_{s,s'}(2\pi)^3\delta^3(\mathbf{p} - \mathbf{p}') \tag{B.37}$$

- The Dirac spinors $u(\mathbf{p},s)$ is a positive-energy eigenstate of momentum $\mathbf{p}$ and of spin $s = \pm\frac{1}{2}$, $v(\mathbf{p},s)$ is a negative-energy eigenstate of the same operators. They are solutions of the Dirac equations

$$(\not{p} - m)u(\mathbf{p},s) = 0 \tag{B.38}$$

$$(\not{p} + m)v(\mathbf{p},s) = 0 \tag{B.39}$$

$\overline{u}(\mathbf{p}, s) = u^\dagger(\mathbf{p}, s)\gamma^0$ and $\overline{v}(\mathbf{p}, s) = v^\dagger(\mathbf{p}, s)\gamma^0$ are solutions of

$$\overline{u}(\mathbf{p}, s)(\not{p} - m) = 0 \tag{B.40}$$

$$\overline{v}(\mathbf{p}, s)(\not{p} + m) = 0 \tag{B.41}$$

- Relations between spinors

$$\overline{u}(\mathbf{p}, r)u(\mathbf{p}, s) = 2m\delta_{r,s} \tag{B.42}$$

$$\overline{v}(\mathbf{p}, r)v(\mathbf{p}, s) = -2m\delta_{r,s} \tag{B.43}$$

$$\overline{u}(\mathbf{p}, r)\gamma^\mu u(\mathbf{p}, s) = 2p^\mu \delta_{r,s} \tag{B.44}$$

$$\overline{v}(\mathbf{p}, r)\gamma^\mu v(\mathbf{p}, s) = -2p^\mu \delta_{r,s} \tag{B.45}$$

$$\sum_s u(\mathbf{p}, s)\overline{u}(\mathbf{p}, s) = \not{p} + m \tag{B.46}$$

$$\sum_s v(\mathbf{p}, s)\overline{v}(\mathbf{p}, s) = \not{p} - m \tag{B.47}$$

- Gordon decomposition

$$\overline{u}(\mathbf{p}', r)\gamma^\mu u(\mathbf{p}, s) = \frac{1}{2m}\overline{u}(\mathbf{p}', r)\left[(p' + p)^\mu + i\sigma^{\mu\nu}(p' - p)_\nu\right] u(\mathbf{p}, s) \tag{B.48}$$

- Explicit expression for the Dirac spinors in the Dirac representation

$$u(\mathbf{p}, s) = \begin{pmatrix} (E_{\mathbf{p}} + m)^{\frac{1}{2}} \\ (E_{\mathbf{p}} + m)^{-\frac{1}{2}}(\sigma \cdot \mathbf{p}) \end{pmatrix} \otimes \chi_s \tag{B.49}$$

$$v(\mathbf{p}, s) = \begin{pmatrix} (E_{\mathbf{p}} + m)^{-\frac{1}{2}}(\sigma \cdot \mathbf{p}) \\ (E_{\mathbf{p}} + m)^{\frac{1}{2}} \end{pmatrix} \otimes \chi_s \tag{B.50}$$

where χ_s are eigenstates of the spin

$$\chi_{+1/2} = \begin{pmatrix} 1 \\ 0 \end{pmatrix}; \qquad \chi_{-1/2} = \begin{pmatrix} 0 \\ 1 \end{pmatrix} \tag{B.51}$$

- Free scalar propagator

$$i\Delta(x) = \langle 0| T\left\{\varphi(x), \varphi^\dagger(0)\right\}|0\rangle = \int \mathrm{d}_4p \frac{i}{p^2 - m^2 + i\varepsilon} e^{-ipx} \tag{B.52}$$

- Free Dirac propagator

$$iS_{\alpha\beta}(x) = \langle 0| T\left\{\psi_\alpha(x), \psi^\dagger_\beta(0)\right\}|0\rangle = \int \mathrm{d}_4p \frac{i(\not{p} + m)_{\alpha\beta}}{p^2 - m^2 + i\varepsilon} e^{-ipx} \tag{B.53}$$

- Free vector-field propagator

$$iD_{\mu\nu}(x) = \langle 0| T\left\{A_\mu(x), A_\nu(0)\right\}|0\rangle = \int \mathrm{d}_4p \frac{i(-g_{\mu\nu} + f_{\mu\nu}(p))}{p^2 - m^2 + i\varepsilon} e^{-ipx} \tag{B.54}$$

where

$$f_{\mu\nu}(p) = \frac{(1-\zeta)p_\mu p_\nu}{p^2 - \zeta m^2 + i\varepsilon} \tag{B.55}$$

It is gauge dependent. The choice $\zeta = 1$ correspond to the Feynman gauge and $\zeta = 0$ to the Landau gauge. For a massless vector field A_μ, the choice $\zeta = 0$ is called Coulomb gauge and correspond to the constraint

$$\langle 0| \partial^\mu A_\mu(x) |0\rangle = 0 \tag{B.56}$$

- Discrete symmetries (in Minkowski space)

	C	P	T
$\phi(x)$	$\eta_C\phi^\dagger(x)$	$\eta_P\phi(x_I)$	$\eta_T\phi(x_T)$
$\partial_\mu\phi(x)$	$\eta_C\partial_\mu\phi^\dagger(x)$	$\eta_P g^{\mu\mu}\partial_\mu\phi(x_I)$	$-\eta_T g^{\mu\mu}\partial_\mu\phi(x_T)$
$\psi_\alpha(x)$	$i\eta_C\gamma^2_{\alpha\beta}\psi^\dagger_\beta(x)$	$\eta_P\gamma^0_{\alpha\beta}\psi_\beta(x_I)$	$i\eta_T(\gamma^5\gamma^0\gamma^2)_{\alpha\beta}\psi_\beta(x_T)$
$\overline{\psi}_\alpha(x)$	$i\eta^*_C(\gamma^0\gamma^2)_{\alpha\beta}\psi_\beta(x)$	$\eta^*_P\gamma^0_{\beta\alpha}\psi_\beta(x_I)$	$i\eta^*_T(\gamma^2\gamma^0\gamma^5)_{\beta\alpha}\psi_\beta(x_T)$
$A_\mu(x)$	$\eta_C A^\dagger_\mu(x)$	$\eta_P g^{\mu\mu}A_\mu(x_I)$	$-\eta_T g^{\mu\mu}A_\mu(x_T)$
$:\overline{\psi}\psi:$	$:\overline{\psi}\psi:$	$:\overline{\psi}\psi:$	$:\overline{\psi}\psi:$
$:\overline{\psi}\gamma^5\psi:$	$:\overline{\psi}\gamma^5\psi:$	$-:\overline{\psi}\gamma^5\psi:$	$:\overline{\psi}\gamma^5\psi:$
$:\overline{\psi}\gamma_\mu\psi:$	$-:\overline{\psi}\gamma_\mu\psi:$	$g^{\mu\mu}:\overline{\psi}\gamma_\mu\psi:$	$g^{\mu\mu}:\overline{\psi}\gamma_\mu\psi:$
$:\overline{\psi}\gamma_\mu\gamma^5\psi:$	$:\overline{\psi}\gamma_\mu\gamma^5\psi:$	$-g^{\mu\mu}:\overline{\psi}\gamma_\mu\gamma^5\psi:$	$g^{\mu\mu}:\overline{\psi}\gamma_\mu\gamma^5\psi:$
$:\overline{\psi}\sigma_{\mu\nu}\psi:$	$:\overline{\psi}\sigma_{\mu\nu}\psi:$	$g^{\mu\mu}g^{\nu\nu}:\overline{\psi}\sigma_{\mu\nu}\psi:$	$-g^{\mu\mu}g^{\nu\nu}:\overline{\psi}\sigma_{\mu\nu}\psi:$

where $\eta_C = \pm 1$ and η_P, η_T are chosen such that $\eta_C\eta_P\eta_T = 1$. Under these definitions for any operator $\mathcal{O}(x)$

$$(CPT)\mathcal{O}_{\mu_1\ldots\mu_n}(x)(CPT)^{-1} = (-1)^n\mathcal{O}^\dagger_{\mu_1\ldots\mu_n}(-x) \tag{B.57}$$

This is known as CPT theorem. Note that $TiT^{-1} = -i$.

- Fierz identities

$$\begin{pmatrix} \overline{u}_1u_2\overline{u}_3u_4 \\ \overline{u}_1\gamma^5u_2\overline{u}_3\gamma^5u_4 \\ \overline{u}_1\gamma^\mu u_2\overline{u}_3\gamma_\mu u_4 \\ \overline{u}_1\gamma^5\gamma^\mu u_2\overline{u}_3\gamma^5\gamma_\mu u_4 \\ \overline{u}_1\sigma^{\mu\nu}u_2\overline{u}_3\sigma_{\mu\nu}u_4 \end{pmatrix} = \frac{1}{4}\begin{pmatrix} 1 & 1 & 1 & 1 & \frac{1}{2} \\ 1 & 1 & -1 & -1 & \frac{1}{2} \\ 4 & -4 & -2 & 2 & 0 \\ 4 & -4 & 2 & -2 & 0 \\ 12 & 12 & 0 & 0 & -2 \end{pmatrix}\begin{pmatrix} \overline{u}_1u_4\overline{u}_3u_2 \\ \overline{u}_1\gamma^5u_4\overline{u}_3\gamma^5u_2 \\ \overline{u}_1\gamma^\mu u_4\overline{u}_3\gamma_\mu u_2 \\ \overline{u}_1\gamma^5\gamma^\mu u_4\overline{u}_3\gamma^5\gamma_\mu u_2 \\ \overline{u}_1\sigma^{\mu\nu}u_4\overline{u}_3\sigma_{\mu\nu}u_2 \end{pmatrix}$$

- Clebsh-Gordan Coefficients, $C^{j,j_1,j_2}_{m,m_1,m_2}$. They can be built by iterative use of the two identities

$$\begin{aligned}\sqrt{j(j+1)-m(m+1)}C^{j,j_1,j_2}_{m+1,m_1,m_2} =& \\ &\sqrt{j_1(j_1+1)-m_1(m_1+1)}C^{j,j_1,j_2}_{m,m_1-1,m_2} + \\ &\sqrt{j_2(j_2+1)-m_2(m_2+1)}C^{j,j_1,j_2}_{m,m_1,m_2-1}\end{aligned} \tag{B.58}$$

$$\begin{aligned}\sqrt{j(j+1)-m(m+1)}C^{j,j_1,j_2}_{m-1,m_1,m_2} =& \\ &\sqrt{j_1(j_1+1)-m_1(m_1+1)}C^{j,j_1,j_2}_{m,m_1+1,m_2} + \\ &\sqrt{j_2(j_2+1)-m_2(m_2+1)}C^{j,j_1,j_2}_{m,m_1,m_2+1}\end{aligned} \tag{B.59}$$

They are different from zero only if

$$m = m_1 + m_2; \qquad |j_1 - j_2| \le j \le |j_1 + j_2| \tag{B.60}$$

B.4 Gauge groups

- Gauge tranfromation on the fields $U = e^{it^a\theta_a} \in SU(N)$

$$\varphi \to U\varphi \tag{B.61}$$
$$\psi \to U\psi \tag{B.62}$$
$$\overline{\psi} \to \overline{\psi}U^{-1}$$
$$A_\mu \to UA_\mu U^{-1} + U\partial_\mu U^{-1} \tag{B.63}$$

- Properties of the group generators t^a

$$\mathrm{tr}(t^a) = 0 \tag{B.64}$$
$$\mathrm{tr}(t^a t^b) = \frac{1}{2}\delta^{ab} \tag{B.65}$$
$$(t^a)_{ij}(t^b)_{kl} = \frac{1}{2}\left[\delta_{il}\delta_{jk} - \frac{1}{N}\delta_{ij}\delta_{kl}\right] \tag{B.66}$$
$$\left[t^a, t^b\right] = if^{abc}t^c \tag{B.67}$$

- Casimir operators (i.e. gauge invariant operators which commute with all the generators of the gauge group):

$$C_F \delta_{ij} = \sum_a (t^a t^{a\dagger})_{ij} \tag{B.68}$$

$$C_A \delta^{ab} = \sum_{cd} f^{cda} (f^{cdb})^* \tag{B.69}$$

$$T_F \delta^{ab} = \sum_{ij} (t^a)_{ij} (t^b)^*_{ji} \tag{B.70}$$

The next table lists the properties of those groups which appear to be the most relevant in physics

group	generators	C_F	C_A	T_F
$U(1)$	1	0	1	1
$SU(2)$	$T_i = \frac{1}{2}\sigma_i$	2	$\frac{3}{4}$	$\frac{1}{2}$
$SU(3)$	$t^a = \frac{1}{2}\lambda^a$	3	$\frac{4}{3}$	$\frac{1}{2}$
$SU(N)$		N	$\frac{N^2-1}{2N}$	$\frac{1}{2}$

(B.71)

- Gell-Mann matrices

$$\lambda^1 = \begin{pmatrix} 0 & 1 & 0 \\ 1 & 0 & 0 \\ 0 & 0 & 0 \end{pmatrix} \qquad \lambda^2 = \begin{pmatrix} 0 & -i & 0 \\ i & 0 & 0 \\ 0 & 0 & 0 \end{pmatrix} \tag{B.72}$$

$$\lambda^3 = \begin{pmatrix} 1 & 0 & 0 \\ 0 & -1 & 0 \\ 0 & 0 & 0 \end{pmatrix} \qquad \lambda^4 = \begin{pmatrix} 0 & 0 & 1 \\ 0 & 0 & 0 \\ 1 & 0 & 0 \end{pmatrix} \tag{B.73}$$

$$\lambda^5 = \begin{pmatrix} 0 & 0 & -i \\ 0 & 0 & 0 \\ i & 0 & 0 \end{pmatrix} \qquad \lambda^6 = \begin{pmatrix} 0 & 0 & 0 \\ 0 & 0 & 1 \\ 0 & 1 & 0 \end{pmatrix} \tag{B.74}$$

$$\lambda^7 = \begin{pmatrix} 0 & 0 & 0 \\ 0 & 0 & -i \\ 0 & i & 0 \end{pmatrix} \qquad \lambda^8 = \frac{1}{\sqrt{3}} \begin{pmatrix} 1 & 0 & 0 \\ 0 & 1 & 0 \\ 0 & 0 & -2 \end{pmatrix} \tag{B.75}$$

The matrices $t^a = \frac{\lambda^a}{2}$ are generators of $SU(3)$ and satisfy the relations

$$t^a t^b = \frac{1}{6}\delta^{ab} + \frac{1}{2}(if^{abc} + d^{abc})t^c \tag{B.76}$$

$$t^a t^a = \frac{4}{3} \tag{B.77}$$

$$t^a t^b t^a = -\frac{1}{6}t^b \tag{B.78}$$

$$t^a t^b \otimes t^a t^b = \frac{2}{9}\mathbf{1}\otimes\mathbf{1} - \frac{1}{3}t^a \otimes t^a \tag{B.79}$$

$$t^a t^b \otimes t^b t^a = \frac{2}{9}\mathbf{1}\otimes\mathbf{1} + \frac{7}{6}t^a \otimes t^a \tag{B.80}$$

where f^{abc} are totally antisymmentric, d^{abc} are totally symmentric and their non vanishing elements are given by

abc	f^{abc}	abc	d^{abc}	abc	d^{abc}
123	1	118	$1/\sqrt{3}$	355	$1/2$
147	$1/2$	146	$1/2$	366	$-1/2$
156	$-1/2$	157	$1/2$	377	$-1/2$
246	$1/2$	228	$1/\sqrt{3}$	448	$-1/2\sqrt{3}$
257	$1/2$	247	$-1/2$	558	$-1/2\sqrt{3}$
345	$1/2$	256	$1/2$	668	$-1/2\sqrt{3}$
367	$-1/2$	338	$1/\sqrt{3}$	778	$-1/2\sqrt{3}$
458	$\sqrt{3}/2$	344	$1/2$	888	$-1/\sqrt{3}$
678	$\sqrt{3}/2$				

(B.81)

B.5 Rules for Dimensional Regularization

In $d = 4 - 2\varepsilon$ dimensions and in Minkowski space.

- Metric

$$g^{00} = 1 \tag{B.82}$$

$$g^{ii} = -1 \text{ for } i = 1, .., 3 - 2\varepsilon \tag{B.83}$$

$$g^{\alpha\beta} = 0 \text{ for } \alpha \neq \beta \tag{B.84}$$

- Relations between γ matrices

$$\{\gamma^\mu, \gamma^\nu\} = 2g^{\mu\nu} \tag{B.85}$$

$$\gamma^\mu \gamma_\mu = 4 - 2\varepsilon \tag{B.86}$$

$$\gamma^\mu \gamma^\nu \gamma_\mu = (2\varepsilon - 2)\gamma^\nu \tag{B.87}$$

$$\gamma^\mu \gamma^\nu \gamma^\rho \gamma_\mu = 4g^{\mu\nu} - 2\varepsilon \gamma^\nu \gamma^\rho \tag{B.88}$$

- Feynman parametrization

$$\frac{1}{\Delta_1^a \Delta_2^b \Delta_3^c} = \frac{\Gamma(a+b+c)}{\Gamma(a)\Gamma(b)\Gamma(c)} \times \int_0^1 \mathrm{d}x \int_0^1 \mathrm{d}y \frac{x^{a-1} y^{b-1} (1-x-y)^{c-1}}{[x\Delta_1 + y\Delta_2 + (1-x-y)\Delta_3]^{a+b+c}} \tag{B.89}$$

- Typical integrals

$$g^2 \mu^{4-d} \int \mathrm{d}_d k \frac{k^{\mu_1} ... k^{\mu_{2m}}}{(k^2 - \Delta + i\varepsilon)^n} = F_{n,m}(\varepsilon, \Delta) P_m^{\mu_1 ... \mu_{2m}} \tag{B.90}$$

$$g^2 \mu^{4-d} \int \mathrm{d}_d k \frac{k^{\mu_1} ... k^{\mu_{2m+1}}}{(k^2 - \Delta + i\varepsilon)^n} = 0 \tag{B.91}$$

where

$$F_{n,m}(\varepsilon) = \frac{ig^2}{16\pi^2} \frac{(-1)^{n+m} \Delta^{2+m-n}}{(m+1)(n-1)!} (1 - \varepsilon \log \frac{\Delta}{4\pi\mu^2}) \Gamma(\varepsilon + n - m - 2) \tag{B.92}$$

and $P_m^{\mu_1 ... \mu_{2m}}$ is a sum with sign over all the possible contractions of the indices. The sign is positive for an even permutation and negative for an odd permutation. For example:

$$P_1^{\mu_1 \mu_2} = g^{\mu_1 \mu_2} \tag{B.93}$$

$$P_2^{\mu_1 \mu_2 \mu_3 \mu_4} = g^{\mu_1 \mu_2} g^{\mu_3 \mu_4} - g^{\mu_1 \mu_3} g^{\mu_4 \mu_2} + g^{\mu_1 \mu_4} g^{\mu_3 \mu_2} \tag{B.94}$$

Using the $\overline{MS}$ prescription (for u.v. divergences)

$$
\begin{aligned}
F_{n,m}(\varepsilon) =& \delta_{(n>m+2)} \frac{ig^2}{16\pi^2} \frac{(-1)^{n+m}(n-m-1)!}{(m+1)(n-1)!} \Delta^{2+m-n} + \\
& \delta_{(n=m+2)} \frac{ig^2}{16\pi^2} \frac{(-1)^{n+m+1}}{(m+1)(n-1)!} \log \frac{\Delta}{\mu^2}
\end{aligned} \tag{B.95}
$$

- Gamma function (for any n positive integer)

$$
\Gamma(n+\varepsilon) = (n-1)! + O(\varepsilon) \tag{B.96}
$$

$$
\Gamma(\varepsilon) = \varepsilon^{-1} - \gamma_E + O(\varepsilon) \tag{B.97}
$$

where $\gamma_E = 0.577..$ is the Euler number.

- Useful integrals

$$
\int_0^1 x^n \log(bx^m) \mathrm{d}x = \frac{\log b}{(n+1)} - \frac{m}{(n+1)^2} \tag{B.98}
$$

Appendix C

Units, Parameters, Particles

- Conversion factors

$$\begin{aligned} 1 \text{ GeV}^{-1} &= 6.5821219(13)\ 10^{-25} \text{ s} \\ &= 0.197327053(59) \text{ fm} \\ &= 0.197327053(59)\ 10^{-15} \text{ m} \end{aligned}$$

- Constants

Quantity	Symbol	Value
speed of light in vacuum	c	299792458 m s^{-1}
Plank constant	$h/2\pi$	1.05457266(63) 10^{-34}J s
Avogadro number	N_A	6.0221367(36) 10^{23}mol^{-1}
Boltzmann constant	k	8.617385(73) 10^{-5}eV K^{-1}
wavelength of $1eV$ particle	hc/e	1.23984277(37) 10^{-6}m

- Parameters of the Standard Model

Symbol	Value	Symbol	Value
m_e	0.51099906(15) MeV	$\alpha = e^2/4\pi$	1/137.035989(6)
m_μ	105.658389(34) MeV	G_F	1.16639(1) 10^{-5} MeV $^{-2}$
m_τ	1777.05(3)MeV	$\alpha_s(m_Z)$	0.1192(2)
m_u	1.5 ÷ 5 MeV	m_d	3 ÷ 9 MeV
m_c	1.3(1) GeV	m_s	65(5) GeV
m_t	174(5) GeV	m_b	4.2(1) GeV
m_W	80.41(10) GeV	m_Z	90.187(7) GeV
$\sin^2\theta_W(m_Z)$	0.2312(3)	Λ_{QCD}	250(50) MeV[136]
m_H	66^{+74}_{-39} GeV		

- Cabibbo-Kobayashi-Maskawa matrix elements

$$\begin{pmatrix} |V_{ud}| & |V_{us}| & |V_{ub}| \\ |V_{cd}| & |V_{cs}| & |V_{cb}| \\ |V_{td}| & |V_{ts}| & |V_{tb}| \end{pmatrix} = \begin{pmatrix} 0.9751(6) & 0.221(2) & 0.003(1) \\ 0.221(3) & 0.9743(7) & 0.041(5) \\ 0.009(5) & 0.040(6) & 0.9991(2) \end{pmatrix}$$

- Examples scalar mesons

Symbol	$q\overline{q}$	I, J^P	mass	Symbol	$q\overline{q}$	I, J^P	mass
π^+	$u\overline{d}$	$1, 0^-$	139	B^+	$u\overline{b}$	$\frac{1}{2}, 0^-$	5278
π^0	$d\overline{u}$	$1, 0^-$	134	B^0	$d\overline{b}$	$\frac{1}{2}, 0^-$	5279
π^-	$u\overline{u} - d\overline{d}$	$1, 0^-$	139	B^-	$b\overline{u}$	$\frac{1}{2}, 0^-$	5278
η	$u\overline{u} + d\overline{d}$	$0, 0^-$	547	$\overline{B}^0$	$b\overline{d}$	$\frac{1}{2}, 0^-$	5279
K^+	$u\overline{s}$	$\frac{1}{2}, 0^-$	493	D_s^+	$c\overline{s}$	$0, 0^-$	1968
K^0	$d\overline{s}$	$\frac{1}{2}, 0^-$	498	B_s^0	$s\overline{b}$	$0, 0^-$	5279
K^-	$s\overline{u}$	$\frac{1}{2}, 0^-$	493	D_s^-	$s\overline{c}$	$0, 0^-$	1968
$\overline{K}^0$	$s\overline{d}$	$\frac{1}{2}, 0^-$	498	$\overline{B}_s^0$	$b\overline{s}$	$0, 0^-$	5369
D^+	$c\overline{d}$	$\frac{1}{2}, 0^-$	1869	η_c	$c\overline{c}$	$0, 0^-$	2979
D^0	$c\overline{u}$	$\frac{1}{2}, 0^-$	1864	...			
D^-	$d\overline{u}$	$\frac{1}{2}, 0^-$	1869				
$\overline{D}^0$	$u\overline{c}$	$\frac{1}{2}, 0^-$	1864				

- Examples of vectorial mesons

Symbol	$q\overline{q}$	I, J^P	mass	Symbol	$q\overline{q}$	I, J^P	mass
ρ	$u\overline{u} - d\overline{d}$	$1, 1^+$	770	D_s^*	$s\overline{c}, c\overline{s}$	$0, 1^-$	782
ω	$u\overline{u} + d\overline{d}$	$0, 1^-$	1419	B_c^*	$c\overline{b}, b\overline{c}$	$0, 1^-$	?
K^*	$s\overline{q}, q\overline{s}$	$\frac{1}{2}, 1^-$	1414	J/ψ	$c\overline{c}$	$0, 1^-$	3096
D^*	$c\overline{q}, q\overline{c}$	$\frac{1}{2}, 1^-$	2006	Υ	$b\overline{b}$	$0, 1^-$	9460
B^*	$b\overline{q}, q\overline{b}$	$\frac{1}{2}, 1^-$	5324	...			

- Examples of Baryons

Symbol	qqq	I, J^P	mass	Symbol	qqq	I, J^P	mass
p	uud	$\frac{1}{2}, \frac{1}{2}^+$	938	Ω^-	sss	$0, \frac{3}{2}^+$	1672
n	udd	$\frac{1}{2}, \frac{1}{2}^+$	939	Λ_c^+	udc	$0, \frac{1}{2}^+$	2285
Δ^{++}	uuu	$\frac{3}{2}, \frac{3}{2}^+$	1232	Σ_c^{++}	uuc	$1, \frac{1}{2}^+$	2452
Δ^+	uud	$\frac{3}{2}, \frac{3}{2}^+$	1232	Σ_c^+	udc	$1, \frac{1}{2}^+$	2453
Δ^0	udd	$\frac{3}{2}, \frac{3}{2}^+$	1232	Σ_c^0	ddc	$1, \frac{1}{2}^+$	2452
Δ^-	ddd	$\frac{3}{2}, \frac{3}{2}^+$	1232	Ξ_c^+	usc	$\frac{1}{2}, \frac{1}{2}^+$	2465
Σ^+	uus	$1, \frac{1}{2}^+$	1189	Ξ_c^-	dsc	$\frac{1}{2}, \frac{1}{2}^+$	2465
Σ^0	uds	$1, \frac{1}{2}^+$	1192	Ξ_b^0	usb	$\frac{1}{2}, \frac{1}{2}^+$	?
Σ^-	dds	$1, \frac{1}{2}^+$	1189	Ξ_b^-	dsb	$\frac{1}{2}, \frac{1}{2}^+$	?
Λ^0	uds	$0, \frac{1}{2}^+$	1115	Λ_b^0	udb	$0, \frac{1}{2}^+$	5624
Ξ^0	uus	$\frac{1}{2}, \frac{1}{2}^+$	1314	...			
Ξ^-	dss	$\frac{1}{2}, \frac{1}{2}^+$	1321				

Appendix D

Feynman Rules

D.1 Feynman rules for QCD and HQET (Minkowski space)

- Gluon Propagator in the Feynman gauge (with an infinitesimal mass λ as infrared regulator)

$$G^{\mu\nu}(p) = \frac{-ig^{\mu\nu}}{p^2 - \lambda^2} \tag{D.1}$$

- Quark Propagator

$$D(p) = i\frac{\not{p} + m}{p^2 - m^2} \tag{D.2}$$

- Quark-Gluon Vertex

$$V_\mu(p, q) = -igt^a\gamma_\mu \tag{D.3}$$

- Static Quark Propagator

$$D_{\mathrm{h}}(p) = \frac{i}{p_0 + i\varepsilon} \tag{D.4}$$

- Static Quark-Gluon Vertex

$$V_{\mathrm{h}\,0}(p,q) = -igt^a \tag{D.5}$$

D.2 Feynman rules for Lattice QCD and HQET (Euclidean space)

In quoting following Feynman rules, we adopt the definitions

$$C_\mu(p) \equiv \cos(p_\mu/2) \tag{D.6}$$
$$S_\mu(p) \equiv \sin(p_\mu/2) \tag{D.7}$$

and all the momenta are in units of the lattice spacing. In the expressions for the vertices, p is intedened to be the momentum of the incoming quark and q is the momentum of the outcoming quark. The symbols $\Delta_i(p)$ are defined later in this Appendix.

- Gluon Propagator in the Feynman gauge (with an infinitesimal mass λ as infrared regulator)

$$G^{\mu\nu}(p) = \frac{\delta^{\mu\nu}}{4\Delta_1(p) + a^2\lambda^2} \tag{D.8}$$

- Quark Propagator

$$D(p) = \frac{-2i\sum_\rho \gamma_\rho C_\rho(p) S_\rho(p) + m + 2r\Delta_1(p)}{\Delta_2(p)} \tag{D.9}$$

- Quark-Gluon Vertex

$$V_\mu(p,q) = -gt^a\Big[i\gamma_\mu C_\mu(p+q) + rS_\mu(p+q)\Big] \tag{D.10}$$

- Improved Quark-Gluon Vertex (from SW "clover" term)

$$V^I_\mu(p,q) = -gt^a\frac{r}{2}\sum_\nu \Big[(\gamma_\mu\gamma_\nu - \gamma_\nu\gamma_\mu)C_\mu(p-q)S_\nu(p-q)C_\nu(p-q)\Big] \tag{D.11}$$

- Quark-two-Gluon Vertex

$$V_{\mu\nu}(p,q) = -g^2\{t^a,t^b\}\frac{r}{2}\delta_{\mu\nu}C_\mu(p+q) \tag{D.12}$$

- Static Quark Propagator

$$D_{\mathrm{h}}(p) = \frac{1}{1-e^{-ip_0}+\varepsilon} \tag{D.13}$$

- Static Quark-Gluon Vertex

$$V_{\mathrm{h}\,0}(p,q) = -igt^a e^{-iq_0/2} \tag{D.14}$$

- Static Quark-two-Gluon vertex

$$V_{\mathrm{h}\,00}(p,q) = -\frac{1}{2}g^2\{t^a,t^b\}e^{-iq_0/2} \tag{D.15}$$

D.3 Example of computation of a Lattice Feynman diagram

As an example the following Feynman diagram that contributes to the one loop correction of the operator $\bar{b}\Gamma q\bar{q}\tilde{\Gamma}b$ will be computed explicitely.

$I =$ 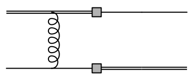 $=$ (D.16)

$$\int\frac{\mathrm{d}^4k}{(2\pi)^4}V_\mu(0,k)D(k)\Gamma\otimes V_{\mathrm{h}\,0}(0,k)D_{\mathrm{h}}(k)\widetilde{\Gamma}G^{\mu 0}(k) = \tag{D.17}$$

$$\frac{g^2}{(4\pi)^2}\frac{1}{\pi^2}\int d^4k\,(i\gamma_0C_0 - rS_0)\,\frac{\left(2i\sum_\rho\gamma_\rho S_\rho C_\rho + 2r\sum_\rho S_\rho S_\rho\right)}{\Delta_2(k)}$$
$$\times\left[\frac{1}{2S_0}+i\pi\delta(k_0)\right]\frac{1}{4\Delta_1(k)}t^a\Gamma\otimes t^a\widetilde{\Gamma} \tag{D.18}$$

The terms $1/2S_0$ and $i\pi\delta(k_0)$ come from the principal value and the pole residue, due to the static quark propagator, respectively. We expand the integrand and observe that

$$\begin{aligned} S_\mu(-k) &= -S_\mu(k) && \text{(D.19)} \\ C_\mu(-k) &= +C_\mu(k) && \text{(D.20)} \\ \Delta_i(-k) &= +\Delta_i(k) && \text{(D.21)} \end{aligned}$$

therefore any term in the integrand with an odd number of S functions vanishes in the integration and just two terms survive:

$$\begin{aligned} I =& \frac{g^2}{(4\pi)^2}\frac{1}{\pi^2}\left[\int \mathrm{d}^4k \frac{-r^2\sum_\rho S_\rho S_\rho - C_0C_0}{4\Delta_1\Delta_2}\right] t^a\Gamma \otimes t^a\widetilde{\Gamma} + \\ & \frac{g^2}{(4\pi)^2}\frac{1}{\pi^2}\left[\int \mathrm{d}^4k \frac{-2r\sum_\rho S_\rho S_\rho \pi\delta(k_0)}{4\Delta_1\Delta_2}\right] t^a\Gamma \otimes t^a\widetilde{\Gamma} \end{aligned} \tag{D.22}$$

Moreover we observe that, due to the lattice hypercubic symmetry,

$$\int \mathrm{d}^4k \frac{C_0C_0}{\Delta_1\Delta_2} = \int \mathrm{d}^4k \frac{C_1C_1}{\Delta_1\Delta_2} = \int \mathrm{d}^4k \frac{C_2C_2}{\Delta_1\Delta_2} = \int \mathrm{d}^4k \frac{C_3C_3}{\Delta_1\Delta_2} \tag{D.23}$$

therefore the following relation holds

$$\int \mathrm{d}^4k \frac{C_0C_0}{\Delta_1\Delta_2} = \frac{1}{4}\int \mathrm{d}^4k \frac{\sum_\rho C_\rho C_\rho}{\Delta_1\Delta_2} = \int \mathrm{d}^4k \frac{1 - \sum_\rho S_\rho S_\rho/4}{\Delta_1\Delta_2} \tag{D.24}$$

Substituting the identity of eq. (D.24) into the first term of eq. (D.22), together with the definition of Δ_1, we obtain

$$\begin{aligned} I =& \frac{g^2}{(4\pi)^2}\frac{1}{\pi^2}\left[\int \mathrm{d}^4k \frac{-r^2\Delta_1 - (1-\Delta_1/4)}{4\Delta_1\Delta_2}\right] t^a\Gamma \otimes t^a\widetilde{\Gamma} + \\ & \frac{g^2}{(4\pi)^2}\frac{-2r}{\pi}\left[\int \mathrm{d}^4k \frac{\Delta_1\delta(k_0)}{4\Delta_1\Delta_2}\right] \gamma^0 t^a\Gamma \otimes \gamma^0 t^a\widetilde{\Gamma} \end{aligned} \tag{D.25}$$

The first integral is divergent therefore we isolate the divergence by adding and substractiong the integrand $\Delta_0(k) = \theta(1-k^2)/(k^2 + a^2\lambda^2)^2$ and we replace the numerical integrals with the symbols d_1 and d_2, defined in eqs. (D.42)-(D.43).

The result reads

$$I = \frac{g^2}{(4\pi)^2}\left(\int \frac{\theta(1-k^2)\mathrm{d}^4k}{\pi^2(k^2+a^2\lambda^2)^2} - d_1\right) t^a\Gamma\otimes t^a\widetilde{\Gamma} + \frac{g^2}{(4\pi)^2}(d_2)\gamma^0 t^a\Gamma\otimes\gamma^0 t^a\widetilde{\Gamma} \tag{D.26}$$

The first integral can be computed analitically (with the appropriate prescription for the pole when $\lambda \to 0$) and we obtain

$$I = \frac{g^2}{(4\pi)^2}\left(\log a^2\lambda^2 - d_1\right) t^a\Gamma\otimes t^a\widetilde{\Gamma} + \frac{g^2}{(4\pi)^2}(d_2)\gamma^0 t^a\Gamma\otimes\gamma^0 t^a\widetilde{\Gamma} \tag{D.27}$$

This is the result quoted in Chapter 3 for the diagram n. 27).

D.4 Definition of useful parameters

$$C_\mu(p) \equiv \cos(p_\mu/2) \tag{D.28}$$

$$S_\mu(p) = \sin(p_\mu/2) \tag{D.29}$$

$$\Delta_0(p) \equiv \theta(1-p^2)/(p^2+a^2\lambda^2)^2 \tag{D.30}$$

$$\Delta_1(p) \equiv \sum_\rho \sin^2(p_\rho/2) \tag{D.31}$$

$$\Delta_2(p) \equiv \sum_\rho \sin^2 p_\rho + (m+2r\Delta_1)^2 \tag{D.32}$$

$$\Delta_3(p) \equiv \sum_\rho \cos^2(p_\rho/2) = (4-\Delta_1) \tag{D.33}$$

$$\Delta_4(p) \equiv \sum_\rho \sin^2 p_\rho \tag{D.34}$$

$$\Delta_5(p) \equiv \sum_\rho \sin^2 p_\rho \sin^2(p_\rho/2) \tag{D.35}$$

$$\Delta_6(p) \equiv \sum_\rho \cos^4(p_\rho/2) \tag{D.36}$$

$$\Delta_7(p) \equiv \sum_\rho \sin^2(p_\rho/2)\cos^6(p_\rho/2) \tag{D.37}$$

$$\Delta_8(p) \equiv \sum_{\rho\neq\xi} \sin^2 p_\rho \cos^2(p_\xi/2) = \Delta_4(4-\Delta_1) - (\Delta_4-\Delta_5) \tag{D.38}$$

Note that $\Delta_2(p)$ only appears for the quark propagator and m is the mass of the quark. For what concerns this thesis we are only interested in massless quarks (chiral limit) therefore m is set equal to zero in the numerical evaluation of the Feynman integrals. Our definitions of the $\Delta_i(p)$ functions are constistent with those of ref. [65] but not with those of ref. [66]

D.5 Definition of useful integrals

In the following definitions, the symbol $\square$ refers to the four dimensional integration domain defined by

$$\square = \{\forall\mu, k_\mu \in [-\pi, +\pi]\} \tag{D.39}$$

Useful integrals:

$$c \equiv -2 + \frac{1}{\pi^2}\int_\square \mathrm{d}^4k \left[\frac{1}{8\Delta_1^2} - 2\Delta_0 - \frac{1}{32\Delta_1}\right] \tag{D.40}$$

$$e \equiv c + \frac{1}{\pi}\int_\square \mathrm{d}^3k\delta(k_0)\left[\frac{1}{4\Delta_1}\right] \tag{D.41}$$

$$d_1 \equiv \frac{1}{\pi^2}\int_\square \mathrm{d}^4k \left[\frac{1}{4\Delta_1\Delta_2} - \Delta_0 - \frac{1-4r^2}{16\Delta_2}\right] \tag{D.42}$$

$$d_2 \equiv -\frac{2r}{\pi}\int_\square \mathrm{d}^3k\delta(k_0)\left[\frac{1}{4\Delta_1}\right] \tag{D.43}$$

$$f \equiv 1 + \frac{1}{\pi^2}\int_\square \mathrm{d}^4k \left[\frac{1}{8\Delta_1} + \Delta_0 - \frac{\Delta_4 - \Delta_5}{16\Delta_1^2\Delta_2} + \frac{r^2}{4}\frac{2-\Delta_1}{\Delta_2}\right] \tag{D.44}$$

$$v_1 \equiv -\frac{1}{\pi^2}\int_\square \mathrm{d}^4k \left[\frac{\Delta_4 - \Delta_5}{\Delta_1\Delta_2^2} - 4\Delta_0 + \frac{2\Delta_1\Delta_4 + 4r^2\Delta_1^3}{4\Delta_1\Delta_2^2}\right] \tag{D.45}$$

$$v_2 \equiv -\frac{1}{\pi^2}\int_\square \mathrm{d}^4k \left[\frac{\Delta_8}{4\Delta_1\Delta_2^2} - 3\Delta_0\right] \tag{D.46}$$

$$v \equiv (v_1 + v_2) \tag{D.47}$$

$$w \equiv \frac{1}{4\pi^2}\int_\square \mathrm{d}^4k \left[-\frac{\Delta_1\Delta_3}{\Delta_2^2} + \frac{\Delta_4}{4\Delta_2^2}\right] \tag{D.48}$$

$$d^I \equiv -\frac{r}{2\pi}\int_\square \mathrm{d}^3k\delta(k_0)\left[\frac{\Delta_4}{4\Delta_1\Delta_2}\right] \tag{D.49}$$

$$f^I \equiv \frac{r^2}{2\pi^2}\int_\square \frac{\mathrm{d}^4k}{4\Delta_1\Delta_2}\left[\Delta_8\left(\frac{\Delta_4}{4}-\frac{\Delta_3}{2}\right)+\Delta_6\left(\frac{\Delta_4}{4}-\Delta_1\right)+\right. \tag{D.50}$$

$$\left.+\frac{\Delta_1\Delta_4}{4}+\Delta_1\Delta_3^2+\Delta_1^2\Delta_3-\Delta_7\right]+\frac{\Delta_4\Delta_8}{16\Delta_1} \tag{D.51}$$

$$h \equiv -\frac{r}{2\pi}\int_\square \mathrm{d}^3k\delta(k_0)\left[\frac{1}{4\Delta_1}\right] \tag{D.52}$$

$$l \equiv -\frac{r^2}{4\pi^2}\int_\square \mathrm{d}^4k\left[\frac{\Delta_8}{4\Delta_1\Delta_2}\right] \tag{D.53}$$

$$m \equiv \frac{r^2}{4\pi^2}\int_\square \mathrm{d}^4k\left[\frac{4\Delta_1\Delta_3-\Delta_4}{4\Delta_1\Delta_2}\right] \tag{D.54}$$

$$n \equiv \frac{r^2}{4\pi^2}\int_\square \mathrm{d}^4k\left[\frac{\Delta_1\Delta_3-\Delta_4}{4\Delta_1\Delta_2}\right] \tag{D.55}$$

$$q \equiv -\frac{r^3}{2\pi}\int_\square \mathrm{d}^3k\delta(k_0)\left[\frac{\Delta_4}{4\Delta_2}\right] \tag{D.56}$$

$$v_1^I \equiv -4w_1^I \equiv -\frac{r^2}{\pi^2}\int_\square \mathrm{d}^4k\left[\frac{\Delta_1\Delta_8}{4\Delta_1\Delta_2^2}\right] \tag{D.57}$$

$$v_2^I \equiv -\frac{r^4}{\pi^2}\int_\square \mathrm{d}^4k\left[\frac{\Delta_1^2\Delta_8}{4\Delta_1\Delta_2^2}\right] \tag{D.58}$$

$$v^I \equiv 2v_1^I+v_2^I \tag{D.59}$$

$$w_1^I \equiv \frac{r^2}{4\pi^2}\int_\square \mathrm{d}^4k\left[\frac{\Delta_1\Delta_8}{4\Delta_1\Delta_2^2}\right] \tag{D.60}$$

$$w_2^I \equiv -\frac{r^2}{4\pi^2}\int_\square \mathrm{d}^4k\left[\frac{\Delta_4\Delta_8}{4\Delta_1\Delta_2^2}\right] \tag{D.61}$$

$$w^I \equiv \frac{1}{2}w_1^I+\frac{1}{4}w_2^I \tag{D.62}$$

$$s_1 \equiv \frac{r^2}{4\pi^2}\int_\square \mathrm{d}^4k\left[\frac{4\Delta_1(\Delta_4-\Delta_5)-\Delta_4^2}{4\Delta_1\Delta_2^2}\right] \tag{D.63}$$

$$s_2 \equiv \frac{r^2}{4\pi^2}\int_\square \mathrm{d}^4k\left[\frac{4\Delta_1\Delta_8}{4\Delta_1\Delta_2^2}\right] \tag{D.64}$$

$$s_3 \equiv s_1+s_2 \tag{D.65}$$

$$s_4 \equiv -\frac{r^2}{4\pi^2}\int_\square \mathrm{d}^4k\left[\frac{\Delta_4\Delta_8}{4\Delta_1\Delta_2^2}\right] \tag{D.66}$$

$$s_5 \equiv -\frac{r^2}{4\pi^2}\int_\Box \mathrm{d}^4k \left[\frac{4\Delta_1^2\Delta_8}{4\Delta_1\Delta_2^2}\right] \tag{D.67}$$

$$s_6 \equiv \frac{r^4}{\pi^2}\int_\Box \mathrm{d}^4k \left[\frac{4\Delta_1^2\Delta_8}{4\Delta_1\Delta_2^2}\right] \tag{D.68}$$

$$s_7 \equiv s_4 \tag{D.69}$$

$$s_8 \equiv -\frac{r^4}{4\pi^2}\int_\Box \mathrm{d}^4k \left[\frac{\Delta_1\Delta_4\Delta_8}{4\Delta_1\Delta_2^2}\right] \tag{D.70}$$

$$s_9 \equiv s_8 \tag{D.71}$$

$$s \equiv 2(s_3+s_5+s_7+s_9) = 2(s_1+s_2+s_4+s_6+s_8) \tag{D.72}$$

$$t_1 \equiv -\frac{r^2}{4\pi^2}\int_\Box \mathrm{d}^4k \left[\frac{\Delta_3}{4\Delta_1}\right] \tag{D.73}$$

$$t_2 \equiv \frac{r^2}{4\pi^2}\int_\Box \mathrm{d}^4k \left[\frac{\Delta_3\Delta_4 + r^2\Delta_1\Delta_4}{4\Delta_1\Delta_2}\right] \tag{D.74}$$

$$t_3 \equiv \frac{r^4}{4\pi^2}\int_\Box \mathrm{d}^4k \left[\frac{\Delta_8}{4\Delta_2}\right] \tag{D.75}$$

$$t_4 \equiv \frac{r^4}{4\pi^2}\int_\Box \mathrm{d}^4k \left[\frac{-\Delta_1\Delta_4 + 4\Delta_1^2(\Delta_4-\Delta_5)}{4\Delta_1\Delta_2^2}\right] \tag{D.76}$$

$$t_5 \equiv \frac{r^4}{4\pi^2}\int_\Box \mathrm{d}^4k \left[\frac{4\Delta_1^2\Delta_8}{4\Delta_1\Delta_2^2}\right] \tag{D.77}$$

$$t_6 \equiv -\frac{r^2}{4\pi^2}\int_\Box \mathrm{d}^4k \left[\frac{\Delta_4^2(\Delta_3+2r^2\Delta_1) + 4r^4\Delta_1^3\Delta_4}{4\Delta_1\Delta_2^2}\right] \tag{D.78}$$

$$t_7 \equiv t_8 \equiv -\frac{r^4}{4\pi^2}\int_\Box \mathrm{d}^4k \left[\frac{\Delta_1\Delta_4\Delta_8}{4\Delta_1\Delta_2^2}\right] \tag{D.79}$$

$$t_9 \equiv \frac{r^4}{16\pi^2}\int_\Box \mathrm{d}^4k \left[\frac{\Delta_4^2\Delta_8}{4\Delta_1\Delta_2^2}\right] \tag{D.80}$$

$$t_{10} \equiv -\frac{r^6}{4\pi^2}\int_\Box \mathrm{d}^4k \left[\frac{\Delta_1^2\Delta_4\Delta_8}{4\Delta_1\Delta_2^2}\right] \tag{D.81}$$

$$t_A \equiv t_1+t_6+t_{10}+2(t_2+t_3+t_8) \tag{D.82}$$

$$t_B \equiv t_4+t_5+t_9+2t_7 \tag{D.83}$$

Bibliography

[1] M. Di Pierro and C. T. Sachrajda, A Lattice Study of Spectator Effects in Inclusive Decays of B-Mesons, Nucl. Phys. **B534** (1998); hep-lat/9805028

[2] G. De Divitiis, L. Del Debbio, M. Di Pierro, J. Flynn, C. Michael and J. Peisa, Towards a lattice determination of the $B^*B\pi$ coupling, 9810:010 JHEP (1998); hep-lat/9807032

[3] M. Di Pierro, Spectator Effects in Inclusive Decays of Beauty Hadrons, to apper in the proceedings of Lattice98 (1998); hep-lat/9809083

[4] M. Di Pierro and C. T. Sachrajda, Spectator Effects in Inclusive Decays of Λ_b from Lattice Simulations (to be submitted).

[5] M. Peskin and D.V. Shroeder, Quantum Field Theory, Addison Wesley (1994)

[6] C. Itzykson and J.-Z. Zuber, Quantum Field Theory, Mc Graw-Hill (1985)

[7] A. Dobado, A. Gómez-Nicola, A.L. Maroto and J.R. Peláez, Effective Theories for the Standard Model, Springer (1997)

[8] J. F. Donoghue, E. Golowich and B. Holstein, Dynamics of the Standard Model Cambridge University Press (1996)

[9] M. Gell-Mann and Y. Neumann, "The Eigthfold Way", Benjamin Press (1969)
M. Gell-Mann, Phys. Lett. **8** (1964) 214

[10] P. W. Higgs, Phys. Lett. **12** (1964) 132
P. W. Higgs, Rev. Lett. **13** (1964) 508
P. W. Higgs, Rev. **145** (1966) 1156

[11] N. Cabibbo, Phys Rev. **10** (1963) 1802
J. Kobayashi and M. Maskawa, Prog. Theor. Phys. **49** (1973) 952

[12] R. P. Feynman, Phys. Rev. **80** (1950) 440

[13] S. L. Glashow, Nucl. Phys. **22** (1961) 579
A. Salam, Nobel Symposium n.8, Almqvist and Wilsell, Stockholm (1968)
S. Weinberg, Phys. Rev. Lett. **31** (1973) 1343

[14] C. N. Yang and R. Mills, Phys. Rev. **96** (1954) 191

[15] D. J. Gross, F. Wilczek, Phys. Rev. Lett. **30** (1973) 1343
H. Fitzsch, M. Gell-Mann and H. Leutwyler, Phys. Lett. **47B** (1973) 365
S. Weinberg, Phys. Rev. **31** (1973) 494

[16] T. Muta, Foundations of Quantum Chromo Dynamics, World Scientific (1987)

[17] W. Marciano and H Pagels, Phys. Rep. **36** (1978) 135

[18] A. V. Smilga, hep-ph/9901412

[19] M. Creutz, Quarks, Gluons and Lattices, Cambridge University Press (1983)

[20] L. Lusanna and P. Valtacoli, Int.J.Mod.Phys. **A27** (1998) 4605

[21] J. L. Hewett, hep-ph/9810316

[22] J. D. Richman, hep-ex/9701014

[23] M. Gell-Mann and F. E. Low, Phys. Rev. **95** (1954) 1300

[24] D. J. Gross and F. Wilczek, Phys. Rev. Lett. **30** (1973) 1343
D. J. Gross and F. Wilczek, Phys. Rev. **D8** (1973) 3633
H. Politzer, Phys. Rev. Lett. **30** (1973) 1346
H. Politzer, Phys. Rep. **14C** (1974) 129

[25] G. 't Hooft, Phys. Rev. (1978) 1

[26] E. Fermi, Z. Phys. **88** (1934) 161

[27] J. D. Bjorken, Phys. Rev. **179** (1969) 1547

[28] BaBar report, SLAC Publication

[29] J. Wolfenstein, Phys. Rev. Lett. **51** (1983) 1945

[30] Y. Nambu, Phys. Rev. Lett. **4** (1960) 380
J. Goldstone, Nuovo Cimento **19** (1961) 154

[31] L. B. Okun, Leptons and Quarks, (italian ed. Editori Riuniti, 1986)

[32] J. M. Rabin, Introduction to Quantum Field Theory for Mathematicians, IAS/Park City Mathematics Series, vol. 1 (1995)

[33] J. Glimm and R. Jaffe, Quantum Physics (second edition), Springer-Verlag (1987).

[34] G. 't Hooft and M. Veltman, Nucl. Phys. **B44** (1972) 189

[35] L. D. Faddeev and V. N. Popov, Phys. Lett. **B25** (1967) 29

[36] G. P. Lepage, nucl-th/970629

[37] S. Weinberg, hep-th/9702027

[38] T. Applequist and J. Carazzone, Phys.Rev. **D11** (1975) 2856

[39] K. Symanzik, Nucl. Phys. **B226** (1983) 187,205

[40] W. Heisenberg and H. Euler, Z. Phys. **98** (1936) 714 J. Schwinger, Phys.Rev. **82** (1951) 714

[41] M. Neubert, Phys. Rep. **245** (1994) 259.

[42] M. Shifman, hep-ph/9510377

[43] S. Weinberg, Physica **A96** (1979) 327
H. Leutwyler, Ann. Phys. **235** (1994) 165

[44] M.B. Wise, Phys. Rev. **D45** (1992) 2188.

[45] B. Grinstein, An Introduction to Heavy Mesons, 6th Mexican School of Particles and Fields, Villahermosa, Tabasco, October 1994, University of California San Diego preprint UCSD–PTH–95–05, hep-ph/9508227.

[46] R. Casalbuoni, A. Deandrea, N. Di Bartolomeo, R. Gatto, F. Feruglio and G. Nardulli, Phys. Rep. **281** (1997) 145 and references therein.

[47] H.-Y. Cheng *et al.*, Phys. Rev. **D49** (1994) 249.

[48] R. Fleischer, Phys. Lett. **B303** (1993) 147.

[49] A. F. falk, H. Georgi and B. Grinstein, Nucl. Phys. **B343** (1990) 1

[50] A.F. Falk and B. Grinstein, Nucl. Phys. **B416** (1994) 771.

[51] I. Montvay and G. Münster, Quantum Fields on a Lattice, Cambridge University Press (1994)

[52] M. Creutz, Quantum Fields on the Computer, World Scientific (1992)

[53] Rothe, Lattice Gauge Theories, World Scientific

[54] R. Gupta, hep-lat/9807028

[55] K. G. Wilson, Phys. rev. **D10** (1974) 2445

[56] B. Sheikoleslami and R. Wolhert, Nucl. Phys. **B259** (1985) 572

[57] M. Luscher, Advanced Lattice QCD, Talk given at Les Houches Summer School in Theoretical Physics, Session 68, (1998); hep-lat/9802029

[58] G. Banhot, The Metropolis Algorithm, Rep. Prog. Phys. 51 (1988) 429

[59] N. Cabibbo and E. Marinari, A new method for updating $SU(N)$ matrices in computer simulations of gauge theories, Phys. Lett. **119B** (1982) 387

[60] C. T. Sachrajda, Lattice Simulations and Effective Theories, Lectures presented at the Advanced School on Effective Theories, Almunecar (Spain) June 1995; hep-lat/960527

[61] C. Bernard in "From Action to Answers", Proceedings of the 1989 TASI in Elementary Particle Physics, Boulder, World Scientific

[62] L. Maiani and M. Testa, Phys.Lett. **B245** (1990) 585-590

[63] E. Eichten, Nucl. Phys. B (Proc. Suppl.) **4** (1988) 147; E. Eichten and B. Hill, Phys. Lett. **B232** (1989) 113.

[64] J. M. Flynn, O. F. Hernández and B. R. Hill, Prof. Rev. **D43** (1991) 3709

[65] A.Borelli and C.Pittori, Nucl.Phys. **B385** (1992) 502

[66] A.Borelli *et al.*, Nucl.Phys. **B409** (1993) 382

[67] UKQCD Collaboration, A.K. Ewing *et al.*, Phys.Rev. **D54** (1996) 3526

[68] V. Giménez and G. Martinelli, Phys.Lett. **B398** (1997) 135

[69] C.G. Boyd and B. Grinstein, Nucl. Phys. **B442** (1995) 205.

[70] G. Burdman, Z. Ligeti, M. Neubert and Y. Nir, Phys. Rev. **D49** (1994) 2331.

[71] For a review, see: V.M. Braun, Light-cone Sum Rules, to appear in Proc. 4th Int. Workshop on Progress in Heavy Quark Physics, Rostock, Germany, September 1997, hep-ph/9801222

[72] A. Khodjamirian, R. Rückl and C.W. Winhart, Phys. Rev. **D58** (1998) 054013

[73] UKQCD Collaboration, L. Del Debbio, J.M. Flynn, L. Lellouch and J. Nieves, Phys. Lett. **B416** (1998) 392.

[74] L. Lellouch, Nucl. Phys. **B479** (1996) 353.

[75] V.M. Belyaev, V.M. Braun, A. Khodjamirian and R. Rückl, Phys. Rev. **D51** (1995) 617.

[76] P. Ball and V.M. Braun, Phys. Rev. **D55** (1997) 556; V.M. Belyaev, A. Khodjamirian and R. Rückl, Z. Phys. **C60** (1993) 349.

[77] R. Dashen and D. J. Gross, Phys. Rev. **D23** (1981) 2340

[78] L. Maiani, G. Martinelli and C. T. Sachrajda, Nucl. Phys. **B368** (1992) 281
V. Giménez, G. Martinelli and C. T. Sachrajda, Phys. Lett. **B393** (1997) 124

[79] J. Shao and D. Tu, The Jackknife and Bootstrap, Springer Verlag (1995)

[80] G. Parisi, R. Petronzio and C. Rapuano, Phys. Lett. **B128** (1983) 418

[81] C. Michael and J. Peisa, Maximal variance reduction for stochastic propagators with applications to the static quark spectrum, Phys.Rev. **D58** (1998)

[82] E. Witten, Nucl. Phys. **12?** (1977) 109

[83] J. Chay, H. Georgi and B. Grinstein, Phys. Lett. **B247** (1990) 399

[84] I.I. Bigi, M.A. Shifman, N.G. Uraltsev and A.I. Vainstein,
Phys. Rev. Lett. **71** (1993) 496

[85] A.V. Manohar and M.B. Wise, Phys. Rev. **D49** (1994) 1310

[86] I. Bigi, M. Shifman and N. Uralstev,
Ann. Rev. Nucl. Part. Sci. **47** (1997) 591

[87] M. Neubert, Int. J. Mod. Phys. **A11** (1996) 4173

[88] I.I. Bigi, N.G. Uraltsev and A.I. Vainstein, Phys. Lett. **B293** (1992) 430; (E) **B297** (1993) 477;

[89] T. Junk, presented at the 2nd International Conference on B-Physics and CP-Violation, Honolulu, Hawai, March 1997, quoted in ref. [90]

[90] M. Neubert, invited talk at the International Europhysics Conference on High-Energy Physics (HEP 97), Jerusalem, Israel, August 1997; hep-ph/9801269

[91] M. Neubert and C.T. Sachrajda, Nucl.Phys. **B483** (1997) 339

[92] M.A. Shifman, A.I. Vainshtein and V.I. Zakharov, Nucl.Phys. **B147** (1979) 385,448

[93] B. Blok and M. Shifman, Proceedings of the 3rd Workshop on the Tau-Charm Factory, Marbella, Spain, June 1993, ed. J. Kirby and R. Kirby (editions Frontières, 1994) (hep-ph/9311331); I.I. Bigi *et al.*, in B-Decays, ed. S. Stone, second edition (World Scientific, Singapore, 1994) p. 134; I.I. Bigi, hep-ph/9508408

[94] J. Christensen, T. Draper and C. McNeile, Phys.Rev. **D56** (1997) 6993

[95] M.A. Shifman and M.B. Voloshin, Sov.J.Nucl.Phys. **41** (1985) 120; JETP **64** (1996) 698

[96] M.A. Shifman and M.B. Voloshin, Sov.J.Nucl.Phys. **45** (1987) 292

[97] H.D. Politzer and M.B. Wise, Phys.Lett. **B206** (1988) 681; **B208** (1988) 504

[98] M. Di Pierro, "**mdpqcd**: Object Oriented Programming for Lattice QCD" hep-lat/9811036

[99] UKQCD Collaboration, C.R. Allton *et al.*, Phys.Rev. **D47** (1993) 5128

[100] S. Güsken *et al.*, Phys. Lett. B227 (1989) 266; UKQCD Collaboration, R.M. Baxter *et al.*, Phys.Rev. **D49** (1994) 1594

[101] H. Cheng and K. Yang, hep-ph/9805222

[102] G. Altarelli and S. Petrarca, Phys.Lett. **B261**, (1991) 303

[103] I. Bigi, B. Block, M.A. Shifman and A. Vainshtein, Phys.Lett. **B323** (1994) 408

[104] B. Guberina, S. Nussinov, R. Peccei and R. Rückl, Phys. Lett. **B89** (1979) 111; N. Bilic, B. Guberina and J. Trampetic, Nucl. Phys. **B248** (1984) 261; B. Guberina, R. Rückl and J. Trampetic, Z. Phys. **C33** (1986) 297

[105] T.-M. Yan, H.-Y. Cheng, C.-Y. Cheung, G.-L. Lin, Y.C. Lin and H.-L. Yu, Phys. Rev **D46** (1992) 1148.

[106] H. Wittig, Int. J. Mod. Phys. **A12** (1997) 4477.

[107] UKQCD Collaboration, C. Michael and J. Peisa, University of Liverpool preprint LTH-420, hep-lat/9802015.

[108] G.M. de Divitiis, R. Frezzotti, M. Masetti and R. Petronzio, Phys. Lett. **B382** (1996) 393.

[109] UKQCD Collaboration, H. Shanahan *et al.*, Phys. Rev. **D55** (1997) 154.

[110] UKQCD Collaboration, P. Lacock, A. McKerrell, C. Michael, I.M. Stopher and P.W. Stephenson, Phys. Rev. **D51** (1995) 6403.

[111] G.P. Lepage and P.B. Mackenzie, Phys. Rev. **D48** (1993) 225.

[112] M. Lüscher, S. Sint, R. Sommer and H. Wittig, Nucl. Phys. **B491** (1997) 344.

[113] E. Gabrielli, G. Martinelli, C. Pittori, G. Heatlie and C.T. Sachrajda, Nucl. Phys. **B362** (1991) 475.

[114] G. Heatlie *et al.*, Nucl. Phys. **B352** (1991) 266.

[115] M. Göckeler *et al.*, Proc. Lattice 96: 14th Int. Symp. on Lattice Field Theory, St. Louis, June 1996, Nucl. Phys. B (Proc. Suppl.) 53 (1997) 896.

[116] E. Eichten and B. Hill, Phys. Lett. **B234** (1990) 511.

[117] X. Ji and M.J. Musolf, Phys. Lett. **B257** (1991) 409.

[118] D.J. Broadhurst and A.G. Grozin, Phys. Lett. **B267** (1991) 105; Phys. Lett. **B274** (1991) 421.

[119] V. Giménez, Nucl. Phys. **B375** (1992) 582.

[120] E. Eichten and B. Hill, Phys. Lett. **B240** (1990) 193.

[121] V. Giménez and J. Reyes, IFIC Valencia preprint, FTUV 98/2, IFIC 98/2, hep-lat/9806023

[122] Particle Data Group, C. Caso *et al.*, Euro. Phys. J. **C3** (1998) 1.

[123] I.W. Stewart, Caltech preprint CALT–68–2160, hep-ph/9803227 v2

[124] ACCMOR Collaboration, S. Barlag *et al.*, Phys. Lett. **B278** (1992) 480.

[125] S. Nussinov and W. Wetzel, Phys. Rev. **D36** (1987) 130.

[126] P. Colangelo, G. Nardulli, A. Deandrea, N. Di Bartolomeo, R. Gatto and F. Feruglio, Phys. Lett. **B339** (1994) 151.

[127] P. Cho and H. Georgi, Phys. Lett. **B296** (1992) 408.

[128] J.F. Amundson *et al.*, Phys. Lett. **B296** (1992) 415.

[129] P. Colangelo, F. De Fazio and G. Nardulli, Phys. Lett. **B334** (1994) 175.

[130] C.G. Boyd, B. Grinstein and R.F. Lebed, Phys. Rev. Lett. **74** (1995) 4603.

[131] UKQCD Collaboration, K. C. Bowler *et al.*, Phys. Rev. **D54** (1996) 3619

[132] I. Bigi, hep-ph/9508408 P. colangelo and F. De Fazio, hep-ph/9604425

[133] Z. Ligeti and A. V. Manohar, hep-ph/9803236

[134] E. Tournefier, Talk given at the 10th Internation Seminar “Quarks98”, Suzdal, Russia (1998); hep-ex/9810042. J. M. Flynn and C. T. Sachrajda, hep-ph/9710057

[135] T. Draper, hep-lat/9810065

[136] E. Tournefier, hep-ex/9810042

[137] M. Artuso, Talk given at Heavy Flavours 1998, Batavia, Illinois (1998); hep-ph/9812372

Index

B_B, 19, 20, 110
$C_\mu(p)$, 146
G_F, 13
$S_\mu(p)$, 146
$W^\pm$, 8
Z^0, 8
Z_A^{light}, 70
Z_A^{static}, 71
Z_{ij}, 55
$\Delta_i(p)$, 146
Λ_{QCD}, 12, 33
β, 46
κ, 46
κ_{crit}, 50
$\tau(B)$, 98
$\tau(\Lambda_b)$, 98
c_{SW}, 46
f_B, 19, 20, 87
f_π, 41
$g_{B^*B\pi}$, 42, 77
z_{ij}, 56

Ahronov-Bohm, 43
anomalous dimension, 57
anomaly, 6
    baryionc and leptonic, 22
    trace, 33
Appelquist-Carazzone theorem, 34
asymptotic freedom, 11, 33

baryon, 16, 141
    Λ_b, 18
Brillouin zone, 45

Casimir operators, 134
chiral extrapolation, 54
CKM matrix, 7, 21, 140
Clebsch-Gordan coefficients, 16
Clebsh-Gordan coefficients, 134
clover term, 46
colour, 3
colour symmetry, 5
commutation relations, 130
confinement, 15
conservation laws, 1
correlation function
    2-point, 49
    3-point, 49
CP symmetry, 23
CPT symmetries, 50, 133
cross section, 125
current
    axial, 22
    baryionic, 22
    colour, 8
    electromagnetic, 8
    leptonic, 22
    PCAC, 21
    weak charged, 8
    weak neutral, 8

decay time, 125
dimensional transmutation, 27
Dirac matrices
    Euclidean, 128
    Minkowskian, 126
divergence
    infrared, 29
    ultraviolet, 29
doubling problem, 45

effective Lagrangian, 34

chiral, ξ, 41
HMχ, 41
Fermi, 12, 37
Heisenberg-Euler, 36
HQET, 38
Lattice QCD, 43
equations of motion, 9

Fermi, Enrico, 12
fermion propagator, 50
Feynman
parametrization, 137
path integral, 123
Feynman rules, 142
Fierz identities, 133
flavour, 3

gauge, 132
Gell-Mann matrices, 135
Gell-Mann-Okubo formula, 22
gluon propagator, 142, 143
Goldstone
bosons, 21, 40
theorem, 21, 40
Gordon decomposition, 131
Green function, 123
group
$SU(2)_W$, 4
$SU(3)_C$, 5
$U(1)_Y$, 4

H symmetry, 50
hadronization, 14
heavy quark symmetry, 39
Higgs
boson, 9
dublet, 4
mechanism, 7
hypercharge, 4

improvement
1-loop, 52
non-perturbative, 52
tadpole, 52
tree-level, 46
integrating out, 36
Isgur-Wise function, 40
isospin, 16

jet event, 14

Lagrangian
electroweak, 8
QCD, 9
QED, 8
lepton, 3
links, 43
LSZ reduction formula, 124

magnetic dipole moment, 10
matching, 54, 55
meson, 16, 140
$B^+, B^-, B^0, \bar{B}^0$, 17
$\pi^\pm, \pi^0, K^\pm, K^0, \bar{K}^0, \eta$, 40
Monte Carlo Algorithm, 48

Nöther's theorem, 122
neutrino, 3
numerical integrals:
$c, e, d_1, d_2, v, w, ...$, 147

Operator Product Expansion, 35
Optical Theorem, 124

propagator
scalar, 132
spinor, 132
vector, 132

quark, 3
mass (lattice), 50
quark propagator
static, 52
light, 142, 143
static, 142, 144
quenching, 37, 47

regularization, 25
dimensional, 29

lattice, 29
momentum cut-off, 29
Pauly-Villars, 29
renormalization, 26
renormalon, 101
RGE, 26, 31, 68
running, 26

S matrix, 124
Sheikoleslami-Wolhert action, 47
Shrödinger equation, 29
smearing
fuzzing, 85
Jacobi, 105
Standard Model (SM), 2
string tension, 10
strong CP probelm, 6
Symanzik improvement, 35

unitarity triangle, 21

valence quark, 18
vector meson dominance (VMD), 78

weak-isospin, 5
Wick rotation, 44, 128
Wolfenstein parametrization, 21

Yukawa
interaction, 7
potential, 9